Universität Trier

Potential candidate genes for neuropsychiatric disorders: *MLC1, C15orf53* and *OXTR*

Dissertation zur
Erlangung des Doktorgrades der Naturwissenschaften
(Dr. rer. nat.)

durch den Fachbereich I – Psychobiologie

der Universität Trier

vorgelegt von

Thorsten Manfred Kranz

Betreuer:
Prof. Dr. Jobst Meyer
Prof. Dr. Claude P. Muller

Trier, 2012

Der Nutzen von Information liegt eindeutig in der Auswahl,

nicht in der Fülle,

in ihrer Relevanz,

nicht im Übertragungstempo.

Die Kunst vernetzt zu denken

Frederic Vester (1925 – 2003), deutscher Biochemiker und Biokybernetiker

Table of Contents

Index of Figures

Index of Tables

List of Abbreviations

11β-HSD	11beta-hydroxysteroid dehydrogenase
A	adenine
AA	amino acid
ABCA13	*ATP-binding cassette, sub-family A (ABC1), member 13*
ACTH	adrenocorticotropic hormone, corticotropin
ADHD	attention deficit hyperactivity disorder
ADI-R	Autism Diagnostic Interview-Revised
ADOS	Autism Diagnostic Observation Schedule
Ala	alanine
Arg	arginine
ANK3	*ankyrin 3, node of Ranvier (ankyrin G)*
ANOVA	Analysis of variance
AQP4	*aquaporin 4*
ASD	Autism Spectrum Disorder
Asp	asparagine
ATXN2	*ataxin 2*
AVP	arginine vasopressin
AVPR	*arginine vasopressin receptor*
BD	bipolar disorder
BDNF	brain-derived neurotrophic factor
ARNTL	*aryl hydrocarbon receptor nuclear translocator-like*
bp	base pair
BRD1	*bromodomain containing 1*
C	cytosine
C15orf53	*chromosome 15 open reading frame 53*
CACNA1C	*calcium channel, voltage-dependent, L type, alpha 1C subunit*
cAMP	cyclic adenosine monophosphate
CAV1	*caveolin 1*
CAR	cortisol awakening response
CBG	*corticosteroid binding globulin* (see *Serpina6*)
CD	cluster of differentiation
CDFE	Cortical Dysplasia–Focal Epilepsy Syndrome
CDK6	*cyclin-dependent kinase 6*
cDNA	complementary deoxyribonucleic acid
CFTR	*cystic fibrosis transmembrane conductance regulator (ATP-binding cassette sub-family C, member 7)*
C. elegans	*Caenorhabditis elegans*

CELSR1	*Cadherin EGF LAG seven-pass G-type receptor 1, human*
Celsr1	*Cadherin EGF LAG seven-pass G-type receptor 1, murine*
CHO	Chinese hamster ovary
Chr	chromosome
CHRNA7	*nicotinic α7 receptor*
CLOCK	*clock homolog (mouse)*
cM	centimorgan
CMD	congenital muscular dystrophies
CNS	central nervous system
CNTNAP2	*contactin associated protein-like 2*
CNV	copy number variation
COMT	*catechol-o-methyltransferase*
DPYD	*dihydropyrimidine dehydrogenase*
CREB	*cAMP responsive element binding protein*
CRH	corticotropin-releasing hormone
CSMD1	*CUB and Sushi multiple domains 1*
Cys	cysteine
D’	D prime (sensitivity index)
DCLK	*doublecortin-like kinase*
df	degree of freedom
DGCR8	*DiGeorge syndrome critical region gene 8*
DGKβ	*diacylglycerol kinase, beta 90kDa*
DISC1	*disrupted in schizophrenia 1*
DIV	days *in vitro*
DLPFC	dorsolateral prefrontal cortex
DLL4	*Drosophila Delta homolog 4*
DMD	*dystrophin*
DNA	deoxyribonucleic acid
DRD	*dopamine receptor D*
DRM	detergent-resistant membrane
DSM-IV	Diagnostic and Statistical Manual of Mental Disorders, fourth edition
ECL	enhanced chemiluminescence
EIF2C	*eukaryotic translation initiation factor 2C*
EMBL	European Molecular Biology Laboratory
ER	endoplasmatic reticulum
ES	embryonic stem cells
FAM98B	*family with sequence similarity 98, member B*
FCS	fetal calf serum
FKBP5	*FK506 binding protein 5*
FLJ	full-length long Japan
FMR1	*fragile X mental retardation 1*

fMRI	functional magnetic resonance imaging
FSK	forskolin
FST	Porsolt Forced Swim Test
G	guanine
GABA	γ-Aminobutyric acid
GAPDH	*Glyceraldehyde 3-phosphate dehydrogenase*
GRCh37	Genome Reference Consortium Human genome
gDNA	genomic deoxyribonucleic acid
GlialCAM	*hepatic and glial cell adhesion molecule*
Glu	glutamine
GRE	glucocorticoid response element
GWAS	genome-wide association study
HB-EGF	*heparin-binding EGF-like growth factor*
His	histidine
HL	high licking
HPA	hypothalamic-pituitary-adrenal
HS	horse serum
HSV-TK	*herpes simplex thymidine kinase*
HTR	*5-hydroxytryptamine (serotonin) receptor*
HVA	homovanilic acid
ICD-10	International Classification of International Statistical Classification of Diseases and Related Health Problems, 10th revision
Ile	isoleucine
iPSC	inducible human pluripotent stem cell
IQ	intelligence quotient
kb	kilobase
KCC2	*Potassium-chloride transporter member 5* (see *SLC12A5*)
kDa	kilodalton
KCNA1	*potassium voltage-gated channel subfamily A member 1*
KO	knock out
KDM1A	*lysine (K)-specific demethylase 1A*
LB	lysogeny broth
LOD	logarithm of the odds
Leu	leucine
Limk1	*LIM domain kinase 1*
LL	low licking
M	molar
MAF	minor allele frequency
MAG	*myelin associated glycoprotein*
MDD	major depressive disorder
MECP2	*methyl CpG binding protein 2 (Rett syndrome)*

MEF	mouse embryonic fibroblasts
Met	methionine
miRNA	microRNA
mM	milimolar
mRNA	messenger ribonucleic acid
NCAM	Neural Cell Adhesion Molecule
Neo	*neomycin resistance gene*
NGF	*nerve growth factor (beta polypeptide)*
NMDA	N-Methyl-D-aspartate
nt	nucleotide
Odds-R	odds ratio of alleles
OMIM	Online Mendelian Inheritance in Men
OXT	*oxytocin*
OXTR	*oxytocin receptor*
MGC	Mammalian Gene Collection
MLC	megalencephalic leukoencephalopathy with subcortical cysts
MLC1	*megalencephalic leukoencephalopathy with subcortical cysts 1, human*
Mlc1	*megalencephalic leukoencephalopathy with subcortical cysts 1, murine*
MAOA	*monoamine oxidase A*
NCBI	National Center for Biotechnology Information
Neo	neomycin
NIMH	National Institute of Mental Health
nM	nanomolar
NPL	non-parametric linkage
NR3C1	*nuclear receptor subfamily 3, group C, member 1 (glucocorticoid receptor)*
NR3C2	*nuclear receptor subfamily 3, group C, member 2 (mineralocorticoid receptor)*
ObsHET	observed heterozygosity
PBMC	peripheral blood mononuclear cell
PCPA	parachlorophenylalanine
PCR	polymerase chain reaction
PCP	phencyclidine
PDD	pervasive developmental disorder
Phe	phenylalanine
pgk	phosphoglycerate kinase
PKA	protein kinase A
PKC	protein kinase C
PMA	phorbol-12-myristate-13-acetate
pmol	picomol
Pol II	RNA polymerase II

PPI	prepulse inhibition
PredHET	predicted heterozygosity
pre-miRNA	precursor micro ribonucleic acid
pri-miRNA	primary micro ribonucleic acid
PRODH2	*proline dehydrogenase (oxidase) 2*
PTSD	posttraumatic stress disorder
PVDF	polyvinylidene fluoride
PVN	paraventricular nucleus
qPCR	quantitative polymerase chain reaction
R^2	R square (coefficient of determination)
RASGRP1	*RAS guanyl releasing protein 1 (calcium and DAG-regulated)*
RELN	*reelin*
REST	*RE1-silencing transcription factor*
RISC	ribonucleic acid induced silencing complex
RLC	ribonucleic acid loading complex
rpm	rounds per minute
RYR3	*ryanodine receptor 3*
SAP	*shrimp alkaline phosphatase*
SCZ	schizophrenia
SCZD10	schizophrenia disorder 10
SDS-PAGE	sodium dodecyl sulfate polyacrylamide gel electrophoresis
SEM	standard error of the mean
Ser	serine
Serpina6	*serpin peptidase inhibitor, clade A (alpha-1 antiproteinase, antitrypsin), member 6, murine*
siRNA	small interfering ribonucleic acid
SLC6A3	solute carrier family 6 (neurotransmitter transporter, dopamine), member 3 (*DAT*)
SLC6A4	*solute carrier family 6 (neurotransmitter transporter, serotonin), member 4*
SLC12A5	*solute carrier family 12 (potassium/chloride transporter), member 5*
SLC12A6	*solute carrier family 12 (potassium/chloride transporters), member 6*
SNP	single nucleotide polymorphisms
SPRED1	*sprouty-related, EVH1 domain containing 1*
SSRI	selective serotonin reuptake inhibitor
STG	superior temporal gyrus
SYNGR1	*synaptogyrin-1*
T	thymine
TCF4	*transcription factor 4*
TDT	transmission disequilibrium test
Thr	threonine

Trp	tryptophan
TRPC1	*transient receptor potential cation channel, subfamily C, member 1*
TRPV4	*transient receptor potential cation channel, subfamily V, member 4*
TSS	transcription start site
TSST	Trier Social Stress Test
U	unit
UBE3A	*ubiquitin protein ligase E3A*
v/v	volume per volume
Val	valine
VMA	vanillylmandelic acid
VMH	ventromedial nucleus of the hypothalamus
VNTR	variable number of tandem repeats
UTR	untranslated region
w/v	weight per volume
w/w	weight per weight
WBP1L	*WW domain binding protein 1-like*
WT	wild type
XPO5	*exportin 5*

1 Introduction

1.1 The short outline on the history of psychiatry from ancient times till present

Disorders that change personal affect and cognition have already been described in ancient times. The ancient civilizations were convinced about the existence of supernatural powers that caused weird behaviors in humans. During the Sumerian, Babylonian and Egyptian Empire, people behaving in an inexplicable and abnormal way from the rest of the society were supposed to be obsessed by demons and handling witchcraft. The western understanding of modern psychiatry is mainly built on the ideas from ancient Greece: the theory of four elements (earth, water, air and fire) which merged into the theory of four body fluids: blood, yellow bile, black bile and phlegm. Hippocrates of Kos (460 – 370 BC) is one of the first physicians that described what we would describe as personality traits nowadays and he had the opinion that each of the basic characteristics of personality traits is caused by one of the four body fluids which is known as the theory of four temperaments (Kapferer and Sticker, 1934). Galen (129 – 199) tried to find the physiological causes for the various human behaviors. Taking into account the four elements, he was convinced that the various human traits are caused either by a balance or an imbalance of those. He invented four categories where the personality traits were allocated to: choleric, sanguine, melancholic and phlegmatic (Linacre and Payne, 1881). From ancient times onwards until the 19th century, due to the dominance of Christianity, most of the persons suffering from delusions or insanity had to undergo exorcism and if this did not bring the expected result, they were mostly considered to be completely obsessed by the devil itself and thus, they were either locked up in "lunatic asylums" which resembled rather a prison than a mental institution or even executed in inquisition-like trials (Catholic Church, 1995; Given, 2001; Mackay *et al.*, 2006). The era of Enlightment mainly in the end of the 18th century opened a new perspective on the "mentally ill", so that physicians started to think about professional care and therapies and that the still predominant conception of being obsessed by demons started declining. In the 19th century in Europe, physicians started to deal actively with the affected persons and developed concepts about the etiology of phenomena such as mania and delusions, which can be considered as the

attempt to categorize abnormal behavioral characteristics into entities. Jeanne Etienne Dominique Esquirol (1772 – 1840) founded the concept of monomanias, where single behavioral characteristics were classified based on external properties that the patient showed (Esquirol, 1838). In parallel, the concept of "phrenology" was introduced by Franz Joseph Gall (1758 – 1828). The concept of phrenology encompassed the conception of the human brain as the organ of the mind and especially, certain brain areas could be allocated to personal traits and characteristics (Simpson, 2005). The term "psychiatry" was introduced by Johann Christian Reil (1759 – 1813) and mentioned 1808 in his article "*Beyträge zur Beförderung einer Kurmethode auf psychischem Wege"* (Marneros and Pillmann, 2005; Marneros, 2008). He assumed that there were physical and mental factors that lead to disorders such as mania and delusion. In 1860, the term "démence précoce", a disorder that predominantly affected young men and led to deterioration and mental disability, was introduced by Bénédict Augustin Morel (1809 – 1873) (Morel, 1860; Noll, 2007). The first classification system on mental disorders was founded by Karl Ludwig Kahlbaum (1828 – 1899). He grouped mental disorders according to course and outcome and defined the syndrome of "catatonia", which is mainly characterized by psychomotoric effects and depression as well as anxiety-like behaviors (Kahlbaum, 1874). His associate Ewald Ecker (1843 – 1909) described and defined hebephrenia ("dementia hebephrenica") (Hecker, 1871) and cyclothymia (Hecker, 2003) during the 1870s, both disorders were the patient mainly shows changes in personal affect. During the 19th century, two major concepts about psychopathology and psychiatry evolved. The "unitary psychosis" concept claimed that all kind of psychiatric disorders are based on common roots and etiology and psychiatric disorders should be considered as a mosaic of single mental patterns. Kahlbaum and Heckel argued against this concept based on their own studies. The valid system on the classification on psychiatric disorders was defined by Emil Kraepelin (1856 – 1926), who is also considered to be the founder of modern psychopathology and who introduced the concept of "dementia praecox" as an entity of diverse psychotic disorders that were previously described by Morel and Kahlbaum. He considered deteriorations and social retraction as a kind of "premature dementia" and delivered the concept of a dichotomy of mental illnesses: manic depression and dementia praecox. Eugen Bleuler (1857 – 1939) revised the "dementia praecox" concept and introduced the term "schizophrenia" in 1911 as well as the term "autism". Bleuler considered the autistic phenotype as a kind of basic symptom of schizophrenia itself, although these patients were mainly characterized by social retraction and a narcistic-like behavior

(McGlashan, 2011). Several different clinical concepts have evolved during the research history on mental disorders to explain their etiologies. The most accepted concept on the etiology of mental disorders is mainly based on neurobiological fundaments. In 1950, Kurt Schneider (1887 – 1967) published his work "Klinische Psychopathologie" which delivered the fundament for the development of the ICD-10 and the DSM-IV diagnostic and statistical manuals (Schneider, 1992).

One of the pioneers on the neurobiological concept of the etiology of mental disorders was Carl Wernicke (1848 – 1905), who is mainly known for his work on brain anatomy. Due to his extended work on neurological diseases ("Lehrbuch der Gehirnkrankheiten") and his research on brain pathology, he also published studies about etiology of psychiatric disorders ("Geisteskrankheiten") (Wernicke, 2007). His student Karl Kleist (1879 – 1960) extended Wernicke's work and is most famous for his studies on "cycloid psychoses" describing the alternation of acute mental disorder state like mania and a long lasting remission phase (Kleist, 1928). Karl Leonhard (1904 – 1988), following the tradition of Wernicke and Kleist, developed the all-time mostly differentiated classification system on mental disorders according to nosological criteria with special dedication to endogenous psychoses (Leonhard and Beckmann, 1999). In the classical German psychiatry, the "schizophrenic" and the "manic-depressive affective" disorders are considered to be endogenous psychoses. Meanwhile, the term endogenous psychosis is not internationally accepted because of its intrinsic problem of hermeneutics and the dogmatization that psychoses are not exogenically triggered. In his publication "Allgemeine Psychopathologie", Karl Jaspers (1883 – 1969) questioned the differentiation between exogenous and endogenous psychoses and criticizes the exclusivity of the endogenous psychoses concept (Jaspers, 1973). Due to the ambiguity of the endogenous psychoses concept, the ICD system does not include these diagnoses (solely endogenous depression). The unitary psychosis concept ("Einheitspsychose") defines endogenous psychoses as a continuum of similar disorders (schizophrenia, depression) with similar causes within an individual. The interpretation according to Wernicke-Kleist-Leonhard is mostly focused on different etiologies and hence, different progression of individual mental disorders. The most recent findings in research on mental disorders seem to confirm the fact that nosology and etiology of mental disorders are of overlapping character, based on both environmental and genetic factors.

1.2 Main characteristics of schizophrenia, bipolar disorder, periodic catatonia (SCZD10) and autism

Schizophrenia (ICD-10 F20.0 – F20.9) is characterized by a combination of symptoms that are grouped into positive and negative ones. During their occurrence, positive symptoms are very obvious, whereas negative symptoms are characterized by behaviors of decreased mental and physical activity. The positive symptoms include disorganized behaviors, delusions and psychomotoric phenomena. The negative symptoms appear depression-like with decreased affect, poverty of speech and impairment of formal thinking. Schizophrenia is not an entity but it forms a spectrum, which can be subdivided into three main branches according to Kraepelin: paranoid-hallucinatory, hebephrenia and catatonia. The paranoid-hallucinatory form of schizophrenia is mainly characterized by its very prominent occurrence of delusions and hallucinations in the acute phase. Patients with hebephrenic schizophrenia mostly appear highly disorganized and reveal low-modulated mood phases. The latter of the three types, the catatonic schizophrenia subtype, becomes apparent by the patients' psychomotor disturbances, including stupor, catalepsia, mutism and echolalia.

Bipolar disorder (ICD-10 F31.0 – F31.9) belongs to the group of affective disorders where mood variability is prominent. The patients' affect alternates from mania episodes to depressive-like states, occurring once or several times during life. Like patients affected by paranoid-hallucinatory schizophrenia, hallucinations and delusions may occur during the manic episodes. Bipolar disorder symptomatology is also known to be rather diverse and thus, it has become accepted that it forms a spectrum depending on severity and endurance of the symptoms, respectively.

Periodic Catatonia (SCZD10, OMIM #605419) is a subtype of unsystematic schizophrenias according to Karl Leonhard's classification system. The symptoms encompass derangements of facial expression and gestures, ataxia and waxy flexibilities of the body extremities. Patients with SCZD10 reveal hyper and parakinetic movements and during their acute states, suffer from hallucinations and delusions. During the remission phase, symptoms from psychomotoric disturbances remain such as stuporous facial expression and impaired grimacing. The phenotype is highly variable due to the underlying symptomatology.

Autism (ICD F84.0 – F84.5) is a mental disorder, where impairments of social and repetitive as well as stereotypic behaviors are most abundant. Like previously mentioned mental disorders, autism also forms a spectrum with respect to its symptomatology, which is known as autism spectrum disorder (ASD). This mental disorder typically occurs during early childhood (age 2 – 5). Children diagnosed with ASD mostly prefer to stay isolated, are occupied with themselves and avoid interaction with peers. The intellectual abilities are very often also impaired or very specific traits are overdeveloped ("savant").

1.3 Neurodevelopmental hypothesis of mental disorders

There exist various hypotheses to explain the different etiologies and pathogeneses. Most prominent are the dopamine and the glutamate hypothesis especially with respect to schizophrenia, although these hypotheses have also been taken into further consideration for other mental disorders. In fact, these hypotheses deliver a biochemical explanation how the brain in patients diagnosed with a mental disorder is influenced and working. The neurodevelopmental hypothesis can be considered as an attempt to encompass these various hypotheses in one, although its main focus is directed to the development of the nervous system during embryogenesis, childhood and early adulthood. Weinberger and colleagues (1986) reported that problems during neurodevelopment as well as brain abnormalities could deliver an explanation for the etiology of schizophrenia (Nasrallah and Weinberger, 1986; Murray and Lewis, 1988; Murray *et al.*, 1992; Murray, 1994; Owen *et al.*, 2011). In patients with mental disorders, comparative studies revealed slight differences in brain morphology. A review of De Peri and colleagues (2012) contains analyses of 45 MRI studies on patients with first-episode schizophrenia and bipolar disorder. There is a significant reduction of grey matter and an enlargement of the lateral ventricles in first-episode schizophrenia patients and a decrease of white matter in bipolar disorder patients (De Peri *et al.*, 2012). Similar results were reported by Nickl-Jockschat and colleagues (2011). Slight morphologic changes identified in the functional cortical areas are linked to language and emotion (Nickl-Jockschat *et al.*, 2011). The prefrontal cortex, which is considered to be the domain of personality, seems to undergo morphological changes as well. Ettinger and colleagues (2011) describe a reduction of grey matter especially in the medial prefrontal, orbitofrontal and the temporal regions (Ettinger *et al.*, 2011). Brain anomalies indeed seem to be a major indicator of mental

disorders. In patients diagnosed with autism, the growth of skull and head circumference is increased (Saitoh and Courchesne, 1998; Courchesne *et al.*, 2007). A multicenter MRI study on 89 autists with various grade of symptom severity revealed various grey and white matter aberrations in cerebellum, amygdala, cingulate cortex and the lateral prefrontal brain areas, which are correlated with symptom severity (Ecker *et al.*, 2012).

Mental disorders form spectra with partially overlapping symptomatologies, thus enabling to extend the neurodevelopmental hypothesis for schizophrenia to other mental disorders. The core ideas of this hypothesis are related to interconnectivity of the different brain areas on the macroscopic level and on neuronal migration and axonal guidance. Altered interconnectivity of brain areas in mental disorder patients in comparison to controls was shown in fMRI studies. A review by Minshew *et al.* (2010) summarizes that in patients diagnosed with autism, the interconnectivity between the frontostriatal areas of cognitive control and the anterior cingulate gyrus are significantly reduced (Minshew and Keller, 2010). Impaired interconnectivity of prefrontal cortical areas and limbic system has been reported in studies on schizophrenia and bipolar disorder (Calhoun *et al.*, 2011; Cerullo *et al.*, 2012), major depression disorder (Hasler and Northoff, 2011) and attention-deficit hyperactivity disorder (Posner *et al.*, 2011; Tomasi and Volkow, 2012). The time of onset of mental disorders is another indication that supports the neurodevelopmental hypothesis. Usually, affective and non-affective mental disorders occur accumulated between the second and the third decade of life. In autism, it even occurs during childhood. Neurodevelopment is a process known to be plastic and mostly adaptive during early childhood and young adulthood. Therefore, the neurodevelopmental hypothesis delivers a good model for explanation of these disorders in combination with environmental factors such as early-life stress as well as physical and psychological violence during early life.

1.4 Biopsychosocial factors trigger the onset of mental disorders: gene – environment interaction

Mental disorder usually cannot be reduced to single pathogens or noxa that cause their onset. In fact, the etiology of mental disorders underlies multifactorial influences, which is expressed by the term “biopsychosocial”. In the previous chapter, it was elucidated that both genetic and environmental factors in a certain composition are necessary to evoke their onset.

Among the environmental factors, chronic physical as well as psychological stress is accepted to be one of the main factors. Stress expresses itself in a variable manner and its quantification is difficult to perform. Interindividually, the absolute stress load is experienced differently and thus, coping strategies of individuals vary. The first encompassing theory about environmental and genetic factors was the vulnerability-stress model, also known as diathesis-stress model (Monroe and Simons, 1991; Beurs *et al.*, 2005). The core information of this model is that early life events during childhood and young adulthood such as physical and psychological trauma, violence and neglect favor the onset of a mental disorder in young adulthood. Nevertheless, this model has to be taken with caution as it only suits for affective and non-affective mental disorders that occur during early adulthood. Patients diagnosed with e.g. autism reveal symptoms at a very early age in their lives, typically between 2 and 5 and thus, the impact of environmental factors is supposed to be rather low here. Therefore, since the model was introduced during the 1960s, it has been extended on the fundament of further studies. The biopsychosocial model (Engel, 1977) encompasses biological, psychological and social factors and takes all three factors equally into account for the etiology of mental disorders. The most recent model on the etiology of psychiatric disorders takes three factors into closer account: genetic susceptibility, environmental factors (stress) and social factors (familial environment and partnerships) (Fischer, 1973; Caspi and Moffitt, 2006). All these models are the center of controversy as none of them is able to explain completely the complex mechanisms that underlie mental disorders. However, the biopsychosocial model provides the best approximation to the complexity of psychiatric disorders until now. A lot of studies indicate that the patients' genetics massively influence the disorders' onset and development. A review by Van Winkel *et al.* (2010) summarizes that there exist many susceptibility loci for mental disorders, which are frequently and repetitively identified, mainly localized on chromosome 15q and 22q (van Winkel *et al.*, 2010). Other studies even reveal that traits, which are associated with psychiatric disorders such as extended aggressiveness and drug dependence, are also highly influenced by specific genotypes, mainly in genes that are involved in the neurotransmitter system. A functional polymorphism in the *SLC6A4* gene, the short allele in the promoter of the serotonin transporter gene, increases the vulnerability to depression in its carriers. In the investigated cohort, the carriers that are homozygous for the short version (s/s) of the promoter had a 70 % probability to develop major depression disorder after childhood maltreatment in comparison to the carriers of the long version (l/l), where the probability was only 30 % (Caspi *et al.*, 2003). Family studies

have discovered candidate genes for traits that are common in psychiatric disorders such as impulsive aggression, rage and exhibitionism. A study by Brunner and colleagues (1993) identified five males in a single family that had a point mutation in the monoamine oxidase A *(MAOA)* gene, where cytosine is replaced by thymine (CAG936TAG) and thus leads to a nonsense mutation. The lack of functional MAOA in these individuals (Brunner syndrome, OMIM: #300615) was accompanied by high impulsive behaviors and a remarkable monoamine metabolism with increased concentrations of 5-hydroxyindole-3-acetic acid (5-HIAA) as well as homovanilic acid (HVA) and vanillylmandelic acid (VMA) in their urine samples (Brunner *et al.*, 1993). Animal studies on a monoamine knockout mouse model (*MAOA* $^{-/-}$) showed up to ninefold serotonin concentrations in catecholaminergic neurons as well as cytoarchitectural changes in the rats' somatosensory cortices including an increased aggressive behavior. The administration of the serotonin synthesis inhibitor parachlorophenylalanine (PCPA) reversed all these effects (Cases *et al.*, 1995). A study on humans by Caspi and colleagues (2002) revealed the interplay of *MAOA* in combination with childhood maltreatment and the development of antisocial behavior (Caspi *et al.*, 2002). *MAOA* is the enzyme that catalyzes the oxidation and thus the inactivation of monoamines and catecholamines such as dopamine, adrenaline, noradrenaline and serotonin. Depending on the length of a variable number tandem repeat (VNTR) polymorphism (30 bp in length) in the *MAOA* promoter (Sabol *et al.*, 1998), carriers either show higher or lower antisocial behaviors. Once the *MAOA* VNTR consists of 3.5 or 4 copies, the MAOA efficacy is 2 – 10 times higher than in those carriers that have 3 or 5 copies of that repeat (Sabol *et al.*, 1998). The gene x environment interaction in the study by Caspi displayed a high significance of antisocial behaviors after childhood treatment in the low-MAOA activity group in comparison to the high-MAO activity group, 85 % of the mistreated children with a low-MAOA activity developed antisocial behavior later on (Caspi *et al.*, 2002). The abundance of distinct genotypes in another candidate gene, the catechol-o-methyltransferase (*COMT*), has been implicated in the development of psychiatric disorders. A single-nucleotide polymorphism (SNP) that either codes for G or A leads to an amino acid exchange (Val158Met). The protein containing the valine at this position reveals a higher enzyme activity due to higher thermostability in comparison to the methyl variant. As COMT is highly expressed in the frontal lobes the two different protein variants are supposed to have tremendous effects on personality traits. A gene by environment interaction study of Caspi and colleagues (2005) implicated that this variant is of special interest in people abusing cannabis, as carriers of the

homozygous valine variant were ten times more likely to exhibit schizophrenic symptoms in comparison to the homozygous methionine variant carriers (Caspi *et al.*, 2005). Fan and colleagues (2005) conducted an association study and a meta-analysis on 862 schizophrenic Han Chinese and 928 non-psychiatric controls. The meta-analysis did not result in an association of the Val variant, neither in the Asian population nor in the European. The Val allele of *COMT* could also not be associated with schizophrenia in Ashkenazi Jewish and Irish subjects (Williams *et al.*, 2005). In spite of these findings, Craddock *et al.* (2006) emphasize in their review that the *COMT* gene remains anyhow in focus of enduring schizophrenia research as aside from the Val158Met variant, there exist other functional variants. As this gene is immediately involved in the degradation of catecholamines, it perfectly serves the hypothesis of enhanced dopaminergic neurotransmission in schizophrenia (Craddock *et al.*, 2006).

1.5 Chronic stress deregulates the hypothalamus-pituitary-adrenal gland (HPA) axis and triggers the onset of psychiatric disorders

Aside from genetic factors, environmental and social factors tremendously favor and modify the onset of mental disorders. Chronic stress is considered to be the major actuating variable. In 1936, Hans Selye (1907 – 1982) defined the term “stress” and in 1946, he defined the “general adaptation syndrome” that humans develop consequently to permanent stressors such as low and high temperature, hunger, thirst or psychological stress. Selye distinguished three steps: at first, the body shows an “alarm state”, which enables the body to elicit energy and to enable the flight, fright and fight mechanism. If the influence of stressors continues, the body reaches the “resistance state”, where secondary effects occur such as ulcers in stomach and duodenum. The last step is the “exhaustion state”, where the body is not able anymore to cope with the stressors. The cortex of the suprarenal gland grows and further secondary diseases such as chronic hypertension, enlargement of heart ventricles and diabetes mellitus occur, which in the worst case can lead to death (Selye, 1946, 1974).

The HPA axis is the neuroendocrine system in higher mammals, which is immediately responsible for acute and chronic stress reactivity of the body. It is a regulatory circuit (feedback system) that contains several distributed endocrine hormone glands. The release of

one hormone is dependent on the other glands' hormone secretion. A part of the hypothalamus, the paraventricular nucleus (PVN), synthesizes the peptides corticotropin-releasing hormone (CRH) and vasopressin (AVP). These hormones stimulate the synthesis of adrenocorticotropic hormone (ACTH) in the anterior lobe of the pituitary gland. The ACTH itself stimulates the synthesis and secretion of glucocorticoids in the adrenal gland, mainly cortisol in humans and corticosterone in rodents. The high abundance of cortisol results in a negative feedback cycle on the anterior lobe of the pituitary gland and moreover on the PVN, hence decreasing the CRH and ACTH production (Chrousos, 1998; de Kloet *et al.*, 2005).

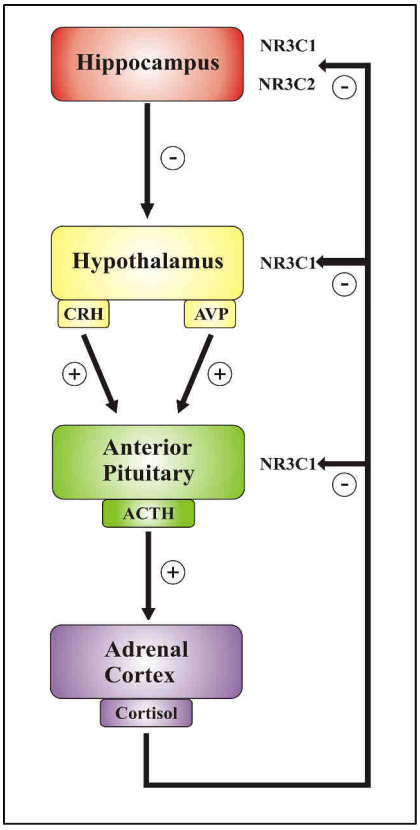

Figure 1.1: Schematic overview over the HPA axis and the hormonal feedback regulation system.

Cortisol as the major effector molecule of stress response is a steroid hormone, which is synthesized from cholesterol and consists of four cycloalkane rings. Three of these rings have cyclohexane (A-C) and one cyclopentane (D) structure and are immediately connected to each other. At position 11 of ring C, cortisol carries a hydroxyl group. The addition or cleavage of the hydroxyl group at position 11 is catalyzed by the enzyme 11-β-hydroxysteroid

hydrogenase (11β-HSD) in the liver, thus leading to physically active cortisol (addition of hydroxyl group) or physically inactive cortisone (cleavage of hydroxyl group). The concentrations of cortisol in the blood follow both a pulsatile and diurnal rhythm. Its concentration is usually the highest around 8:00 to 09:00 a.m., a phenomenon called cortisol awakening response (CAR). The cortisol level reaches its highest concentration 20 to 45 minutes after awakening in 50 % of investigated people (Wust *et al.*, 2000). The CAR follows a diurnal rhythm, which is stimulated by the suprachiasmatic nucleus (SCN), a region in the brain controlling circadian rhythms (Fries *et al.*, 2009) and it increases once the persons wake up in light around 800 lux in the morning (Scheer and Buijs, 1999). The highest level of cortisol in the morning declines over day to a minimum around midnight, whereas glucocorticoids such as cortisol are released in an approximately hourly rhythm (Lightman *et al.*, 2008). This rhythm consequently triggers the expression of the glucocorticoids' target molecules, the glucocorticoid receptor (*NR3C1*) and the mineralocorticoid receptor (*NR3C2*). Steroid hormones such as cortisol and corticosterone are highly lipophilic; hence they are highly insoluble in blood and further hydrophilic media. Their transport to their target organs is enabled by transport globulins such as serpin peptidase inhibitor, clade A (alpha-1 antiproteinase, antitrypsin), member 6 (*SERPINA6*), also known as corticosteroid binding globulin (*CBG*) and by serum albumin. Once the target organ is reached, cortisol dissociates from SERPINA6, permeates the cell membrane and binds to NR3C1 or NR3C2, stimulating them to homodimerize (de Kloet *et al.*, 2005). The dimers interact with transcription factors and other multiple co-regulators. This complex permeates into the nucleus of the cell, where it preferably targets glucocorticoid response elements (GREs) and thus, activating transcription of stress-associated genes, increasing gluconeogenesis and inducing anti-inflammatory effects. Chronic stress facilitates the disruption of the fine-tuned feedback mechanism leading to a disorder called Cushing's syndrome (ICD-10 E24) ("hypercortisolism"), which is characterized by permanently elevated cortisol levels after the dexamethasone suppression test. The cardinal symptoms of this disorder are swelling of the face, hyperhidrosis, central obesity and skin atrophy. Furthermore, psychiatric-like traits are likely to occur such as euphoria, depression and anxiety (Wolkowitz *et al.*, 2009; Pereira *et al.*, 2010; Sonino *et al.*, 2010). The equivalent disorder to hypercortisolism is hypocortisolism, known as Addison's disease (ICD-10 E27.1) or "primary adrenocortical insufficiency". In most of the cases the patients suffer from an autoimmune disease, where the body has generated antibodies against the cortisol-producing cells in the zona fasciculata of the adrenal cortex. The main symptoms

of Addison's disease are fatigue, nausea, vomiting, and hypotension that very often leads to an exaggerated demand for sodium chloride in food.

Patients suffering especially from psychiatric disorders in the affective spectrum like bipolar disorder, ADHD, eating disorders, social phobia and post-traumatic stress disorder are known to report either extreme single or chronically stressful life events before the onset of their disorder (Hudson *et al.*, 2003; Hillegers, 2004). Furthermore, these disorders show familial aggregation, which supports the idea of a high heritability. To date, there is no clear mechanism known how much "stress" is needed to elicit a psychiatric disorder because quality and quantity are difficult to judge. The disorder that shows the best correlation of stressful single or chronic life events to its development is PTSD. PTSD is characterized by the inability of the patients' limbic system to facilitate fear extinction. Typically, patients underwent extreme stressful life events, such as the loss of comrades and colleagues during war battles or rescue operations as they occur during war or terror attacks. It is reported that a modulator of the *NR3C1,* called *FKBP5,* seems to predispose for PTSD risk in survivors of the World Trade Center Terror attacks (Sarapas *et al.*, 2011; Yehuda *et al.*, 2011) and for PTSD after childhood trauma (Binder *et al.*, 2008; Binder, 2009). Patients diagnosed with PTSD show an increased response after the dexamethasone suppression test (Yehuda *et al.*, 2002; Yehuda *et al.*, 2004) and elevated levels of CRH in the blood (de Kloet *et al.*, 2008). Yehuda and colleagues (2001) are convinced that the strong effect of the dexamethasone suppression test is due to an enhanced negative feedback by cortisol and an increased sensitivity of NR3C1 (Yehuda, 2001). Aside from the massive environmental effect that evokes PTSD, it is also supposed to be highly heritable. A twin study on 4,042 monozygotic and dizygotic Vietnam era veterans revealed that monozygotic twins show a higher avoidance of combat exposure than dizygotic twins (True *et al.*, 1993). The example of anxiety disorders, especially PTSD, demonstrates that environmental and genetic factors either contribute to their etiology or act in a protective manner.

1.6 Mental disorders follow a complex inheritance mode but in rare cases they appear to accumulate in multiplex families

Mental disorders are supposed to be caused by multiple factors (Kato, 2007; Nothen *et al.*, 2010). On the one hand, environmental factors such as stressful life events seem to trigger their onset. On the other hand, multiple genes seem to be causative for their etiology and pathophysiology as mental disorders usually do not accumulate within families. Conservative estimations predict a lifetime prevalence of about 0.3 % to 1 % in the worldwide population, depending on which kind of mental disorder (Bhugra, 2005; Fombonne, 2003, 2009; Perälä *et al.*, 2007; van Os and Kapur, 2009). Twin studies on monozygotic twins reveal that schizophrenia and bipolar disorder show a concordance rate of up to 85 %, whereas in dizygotic twins it is about 15 % (Cannon *et al.*, 1998; Sullivan *et al.*, 2003; Perälä *et al.*, 2007; Edvardsen *et al.*, 2008;). These values indicate that mental disorders indeed seem to have a genetic component, especially once the individuals share common genes as monozygotic twins. Nevertheless, regarding the heritability values for dizygotic twins it becomes evident that environmental factors play a major role in the onset of mental disorders.

To date, no single causative gene for mental disorders is clearly known. However, many family and population based studies have been accomplished to find causative variants or genes for their etiology. There are few studies that report a Mendelian inheritance mode of mental disorders, among those schizoaffective and schizophrenic subtypes (St Clair *et al.*, 1990) and a CAG repeat in a gene that is located on chromosome 22q called synaptogyrin-1 (*SYNGR1*) supposed to cause schizophrenia (Verma *et al.*, 2004). Another study reports the disruption of a lipid transporter gene called *ABCA13*, which was found to be disrupted in a schizophrenic patient and which is supposed to be involved in the etiology of schizophrenia, bipolar disorder and depression (Knight *et al.*, 2009). Aside from these findings, most of the available and recently investigated susceptibility loci were found by family-based and genome wide association studies. Susceptibility loci that contribute to the etiology of mental disorders have been found all over the human genome (1q, 3p, 5q, 6p, 6q, 8p, 10p, 11q, 14p, 15q, 16q, 17q, 18q, 20q, 22q) (Lewis *et al.*, 2003), although some chromosomes appear to be “hotspots” that favor their development, among that chromosome 3p (Knight *et al.*, 1995; Muhle *et al.*, 2004), chromosome 15q (Lewis *et al.*, 2003; Abrahams and Geschwind, 2008b; Abrahams

and Geschwind, 2010), and chromosome 22q (Lasseter *et al.*, 1995; Mowry *et al.*, 2004; Abrahams and Geschwind, 2008a).

1.7 Multiplex families segregating periodic catatonia (SCZD10, OMIM: #605419) reveal susceptibility loci on chromosome 15q and 22q

In this study, multiplex families have been investigated that had been previously diagnosed with a type of unsystematic schizophrenia according to Leonhard's classification system, termed periodic catatonia (Leonhard and Beckmann, 1999). In our previous SCZD10 genome wide linkage study with 356 polymorphic markers in twelve multiplex families comprising 57 patients, we could show that SCZD10 is distinctly inherited within these families. Two chromosomal candidate loci were detected on chromosome 15q14 (confirmed) and chromosome 22q13.33 (suggestive) by non-parametric linkage (NPL) analyses (Stober *et al.*, 2000). In a second genome wide linkage analysis with four multiplex families containing 21 SCZD10-affected individuals, the chromosome 15 locus was confirmed and the borders refined to an 11 cM region between microsatellite markers D15S1042 and D15S659 (Stober *et al.*, 2001; Stober *et al.*, 2002). This fine-mapping already excluded several brain-expressed genes such as *SLC12A6* and *RYR3*. By further narrowing down the borders to a 7.7 cM interval on chromosome 15q14-15.1 in these families, the nicotinic α7 receptor gene (*CHRNA7*) was also excluded (Meyer *et al.*, 2002; Meyer *et al.*, 2003) as well as *DLL4* (McKeane *et al.*, 2005). The strong positional candidate genes *SPRED1*, *FAM98B*, *RASGRP1* and *C15orf53* identified in two genome-wide association studies (GWAS) on bipolar disorder (BD) (Ferreira *et al.*, 2008; Smith *et al.*, 2009) are located exactly in the region defined by our SCZD10 families on chromosome 15q14-15.1. Mutational analysis of *SPRED1* additionally excluded this gene to be causative for the etiology of SCZD10, nor being associated with it (Ekawardhani, 2008). The previous findings within the families that support the susceptibility locus on chromosome 15q14-15 in combination with the high and independently generated association signals of a SNP in *C15orf53* evoked the interest to focus on that gene during this thesis. A second genome scan by Stöber and colleagues (2001, 2002) confirmed the previous results and confined the susceptibility regions on chromosome 15q14-15 and chromosome 22q13.33 (Stober *et al.*, 2001; Stober *et al.*, 2002). The susceptibility region on chromosome 15q14-15 has been further confined (Ekawardhani, 2008), leading to a low number of

susceptibility genes on chromosome 15q14-15 including *C15orf53,* which is further investigated in this study.

Meyer and colleagues (2001) identified a variant in the gene *MLC1* (Leu309Met) located on chromosome 22q13.33 segregating with SCZD10 in a large pedigree (Meyer *et al.*, 2001). Several candidate genes for SCZD10 in this chromosomal region have already been excluded (Realmuto and August, 1991; Ekici, 2004; Ekawardhani, 2008). One of these potential candidate genes is *BRD1,* which had been associated with schizophrenia and bipolar disorder. This gene was first cloned and described by McCullagh and colleagues (McCullagh *et al.*, 1999). Immunohistochemical characterization of this gene resulted in an expression in almost all human tissues but especially high abundance in oligodendrocytes and astrocytes (Bjarkam *et al.*, 2009). The same group that had previously investigated the Faroese sample on common haplotypes on chromosome 22q in bipolar patients did an association study encompassing five genes in this area in a case-control design with 162 bipolar disorder patients, 103 schizophrenia patients and 200 controls (Jorgensen *et al.*, 2002). The gene *BRD1*, supposedly acting as a regulator of transcription, showed association with both disorders at SNP rs138880 ($p = 0.0046$) (Severinsen *et al.*, 2006). Investigations of this SNP in our families showing linkage to chromosome 22q13.33 did not reveal any association with SCZD10 (Ekawardhani, 2008), hence excluding *BRD1* as a candidate gene in our families. Further evidence is provided with the finding that SNPs of *BRD1* and *MLC1* did not show a significant LD in their samples (Severinsen *et al.*, 2006). Kushima and colleagues (2010) additionally excluded *BRD1* as a candidate gene in their sample. They accomplished an association study of ten SNPs located in *BRD1* in a Japanese cohort consisting of 626 schizophrenia patients and 770 controls and additionally, the mRNA levels of *BRD1* based on lymphoblastoid cell lines derived from 29 cases and 30 controls. None of the SNPs showed association with schizophrenia (SCZ) and the mRNA levels of *BRD1* did not significantly differ between cases and controls (Kushima *et al.*, 2010). A replication analysis using a combined caucasian sample from Denmark and Great Britain with 490 BD patients, 527 SCZ patients and 601 controls confirmed the results of the study by Severinsen and colleagues (2006) and found in total five SNPs significantly associated with SCZ but not with BD (Nyegaard *et al.*, 2010). However, the negative findings in our families excluded *BRD1* as a candidate gene for SCZD10. In 2000, Yagi and Takeichi hypothesized the implication of cadherin molecules, which are responsible in cell-cell interaction and communication in neurological and psychiatric disorders (Yagi and Takeichi, 2000). The gene *CELSR1*, which is

responsible for cell-cell interactions in cadherin domains, was considered to be a candidate gene in our families due to its location within the susceptibility locus on chromosome 22q13.33. The murine orthologue *Celsr1* shows expression in the CNS, namely developing brain, choroid plexus, spinal cord, area postrema and ependymal cell layer (Hadjantonakis *et al.*, 1997). Mutational analysis of *CELSR1* in two SCZD10-affected family members from a family supporting locus 22q13.33 and three controls did not reveal any mutation, which excluded *CELSR1* as a candidate gene for SCZD10 in our family (Gross *et al.*, 2001). In conclusion, the linkage study by Savira Ekawardhani (Ekawardhani, 2008) and the exclusion of candidate genes of previously listed candidate genes in the 22q13.33 locus (Gross *et al.*, 2001; Ekici, 2004) directed our interest on *MLC1* as a putative candidate gene for the etiology of SCZD10.

1.8 *MLC1* mutations cause megalencephalic leukoencephalopathy with subcortical cysts (MLC)

Independently from our study, the locus $22q_{tel}$ had already been found in linkage study on MLC accomplished with ten consanguineous families and three families with no known relationship. The linkage interval is located between the polymorphic markers D22S1161 (centromeric) and n66c4 (telomeric), including *MLC1* (Topçu *et al.*, 2000). Furthermore, Leegwater and colleagues (2001) reported a linkage analysis on 16 MLC-affected patients from 11 families of different ethnic origin with linkage between the MLC affected patients and chromosome $22q_{tel}$ (Leegwater *et al.*, 2001). The autosomal recessive inherited syndrome MLC (OMIM: *605908), also known as Van-der-Knaap disease (van der Knaap *et al.*, 1995), is characterized by a megalencephaly and cerebral leukoencephalopathy including ataxia, spasticity, seizures as well as delayed motor development and mental retardation, which is caused by numerous nonsense, missense and splicing mutations (Leegwater *et al.*, 2001; Leegwater *et al.*, 2002; Ben-Zeev *et al.*, 2002; Wang *et al.*, 2011; Yüzbaşioğlu *et al.*, 2011). 80 % of patients diagnosed with MLC show mutations in *MLC1,* whereas 20 % do not show any in this gene (Blattner *et al.*, 2003; Patrono *et al.*, 2003; Boor *et al.*, 2006). The fact that mutations and polymorphisms in *MLC1* have been identified both in MLC as well as in SCZD10 makes it a candidate gene for the development of neurological as well as neuropsychiatric disorders.

1.9 SCZD10 (periodic catatonia): an entity on its own in psychiatric classification?

The term "SCZD10" already points to a relationship with schizophrenia, although there is high evidence that it is not legitimate to merge these diagnoses without restrictions. Most recent studies have shown that there is high overlap of symptomatology and etiologies among mental disorders (Fallin *et al.*, 2005; Carroll and Owen, 2009; Millan *et al.*, 2012). The application of ICD criteria would most likely give both BD and SCZ as the equivalent diagnosis for SCZD10 (Taylor and Fink, 2003). This observation has already started a scientific discussion, if SCZD10 is an own psychiatric category instead of a symptom amongst other mental disorders. In their most recent reviews, Fink and colleagues (2009, 2010) argue that SCZD10 should be considered as an entity on its own in the psychiatric classification system. It occurs in multiple mental disorders, among SCZ and BD having its own specific and characteristic symptomatology (Fink and Taylor, 2009; Fink *et al.*, 2010). Further emphasis is given by an example of a single patient, who had had multiple diagnoses on mental disorders (MDD, schizoaffective disorder, adjustment disorder, PTSD, selective aphasia, alcohol abuse) and who was finally also co-diagnosed with SCZD10 (Carroll *et al.*, 2011).

1.10 Candidate genes for SCZD10, BD and ASD: *C15orf53* (Chr. 15q14), oxytocin receptor (*OXTR*, Chr. 3p25) and *MLC1* (Chr. 22q13.33).

C15orf53

The further interest in the gene *C15orf53,* which is located on chromosome 15q14 in the human genome, is based on coinciding findings: 1.) the genome-wide linkage studies in our families segregating SCZD10 pointed to a susceptibility locus in this genomic region, which was further confined in our group, and already excluded strong candidate genes such as *CHRNA7* (Meyer *et al.*, 2002; Meyer *et al.*, 2003) *DLL4* (McKeane *et al.*, 2005), *SLC12A6*, *RYR3* and *SPRED1* (Stober *et al.*, 2000, 2001, 2002; Ekawardhani, 2008); 2.) two genome-wide association studies on BD in European American and African American individuals mapped to *C15orf53* as a susceptibility locus for BD and hence directed our attention to this

gene (Ferreira *et al.*, 2008; Smith *et al.*, 2009); 3.) this gene has an unknown function and has not yet been investigated in psychiatric disorders. *C15orf53* encompasses 3.44 kb in the human genome and the only identified transcript is 2,043 bp in length. It is putatively a protein coding gene resulting in a protein with 179 AA. None of the transmembrane prediction tools predicted a transmembrane domain and thus, it is considered to code for a soluble protein (Predict Protein server, http://www.predictprotein.org).

OXTR

Furthermore, the oxytocin receptor (*OXTR*) is investigated in the present study as a putative candidate gene that is supposed to increase the susceptibility for the etiology of ASDs. One of the main symptoms in ASDs is the decreased ability of social interaction and impaired social bonding. As the nonapeptide oxytocin, also known as "trust and love hormone" (Kosfeld *et al.*, 2005), acts through its own receptor (*OXTR*), genetic variations in that specific gene have been associated with ASD. Like CRH, oxytocin is mainly synthesized in the PVN, a part of the hypothalamus. A small share of oxytocin is produced in the SCN. Unlike CRH, oxytocin is transported via the blood stream to the neurohypophysis ("posterior pituitary gland") in the Herring bodies (Jirikowski *et al.*, 1990). It is released on demand into circulation and reaches targets all over the body (Lee *et al.*, 2009). Oxytocin binds to OXTR and elicits parturition, lactation and social bonding between mother and child (Lee *et al.*, 2009; Ebstein *et al.*, 2009) and has been found to improve symptomatology once administered intranasally or intravenously into humans (Hollander *et al.*, 2007; Bartz and Hollander, 2008; Guastella *et al.* 2010). Levels of oxytocin in the cerebrospinal fluid are known to change in affective disorders. A study by Scantamburlo *et al.* (2007) found an increase of oxytocin-producing cells in the PVN in human *post-mortem* tissue and they identified a negative correlation of oxytocin levels and the severity of major depression symptoms (Scantamburlo *et al.*, 2007). As oxytocin is the facilitator of trust and social bonding between individuals, it has also been implicated in the fine-tuning of the HPA axis and coping of individuals with psychosocial stress. In a placebo-controlled double-blind study, 37 healthy men underwent the Trier Social Stress Test (TSST) (Kirschbaum *et al.*, 1993), which is an internationally accepted model for acute psychosocial stress in a lab setting. Fifty minutes prior to the onset of stressors, the participants (n = 37) received either intranasal oxytocin or a placebo. The salivary cortisol levels were significantly decreased after stress in comparison to the placebo group, thus

supporting its therapeutic abilities for coping with stress (Heinrichs *et al.*, 2003). *OXTR* is located on chromosome 3p25 in the human genome with a genomic size of 19.22 kb. The major variant of *OXTR* consists of 4 exons; the predominant transcript has a size of 4,364 bp and codes for a protein consisting of 389 amino acids (AA). The first two exons are non-coding, the translation start site (ATG) is located in exon 3 (Inoue *et al.*, 1994). OXTR is expressed in the periphery of the body (uterus, kidney, ovary, testis, thymus, heart, vascular endothelium, myometrium of the uterus and mammal glands) and the central nervous system (Gimpl and Fahrenholz, 2001; Zingg and Laporte, 2003). The rat orthologue of the human *OXTR* gene (92 % AA homology, Uniprot.org) shows the highest expression in the limbic system, especially in the amygdala and the ventromedial nucleus of the hypothalamus (VMH), both mediators of anxiety and sexual behaviors (Bale *et al.*, 2001). Urinary sample assays from children that have been suffering from severe social deprivation (n = 21) and have grown up in orphanages compared to controls had half the oxytocin levels than children that had no history in social deprivation (Wismer *et al.*, 2005). Intranasal application of oxytocin in an fMRI study reduced the activation of bot amygdala and of brain areas that are involved in the manifestation of fear in 15 healthy males in a double-blind crossover trial (Kirsch *et al.*, 2005). These data underline the importance of oxytocin for social bonding. As social bonding is supposed to be highly impaired in ASD patients, manifold association studies of *OXTR* with ASD have been accomplished in samples of various ethnicities (Wu *et al.*, 2005; Jacob *et al.*, 2007; Lerer *et al.*, 2008; Liu *et al.*, 2010). Each of the association studies identified different SNPs in *OXTR* associated with ASD, whereas the finding by Lerer and colleagues is the most intriguing one. They investigated 18 SNPs in *OXTR* in 152 ASD patients and found a haplotype consisting of five SNPs (rs237897-rs13316193-rs237889-rs2254298-rs2268494) that was significantly associated with ASD ($p = 0.009$). One study completely opposes the idea of association of *OXTR* with ASD. By allelic expression imbalance assay and the consideration of RNA levels and the genotype in the amygdala, none of the 18 investigated SNPs survived the multiple corrections for association with ASD in a combined sample of 436 individuals (Tansey *et al.* 2010). Further studies elucidated the therapeutic potential of oxytocin. Popik *et al.* (1992) reported that low-dosed oxytocin improve the social cognition in rats in repeated encounters of the oxytocin-receiving animal with those who did not (Popik *et al.*, 1992). Oxytocin is obviously crucial for the consolidation of short-term olfactory memory in rats. Female Wistar rats showed increased exploratory behaviors towards juvenile rats in comparison to those that they previously

encountered; the only condition was that the time delay did not exceed 180 minutes. The application of an oxytocin receptor antagonist (des-Gly-NH2 d(CH2)5[Tyr(Me)2Thr4]OVT) reversed these effects (Engelmann *et al.*, 1998). In another study it was discovered that male oxytocin knockout mice (*Oxt* $^{-/-}$) revealed social amnesia towards conspecifics in their cage. The social memory could be reestablished after intervention with oxytocin (Ferguson *et al.*, 2000). There exists a conditional knockout mouse model of the oxytocin receptor (*Oxtr* $^{-/-}$). The lack of *Oxtr* expression has especially massive effects on the formation of interconnectivity within the central nervous system. From *Oxtr* $^{-/-}$ mice it is reported that they show obvious disabilities to recognize their family members ("social amnesia") and showed increased aggressive behaviors, hence supporting its implication in the pathogenesis of psychiatric disorders such as ASD. Female *Oxtr* $^{-/-}$ mice show impairments in maternal behaviors. They spent significantly less time with crouching over their pups and additionally, the pups are more often scattered around the cage in comparison to WT mice (Takayanagi *et al.*, 2005). Low functioning autistic children that were demanded to speak in public showed increased basal oxytocin levels but normal cortisol levels in comparison to healthy controls (Jansen *et al.*, 2006). Intervention studies of oxytocin in ASD patients demonstrate the positive effects on cognitive abilities. Stereotypies, such as repetitive behaviors, were significantly reduced over time subsequently to four hours of oxytocin infusion in patients diagnosed with Asperger syndrome and autism in comparison to the placebo group. The more often the patients were infused with oxytocin, the better they performed during the repetitive autistic behaviors tests (Hollander *et al.*, 2003). Similar results could be achieved in a further double-blind controlled intervention study on 15 patients, nine diagnosed with Asperger's syndrome and six with autism. The participants either received four hours of oxytocin or placebo infusion. At baseline and continuously each 30 min up to 240 min after intervention start, the comprehension of affective speech was tested. Patients that had received oxytocin performed better in the affective speech test and showed less social retention versus the placebo group (Hollander *et al.*, 2007). The therapeutic implications and their potential in treatment of ASDs have been summarized in a review by Bartz and Hollander (Bartz and Hollander, 2008).

MLC1

In 2001, Meyer and colleagues detected a rare genetic variant (Leu309Met) in the *MLC1* gene, which segregates within an extended pedigree in seven SCZD10-affected members (F21) and which was not found in 327 unrelated controls (Meyer *et al.*, 2001). The affected patients were heterozygous for this mutation (Leu/Met), which led to the conclusion that SCZD10 could be inherited via an autosomal-dominant inheritance mode with variable penetrance. Another study investigating 140 individuals affected by SCZD10 and a further family with SCZD10-affected members revealed two affected patients among the SCZD10 individuals carrying the Leu309Met variant in *MLC1*; this variant did not furthermore segregate among the SCZD10-affected members of the investigated family (Rubie *et al.*, 2003). Despite that, it is still considerable finding as the investigated family in the study by Rubie and colleagues originates from the same local area as those investigated in the studies by Stöber and colleagues as well as Meyer and colleagues. A founder effect is a possibility to explain the abundance of this variant within these families. The genetic variant was transmitted by the father, who had not been previously explicitly diagnosed with SCZD10, yet showing symptoms similar to dementia (Ekawardhani, 2008). Variable penetrance could be an explanation for the transmission of this variant from the allegedly healthy father to his child. Further association and mutation analysis studies on SCZD10, BD and SCZ-affected patients could not identify the Leu309Met variant (McQuillin *et al.*, 2002; Devaney *et al.*, 2002; Jorgensen *et al.*, 2002; Kaganovich *et al.*, 2004). Ewald and colleagues commented the study conducted by Meyer and colleagues in 2001. Although they were not able to identify the Leu309Met variant in any of the investigated persons (80 BD and 84 control patients from Denmark), they emphasized that this variant remains a promising risk allele for SCZ (Ewald and Lundorf, 2002). Furthermore, a protein sequence similarity of *MLC1* with the *potassium voltage-gated channel subfamily A member 1* (*KCNA1*) at about 24 % indicates that MLC1 could possibly function as an ion channel (Meyer *et al.*, 2001; Crespi and Thiselton, 2011). Electrophysiological experiments conducted by Kaganovich and colleagues on MLC1 expressed in Chinese hamster ovary (CHO) cells led them to the conclusion that MLC1 does not show any voltage-gated ion channel activity (Kaganovich *et al.*, 2004). Yet, ion channel activity of MLC1 cannot be excluded for sure. The ion channels KCNA1, which revealed a sequence similarity of 24 % with MLC1, serves as a good example for the complexity of these proteins. KCNA1, a heteromultimer, is highly expressed in the central nervous system. Depending on the target tissue, the KCNA1 channel forms combinations with different

subunits. In three different tissues (white matter, grey matter and spinal cord), the Kv1.1 subunit encoded by *KCNA1* forms oligomeric compositions with further Kv1.x subunits: five in the grey matter, two in the white matter and two within the spinal cord (Coleman *et al.*, 1999). This fact is of special interest since manifold mutations in the *KCNA1* gene have been described to cause a disorder called episodic ataxia, in which patients suffer from stress-induced motor impairments with predominant manifestation during early adulthood (Browne *et al.*, 1994; Browne *et al.*, 1995; Adelman *et al.*, 1995; Comu *et al.*, 1996). The motor impairment as main characteristic in familial episodic ataxia indicates the putative relationship to SCZD10. The different ion channel assembly is linked to altered excitability. Heterologous co-expression of *KCNE4* in Xenopus oocytes and mammalian HEK293 cells has a significant effect on the excitability of KCNA1 heteromeric complexes but none on KCNA1 homomeric ones (Grunnet *et al.*, 2003). In mouse primary hippocampal cultures, there is a clear correlation between days *in vitro* (DIV) and the expression of different Kv1.x subunits (Grosse *et al.*, 2000). At first, KCNA1 is expressed at DIV 10-12, KCNA2 at DIV 12-14 and at DIV 16-20, KCNA1 to KCNA6 are expressed in these primary cultures. Quaternary structural effects also have an impact on the ion-channels' functionality. Adjacent positioning of *KCNA* genes had a significant effect on the activation and inactivation kinetics in comparison to diagonally positioned ones (Al-Sabi *et al.*, 2010). Teijido and colleagues co-expressed MLC1 and KCNA1 due to their sequence similarities in Xenopus oocytes and a HEK293-derived cell line. No ion channel activity could be detected after application of whole-cell patch clamp pulse protocols from -140 mV up to +100 mV. Even after pharmacological intervention which increases cytosolic cAMP, no ion channel activity could be measured (Teijido *et al.*, 2004). Thus, it is very likely that MLC1 needs an interaction partner to assemble in order to receive an ion channel function. One example for that is given by a study of López-Hernández and colleagues (2011). They show that the protein GlialCAM is co-localized with MLC1 in astrocyte junctions and that a mutated version of GlialCAM leads to a disruption of the MLC1-GlialCAM complex (López-Hernández *et al.*, 2011). Perhaps this had been the missing subunit or interaction partner of MLC1 in the electrophysiological experiments by Teijido and colleagues (2007), which had led to a failure of identifying MLC1 ion channel activity. Once known, MLC1 should be investigated in an *in vitro* study focusing on the time course of protein expression in combination with electrophysiological investigation.

The *MLC1* gene produces transcripts of variable length but predominately one of 3,933 bp in size, coding for a protein consisting of 377 AA (Ensembl genome browser, rel. 66). The predominant transcript consists of twelve exons and to date, multiple transcription start sites (TSS) have been identified, although not otherwise specified yet. *MLC1* is located on the reverse strand and encompasses a length of almost 26 kb in the human genome. Its implication in the etiology of SCZD10 is supported by the high abundance of this protein in the human brain, especially in glial cells, where it co-localizes with the dystrophin-glycoprotein complex in astrocytic endfeet of the blood-brain-barrier (Teijido *et al.*, 2004; Boor *et al.*, 2005; Ambrosini *et al.*, 2007; Teijido *et al.*, 2007). The identification of two further non-synonymous coding polymorphisms (Arg328His, Leu308Gln) in BD and SCZ patients supports the importance of this gene (Verma *et al.*, 2005). Both mutations are located in the same exon as the one that was found segregating in our families (Leu309Met). Two of these mutations (Leu308Gln and Leu309Met) affect amino acids in immediate vicinity. According to the applied transmembrane domain prediction tool and model, *MLC1* either consists of seven or eight transmembrane domains (Predict Protein Server) consisting of 43.2 % very hydrophobic amino acids (Val, Ile, Leu, Phe, Trp and Cys, PredictProtein Server). In all applied models, the N-terminal and C-terminal region are predicted to be inside the cytoplasm and the Leu309Met variant is located in a predicted transmembrane domain.

The *MLC1* gene has orthologues in a variety of vertebrate species and is highly conserved, whereas it is not present in eukaryotes that do not produce myelin (Boor *et al.*, 2005). The similarity of the human gene with the murine orthologue is 83 % on the nucleotide and 87 % on the protein level (Ensembl rel. 65, December 2011). Investigations on the murine orthologue, *Mlc1*, have shown that its gene expression already starts at early stages of mouse embryonic development. In murine forebrain, midbrain and hindbrain, *Mlc1* expression is detectable at E13 and steadily increases into adulthood. Immunohistochemistry and *in situ* hybridization experiments performed on murine tissues reveal that *Mlc1* is expressed both in the central nervous as well as the peripheral nervous system, with highest abundances in the glial cells (Schmitt *et al.*, 2003), especially astrocytic endfeet (Boor *et al.*, 2007), medulla, dorsal root ganglia, lung, heart (Teijido *et al.*, 2007) and all kind of leukocytes (Boor *et al.*, 2005). Teijido *et al.* (2004) performed an intense biochemical characterization of the murine Mlc1 protein. They showed that Mlc1 assembles oligomers during embryogenesis, which cannot be inhibited even in reducing conditions; Mlc1 has a putative glycosylation site at position Asn136Ala, which was assumed to cause the obvious motility shift in SDS-PAGE.

After Endo F peptidase digestion, no changes occurred in electromotility of Mlc1, which either means that the putative glycosylation site is a false-positive prediction or that different post-translational modifications are responsible to explain this observation. They analyzed, if Mlc1 undergoes post-translational modifications in the endoplasmatic reticulum (ER), a typical procedure for membrane proteins before trafficked to the plasma membrane via the secretory pathway. A retention test was applied to elucidate the cause of oligomerization and if the modification of a retention signal could lead to different biochemical properties of the protein (Berney, 2000). The introduction of an N-terminal retention signal led to a significant reduction of Mlc1 plasma membrane expression. Co-expression of Mlc1 including the retention signal (R5-HAL) with native Mlc1 resulted in a reduced plasma membrane expression. Hence, Mlc1 oligomerizes in the ER and according to the molecular weight detected on immunoblots, with itself (homooligomerization) (Teijido *et al.*, 2004). Mlc1 is already expressed at E13 and predominantly in the complete hippocampus, Bergman glia, but not in oligodendrocytes (Teijido *et al.*, 2004, 2007). This allows two conclusions: 1.) early gene expression during embryogenesis and especially neurogenesis emphasizes the obvious importance of Mlc1 in the central nervous system (CNS), especially the high expression of Mlc1 in the subventricular zone (Schmitt *et al.*, 2003). Since Mlc1 is not expressed in oligodendrocytes, it does not seem to be involved in the development of myelin sheaths in the CNS. High abundance in Bergman glia underlines the putative involvement of this protein in neurogenesis and even perhaps in neuronal guidance (Yamada and Watanabe, 2002). Bergman glial cells are known for their high GABA receptor expression (Riquelme *et al.*, 2002). These receptors are the target sites for benzodiazepine, conveying anxiolysis, muscle relaxation and sedation. Furthermore, the atypical neuroleptic agent olanzapine targets the GABA receptor and possesses its highest affinity to the dopamine receptor D1 (*DRD1*) and the serotonin receptor 3A (*HTR3A*). DRD1 and HTR3A themselves have a modulating effect on the GABA receptor (Bymaster *et al.*, 1996, 1997). The PubMed database (May 2012) contains two pharmacological studies on the treatment of SCZD10: one testing risperidone (Duggal and Gandotra, 2005) and another one testing olanzapine (Guzman *et al.*, 2008). Potentially, there is a connection of *MLC1* and the compound treatment, which has not been elucidated yet. There is a potential link to a protein called doublecortin-like kinase (DCLK). Like *Mlc1*, *DCLK* is also expressed at a very early time during embryogenesis. This protein is responsible for the mitotic spindle integrity during neurogenesis and contributes to neuronal migration (Vreugdenhil *et al.*, 2007). MLC1 is co-localized with aquaporin 4 (AQP4) at

astrocytic endfeet and the blood-brain-barrier (Boor *et al.*, 2005; Teijido *et al.*, 2007). 2.) The biochemical properties of MLC1 indicate that it is either an ion channel or a transport protein. Ambrosini and colleagues (2007) confirmed that MLC1 builds oligomers and that it co-localizes with the dystrophin-glycoprotein complex in astrocytic endfeet, a location for manifold transporters and ion channels (Ambrosini *et al.*, 2007). The immunoreactive band of MLC1 occurring at a molecular weight of 36 kDa disappeared under reducing conditions (dithiotreitol, DTT). Mutational analysis conducted by Duarri and colleagues (2008) on *MLC1* indicated protein misfolding and rapid degradation in the proteasomes (Duarri *et al.*, 2008). In 2009, it was demonstrated that protein kinas C (PKC) and protein kinase A (PKA) activating agents such as phorbol-12-myristate-13-acetate (PMA) and forskolin (FSK) influence MLC1 trafficking in astrocytes. Furthermore, it could be shown that MLC1 gets phosphorylated after post-translational modifications in the ER. The localization of MLC1 is dependent on caveolin 1 (*CAV1*), a marker for detergent-resistant membranes (DRM), which are characterized by extraordinary cholesterol levels and high contents of sphingolipids (Lanciotti *et al.*, 2008). The fact that MLC1 forms several populations of mono and oligomers, which are either present in soluble or insoluble membrane fractions, supports the idea that *MLC1* is a potential ion channel or a transport protein. The membrane protein *SLC12A5*, known as *KCC2*, shows similar biochemical properties. The oligomer of *KCC2* accumulates in the soluble, whereas the monomeric form remains in the insoluble fraction (Hartmann *et al.*, 2009). Further evidence is provided by studies on the dystrophin-glycoprotein complex and especially on one of its proteins named syntrophin, which is as well located in membrane rafts (Song *et al.*, 1996). Syntrophin is responsible for the organization and distribution of ion channels such as the voltage-gated potassium channels (Schultz *et al.*, 1998), brain sodium channels (Gee *et al.*, 1998) and *TRPC1* channels (Vandebrouck *et al.*, 2007). Brignone and colleagues (2011) identified the Na^+-K^+-ATPase as an interaction partner of MLC1. The creation of a hypo-osmotic environment leads to an increase of the MLC1 in the cell membrane and a concomitant overrepresentation of the Na^+-K^+-ATPase (*ATP1A* family) (Brignone *et al.*, 2011). The vacuoles observed in patients affected by MLC can be explained with alterations of mechanisms that regulate both, the osmotic balance and the cell volume. These mechanisms have been described as causative for the pathophysiology of congenital muscular dystrophies (CMD), where aberrations such as vacuoles in the white matter occur (Reed, 2009). Thus, the *ATP1A* family provides ideal interaction partners for co-transfection experiments in astrocytes. Subsequent electrophysiological experiments could elucidate, if

MLC1 reveals transport activity or not. A very supportive experiment correlating MLC1 with vacuoles formation was accomplished by Duarri and colleagues (2011), proposing a new disease model for MLC. The application of small hairpin RNA (shRNA) targeting *Mlc1* transcripts and evoking their degradation led to the formation of vacuoles in primary rat astrocytes (Duarri *et al.*, 2011). Although not yet proven for MLC1, it seems to play a major role in the homeostasis of intra– and extracellular ion concentrations, especially chloride. Patch clamp experiments reveal an association of MLC1 and anion channels; a chloride-free environment and disease-causing mutations in MLC1 lead to electrical inactivity in astrocytes. The same effect was achieved once endogenous MLC1 was downregulated by small interfering RNA (siRNA). Concomitantly, the MLC1 knockdown caused cell swelling, which is a cardinal symptom of MLC (Ridder *et al.*, 2011). The latest study published on MLC1 reports an association of this protein with the transient receptor potential cation channel subfamily V member 4 (*TRPV4*), a nonselective ion channel mainly known in Ca^{2+} signaling and its function in osmotic pressure (Harteneck and Reiter, 2007), and the Na^{+}-K^{+}-ATPase. Mutations in *MLC1*, especially highly abundant ones like Ser280Leu and Cys125Arg, lead to a decreased interaction with the previously described interaction partners (Lanciotti *et al.*, 2012). These and the previously presented data indicate that MLC1 is a "key player" in the osmo-homeostasis of astrocytes and that it is at least a cofactor for the correct function of further ion channels.

These data evoked the interest for further investigation of MLC1 in a transgenic mouse model. The murine *Mlc1* gene is located on chromosome 15E3 and like its human orthologue, the gene consists of 12 exons and the translation start site (ATG) is located in exon 2. The protein size is 382 AA and the sequence identity of the murine and the humane gene on the amino acid level is 87 % (Uniprot.org; Henseler, 2010). Cell culture studies in our facilities on the murine *Mlc1* have revealed an unusual 5'-regulatory structure and the lack of promoter-specific elements (Henseler *et al.*, 2011).

1.11 Non-coding RNAs and their influence in pathophysiology: regulation of microRNAs (miRNAs) in psychiatric disorders

Manifold regulatory mechanisms are embedded in gene expression and protein synthesis. Their effect is mediated by effector molecules such as non-coding RNAs. Among the non-coding RNAs, a new class has recently been identified: so-called microRNAs (miRNAs). Once the first draft of the human genome was published in 2001, researchers were assuming that more than 98 % of the human genome is non-coding. This non-coding DNA was specified as "junk DNA" with so far unknown function (Lander *et al.*, 2001). Especially introns and intergenic DNA were believed to be transcriptionally inactive. In fact, the biggest share of the human genome does not code for proteins but is nevertheless transcriptionally active (Elgar and Vavouri, 2008). Recent Whole Transcriptome Shotgun Sequencing (RNAseq) approaches of the human transcriptome elucidated that 58 % of the transcriptionally active clusters are located in intergenic regions (Sultan *et al.*, 2008). A study by Cawley and colleagues (2004) applying DNA tiling arrays revealed that 36 % of transcription factor binding sites are located 3' to genes and are correlated with non-coding RNAs while only 22 % are located in the 5' area of protein encoding genes (Cawley *et al.*, 2004). The first miRNA ever described was *lin-4* in *Caenorhabditis elegans* (*C. elegans*), which encodes a 22 bp non-coding RNA decreasing the translation of *lin-14* (Ambros, 2011). Another non-coding 21 bp RNA was discovered, *let-7*, which decreases the translation of the *lin-41* mRNA, a gene involved in the morphogenesis of *C. elegans* (Reinhart *et al.*, 2000; Del Rio-Albrechtsen *et al.*, 2006). In 2001, these non-coding RNAs were named miRNAs and bioinformatic analysis confirmed their high conservation in invertebrates and vertebrates (Lagos-Quintana *et al.*, 2001; Lee and Ambros, 2001). The most recent version of miRBase release 18, November 2011, (http://www.mirbase.org), a database for miRNA entries, reports 18,226 entries (precursor miRNAs) expressing 21,643 mature miRNA products in 168 different species. The first version of miRBase was released in December 2002 and comprised 218 entries, release 13 in September 2009 already contained 9,623 entries and within three years, the amount of entries almost doubled up to 18,226 entries in release 18 of November 2011. This underlines the exponential research going on in this area and the obvious necessity of miRNAs in gene regulation across species.

The class of miRNAs is characterized by single stranded molecules with a variable length between 19–25 nucleotides, in average 22 nucleotides, originating from hairpin RNA (Bartel, 2004). The majority of miRNAs are transcribed by RNA polymerase II (Pol II) in the nucleus. This primary transcript with an average length of about 1 kb is called "pri-miRNA" and is a double-stranded RNA molecule with a hairpin-structure carrying a 7-methylguanosine-cap at its 5' terminus and a poly-A-tail at its 3' terminus (Lee *et al.*, 2002). The pri-miRNA is cleaved by the multiprotein complex of RNase II enzyme called Drosha and DGCR8/Pasha leads to a stem-loop structure of about 70 nt, which is called "pre-miRNA" (Lee *et al.*, 2003; Yeom *et al.*, 2006). The pre-miRNA is transferred to the cytosol by Exportin 5 (*XPO5*), a member of the karyopherin family that enables the nucleocytoplasmatic transport (Brownawell and Macara, 2002; Yi, 2003).

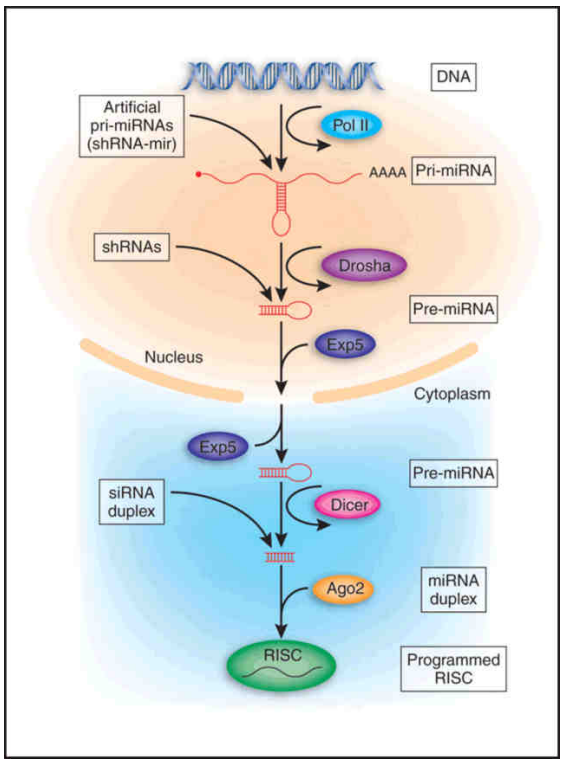

Figure 1.2: Pathway of miRNA biogenesis and processing in vertebrates (Cullen, 2005)

In the cytoplasm, the pre-miRNA is further processed by the class 3 RNase III enzyme called Dicer. This enzyme cleaves the stem-loop resulting in a double-stranded RNA molecule of 21-23 bp in length and two nucleotide 3' overhangs at each end (Zamore *et al.*, 2000;

Bernstein *et al.*, 2001; Vermeulen *et al.*, 2005). Dicer is part of the RNA-induced silencing complex (RISC), a multiprotein complex, in combination with the endonuclease of the Argonaute family (*EIF2C1-4*), although exclusively *EIF2C2* has been reported to be involved in the cleavage of target mRNA (Liu *et al.*, 2004). From the double-stranded RNA, the 5' end with the lowest thermodynamic stability is favored to become the guide strand and is loaded into the RISC (Siomi and Siomi, 2009). The other strand called passenger strand is degraded (Gregory *et al.*, 2005). The RISC complex is assembled by the RISC loading complex (RLC) and this process is responsible for the correct loading of the miRNA (Tang, 2005).

The identification of the target mRNA increases with the degree of miRNA complementarity. The RISC complex, including the guide strand, binds with its seed region at the 5' end of the miRNA (5–8 nt) to the complementary sequence in the 3'–UTR of the target mRNA (Bartel, 2004). The bound miRNA either acts via translational repression or via degradation of the target mRNA, both leading to a less abundant protein concentration (Pillai *et al.*, 2005; Bushati and Cohen, 2007; Bartel, 2009).

Recent research is focusing on the impact of miRNAs in the etiology of psychiatric diseases. It has been reported that approximately 60 % of all protein-coding genes are regulated by miRNAs (Friedman *et al.*, 2008). Especially for the CNS, it has been shown in various studies that miRNAs execute essential regulatory functions in neuronal development and formation. The human brain shows an enrichment of miR-124 and it has been demonstrated that it represses about 200 genes in the brain (Lim *et al.*, 2005). In the brain, miR-124 is involved in the regulation of neuronal precursor fate, meaning the regulation of glial and neuronal gene expression patterns (Krichevsky *et al.*, 2006). During adulthood, some miRNAs are involved in the regulation of synaptic plasticity and circadian rhythm. The most prominent example is miR-134, which has been proven to be a regulator of RNA translation in dendritic spines. The protein kinase Limk1, which controls spine development, is negatively regulated by miR-134. Spine development is one of those mechanisms that are impaired in disorders like Tourette's syndrome and Parkinson's disease (Schratt *et al.*, 2006). Concerning circadian rhythm, miR-132 and miR-219 have been shown to be crucial for proper function. Both of these miRNAs are expressed in the SCN and their transcription is induced by the CLOCK, ARNTL and CREB proteins (Cheng and Obrietan, 2007). The protein FMRP is encoded by the gene *FMR1*. The lack of FMRP protein causes the Fragile X syndrome; it leads to a disturbed function of the RISC-mediated gene silencing and an altered synaptic development

(Jin *et al.*, 2004). Most atypical antipsychotics act on the dopaminergic system with the highest affinity to the dopamine D2 receptor (*DRD2*), although these effects are not very specific. Most of the antipsychotics additionally act on further neurotransmitter systems such as the serotoninergic, muscarinic and histaminergic ones (Meltzer and Huang, 2008). Psychiatric disorders are characterized by dysfunctions in neurotransmitter systems. Due to the effects that atypical antipsychotics have on the improvement in schizophrenic patients, the dopaminergic system is of major research interest despite the fact that negative symptoms are not improved by atypical antipsychotics. Another neurotransmitter system, the glutamatergic system, has attracted notice to researchers of psychiatric disorders. Application of *N*-methyl-D-aspartate (NMDA) receptor antagonists such as phencyclidine (PCP) and MK-801 have been proven to evoke psychosis and cognitive impairment in humans while the NMDA receptor density is lowered in schizophrenic subjects (Pilowsky *et al.*, 2006). A study by Beveridge and colleagues (2010) reported a significant upregulation of the miRNA-15 family in the superior temporal gyrus (STG) of schizophrenic patients, which is predicted to target genes that are implicated in schizophrenia: *BDNF*, *RELN*, *DRD1* and *ATXN2*. In addition, 9.5 % of the miRNAs are upregulated in the dorso-lateral prefrontal cortex (DLPFC) (Beveridge *et al.*, 2010). Perkins and colleagues (2007) investigated *post-mortem* brain tissue of thirteen schizophrenic and two schizoaffective disorder patients. The expression level of 15 miRNAs was lowered in comparison to psychiatrically unaffected control subject *post-mortem* brains (Perkins *et al.*, 2007). Mouse embryonic stem carrying a knockout of the RISC complex gene *DGCR8* revealed that this gene is essential for the processing of pre-miRNAs to mature miRNAs (Wang *et al.*, 2007). This gene is also dysfunctional in a transgenic mouse model from the Karayiorgou lab. They created a mouse model, where the murine syntenic region of the human genomic area 22q11.2 is missing hemizygously. The mouse model reveals increased hyperactivity, poor pre-pulse inhibition and a reduced spine density including an upregulation of pri-miRNAs and a downregulation of mature miRNAs in the murine brain (Karayiorgou *et al.*, 1995; Stark *et al.*, 2008). Some chromosomal regions are considered to be “hotspots” for the susceptibility of neuropsychiatric disorders and other diseases. Aside from chromosome 22q11.2, chromosome 8p has shown up to be a promising susceptibility region for schizophrenia, autism and cancer. In a review by Tabares-Seisdedos and Rubenstein (2009), a CNV hotspot at chromosome 8p21-23 is linked to SCZ. Furthermore, this chromosomal region harbors six miRNAs, among them miR-124 (Tabares-Seisdedos and Rubenstein, 2009). The protein BDNF has been implicated as well in the

etiology of neuropsychiatric diseases (Dwivedi, 2009; Xiu *et al.*, 2009). Mellios *et al.* (2008) discovered two miRNAs in the human prefrontal cortex: miR-30a and miR-195. They both target the 3'-UTR of the *BDNF* mRNA, hence decreasing BDNF expression (Mellios *et al.*, 2008). The gene *MECP2*, whose knockout leads to the Rett syndrome, is also targeted by miR-132. The lack of MECP2 expression thereby leads to an increased expression of the RE1 silencing transcription factor (REST) that itself decreases BDNF expression (Abuhatzira *et al.*, 2007; Klein *et al.*, 2007). These findings support a connection between schizophrenia, Rett syndrome and autism-like phenotypes on the molecular level. Among the various miRNAs, miR-137 appears to be a candidate miRNA because of its implication in neurodevelopment and thus, a possible link to the pathophysiology of mental disorders. In a study on anaplastic astrocytoma in humans it has been shown that some miRNAs are significantly downregulated. In neoplastic brain tissue, miR-124 reveals a 26 fold change and miR-137 a 66 fold change in comparison to non-neoplastic brain tissue (Silber *et al.*, 2008). Smrt and colleagues (2010) report that miR-137 is enriched in neurons and highly expressed in the dentate gyrus and the molecular layer of hippocampi in C57BL/6 mice (Smrt *et al.*, 2010). In mouse embryonic stem cells, miR-137 is mandatory for proper differentiation (Tarantino *et al.*, 2010). In 2011, the most extended GWAS on schizophrenia was published. The stage 1 phase contained 21,856 individuals of European ancestry and the replication sample 29,839 individuals. The analysis of the combined sample including more than 50,000 individuals revealed the strongest signal on rs1625579 within miR-137 ($p = 1.6 \times 10^{-11}$). Four genes, all conferring to SCZ and BD, have reached genome-wide significance (*TCF4*, *CACNA1C*, *CSMD1* and *WBP1L*) and harbor potential miR-137 target sites at once (Ripke *et al.*, 2011). Thus, miR-137 is a potential candidate miRNA that is implicated both in the etiology and modification SCZ and BD. Willemsen and colleagues (2011) investigated five patients with intellectual disability by genome-wide array analysis and found a deletion on chromosome 1p21.3 with an overlapping region in all patients containing the gene dihydropyrimidine dehydrogenase (*DPYD*) and miR-137. Previously, hemizygous *DPYD* deletions have been implicated to cause an autism-like phenotype and speech delay. All five patients revealed a significant decrease of pri-, pre- and mature miR-137 levels (Willemsen *et al.*, 2011). A recent publication has delivered the biological confirmation of the findings by Ripke and colleagues, who had identified five new potential susceptibility loci for SCZ, including miR-137 and four potential target genes. Kwon and colleagues (2011) cloned the 3'-UTRs of the potential target genes (*CSMD1*, *WBP1L*, *CACNA1C* and *TCF4*) into Renilla

luciferase reporter constructs. They overexpressed these constructs either together with a control vector for normalization and an empty construct for internal control. Indeed, all four constructs containing the 3'-UTRs of the predicted susceptibility loci showed a significant decrease in luminescence after miR-137 transfection (Kwon *et al.*, 2011).

In this study, the effects of miR-137 were investigated, as a potential and exclusive target site was predicted within the 3'-UTR of *MLC1*. Due to the unavailability of a suitable antibody to produce illustrative and distinct immunoblots of MLC1, the research focus was directed to the NR3C1 protein. NR3C1 is the major molecule in the conveyance of stress response, shows a predicted miR-137 target site like MLC1 and thus, reveals a possible link of MLC1 and NR3C1 in the pathophysiology of mental disorders.

1.12 Transgenic mouse models are a suitable approach to investigate the etiological mechanisms of mental disorders

The investigation of human diseases in rodent models has proven to be suitable in many cases. This is due to the high genetic relationship between humans and rodents: over 80 % of all genes are highly conserved (Waterston *et al.*, 2002). Knockout mice carry a dysfunctional gene in their genome and the effects on phenotype and behavior can be observed from embryogenesis until adulthood. In addition, mice are handy with respect to genetic manipulation, easy to breed and have a high reproduction rate, which makes them the ideal animal model for behavioral studies. Especially for monogenetic diseases in humans, mouse models have been useful to gain an understanding about aberrant mechanisms that cause the disease: cystic fibrosis, caused by mutations in the *CFTR* gene located on chromosome 7q31.2 (Grubb and Gabriel, 1997; Devuyst and Guggino, 2002), muscular dystrophy Duchenne type, caused by mutations in the *DMD* gene on chromosome Xp21.2-21.1 (Vainzof *et al.*, 2008; Willmann *et al.*, 2009), X-chromosome linked mental retardation such as the Rett syndrome, caused by mutations in the *MECP2* gene located on chromosome Xq28 (Gura, 1999; Guy *et al.*, 2001) and the Fragile X syndrome, caused by trinucleotide expansions in the *FMR1* gene on chromosome Xq27.3 (D'Hulst and Kooy, 2009; Liu *et al.*, 2012).

Psychiatric disorders are considered to be caused in a multifactorial manner. In contrast to monogenetic diseases, more than one gene is involved in the etiology and pathophysiology of

these disorders, which are modified by environmental factors such as daily nutrition and the individual intrinsic stress load. The phenotype of psychiatric disorders is not very specific, on the contrary, there are spectra within the affective and non-affective disorders and the characteristics of the symptoms vary among individuals. Furthermore, animal models show intrinsic limitations concerning behavior and intellectual abilities, as many qualities that are represented in humans cannot be assigned to animals. This includes e.g. suicidality and self-reflection, both traits that are often occurring or aberrant in patients affected by depression or SCZ. Hence, there is no perfect mapping of human traits like "autistic" or "schizophrenic" behaviors in a knockout mouse model, where all kind of human symptoms are equally represented. Takao and colleagues (2007) discuss the general requirements that animal models of psychiatric disorders have to fulfill. They present a "comprehensive behavioral test battery" consisting of 18 items for the investigation of knockout mice and the assignability of these findings to the human situation. Diverse aspects are discussed such as construct, predictive and face validity. "Construct validity" describes the task to find a first rationale link of the cause of a disease in an animal model, meaning the animal pathophysiology should somehow resemble the human one. The term "predictive validity" means that once a specific medical treatment in a particular disease in a mouse model is efficient, its predictive validity is high. The term "face validity" explains how far the animal model mimics symptoms of a specific neuropsychiatric disease, whereas Takao and colleagues admit that this task is the most difficult one to evaluate due to limited assignment between animal models and complex human traits (Takao *et al.*, 2007). Thus, animal models cannot and should not be anthropomorphized to their full range. Nevertheless, psychiatric disorders in humans reveal intermediate phenotypes, which can be modeled in knockout mice. Intermediate phenotypes are traits occurring at a high frequency in affected individuals in comparison to the full symptomatic spectrum. The reduction of the symptomatology of psychiatric disorders to specific traits that are characteristic for a certain disorder enables more focused research. There are various examples for intermediate traits on different levels. In SCZ, many patients show a reduced dopamine release in the prefrontal cortex and an increased volume of the ventricles as well as a reduced prepulse inhibition (PPI). Autists often have a larger brain volume and show low social interaction. Patients with depression are often characterized by increased anxiety and a reduced hippocampal volume (Seong *et al.*, 2002). Candidate genes in humans that are supposed to be involved in the etiology of psychiatric disorders have been predominantly identified by linkage or physiological studies. Modahl *et al.* (1998) measured

the plasma oxytocin level in 29 autistic and 30 normal children and identified a significantly lower plasma oxytocin level in autistic children in comparison to non-affected ones (Modahl *et al.*, 1998). In an oxytocin knockout mouse model (*Oxt* $^{-/-}$), mice lacking the *Oxt* gene were unable to develop social memory in comparison to wild type (WT) mice, a behavior that mimics the autistic phenotype of humans. In schizophrenic patients, the cerebrospinal fluid (CSF) level of cN-CAM, a protein involved in neural cell adhesion and synaptic plasticity, was increased and correlated with ventricle enlargement (Vawter *et al.*, 2001). Mice lacking the isoform Ncam-180 of the gene *Ncam1* revealed increased lateral ventricles and additionally to that, a decreased PPI (Wood *et al.*, 1998). One study with three independent patient samples analyzing linkage disequilibrium (LD) identified the *PRODH2* locus on chromosome 22q11 in humans as a susceptibility locus for SCZ (Liu *et al.*, 2002). Previously, hemizygous deletions of the chromosome 22q11 locus had already been identified in schizophrenic patients (Karayiorgou *et al.*, 1995). *Prodh* homozygous mutant mice show impairments in PPI, so these mice have an aberrant sensorimotor gating and show a "schizophrenia-like" phenotype (Gogos *et al.*, 1999).

Pharmacological and behavioral studies of promising knockout mouse models for intermediate phenotypes of psychiatric disorders in humans helps to further validate the appropriateness of the model. The efficacy of antidepressants in the preclinical context is most commonly investigated by the help of the Porsolt Forced Swim Test (FST) (Porsolt *et al.*, 1977). In this test, a rodent is placed in an inescapable cylinder filled with water. Due to the inescapability, rodents adapt to the situation and start floating on the surface. Repeating the test 24 h later leads to a quick repeat of the rodents' behavior, they float again on the surface. The result of this test can be either interpreted as behavioral despair due to inescapability or as passive behavior because the animal cannot cope with stress stimuli actively (Lucki, 1997). The administration of antidepressants between the two testing episodes leads to the effect that rodents will try for an extended time to escape the cylinder in comparison to vehicle treatment. This test just serves as a good indicator for the efficacy because the specificity of the applied drug cannot be tested. The limitation of the test is due to individual strain differences. In a study by Lucki *et al.* (2001), eleven different mice strains were tested in the FST after administration of desipramine, a norepinephrine reuptake inhibitor, and fluoxetine, a selective serotonin reuptake inhibitor. In seven of the strains, the immobility was reduced after administration of desipramine; after administration of fluoxetine, only three of eleven mouse strains showed a reduction in immobility. This

confirms that genetic factors essentially contribute to behavioral performance (Lucki *et al.*, 2001). These findings have led to intensive testing of mouse strains with respect to their responsiveness to certain behavioral tests, resulting in high and low FST-responding mice strains (Schatzberg and Nemeroff, 2009).

One example for an intermediate phenotype of SCZ is the conditional *Hb-egf* knockout mouse. Once Hb-egf is knocked out in the ventral forebrain, mice reveal behavioral abnormalities as seen in SCZ. These behavioral abnormalities can be improved by administration of antipsychotics. Haloperidol, a typical antipsychotic, reduced the locomotor activity of these mice, whereas the administration of clozapine and risperidone, both atypical antipsychotics, improved social interaction and PPI. Furthermore, in this mouse model the abundance of *Grin1* is reduced, which supports the glutamate hypothesis of SCZ (Oyagi *et al.*, 2009). Another model for SCZ is the *Grin1* knock down mouse. In this mouse model, the NMDA receptor is knocked down to a minimum level and these mice exhibit behaviors that resemble a pharmacological NMDA receptor blockade. These behavioral similarities are also known from schizophrenic patients (Ramsey, 2009). In human prefrontal cortices of BD patients, an isoform of the *DGKB* gene (GenBank accession number: AF019352) has been reported to be differentially expressed and thus it is implicated in BD pathogenesis (Yolken, 2002; Caricasole *et al.*, 2002). *Dgkb* knockout (KO) mice reveal higher locomotor activity and in the open field test, KO mice show a higher travel distance than WT mice. In addition, they show less anxiety and decreased immobility in the forced swim test. The hyperactivity could be attenuated by application of lithium chloride (LiCl), whereas this administration did not affect WT mice. *DGKβ* KO mice neither show impairments of sensorimotor gating nor social interaction (Kakefuda *et al.*, 2010). Yamashita and colleagues (2006) performed PPI experiments on dopamine transporter knockout (*Slc6a3* KO) and WT mice. The administration of dopamine, noradrenaline and serotonin reuptake inhibitors (SSRIs) such as methylphenidate and cocaine resulted in an impairment of PPI in WT mice, but caused an improvement of PPI in the *Slc6a3* KO mice. PPI could also be manipulated by administration of the SSRI fluoxetine, whereas the SSRI citalopram did not reveal any effect in *Slc6a3* KO mice (Yamashita *et al.*, 2006). In their review articles, Groenink *et al.* (2003) and Gardier (2009) focus on behavioral aspects of knockout mouse models of serotonin receptor 1A (*Htr1a* KO) and 1B (*Htr1b* KO). *Htr1a* KO mice reveal higher anxiety than WT mice, whereas *Htr1b* KO mice show higher levels of aggression and susceptibility to cocaine (Groenink *et al.*, 2003; Gardier, 2009). Another explanation for the etiology of SCZ is the

existence of white matter aberrations. Microarray studies on schizophrenic patients revealed that myelin-related genes show decreased expression levels, among those the myelin-associated glycoprotein (*MAG*). Morphological studies on *Mag* KO mice brains resulted in changes of dendritic patterns of pyramidal cells and loss of axonal stability (Segal *et al.*, 2007; Nguyen *et al.*, 2009).

Various mouse models have been implicated for the investigation of ASD. Nishimori *et al.* (1996) observed that female oxytocin knockout mice (*Oxt* KO) were unable to care for their offspring (Nishimori *et al.*, 1996). Besides the effects of the peptide oxytocin itself, the effects of the oxytocin receptor knockout have been in focus of ASD research. Behavioral experiments on oxytocin receptor knockout (*Oxtr* KO) mice revealed the inability of male knockout mice to establish a social memory. The administration of an oxytocin antagonist in WT mice led to behavioral modifications that mimic the findings of studies in *Oxtr* KO mice; it produced a social-amnesia like effect (Ferguson *et al.*, 2000). Another neuropeptide receptor, which has been implicated in the etiology and pathogenesis of ASD, is the arginine vasopressin receptor (AVPR). Vasopressin is a nonapeptide, which is closely related to oxytocin in structure and function. Egashira and colleagues (2007) performed behavioral tests on arginine vasopressin receptor 1A (*Avpr1a* KO) mice and observed impairment of social interaction and reduced anxiety-related behaviors in the elevated plus-maze. Furthermore, these mice had problems with spatial learning and sensorimotor gating (Egashira *et al.*, 2007). All these findings receive further support by the knockout mouse model of the *CD38* gene. It encodes a transmembrane glycoprotein, which catalyzes the hydrolysis of cyclic ADP-ribose to ADP-ribose (Malavasi *et al.*, 2008). *Cd38* KO mice show higher locomotor activity as well as impairments in maternal nurturing and social behaviors. Additionally to these findings, the plasma level of oxytocin was significantly decreased in *Cd38* KO mice (Jin *et al.*, 2007; Higashida *et al.*, 2011).

All these examples demonstrate the strengths and weaknesses of animal models. The knockout of a single gene is obviously sufficient to mimic specific symptoms of a psychiatric diseases but it is impossible to create a complete image of a neuropsychiatric disorder within a mouse model. A major problem to overcome in the future is the different effects of gene knockouts on phenotype and behavior depending on the used mouse strain. Koike and colleagues (2006) published a study on a knockout mouse model of the gene *Disc1*, whose human orthologue had been identified as a candidate gene for SCZ and BD in an extended

Scottish family (St. Clair *et al.*, 1990). They created two *Disc1* KO mice: one in the strain 129S6/SvEv and one in C57BL/6J. The gene knockout in the 129S6/SvEv strain revealed both normal working memory and PPI in contrast to the C57BL/6J strain, where working memory and PPI were impaired (Koike, 2006). This leads to the conclusion that the effects of gene knockouts in various mouse strains reveal variable penetrance. Based on these observations, Takao *et al.* (2007) suggest creating a substantial number of gene knockouts in various mouse strains in an international context. Once a substantial number of "psychiatric mouse models" in different strains exists, an "animal-model-array" should be set up to identify the most appropriate mouse model for studies on a specific gene (Takao *et al.*, 2007).

1.13 Research objective

Two GWAS on BD patients on individuals of European ancestry mapped to a susceptibility locus in vicinity of *C15orf53* on chromosome 15q14. This genomic area had been previously confined in our SCZD10 multiplex families by linkage analysis and thus, the investigation of *C15orf53* as a potential candidate gene for the etiology of SCZD10 became self-evident. There is hardly any information available about *C15orf53*. The hypothesis shall be verified, if *C15orf53* is causative for the etiology of SCZD10 in our multiplex families. Gene expression analysis on humane immune and CNS-derived cell lines and human *post-mortem* brain tissue is conducted and delivers information about tissue-specific gene expression patterns of *C15orf53*. DNA sequencing of this gene in SCZD10-affected patients is conducted to identify putative disorder-causing mutations. A case-control association analysis on SCZD10 and BD individual samples is conducted to support the findings from the family studies and the identification of a possible association of *C15orf53* with SCZD10 and/or BD in a population-wide context.

OXTR is the receptor for the "trust hormone" oxytocin and has been implicated in the etiology of ASD in functional and association studies. The hypothesis of this study is the identification of a possible association the *OXTR* gene with ASD in our cohort. Five SNPs located in the *OXTR* gene are genotyped in parents-child trios with one ASD-affected child. The ASD-affected children are dichotomized into the complete cohort and those with an IQ above 70. A transmission-disequilibrium test (TDT) is performed in both groups. Possible SNP and haplotype associations with ASD are identified in the complete cohort and/or the subpopulation with children having an IQ above 70. Two different tools, Haploview and UNPHASED, are used for the TDT and the results are compared to each other with respect to data robustness and validity.

In a previous genome-wide linkage analysis in multiplex families segregating SCZD10, a non-synonymous amino acid exchange (Leu309Met) was identified in the gene *MLC1* on chromosome 22q13.33. The function of the human *MLC1* gene still remains mostly unknown to date. This study aims to extend the knowledge about functional properties of the MLC1 protein and potential regulatory effects of miR-137 on MLC1 and NR3C1 protein expression. A constitutive knockout mouse of the murine orthologue *Mlc1* is planned to enable extensive morphological and behavioral research in an animal model. *In silico* analysis of the 3'-UTRs

of *MLC1* and *NR3C1* has predicted a putative miR-137 target site in both genes. The *in silico* predictions are biologically validated through *in vitro* experiments on glial and neuronal cell lines, which are transfected with miR-137. The regulatory feature of miR-137 on gene expression of *NR3C1* is evaluated on the protein level by immunoblot analysis.

2 Material & Methods

2.1 Psychiatric disorder sample collections

From all affected and non-affected individuals, 10 ml of whole blood was drawn and by salting out procedure, the DNA was extracted (Miller *et al.*, 1988). All participants gave written informed consent after oral and written explanation about the aim and scope of the investigation. The families segregating SCZD10 were ascertained and diagnosed at the Department of Psychiatry, Psychosomatics and Psychotherapy, Würzburg University Hospital, Würzburg, Germany by Stöber and colleagues (Stober *et al.*, 2000, 2001). Differential diagnosis of the bipolar and SCZD10 individual samples was accomplished in the Department of Psychiatry, Psychosomatics and Psychotherapy, Würzburg University Hospital, Würzburg Germany by Reif and colleagues (Meyer *et al.*, 2005). Parent offspring trios (non-affected parents and one affected child) were recruited and diagnosed at the Department of Child and Adolescent Psychiatry, Saarland University Hospital, Homburg, Germany and at the Department of Child and Adolescent Psychiatry, Psychosomatics and Psychotherapy, Johann Wolfgang von Goethe University, Frankfurt/Main, Germany, by Christine M. Freitag and colleagues. The children were diagnosed according to the Autism Diagnostic Observation Schedule (ADOS) (Lord *et al.*, 2000) and/or the Autism Diagnostic Interview – Revised (ADI-R) (Lord *et al.*, 1994).

2.2 Individual patient samples (non-related)

2.2.1 Bipolar disorder (BD) patients

The investigated BD sample consisted of 203 patients, which were described by our group (Meyer *et al.*, 2005). The anamnesis included the first onset of the disorder, attempted suicide, familial background as well as age and sex. The mean age of the male patients was 28.9 ± 10.3 years; that of the female patients was 29.7 ± 9.8 years.

2.2.2 Periodic catatonia (SCZD10) patients

The individual SCZD10 sample consisted of 71 patients. For the SCZD10 patients, the differential diagnosis also encompassed the first onset of the disorder, attempted suicide, familial background as well as age and sex (Andreas Reif, personal communication). The mean age of the male patients was 23.4 ± 7.4 years; that of the female patients was 27.2 ± 10.1 years.

2.3 Parents-offspring trios and multiplex families (related)

2.3.1 Parents-offspring trios with autism spectrum disorder (ASD)

In the present study, 574 subjects were considered for further investigation, consisting of 207 children diagnosed with ASD and 367 parents without any psychiatric history.

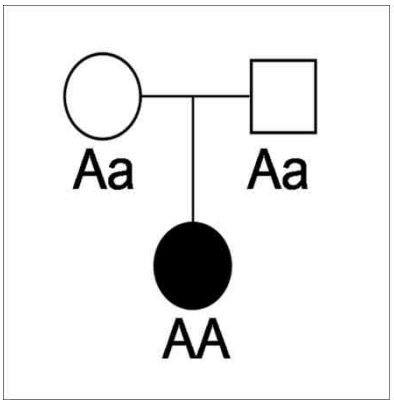

Figure 2.1: Parents-offspring trio with at least one heterozygous parent and one affected child.

All parents-offspring trios were of Caucasian origin and live in the south of the federal states Rhineland-Palatinate and Saarland, Germany. The mean age of the male patients was 10.6 ± 5.6 years; that of the female patients was 10.7 ± 5.8 years.

2.3.2 Multiplex families segregating SCZD10

Seven of eleven families (F05, F09, F11, F13, F17, F19 and F24) including 56 SCZD10-affected and 30 non-affected family members were considered for investigation due to a segregating susceptibility region on chromosome 15q14-15.1 (Stober *et al.*, 2001).

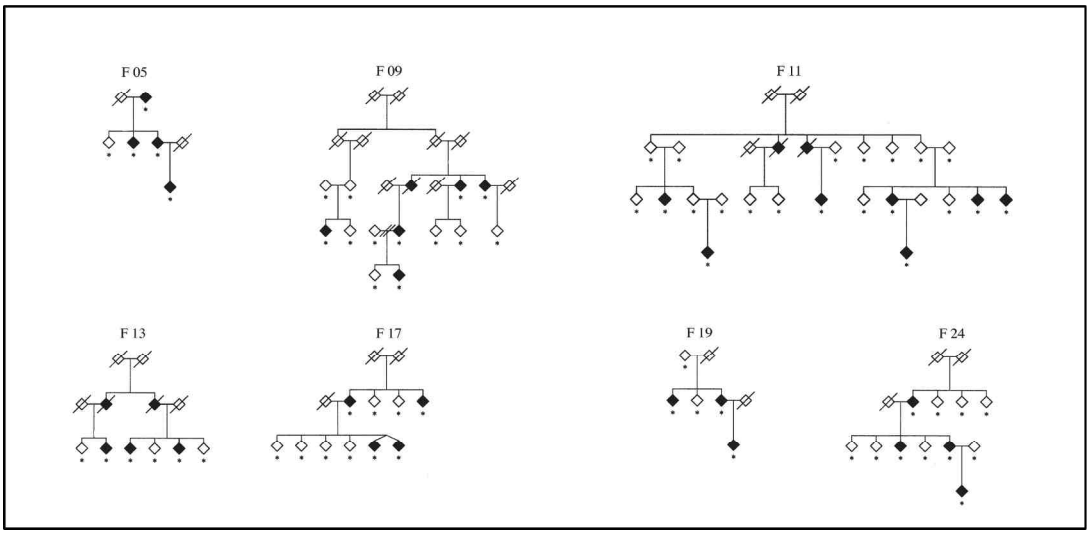

Figure 2.2: Multiplex pedigrees segregating SCZD10 (adapted from Stober *et al.*, 2001). Blank symbol: unaffected individual, filled symbol: affected individual, slashed symbol: individual deceased, asterisk: available DNA specimen

2.4 Cell lines

2.4.1 Cell lines used for expression analysis and knock down experiments of *MLC1*

Table 2.1: Cell lines used for experiments

cell lines	reference	cell type, origin	species
PC12	ECACC: 88022401	adrenal phaeochromocytoma	*Rattus norvegicus*
SH-SY5Y	ECACC: 94030304	Neuroblastoma	*Homo sapiens*
SK-N-MC	ECACC: 90022302	Neuroepithelioma	*Homo sapiens*
TR14	Rupniak *et al.*, 1984	Neuroblastoma	*Homo sapiens*
U373MG	ECACC: 08061901	glioblastoma astrocytoma	*Homo sapiens*

All listed cell lines were used for investigation of MLC1 protein expression, validation of the MLC1 antibody and for testing and modification of transfection conditions with the miRNA precursor molecules. For experiments with miR-124 and miR-137 and their regulatory influence MLC1 protein expression, the cell lines SK-N-MC and U373MG cells were used.

2.4.2 Cell lines cDNA used for gene expression analysis of *C15orf53*

Table 2.2: Cell lines cDNA used for *C15orf53* gene expression analysis

number	cell lines	cell type
1	A431	epidermoid carcinoma
2	Jurkat	T cell leukemia
3	U-937	histiocytic lymphoma
4	EBV-WMPT	B cell line
5	HT29	colon adenocarcinoma
6	K-562	chronic myeloid leukemia
7	HEL	Erythroleukemia
8	Jurkat	T cell leukemia
9	TF-1	Erythroleukemia
10	U-937	histiocytic lymphoma
11	Raji	Burkitt lymphoma
12	A-549	lung carcinoma
13	CCL 75	diploid fibroblast
14	CCRF-CEM	T-lymphoblastoid
15	DAUDI	B-lymphoblast
16	HSB-2	lymphoblastic leukemia
17	KG1	acute myelogenous leukemia
18	TT 830-845	T cell clone
19	MelJuSo-wt	Melanoma
20	HELA S3	Carcinoma
21	LL87-CD4 CCR	Neuron
22	BC2	Hepatocyte
23	NCI-H82	lung epithelial
24	KG1 (2)	acute myelogenous leukemia
25	K562	chronic myelogenous leukemia
26	THP-1	Monocyte
27	Hep G2	liver epithelium
28	MCF-7	breast epithelial
29	MCF 1DA	breast cancer

number	cell lines	cell type
30	HaCaT p42	human keratinocyte
31	PC-3	prostate cancer
32	HEK 293T	human embryonic kidney cells
33	HL60	promyelocytic leukemia
34	Jeg 3	choriocarcinoma cell line
35	MeWo	human melanoma cell line
36	Ptak	monocytic cell line, unspecified
37	Ww9	monocytic cell line, unspecified
38	U4C	fibrosarcoma cell line
39	HEK-293	human embryonic kidney cells
40	MonoMac	monocytic cell line

2.5 Bacterial strains & transformation of DNA

The following chemically competent bacterial strains were used:

Table 2.3: Bacterial strains and genotypes

strain	genotype	catalogue number	Supplier
Escherichia coli DH5α	*F- φ80lacZΔM15 Δ(lacZYA-argF)U169 deoR recA1 endA1 hsdR17(rk -, mk+) phoA*	18263-012	Invitrogen, Carlsbad, USA
Escherichia coli K12, XL1-Blue	*recA1 endA1 gyrA96 thi-1 hsdR17 supE44 relA1 lac [F´ proAB lacIqZΔM15 Tn10 (Tetr)]*	#200249	Stratagene, La Jolla, USA
Escherichia coli K12, XL10-Gold	*Tet^r D(mcrA)183 D(mcrCB-hsdSMR-mrr)173 endA1 supE44 thi-1 recA1 gyrA96 relA1 lac Hte [F¢ proAB lacI ^{q}ZDM15 Tn10 (Tet^r) Amy Cam^r]*	#200315	Stratagene, La Jolla, USA
Escherichia coli TOP10	*F- mcrA Δ(mrr-hsdRMS-mcrBC) φ80lacZΔM15 ΔlacX74 recA1 araD139 Δ(ara-leu) 7697 galU galK rpsL (StrR) endA1 nupG λ-*	C4040-10	Invitrogen, Carlsbad, USA

The bacterial strains were used for cloning procedures. The *Mlc1* knockout vector (pMlc1_KO_mod) construct was transformed into the bacterial strains DH5α and XL1-blue. For investigation of the human *NR3C1* 3'-UTR, sized 2,475 bp (based on

Genbank: NM_000176), a 628 bp fragment of the 3'-UTR was cloned into the pMIR-REPORT vector. The strains XL10-Gold and TOP10 were used for transformation with the pMIR-REPORT_NR3C1 construct (2.17.5).

2.6 Bacterial DNA vectors

Cosmid and plasmid vectors that were used in the studies are listed in the following table:

Table 2.4: DNA vectors

name	supplier / origin	description
MPMGc121K08537Q2	Klaus-Peter Lesch, Würzburg, Germany	Cosmid
pENTR / D-TOPO	Invitrogen, Carlsbad, USA	Plasmid
pMIR-REPORT	Ambion, Austin, USA	Plasmid
pMlc1_KO_mod	Savira Ekawardhani, based on pUC19	Plasmid

2.7 Human brain tissue

Human *post-mortem* limbic brain tissue samples (amygdala, hippocampus, inferior gyrus, cingulate gyrus and nucleus accumbens) from six donors free of CNS diseases and without a history of long term psychotropic medication were obtained from the Dutch Brain Bank (Netherlands Institute of Neuroscience). All patients provided pre-mortem consent for brain autopsy and use of brain material for research purposes as previously reported (Alt *et al.*, 2010).

2.8 Genomic murine DNA & murine embryonic stem cells (ES)

Genomic DNA (gDNA) from *Mus musculus domesticus Black 6* was given as a courtesy from Klaus-Peter Lesch, Laboratory of Translational Neuroscience, Department of Psychiatry, Psychosomatics and Psychotherapy, University of Würzburg. The transfection of ES was accomplished in the facilities of Michael Sendtner, Department of Clinical Neurobiology,

University of Würzburg. ES that had been electroporated with the knockout construct pMlc1_KO_mod and had survived the selection process (2.15.1) were sent to our department for further investigation. DNA of ES was isolated by application of the QIAamp DNA Micro Kit (Table 2.10) and further analyzed by PCR.

2.9 Buffers, media and reagents

2.9.1 Used buffers and media

Table 2.5: Buffer and media list

name	components	additional information
Cell culture growth medium for cell lines: SH-SY5Y, SK-N-MC, TR14 and U373MG	DMEM High Glucose 4.5 g/l	after defrosting, cells were first cultivated in 15 % (v/v) FCS, after two passages in 10 % (v/v) FCS
	15 % (v/v) FCS, 10 % (v/v) FCS	
	1 % (v/v) GlutaMAX	
Cell culture growth medium for cell lines: SH-SY5Y, SK-N-MC, TR14 and U373MG	DMEM High Glucose 4.5 g/l	after defrosting, cells were first cultivated in 15 % (v/v) FCS, after two passages in 10 % (v/v) FCS
	15 % (v/v) FCS, 10 % (v/v) FCS	
	1 % (v/v) GlutaMAX	
	1 % (v/v) P/S	
Cell culture growth medium for cell line: PC12	RPMI 1640	after defrosting, cells were first cultivated in 15 % (v/v) HS, after two passages in 10 % (v/v) FCS
	5 % (v/v) FCS	
	1 % (v/v) GlutaMAX	
	10 % (v/v) Horse serum	
DNA loading buffer (6x)	0.25 % (w/v) bromophenolblue or 0.25 % (w/v) xylene cyanol	complete volume with H_2O
	15 % (w/v) Ficoll	
Erythrocytes lysis buffer (pH 7.4)	155 mM NH_4Cl	complete volume with H_2O
	10 mM $KHCO_3$	
	0.1 mM EDTA	
LB agar (pH 7.0)	10 g/l tryptone	autoclave at 121 °C, add 100 µg / ml ampicillin or 30 µg / ml kanamycin
	5 g/l yeast extract	

name	components	additional information
	10 g/l NaCl	
	15 g/l agar	
LB medium (pH 7.0)	10 g/l tryptone	autoclave at 121 °C, add 100 µg / ml ampicillin or 30 µg / ml kanamycin
	5 g/l yeast extract	
	10 g/l NaCl	
Luminol solution	200 ml 0.1 M Tris-HCl pH 8.0	
	50 mg sodium luminol	
	60 µl 30 % (w/w) H_2O_2	
Nuclear lysis buffer (pH 8.2)	10 mM Tris-HCl (pH 8.0)	
	400 mM NaCl	
	2 mM EDTA (pH 8.2)	
PCR buffers	500 mM KCl	buffer A: 7.5 mM $MgCl_2$ buffer B: 10 mM $MgCl_2$ buffer C: 15 mM $MgCl_2$ buffer D: 20 mM $MgCl_2$ buffer E: 25 mM $MgCl_2$ buffer F: 30 mM $MgCl_2$ buffer G: 35 mM $MgCl_2$ buffer H: 40 mM $MgCl_2$
	100 mM Tris-HCl (pH 8.3)	
	0.25 % (v/v) Tween-20	
	0.25 mg/ml BSA	
Polyacrylamid running gels (10 %)	4.8 ml H_2O	quantities for two gels
	2.5 ml 1.5 M Tris-HCl pH 6.8	
	2.5 ml Acrylamide/Bisacrylamide (29:1)	
	100 µl of 10 % (w/v) SDS	
	85 µl of 10 % (w/v) APS	
	6 µl TEMED	
Polyacrylamid stacking gels (10 %)	3.8 ml H_2O	quantities for two gels
	1.5 ml 0.5 M Tris-HCl pH 6.8	
	600 µl Acrylamid/Bisacrylamide (29:1)	
	60 µl of 10 % (w/v) SDS	
	37.5 µl of 10 % (w/v) APS	
	10 µl TEMED	
Protein blotting buffer (3x)	250 mM Tris	complete volume with H_2O
	1.15 M glycine	
	20 % (v/v) methanol	

name	components	additional information
Protein electrophoresis buffer (5x)	250 mM Tris	complete volume with H_2O
	1.92 M glycine	
	1 % (w/v) SDS	
Protein lysis buffer (1x)	150 mM NaCl	add complete mini protease inhibitor immediately prior to use, complete volume adding H_2O
	1 % (w/v) NaDOC	
	1 % (v/v) NP-40	
	0.1 % (w/v) SDS	
	50 mM Tris-HCl pH 7.4	
Protein sample buffer (1x)	12.5 % (v/v) 0.5 M Tris-HCl pH 6.8	add bromophenolblue and β-mercaptoethanol just prior to use, complete volume adding H_2O
	10 % (v/v) glycerol	
	3 % (w/v) SDS	
	0.2 % (v/v) bromophenol blue	
	2.5% (v/v) β-mercapto-ethanol	
TAE buffer (10x, pH 8.5)	400 mM Tris	
	200 mM acetic acid	
	10 mM EDTA	
TBE buffer (10x, pH 8.3)	890 mM Tris	
	890 mM boric acid	
	20 mM EDTA	
TBST (pH 8.0)	50 mM Tris	complete volume adding H_2O
	150 mM NaCl	
	0.2 % (v/v) Tween-20	
TE-buffer (pH 8.0)	10 mM Tris-HCl	
	0.1 mM EDTA	

2.10 Reagents

Table 2.6: Reagents and consumables

reagent / consumables	Supplier
Acrylamid / Bisacrylamid (30 % / 0.8 %)	Bio-Rad, Hercules, USA
Agarose	Roth, Karlsruhe, Germany
Agar	Roth, Karlsruhe, Germany
Ammonium persulfate (APS)	Roth, Karlsruhe, Germany
Ampicillin	Roth, Karlsruhe, Germany
β-mercaptoethanol	Merck, Darmstadt, Germany

reagent / consumables	Supplier
Bovine Serum Albumine (BSA)	New England Biolabs, Ipswich, USA
Bromophenol blue	Merck, Darmstadt, Germany
Cell culture flasks 25 cm^2, 75 cm^2, 175 cm^2	Life Technologies, Carlsbad, USA
Cell culture plates 6 wells, 12 wells, 24 wells	Life Technologies, Carlsbad, USA
Centrifuge tubes 15 ml, 50 ml	Sarstedt, Nümbrecht, Germany
Complete Mini Protease Inhibitor	Roche Diagnostics, Risch, Switzerland
Coomassie Brilliant Blue R-250	Sigma-Aldrich, St.-Louis, USA
Cultivation tubes 12 ml	Roth, Karlsruhe, Germany
Dimethylsulfoxide (DMSO)	Merck, Darmstadt, Germany
Dulbecco's Minimal Essential Medium (DMEM) High Glucose	BioWest, Nuaillé, France
Phosphate Buffered Saline (PBS)	BioWest, Nuaillé, France
Enhanced chemiluminescence (ECL)	GE Healthcare, Little Chalfont, UK
Ethylenediaminetetraacetic acid (EDTA)	Merck, Darmstadt, Germany
Ethanol	Roth, Karlsruhe, Germany
Ethidium bromide	Roth, Karlsruhe, Germany
Exonuclease I & 10x reaction buffer	Thermo Fisher Scientific, Waltham, USA
Fetal Calf Serum (FCS)	Life Technologies, Carlsbad, USA
GeneAmp PCR buffer (10x)	Life Technologies, Carlsbad, USA
GeneRuler 100 bp DNA ladder plus	Thermo Fisher Scientific, Waltham, USA
GeneRuler 1 kb DNA ladder	Thermo Fisher Scientific, Waltham, USA
GlutaMAX	Life Technologies, Carlsbad, USA
Glycerol	Roth, Karlsruhe, Germany
HindIII	Thermo Fisher Scientific, Waltham, USA
Hydrogen peroxide	Roth, Karlsruhe, Germany
Horse serum (HS)	Life Technologies, Carlsbad, USA
Incidin Plus disinfectant	Ecolab, St. Paul, USA
Indicator tape	3M, St. Paul, USA
Isopropyl alcohol	Roth, Karlsruhe, Germany
Latex gloves	Roth, Karlsruhe, Germany
Lipofectamine 2000 Transfection Reagent	Life Technologies, Carlsbad, USA
Low-fat milk powder	Nestlé, Vevey, Switzerland
Kanamycin	Roth, Karlsruhe, Germany
Magnesium chloride ($MgCl_2$)	Roth, Karlsruhe, Germany
N,N,N',N'-Tetramethylethylenediamine (TEMED)	Roth, Karlsruhe, Germany
Pasteur pipettes	Hirschmann, Eberstadt, Germany
PCR plates 96 well	Sarstedt, Nümbrecht, Germany
PCR single tubes 200 µl	Sarstedt, Nümbrecht, Germany

reagent / consumables	Supplier
Penicillin / Streptomycin (P/S)	BioWest, Nuaillé, France
PeqGOLD RNA Pure	PEQLAB, Erlangen, Germany
Petri dishes 50mm x 20 mm, 100 mm x 20 mm, 175 mm x 20 mm	Sarstedt, Nümbrecht, Germany
Pipette tips, barrier, 10 µl, 200 µl, 1000 µl	Biozym, Hessisch Oldendorf, Germany
Pipette tips, non-barrier, 10 µl, 200 µl, 1000 µl	Sarstedt, Nümbrecht, Germany
Platinum *Taq* DNA Polymerase	Life Technologies, Carlsbad, USA
Proteinase K	Sigma-Aldrich, St.-Louis, USA
*Pst*I	Promega, Madison, USA
*Sac*I	Promega, Madison, USA
RPMI 1640	BioWest, Nuaillé, France
Sample loading solution (SLS)	Beckman Coulter, Brea, USA
SAP & SAP buffer (10x)	Thermo Fisher Scientific, Waltham, USA
Serological pipettes 5 ml, 10 ml, 25 ml	Sarstedt, Nümbrecht, Germany
Size standard 80	Beckman Coulter, Brea, USA
*Sma*I	Thermo Fisher Scientific, Waltham, USA
Sodium acetate	Roth, Karlsruhe, Germany
Sodium chloride	Roth, Karlsruhe, Germany
Sodium dodecyl sulfate (SDS)	Sigma-Aldrich, St.-Louis, USA
Sodium hydroxide	Roth, Karlsruhe, Germany
Sodium luminol	Sigma-Aldrich, St.-Louis, USA
*Spe*I	Promega, Madison, USA
SuperFect Transfection Reagent	Qiagen, Hilden, Germany
SYBR green I	Life Technologies, Carlsbad, USA
T4 DNA Ligase	Thermo Fisher Scientific, Waltham, USA
Taq-Polymerase	In-house production
Tris-Borate-EDTA (TBE) buffer 10x	Roth, Karlsruhe, Germany
Tris(hydroxymethyl)aminomethane (TRIS)	Roth, Karlsruhe, Germany
Trypane blue	BioWest, Nuaillé, France
Trypsin	BioWest, Nuaillé, France
Trypton / Pepton	Roth, Karlsruhe, Germany
Tween-20	Roth, Karlsruhe, Germany
*Xba*I	Thermo Fisher Scientific, Waltham, USA
*Xho*I	Thermo Fisher Scientific, Waltham, USA
Xylene cyanol	Roth, Karlsruhe, Germany

2.11 Oligonucleotides

2.11.1 Oligonucleotides ("primers") used for PCR reactions

All oligonucleotides were manufactured and obtained from MWG Biotech, Ebersberg, Germany and Biomers.net, Ulm, Germany.

Table 2.7: Overview of investigated genes and applied oligonucleotides

name (approved symbol)	Genbank / UniSTS acc. nr.	oligo name	oligo sequence (5' to 3')
Bromodomain containing 1 (*BRD1*) NM_014577		rs138880 for	CTGCCAAGGCTCTGCAGAA
		rs138880 rev	CCTAAACCACTCTTCCCC
		rs4468 for	CAGTGAATTTGTTAGATGATTA
		rs4468 rev	CTTTATTCTCCCCTCTTTCCAC
C15orf53 NM_207444		*C15orf53* Exon1 nested forward	CTGTCTCCAGGCGTCTGTTT
		C15orf53 Exon 1 nested reverse	TGGAGAAGAGAAGGGAAGCA
		C15orf53 Exon 1 Primer1 forward	CAAGAGGACCTGGGCATTT
		C15orf53 Exon1 Primer 1 reverse	CACTTCTGGGCTTCTCTTGG
		C15orf53 expression for	GCGTCTGTTTGGATGGCTGGAGG
		C15orf53 expression reverse	GGAAGTGGTGAACGGCGGGG
		C15orf53 for	CCAGGAAGCAAGGCTAAGG
		C15orf53 rev	TGGAGAAGAGAAGGGAAGCA
		C15orf53 rs717 rs716 f	TGTGGTTGAGAACCCATCA
		C15orf53 rs717 rs716 r	CAGGCTGGAGGTGTCTGAAT

name (approved symbol)	Genbank / UniSTS acc. nr.	oligo name	oligo sequence (5' to 3')
		C15orf53 rs2172835 f	AGAGCTGCCACCAAGGAAC
		C15orf53 rs2172835 r	CCTCAGCTTTCCTCCCTGTA
Glyceraldehyde-3-phosphate dehydrogenase (*GAPDH*) NM_002046		GAPDH for	GAAGGTGAAGGTCGGAGTC
		GAPDH rev	GAAGATGGTGATGGGATTTC
Megalencephalic leukoencephalopathy with subcortical cysts 1 homolog, human (*Mlc1*), NM_133241.2		SA Mlc1 for TK	GGACGACAGCAGAGGTAAGC
		Mlc1 integ f SS	TATGGACGCTGGGAACTGAAC
		Mlc1 up3 f SS	AGGGAGGAACTGGGCTATGAC
		Mlc1 integ ex f	AGGGTGCCAATGTCTCCA
		Mlc1 nested SA f	CTGACTCAAAGCCCAAGGAC
		Mlc1 pgk prom f	ATTCTCGCACGCTTCAAAAG
		SA Mlc1 for TK	GGACGACAGCAGAGGTAAGC
		Mlc1 integ ex rev	AGGCACACAGCTTCCTGAAT
		Mlc1 in1 for TK	CTGCATAGGAGGGAATGGTGGTC
		Mlc1 ex1 nest f	CCAATGTCTCCAGGCAAATG
		Mlc1 int nest r	CTGTTGTGCCCAGTCATAGC
		mmMlc1 Integ SA forward	TCCAGGCAAATGAAGCACATTCA
		mmMlc1 Integ SA reverse	CGGACAGGTCGGTCTTGACAAAA
Megalencephalic leukoencephalo-pathy with subcortical cysts 1 (*MLC1*), NM_015166.3		hsMLC1 fragment 1 miR137 for	GGGTCTGCTCCTGGGAATGG
		hsMLC1 fragment 1 miR137 rev	CAGTAAGCTTCTCTAGGG-GTTACACAAATC
Neomycin resistance gene (*NeoR*), AY497508.1		Neo rev SS	AGCCGATTGTCTGTTGTGCCC
		Neo 340 rev TK	ATACTTTCTCGGCAGGAGCA

name (approved symbol)	Genbank / UniSTS acc. nr.	oligo name	oligo sequence (5' to 3')
		Neo do3 rev SS	CGGTGGATGTGGAATGTGTGC
Nuclear receptor subfamily 3, group C, member 1 (*NR3C1*), NM_001204258		hsGR frag2 SpeI SacI miR183 - miR410 for	TGGCACTAGTCCCATT-TTCACATTCCCATC
		hsGR frag2 SpeI SacI miR183 - miR410 rev	TTTGGAGCTCGAGACC ATCGCTGCCTGTAT
Oxytocin receptor (*OXTR*), NM_000916		hsOXTR rs237906 non-syn Exon 3 for	AGCCGTAAAGGGCTCGAA
		hsOXTR 4 SNPs Intron 3 for	TTGGCGTGTGTGTATGTGTG
		hsOXTR 4 SNPs Intron 3 rev	AGCAGAAACTGTGGGTGTCC
		hsOXTR rs237897 Intron 3 for	GTAGTTGAAGGGGGTGTTGG
		hsOXTR rs237897 Intron 3 rev	ACAGGCCAAGAATGGACAAT
		hsOXTR rs237897 Intron 3 nfor	CCAAGGGAGAGGTGAAGACA
		hsOXTR rs237897 Intron 3 nrev	CCTCCCCCTCAAACTTGAAT
		hsOXTR rs237906 non-syn Exon 3 rev	GGCGATGCTTAGGTGCTT
		hsOXTR rs4686302 ns Exon 3 for	GGCCTACATCACATGGATCA
		hsOXTR rs4686302 ns Exon 3 rev	CTTGACGCTGCTGACACG
		OXTR 237906 nfor	CCGTAAAGGGCTCGAAGG

name (approved symbol)	Genbank / UniSTS acc. nr.	oligo name	oligo sequence (5' to 3')
		OXTR 237906 nrev	ATGAGCAGCAGCAGGTAGGT
		OXTR rs4686302 nfor	CATCACCTTCCGCTTCTACG
		OXTR 237906 for	CTCATTTGCAGTGGCTCAGA
		OXTR 237906 rev	CAGGAGCAGGATGAGACACA

2.11.2 Oligonucleotides ("primers") used for SNP detection

name (approved symbol)	Genbank / UniSTS acc. nr.	oligo name	oligo sequence (5' to 3')
Oxytocin receptor (*OXTR*), NM_000916		OXTR rs237889 det for	AAAAAAATGATTTGCCGCTTTC-CACAAGTTCCT
		OXTR rs2254298 det rev	AAAAAAAAAAAAATTCAGAGG-AAGAAGCCCCGCAAACTG
		OXTR rs2268494 det for	AAAAAAAAAAAAAAAAATCCT-GCGGCCAGCTGCTGACATGCATA
		OXTR rs237897 det for	AAAAAAAAAAAAAAAAAAAAA-AAAATGCAGAGAGGTGAGTACT-GCAAGGAG
		OXTR rs4686302 det for	AAAAAAAAAAAAAAAAAAAAA-AAAAAAAATACATCGTGCCGGT-CATCGTGCTCGCT

2.11.3 Oligonucleotides ("primers") used for sequencing reactions

name (approved symbol)	Genbank / UniSTS acc. nr.	oligo name	oligo sequence (5' to 3')
C15orf53 NM_207444		*C15orf53* frag1 seq f	TGTGGTTGAGAACCCATCA
		C15orf53 frag1 seq r	CAGGCTGGAGGTGTCTGAAT
		C15orf53 frag2 seq f	GCAGGGTTCTCAGTTTCTGC
		C15orf53 frag2 seq r	CCACACTTGCAAAATCCTGTT
		C15orf53 frag3 seq f	GACAGAAAGATGCCCACTCC

name (approved symbol)	Genbank / UniSTS acc. nr.	oligo name	oligo sequence (5' to 3')
		C15orf53 frag3 seq r	CCAAAACTTTACAGCTTAAAAC
		C15orf53 frag4 seq f	AGAGCTGCCACCAAGGAAC
		C15orf53 frag4 seq r	CCTCAGCTTTCCTCCCTGTA
		C15orf53 frag5 seq f	GTCAGTCAGTGGCTCCATCC
		C15orf53 frag5 seq r	CCTAGTTTGGGTGGGGAAAG
		C15orf53 frag6 seq f	GCATGCCAATCTCTCCTCTC
		C15orf53 frag6 seq r	CAAGCCAGGGATGAAACAAT
		C15orf53 frag7 seq f	GTTCCTTCTGGGGTCACTCA
		C15orf53 frag7 seq r	ATGTTTCCGGTAACCAGCAG
		C15orf53 frag8 seq f	CCCAGACTTCTTGGATGGAC
		C15orf53 frag8 seq r	CCCACTGCATTTCTTCACCT
		C15orf53 frag9 seq f	TTTGCCAAACTGGAACACAA
		C15orf53 frag9 seq r	TCTCCCTCCTGCCTGACTAA
NR3C1 NM_000176		Seq_pMIR_REPORT_for_TK	AGGCGATTAAGTTGGGTA
		Seq_pMIR_REPORT_rev_TK	GGAAAACTCGACGCAAGAAA

2.12 Precursor sequences of miRNAs and applied antibodies

Table 2.8: Nucleotide precursor sequences of miRNAs

name (approved symbol)	miRBase acc. nr.	precursor sequence
hsa-mir-124-1 (MIR124-1)	MI0000443	AGGCCUCUCUCUCCGUGUUCACAGCGGACCU-UGAUUUAAAUGUCCAUACAAUUAAGGCACG-CGGUGAAUGCCAAGAAUGGGGCUG
hsa-mir-137 (MIR137)	MI0000454	GGUCCUCUGACUCUCUUCGGUGACGGGUAU-UCUUGGGUGGAUAAUACGGAUUACGUUGUU-AUUGCUUAAGAAUACGCGUAGUCGAGGAGA-GUACCAGCGGCA

Table 2.9: Antibody list

name	working concentration	manufacturer
rabbit anti-human GRα (H-300)	1:1000	Santa Cruz Biotech, Santa Cruz, USA
rabbit anti-human MLC1	1:200	Abcam, Cambridge, UK
rabbit anti-human MLC1 (N-18), sc-86741	1:200	Santa Cruz Biotech, Santa Cruz, USA
rabbit anti-mouse α-tubulin (H-300)	1:5000	Santa Cruz Biotech, Santa Cruz, USA

2.13 Commercial kits

Table 2.10: Commercial kits list

name	manufacturer / supplier
BigDye Terminator v3.1 Cycle Sequencing Kit	Life Technologies, Carlsbad, USA
dNTPs (ATP, CTP, GTP, TTP)	Thermo Fisher Scientific, Waltham, USA
GeneJET Gel Extraction Kit	Thermo Fisher Scientific, Waltham, USA
GenomeLab DTCS Quick Start Kit	Beckman Coulter, Brea, USA
GenomeLab SNPStart Primer Extension Kit	Beckman Coulter, Brea, USA
High Pure RNA Isolation Kit	Roche Diagnostics, Risch, Switzerland
MACS MicroBeads	Miltenyi, Bergisch Gladbach, Germany
MinElute Gel Extraction Kit	Qiagen, Hilden, Germany
MinElute PCR Purification Kit	Qiagen, Hilden, Germany
peqGOLD Gel Extraction Kit	PEQLAB, Erlangen, Germany
peqGOLD Plasmid Miniprep Kit II	PEQLAB, Erlangen, Germany
peqGOLD RNA Pure	PEQLAB, Erlangen, Germany
Phusion High-Fidelity DNA Polymerase	Thermo Fisher Scientific, Waltham, USA
QIAamp DNA Micro Kit	Qiagen, Hilden, Germany
QIAGEN Plasmid Maxi Kit	Qiagen, Hilden, Germany
QIAGEN Plasmid Midi Kit	Qiagen, Hilden, Germany

2.14 Equipment, bioinformatic tools & databases

2.14.1 Equipment

Table 2.11: Equipment and manufacturer list

name	manufacturer / supplier
ABI 3100 Genetic Analyzer	Life Technologies, Carlsbad, USA
AccuJet Pipette Controller	Brand, Wertheim, Germany
Agencourt SPRIPlate 96R Magnet Plate	Beckman Coulter, Brea, USA
Analytical balance L 420 P	Sartorius, Göttingen, Germany
Autoclave GVA 570	Gössner, Hamburg, Germany
Avanti Centrifuge J-25 I	Beckman Coulter, Brea, USA
Balance Europe 4000 AR	Gibertini, Novate Milanese, Italy
Beckman Coulter CEQ 8000 Genetic Analysis System	Beckman Coulter, Brea, USA
Cabinet dryer	WTB Binder, Tuttlingen, Germany
Cabinatic pH-Meter 766	Knick, Berlin, Germany
Digital camera D50	Nikon, Tokio, Japan
DNA Engine Opticon 2 Real-Time PCR Detection System	Bio-Rad, Hercules, USA
Electrophoresis chamber CTI, LKB, GNA 200	Pfizer, New York City, USA
Electrophoresis chamber Sub-Cell GT	Bio-Rad, Hercules, USA
Electrophoresis power supply Consort E865	Consort, Turnhout, Belgium
Electrophoresis power supply EPS 3500 XL, EPS 200	Pfizer, New York City, USA
Electrophoresis power supply PowerPac 300	Bio-Rad, Hercules, USA
Eppendorf Thermomixer 5436	Eppendorf, Hamburg, Germany
Fume hood Maxima 17840 WRT	Hemling, Ahaus, Germany
GeneQuant II Spectrophotometer	Pfizer, New York City, USA
Hellma Suprasil cuvette, bluespot, 10 mm thickness, 15 mm center	Hellma, Müllheim, Germany
Hettich Rotina 48RC	Hettich, Tutlingen, Germany
Incubator	Heraeus, Hanau, Germany
IR sensor CO2 incubator	Sanyo, Moriguchi, Japan
Julabo waterbath UC	Julabo, Seelbach, Germany
Laboratory dish washer Mielabor G7783 Multitronic	Miele, Gütersloh, Germany
Laminar flow Jouan MSC-12	Thermo Fisher Scientific, Waltham, USA
Light microscope Kulowert	Hundt, Wetzlar, Germany
Magnetic stirrer Monotherm	Faust, Schaffhausen, Switzerland
Microcentrifuge C1301B	Labnet, Woodbrigde, USA
Microwave oven Micromat	AEG-Electrolux, Nürnberg, Germany

name	manufacturer / supplier
Multichannel (8) pipettes 1 – 10 µl, 5 – 50 µl	Biohit, Helsinki, Finland
Nanodrop ND-1000	Thermo Fisher Scientific, Waltham, USA
PCR workstation P-036	C.B.S. Scientific, Del Mar, USA
Rotating incubator Gallenkamp	Sanyo, Moriguchi, Japan
Schutron Schnipptherm heat block	Wolflabs, York, UK
Single channel pipettes 0.5-10 µl, 20 – 200 µl, 100 – 1000 µl	Biohit, Helsinki, Finland
Tabletop centrifuge Z233M	Hermle, Wehingen, Germany
Tabletop centrifuge Z233MK-2	Hermle, Wehingen, Germany
Thermocycler GeneAmp 9600	PerkinElmer, Waltham, USA
Thermocycler GeneAmp PCR System 9700	PerkinElmer, Waltham, USA
Thermocycler Multigene Gradient TC-9600-G	Labnet, Woodbridge, USA
TKA Micropure water system	Thermo Fisher Scientific, Waltham, USA
UV screen N-90M	Intas, Göttingen, Germany
Vortex Mixer Neolab	Neolab, Heidelberg, Germany
Vortexer Vortex Genie 2	Scientific Industries, Bohemia, USA
Waterbath Julabo SW21	Julabo, Seelbach, Germany

2.14.2 Bioinformatic tools & databases

Table 2.12: Applied bioinformatic tools and databases

name	URL / manufacturer
ChromasLite	Technelysium Ltd.
ClustalW	http://www.ebi.ac.uk/Tools/msa/clustalw2/
DBTTS	http://dbtss.hgc.jp/
Ensembl Genome Browser	http://www.ensembl.org/
GeneCards	http://www.genecards.org/
Haploview	Broad Institute, Cambridge, USA
ImageJ	NIH, Bethesda, USA
miRBase	http://www.mirbase.org/
NCBI	http://www.ncbi.nlm.nih.gov/
NEBCutter	http://tools.neb.com/NEBcutter2/
Primer3	http://frodo.wi.mit.edu/primer3/
Pubmed	http://www.ncbi.nlm.nih.gov/pubmed/
SPSS	IBM corporation, Armonk, USA
TargetScan	http://www.targetscan.org/
UCSC Genome Browser	http://genome.ucsc.edu/

name	URL / manufacturer
Unphased	MRC Biostatistics Unit, Cambridge, UK
VectorNTI	Life Technologies, Carlsbad, USA

2.15 Methods

2.15.1 Non-conditional murine *Mlc1* knockout mouse procedure

In order to investigate the function of *Mlc1* during development, a constitutive knockout mouse model was planned. In a constitutive knockout mouse, the gene of interest is inoperable in all somatic cells throughout all developmental stages of the organism. The knockout procedure is illustrated by the subsequent scheme (Figure 2.3).

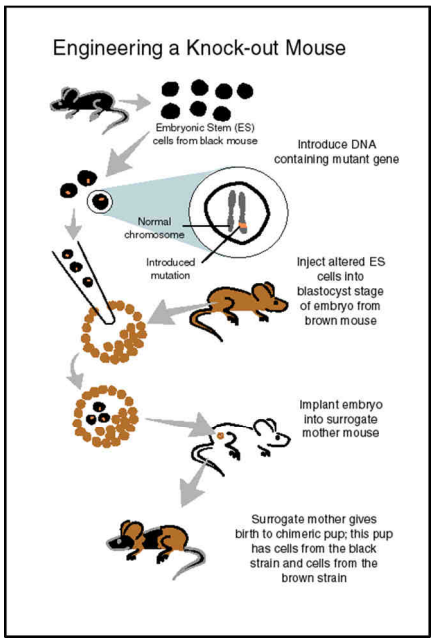

Figure 2.3: Simplified illustration of the knock out procedure (http://tinyurl.com/5sp2373). Embryonic stem cells (ES) are isolated from one mouse strain (black). The knockout vector (DNA containing mutant gene) is electroporated into the ES. Due to homologous recombination, the original chromosomal DNA sequence is replaced by an inoperable DNA sequence leading to a gene knockout. The recombinant ES are introduced into a blastocyst of a different mouse strain (brown). The blastocyst containing the recombinant ES is implanted into a surrogate mother mouse. The offspring are chimeric; they merge qualities of the donor (black) and the acceptor (brown) mouse strain, which is especially indicated by the color of the fur (black and brown).

The knockout vector pMlc1_KO_mod (Figure 2.3) created by Savira Ekawardhani (Ekawardhani, 2008) was used during the *Mlc1* knockout process, which was performed at the Institute for Clinical Neurobiology (head of department: Professor Michael Sendtner), SFB 581 "Molecular models for diseases of the nervous system", University of Würzburg, Germany. The subsequently described procedure was given as a courtesy of the Department of Clinical Neurobiology.

Procedure

Mouse embryonic fibroblasts (MEF) were seeded in 75 cm^2 cell culture flasks and incubated at 37 °C at 95 % O_2 / 5 % CO_2 in humidified air until they reached confluence. The MEF cells served as the attachment layer (so-called "feeder cells"). Murine embryonic stem cells (ES) from the 129/Ola mouse strain were seeded on top of the MEF layer and incubated for 96 h until they reached confluence. After 96 h, the ES–MEF matrix was trypsinized and the cell matrix detached from the flask bottom. The cell suspension was singularized by aspiration with a 25 ml serological pipette. For subsequent electroporation, the ratio of ES to MEF was determined. An aliquot of the ES–MEF suspension was transferred into a cuvette and electroporated with the knockout vector construct "pMlc1_KO_mod" (Figure 2.4).

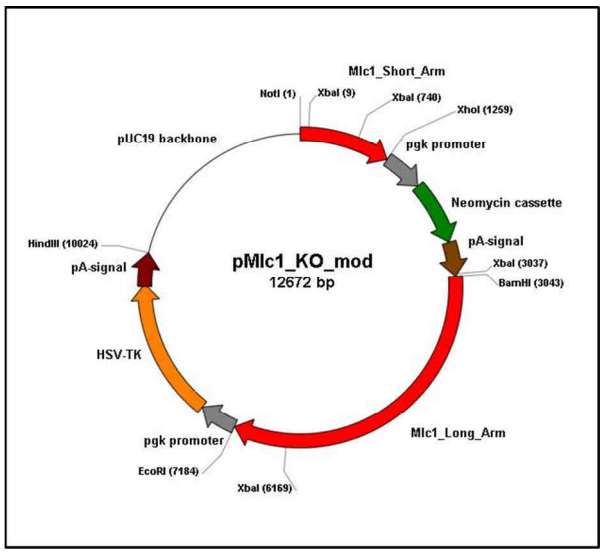

Figure 2.4: Validated *Mlc1* promoter construct pMlc1_KO_mod. The short arm of *Mlc1* encompasses the first and the second exons, the long arm intron three to intron five of *Mlc1* (Ekawardhani, 2008).

After electroporation, the cell suspension was plated into a 10 cm^2 petri dish that had been previously covered with MEF cells and supplied with the appropriate cell culture medium. The ES suspension was left overnight for attachment of the ES with the MEF matrix. The next day, the selection process with G418 was started. This selection process was repeated at least three times.

For positive selection, i.e. for validation of successful integration of the knockout construct into the genome, the neomycin (*NeoR*) resistance gene had been integrated into the knockout vector construct. By application of the antibiotic G418, recombinant embryonic stem cells could be selected from non-recombinant ones. For negative selection, i.e. if the presumed homologous recombination had occurred at the correct position in the mouse genome or not, the Herpes simplex virus thymidine kinase gene (*HSV-TK*) had been additionally integrated into the knockout construct. The application of the drug ganciclovir, an analogon of the nucleoside guanosine that by phosphorylation leads to the termination of DNA elongation, led to the elimination of those cells that had not inserted the knock out construct at the correct position in the mouse genome, i.e. non-homologous recombination (Figure 2.5).

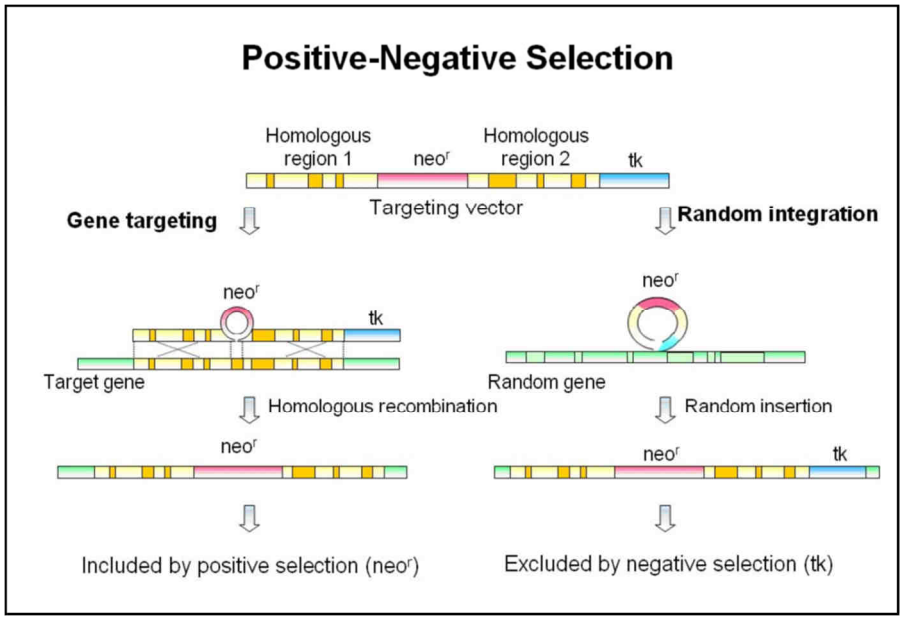

Figure 2.5: Integration of the knockout construct into the mouse genome (Tsai *et al.*, 2007). Left: homologous recombination with the neomycin resistance gene (neo^r) disrupting the gene of interest. Right: non-homologous recombination with complete insertion of the knockout construct including the tk gene.

Those ES that had survived the selection process (G418 and ganciclovir-resistant) were isolated and transferred to 96 well plates. Backups of the positively tested ES were transferred to a 24 well plate. Once the ES backup sample had reached confluence of 80 %, these cells were partially transferred to six well plates and ultra-deep frozen at -80 °C. The backup plates with the remaining ES that had presumably undergone homologous recombination were sent to our department for further verification and validation via genome integration-specific PCR.

2.16 PCR reactions on gDNA of ES

2.16.1 Estimation of ES gDNA amount by PCR on *Serpina6*

The total gDNA content from each well of the 96 well plates was below the measurement range of the spectrophotometer. A PCR reaction on the gene *Serpina6* was set up to validate the yield of the ES gDNA. Serpina6 is the major transport protein for glucocorticoids in the blood in most of the vertebrates. The PCR conditions were optimized on gDNA from C57BL/6 mice. After optimization, ES gDNA was taken as a template for PCR. C57BL/6 gDNA was used as a positive control, H_2O served as the negative control. The expected PCR product had a size of 300 bp.

- 5 µl of ES gDNA
- 10 pmol primer "mmCBG Exon 3 for"
- 10 pmol primer "mmCBG Exon 3 rev"
- 0.2 mM dNTPs
- 5 µl buffer B
- 1 U *Taq* – Polymerase

PCR conditions: 5 min at 94 °C for initial denaturation followed by 35 cycles (30 s at 94 °C, 30 s at 54 °C, 30 s at 72 °C) and a final extension step for 10 min at 72 °C.

PCR products were separated on a 1.5 % agarose gel at 140 V for 1.5 h.

2.16.2 Detection of aberrant *Mlc1* gDNA sequence into ES genome

A PCR reaction with pMlc1_KO_mod-specific primers was conducted to check, if recombination between the *Mlc1* knockout construct and the ES genome had occurred. Prior to PCR, the ES gDNA was isolated with the QIAamp DNA Micro Kit (Table 2.10) according to the manufacturer's protocol. The expected PCR product had a size of 430 bp. The subsequent description is valid for one single PCR reaction. Each PCR reaction was completed with H_2O until a total volume of 50 µl. As a positive control, 10 ng of pMlc1_KO_mod was used. H_20 served as a negative control.

- 10-20 ng of ES DNA
- 10 pmol "Mlc1 pgk prom f"
- 10 pmol "Neo 340 rev TK"
- 0.2 mM dNTPs
- 5 µl buffer B
- 1 U *Taq* – Polymerase

PCR conditions: 5 min at 94 °C for initial denaturation followed by 35 cycles (30 s at 94 °C, 30 s at 54 °C, 30 s at 72 °C) and a final extension step for 10 min at 72 °C.

PCR products were separated on a 1.5 % agarose gel at 140 V for 1.5 h.

2.16.3 Detection of homologous recombination of aberrant *Mlc1* into ES genome

Subsequent to the detection of aberrant *Mlc1* gDNA in the ES genome, the homologous recombination had to be verified. If homologous recombination of the aberrant *Mlc1* sequence and the ES genome had been successful, a positive clone would have been identified to continue with in the knockout process. To verify the success of the homologous recombination, a PCR with integration-specific primers was conducted. The forward primer binds in the ES genome, in 5' orientation to the putative integration site. The reverse primer binds to the phosphoglycerate kinase (pgk) promoter sequence (Figure 2.4). The pMlc1_KO_mod vector and H_2O served as negative controls. The expected product size was 1,398 bp.

- 10 – 20 ng of ES DNA
- 10 pmol primer “Mlc1 integ ef f”
- 10 pmol primer “Neo do3 rev SS”
- 0.2 mM dNTPs
- 5 µl buffer B
- 1 U *Taq* – Polymerase

PCR conditions: 5 min at 94 °C for initial denaturation followed by 35 cycles (30 s at 94 °C, 30 s at 52 - 58 °C, 30 s at 72 °C) and a final extension step for 10 min at 72 °C.

PCR products were separated on a 1.0 % agarose gel at 140 V for 1.5 h.

2.16.4 *In silico* predicition of miRNA target sites in 3’-UTRs of *MLC1* and *NR3C1*

The 3’-UTR of the human *MLC1* was investigated by the bioinformatic tool TargetScan human, release 5.1 (Table 2.12). Exactly one putative miRNA binding site (miR-137) was predicted for the 3’-UTRs of both, *MLC1* and *NR3C1* (Figure 2.6, http://tinyurl.com/3lbv7ag).

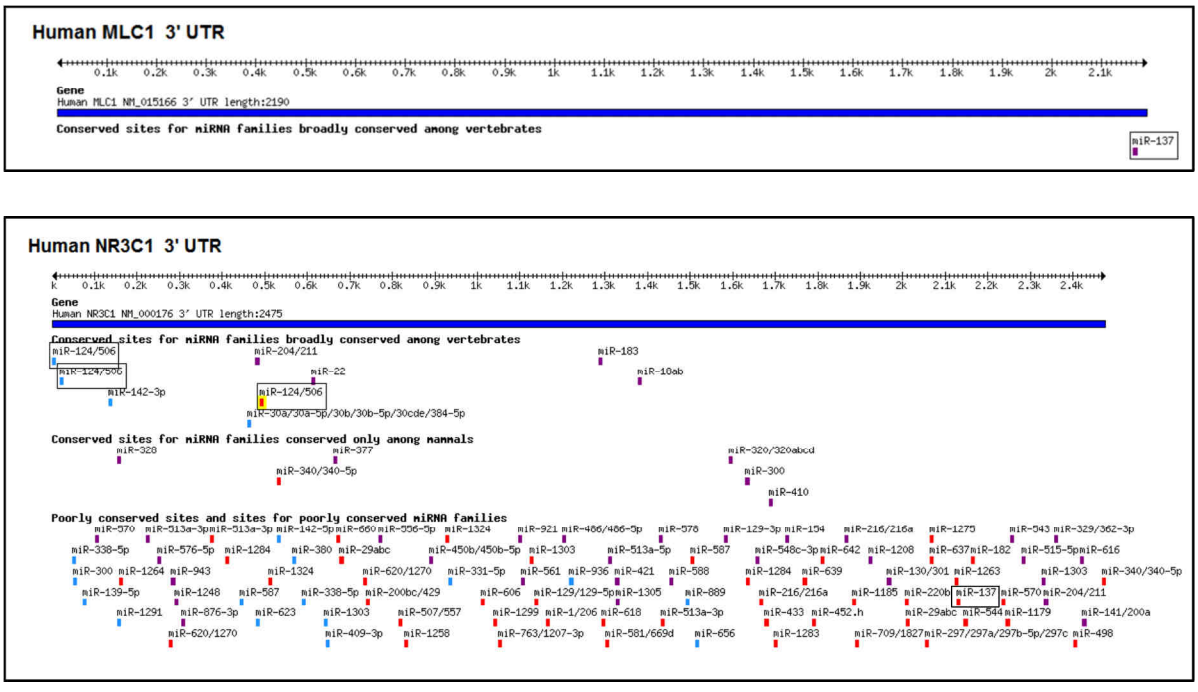

Figure 2.6: 3'-UTRs of *MLC1* and *NR3C1*. Only one target site (miR-137) was predicted for each gene (black box on right end of 3’-UTRs).

To verify a possible effect of miR-137 on *MLC1* and *NR3C1* translation, the miR-137 precursor molecule was transfected into SK-N-MC, U373MG and PC12 cells. As a negative control, miR-22 was used as no binding site for this miRNA has been predicted for *MLC1* and as it has been empirically proven not to affect *NR3C1* translation. As a positive control, miR-124 was applied as it has been empirically proven that this miRNA negatively affects *NR3C1* translation.

2.16.5 Heat inactivation of fetal calf (FCS) and horse serum (HS)

FCS is derived from new born calfs and is a mandatory component for cell culture work, as it contains high levels of growth factors. Pure FCS also contains high concentrations of complement system cells that disturb during cell culture work because they interact with alien cells and destroy them. The complement system cells are heat sensitive. Hence, the FCS bottle was placed in a water bath at 56 °C for 30 min and stirred regularly to degrade them. An extended incubation time at this temperature would lead to the degradation of growth factors, vitamins and amino acids.

2.16.6 Depletion of steroids in FCS and HS by charcoal filtering

The heat inactivated FCS and HS still contain high levels of steroids such as glucocorticoids and cholesterol. Endogenous glucocorticoids like cortisol bias cell culture experiments focusing on glucocorticoid expression and effects. The interference by glucocorticoids can be lowered to a minimum by depletion with charcoal (Roel de Rijk, personal communication). 10 g of charcoal were added to 500 ml heat-inactivated FCS and agitated overnight at 30 rpm and 4 °C. The next day, the serum was divided over sterile 50 ml tubes and centrifuged at 4,500 g for 10 min. The supernatant was filtered twice with sterilizing grade filters (0.1 µM) to remove to charcoal. The complete procedure was repeated once. The remaining and two times steroid-stripped FCS was aliquoted in sterile 50 ml tube and stored at -20 °C.

2.17 Cell culture experiments with miR-137, miR-22 and miR-124

SK-N-MC and U373MG

Aliquots of SK-N-MC and U373MG cells were taken from the liquid nitrogen storage and quickly thawed at 37 °C in a water bath and added to a 75 cm^2 cell culture flask containing DMEM High Glucose with 15 % (v/v) steroid-depleted FCS, 1 % (v/v) Penicillin / Streptomycin (P/S) and 1 % (v/v) GlutaMAX. After 24 h, the medium was completely removed and replaced to deplete the cell-toxic DMSO. U373MG and SK-N-SH cells were split at a confluence of 80 %. The complete medium was removed by a vacuum suction device. The cells were washed by adding 20 ml of PBS $^{-/-}$ and tilting the cell culture flask several times. The PBS $^{-/-}$ was removed and 3 ml of prewarmed Trypsin-EDTA was added to detach the cells from the bottom and to enable singularization. The cell culture flask was placed into the incubator at 37 °C and afterwards hit several times to support the cell detachment. The cells were supplied with 15 ml of DMEM High Glucose with 15 % (v/v) FCS, 1 % (v/v) P/S and 1 % (v/v) GlutaMAX. A part of the cell suspension was transferred to new cell culture flasks; the rest was centrifuged at 300 g and 4 °C for 10 min. The resulting pellets were resuspended in 1 ml freezing medium consisting of 70 % (v/v) DMEM High Glucose, 20 % (v/v) steroid-depleted FCS and 10 % (v/v) DMSO. The cell suspension was transferred to cryoconservation tubes and these were stored at -80 °C in a cryoconservation box enabling a cooling-down of 1 °C / min. The next day, the cryoconservation tubes were transferred to liquid nitrogen for long-term storage.

For experimental use, U373MG and SK-N-SH cells were seeded 24 h prior to transfection in cell culture plates containing six wells at a concentration of 5 x 10^5 cells per well and incubated in DMEM High Glucose containing 15 % (v/v) steroid-depleted FCS. Cells were incubated in humidified air with 5 % CO_2. After 20 h, the medium was removed and the cells were rinsed once with prewarmed PBS $^{-/-}$. The prewarmed PBS $^{-/-}$ was removed and 2 ml of serum-free DMEM High Glucose was added to each well. For transfection, the concentration of 100 µM miR-137, miR-22 and miR-124 was used. Transfection was done with Lipofectamine RNAiMAX according to the manufacturer's protocol exactly 24 h after seeding. 4 h after transfection, the serum-free medium was removed and 2 ml of prewarmed DMEM High Glucose containing 15 % (v/v) steroid-depleted FCS was added to each well. The medium of each well was renewed 24 and 48 h after transfection and replaced by DMEM

High Glucose supplemented with 15 % (v/v) steroid-depleted FCS, 1 % (v/v) GlutaMAX and 1 % (v/v) P/S. 72 h after transfection, the cells were harvested in 1 ml protein lysis buffer and stored on ice. Protein quantification was performed by applying the Bradford Assay using standard protocols.

PC12

PC12 cells derived from a rat pheochromocytoma (tumor of the renal medulla) and it has been proven to be an appropriate model system for the investigation of neuronal phenotypes (Martin and Grishanin, 2003). The application of nerve growth factor (NGF) leads to a differentiation of these cells into a neuronal phenotype. Aliquots of PC12 cells were taken from the liquid nitrogen storage and quickly thawed at 37 °C in a water bath and added to a 75 cm^2 collagen-coated cell culture flask containing RPMI-1640 with 10 % (v/v) steroid-depleted HS, 5 % (v/v) steroid-depleted FCS, 1 % (v/v) P/S and 1 % (v/v) GlutaMAX. 24 h later, the medium was completely removed and replaced to deplete the cell-toxic DMSO. PC12 cells were split at a confluence of 80 %. The complete medium was removed by a vacuum suction device. The cells were washed by adding 20 ml of $PBS^{-/-}$ and tilting the cell culture flask several times. The $PBS^{-/-}$ was removed and 3 ml of prewarmed Trypsin-EDTA was added to detach the cells from the bottom and to enable singularization. The cell culture flask was placed into the incubator at 37 °C and afterwards hit several times to support the cell detachment. 15 ml of RPMI-1640 with 10 % (v/v) steroid-depleted HS, 5 % (v/v) FCS, 1 % (v/v) P/S and 1 % (v/v) GlutaMAX was added to the cell culture flask. A part of the cell suspension was transferred to new cell culture flasks; the rest was centrifuged at 300 g and 4 °C for 10 min. The resulting pellets were resuspended in 1 ml freezing medium consisting of 70 % (v/v) DMEM High Glucose, 10 % (v/v) steroid-depleted HS, 5 % (v/v) steroid-depleted FCS and 10 % (v/v) DMSO. The cell suspension was transferred to cryoconservation tubes and put into a cryoconservation box at -80 °C enabling a cooling-down of 1 °C / min. The next day, the cryoconservation tubes were transferred to liquid nitrogen for long-term storage.

For experimental use, undifferentiated PC12 cells were seeded 24 h prior to transfection in collagen-coated cell culture plates containing six wells at a concentration of 5 x 10^5 cells per well and incubated in RPMI-1640 containing 10 % (v/v) steroid-depleted HS, 5 % (v/v)

steroid-depleted FCS, 1 % (v/v) P/S and 1 % (v/v) GlutaMAX. Cells were incubated in humidified air with 5 % CO_2. After 20 h, the medium was removed and the cells were rinsed once with prewarmed PBS $^{-/-}$. The prewarmed PBS $^{-/-}$ was removed and 2 ml of serum-free RPMI-1640 was added to each well. For differentiation of PC12 cells into a neuronal phenotype, 100 ng / ml NGF was added to each well and incubated for at least seven days. For transfection, the concentration of 100 µM miR-137, miR-22 and miR-124 was used. Transfection was done with Lipofectamine RNAiMAX according to the manufacturer's protocol exactly 24 h after seeding. 4 h after transfection, the serum-free medium was removed and 2 ml of prewarmed RPMI 1640 containing 10 % (v/v) steroid-depleted HS and 5 % (v/v) steroid-depleted FCS was added to each well. The medium of each well was renewed 24 and 48 h after transfection and replaced by DMEM High Glucose supplemented with 15 % (v/v) steroid-depleted FCS, 1 % (v/v) GlutaMAX and 1 % (v/v) P/S. 72 h after transfection, the cells were harvested in 1 ml protein lysis buffer and stored on ice. Protein quantification was performed applying the Bradford Assay using standard protocols.

2.17.1 Immunoblot analysis of miR-137, miR-22 and miR-124 effects on NR3C1 expression

The samples were all diluted to a total protein concentration of 1.5 µg / µl; 20 µg total protein of each sample was used for immunoblot analysis. Prior to gel loading, samples were denaturated with β-mercaptoethanol for 5 min at 94 °C. Proteins were separated via SDS-PAGE and subsequently transferred to a PVDF membrane. The blots were blocked for 1 h in TBST and 5 % (w/v) low-fat milk powder. The primary antibodies anti-MLC1 (1:200), anti-GRα (1:1000) and anti-α-tubulin (1:5000) were added after blocking for 2 h at room temperature (25 °C) or overnight at 4 °C. Blots were washed three times with TBST prior to incubation with horseradish peroxidase-conjugated secondary antibodies. Antibody binding was detected by enhanced chemiluminescence (ECL).

2.17.2 Amplification of *NR3C1* 3'-UTR fragment

For investigation of miRNA effects on the 3'-UTR of *NR3C1*, a 628 bp section of the 3'-UTR (Chr 5: 142.660.301 – 142.659.674, GRCh37) was amplified by PCR using primers

containing the recognition sites for the restriction enzymes *Spe*I (hsGR frag2 SpeI SacI miR183 - miR410 for) and *Sac*I (hsGR frag2 SpeI SacI miR183 - miR410 rev). Human gDNA was used as a template, H_2O served as a negative control. PCR reactions were accomplished in a total volume of 50 µl.

NR3C1 3'UTR 628 bp fragment PCR

- 100 ng human gDNA
- 10 pmol "hsGR frag2 SpeI SacI miR183 - miR410 for"
- 10 pmol „hsGR frag2 SpeI SacI miR183 - miR410 rev"
- 0.2 mM dNTPs
- 5 µl HF – buffer
- 1 U Phusion *Taq* Polymerase

PCR conditions: 5 min at 94 °C for initial denaturation followed by 25 cycles (30 s at 94 °C, 30 s at 60 °C, 30 s at 72 °C) and a final extension step for 5 min at 72 °C.

PCR products were separated on a 1.5 % agarose gel at 140 V for 1.5 h.

2.17.3 Verification of *NR3C1* 3'-UTR fragment by enzymatic restriction

The putative *NR3C1* fragment was extracted from the agarose gel applying the MinElute Gel Extraction Kit (Table 2.10) according to the manufacturer's protocol. The DNA yield was checked with the spectrophotometer Nanodrop ND-1000 (2.7.4). The DNA fragment was verified by an enzymatic restriction reaction with *Pst*I. The restriction reaction was carried out in a 1.5 ml reaction tube in a total volume of 20 µl. In the negative control, H_2O was used as the template.

Enzymatic restriction reaction of NR3C1 3'-UTR fragment

- template: 500 ng (5 µl) DNA from PCR reaction or H_2O
- 2 µl 10x MULTI-CORE buffer
- 0.5 µl *Pst*I (5 U / µl)
- 12.5 µl H_20

The reaction tube was centrifuged for 10 s at 10,000 g to concentrate the liquid in the bottom part of the tube. The reaction was carried out at 37 °C for 3 h in a water bath. The tube was taken out and centrifuged another time for 10 s at 10,000 g. The restriction reaction was stopped by incubation of the tube at 80 °C for 15 min. The reaction tube was centrifuged another time for 10 s at 10,000 g. The cleaved DNA fragment was loaded on a 1.5 % agarose gel and run at 140 V for 1.5 h to check if the restriction had worked properly. Two fragments were expected with a size of 442 and 186 bp.

2.17.4 Cloning of *NR3C1* 3'-UTR fragment into pMIR-REPORT vector

After verification of the *NR3C1* fragment (2.17.3), the pMIR-REPORT vector and the *NR3C1* fragment were cleaved with *Spe*I and *Sac*I simultaneously.

Enzymatic restriction reactions were accomplished in a volume of 20 µl in 1.5 ml reaction tubes. H_2O served as a negative control.

Restriction of *NR3C1* fragment & pMIR-REPORT

- 1 µg PCR product (*NR3C1* 3'-UTR) respectively pMIR-REPORT or H_2O
- 2 µl 10x MULTI-CORE buffer
- 0.5 µl each *Spe*I & *Sac*I (each 5 U / µl)
- filled up to 20 µl with H_2O

The enzymatic restriction reactions were carried out according to the conditions that were previously described. The cleaved DNA fragments were checked on a 1.5 % agarose gel at 140 V for 2 h. 100 ng of non-cleaved *NR3C1* fragment DNA and pMIR-REPORT were used as a control.

The cleaved pMIR-REPORT vector was treated with shrimp alkaline phosphatase (*SAP*). *SAP* dephosphorylates the 5' ends of nucleotides and prevents a religation of the linearized vector. The reaction volume was 20 µl.

SAP-treatment of *Spe*I and *Sac*I cleaved pMIR-REPORT

- 1 µg *Spe*I – *Sac*I cleaved pMIR-REPORT
- 2 µl 10x *SAP* reaction buffer
- 1 µl *SAP* (1 U / µl)
- 11 µl H2O

The reaction was carried out in a 1.5 ml reaction tube. The sample was quickly mixed and centrifuged for 10 s at 10,000 g and incubated at 37 °C for 30 min. The *SAP* was inactivated by incubation of the sample at 65 °C for 20 min.

For ligation of the insert DNA into the vector, the amounts of insert DNA and vector DNA were calculated according to this equation (Promega, Madison, USA).

$$\frac{\text{length of insert (kb)}}{\text{length of vector (kb)}} \times \text{ng of vector} = \text{ng of req. insert for a } 1{:}1 \text{ insert} - \text{vector ratio}$$

Ligations were set up in 1:1, 1:3 and 3:1 ratios. The ligation reactions were set up with the appropriate insert – vector DNA ratios, 2 µl of 10x Ligase Buffer, 1 µl T4 DNA Ligase (5 U / µl) and filled up with H_2O to a volume of 20 µl. The reaction samples were incubated at 16 °C overnight (12 – 16 h).

2.17.5 Transformation of pMIR_REPORT_*NR3C1* construct into bacterial strains TOP10 & XL10-Gold

The bacterial strains TOP10 and XL10-Gold are chemically competent: due to a prior chemical treatment, the bacterial cell walls are able to uptake exogenous DNA. From each of the bacterial strains, three 50 µl aliquots were taken and defrosted on ice and 10 µl of each ligation reaction (2.17.4) was added to each bacterial sample. A pure bacterial aliquot supplied with H_2O instead of the plasmid served as negative control. The bacteria – ligation mixes and the negative control were incubated for 30 min on ice, which was followed by a heat shock of 45 s at 42 °C. Immediately after the heat shock, bacteria – ligation mixes were

put on ice for 2–3 min. Subsequently, the samples were supplied with 300 µl prewarmed antibiotics-free LB medium (Table 2.5) and incubated in a rotating incubator for 1 h at 37 °C and 180 rounds per minute (rpm). 150 µl of the bacterial suspension was taken and spread over prewarmed LB agar plates (Table 2.5) containing 50 µg / ml ampicillin. The inoculated plates and a sterile one (further negative control) were placed into an incubator overnight (12–16 h) at 37 °C.

2.17.6 Inoculated agar plates & liquid bacterial cultures

The agar plates were checked 12–16 h after inoculation for bacterial colonies. The two negative controls (pure agar plate and bacteria transformed with H_2O) did not show any, the agar plates with an insert – vector ratio of 3:1 showed the most (both XL10-Gold and TOP10 cells). 22 colonies were chosen and transferred to a backup agar plate ("Master plate"). The same colonies were taken to set up liquid bacterial cultures by inoculating 2 ml of LB medium supplied with 50 µg / ml ampicillin as a selection marker. The liquid cultures were incubated for 16 h in a rotating incubator at 37 °C and 180 rpm. Those colonies that gave a positive signal in the colony PCR (2.17.7) were collected, negative colonies were discarded. After 16 h, 500 µl of the densely grown bacterial cultures was properly mixed with 700 µl sterile glycerol in a 1.5 ml cryoconservation tube and stored in an ultra-deep freezer at -80 °C. 500 µl of the bacterial culture was taken as a starter for the inoculation of 100 ml LB medium supplied with 50 µg /ml ampicillin. 16 h after inoculation, the pMIR-REPORT construct was extracted by using the QIAGEN Plasmid Maxi Kit (Table 2.10) according to the manufacturer's protocol.

2.17.7 Colony PCR on selected bacterial colonies

The colony PCR is a favorable and time-efficient method to verify and validate the ligation and transformation process. A PCR reaction with a colony as a template that contains the cloned fragment ("positive colonies") would show the expected band size on the agarose gel. Negative colonies will either show no fragment or a fragment of aberrant size. The 22 colonies from the backup plate (2.17.6) were used as templates for the PCR reactions. The

expected fragment size was 915 bp (287 bp from the vector sequence plus 628 bp from the *NR3C1* 3'-UTR fragment). Two negative controls were used, the empty pMIR-REPORT DNA and H_2O. The templates were added to the previously created PCR master mix.

Colony PCR on pMIR-REPORT *NR3C1* 3'-UTR transformed bacteria

- bacterial colony as template selected with a pipette tip
- 10 pmol primer "Seq_pMIR_REPORT_for_TK"
- 10 pmol primer "Seq_pMIR_REPORT_rev_TK"
- 0.2 mM dNTPs
- 5 µl HF – buffer
- 1 U Phusion *Taq* Polymerase
- filled up with H_2O until 50 µl

PCR conditions: 2 min at 94 °C for initial denaturation followed by 25 cycles (30 s at 94 °C, 30 s at 56 °C, 30 s at 72 °C) and a final extension step for 5 min at 72 °C.

PCR products were separated on a 1.5 % agarose gel at 140 V for 1.5 h.

2.17.8 Quantification of immunoblot signals

The films were scanned and optical density of each band was evaluated using the Image J Software (Image J Gel Analysis method). Optical density of each band was divided by the respective α-tubulin band (relative optical density ratio).

2.18 Investigation of *C15orf53* in BD and SCZD10 patients

A fine-mapping on seven families segregating SCZD10 by Savira Ekawardhani revealed a segregating genomic area on chromosome 15q14-15.1 (Ekawardhani, 2008). Two genome-wide association studies by Ferreira and colleagues (Ferreira *et al.*, 2008) and Smith and colleagues (Smith *et al.*, 2009) identified independently from each other an association signal amongst others on chromosome 15q14 in the gene *C15orf53*. The segregating region in our

seven SCZD10 multiplex families contains four genes (*SPRED1, FAM98B, RASGRP1* and *C15orf53*), whereof *C15orf53* and *SPRED1* were further investigated. Results of the investigation on *SPRED1* were explicitly described in the dissertation of Savira Ekawardhani (Ekawardhani, 2008). In this study, we investigated 203 BD-affected individuals, 71 SCZD10-affected individuals and 230 healthy control individuals with no psychiatric history; additionally, we investigated our seven SCZD10 multiplex families containing 30 SCZD10-affected family members (Figure 2.2).

2.18.1 Mutational analysis of *C15orf53*

Primers encompassing the proximal promoter region, 5'-UTR, coding regions and intron-exon boundaries of *C15orf53* were used for genomic DNA amplification. Two affected members from family 11 (F11, 7 SCZD10-affected in total) and one from family 9 (F9, 5 SCZD10-affected in total) were used for further mutational analysis of *SPRED1* (Ekawardhani, 2008). For mutational analysis of *C15orf53*, seven patients (one from each SCZD10-affected family) were examined. For mutational analysis of *SPRED1* and *C15orf53*, a 50 µl PCR reaction containing 100 ng of SCZD10 affected patient's genomic DNA, 10 pmol gene specific primers, 200 µM dNTPs, 0.75 to 1.5 mM $MgCl_2$, 50 mM KCl, 10 mM Tris-HCl (pH 8.3 at 25 °C), 0.0025 mg/ml BSA, 0.25 % Tween-20 and 1 U of *Taq* Polymerase was conducted. Amplicons were separated on a 2 % agarose gel, purified using a gel purification kit and directly sequenced. Sequencing reactions were performed for both DNA strands with the sequencing primers (2.11.3) using the CEQ DTCS Quick Start Kit according to the manufacturer's protocol and analyzed using the ChromasLite program and the reference sequence from the Ensembl genome browser.

2.18.2 Genotyping of *C15orf53* in SCZD10 and BD individual samples and SCZD10 families

For genotyping, we chose three SNPs in *C15orf53*, namely rs7171233, rs7165988 and rs2172835. PCR reactions of the genomic regions encompassing these SNPs were carried out in a total volume of 50 µl with 100 ng of genomic DNA, 10 pmol of each primer, 200 µM dNTPs, 2.0 or 2.5 mM $MgCl_2$, 50 mM KCl, 10 mM Tris-HCl (pH 8.3 at 25 °C), 0.0025 mg/ml

BSA, 0.25 % Tween-20 and 2.5 U Taq Polymerase and 5 % (v/v) dimethylsulfoxide (DMSO). All PCR reactions were performed in a Multigene-Thermocyler TC9600. Conditions for PCR reactions were: 5 min at 94 C followed by 40 cycles (45 s at 94 °C, 45 s at 56 °C or 58 °C, 45 s at 72 °C) and a final extension for 7 min at 72 °C. PCR products were separated and visualized on a 1.5 % agarose gel. The subsequent genotypes of the SNPs rs7171233 and rs7165988 were determined by restriction digestion with *Rsa*I and those of SNP rs2172835 with *Hin*1II, all incubated at 37 °C for 4 h. Restriction products were separated and visualized on 2 % agarose gels.

2.18.3 Case-control association analysis of *C15orf53* with BD and SCZD10

Linkage disequilibrium (LD) among the previously described SNPs was determined and haplotypes were estimated using Haploview Version 4.2, (Barrett *et al.*, 2005) (2.14.2). Only haplotypes with a frequency above two percent were included in the analysis. We tested the haplotypes for association in a case-control design for the following groups: a) BD-affected (203 subjects) versus controls (230 subjects), b) SCZD10-affected (71 subjects) versus controls, c) pooled sample of BD and SCZD10-affected (274 subjects) versus controls.

2.18.4 *C15orf53* gene expression analysis in human *post-mortem* brain tissue and leukocyte subpopulations

For cDNA synthesis, total RNA was isolated from human *post-mortem* limbic brain tissues of six patients (2.7). Furthermore, total RNA was isolated from $CD4^+$, $CD8^+$, $CD14^+$, $CD19^+$ positive cells and peripheral blood mononuclear cells (PBMCs) derived from fresh blood of one healthy donor. The cDNA from *post-mortem* Thai brain regions and 40 cell lines was given as a courtesy by Claude P. Muller and Jonathan D. Turner from the Laboratoire National de Santé, Luxembourg-City, Luxembourg. MACS MicroBeads Kits were used for the enrichment of the appropriate leukocyte subpopulations. Total RNA was purified with the High Pure RNA Isolation Kit by following the manufacturer's instructions. The cDNA was synthesized using the iScript cDNA synthesis kit. Both, total RNA isolation and cDNA synthesis were accomplished according to the manufacturers' protocols. Quantitative PCRs

(qPCR) on *C15orf53* with exon-spanning primers (Table 2.7) were performed in duplicates; Glyceraldehyde-3-phosphate dehydrogenase (*GAPDH*) expression was measured and included as an internal control. The qPCR reactions were conducted in a total volume of 25 µl containing 50 mM KCl, 200 mM dNTPs, 20 mM Tris-HCl (pH 8.3 at 25 °C), 2.5 U Platinum Taq Polymerase and 1x concentrated SYBR green I. The thermal cycling was carried out in a DNA Engine Opticon 2. The cycling conditions for *C15orf53* were as follows: 2 min at 95 °C followed by 44 cycles (20 s at 95 °C, 25 s at 71 °C, 20 s at 72 °C); for *GAPDH:* 2 min at 95 °C followed by 44 cycles (20 s at 95 °C, 25 s at 60 °C, 20 s at 72 °C). The qPCR products were separated and visualized on a 2 % agarose gel. The amplified fragments were directly sequenced and confirmed.

2.19 Association study of the human oxytocin receptor (*OXTR*) with ASD

We investigated 203 children diagnosed with ASD and 356 parents without any psychiatric history. Five SNPs located in *OXTR* (rs237897, rs237889, rs2254298, rs2268494 and rs4686302) were genotyped. All of these SNPs except rs4686302 are located in the non-coding genomic area (Intron 3) of *OXTR*. The SNP rs4686302 is located in the coding genomic area (Exon 3) and leads to a non-synonymous amino acid exchange (Ala218Thr). The genotyping process consisted of two steps: The first step was the amplification of the genomic region encompassing the SNPs. The second step was the SNP analysis, a process that is based on the principles of the dye-terminator sequencing. The association analysis was performed by Christine M. Freitag and colleagues from the Department of Child and Adolescent Psychiatry, Saarland University Hospital, Homburg, Germany and at the Department of Child and Adolescent Psychiatry, Psychosomatics and Psychotherapy, Johann Wolfgang von Goethe University, Frankfurt/Main, Germany.

2.19.1 PCRs of SNP-encompassing genomic regions in *OXTR*

Three different PCR reactions were carried out to amplify the genomic regions containing the SNPs. All PCR reactions were performed in a total volume of 25 µl with 0.2 mM dNTPs,

1 U Taq Polymerase and 100 ng genomic DNA. As a negative control, H_2O was used. The PCR products were separated on a 1.5% agarose gel for 1.5 h.

PCR 1 (rs237889 – rs2254298 – rs2268494)

- 3 mM $MgCl_2$
- 1 pmol primer "hsOXTR 4 SNPs Intron 3 for"
- 1 pmol primer "hsOXTR 4 SNPs Intron 3 rev"

Cycling program: 5 min at 94 °C for initial denaturation followed by 40 cycles (30 s at 94 °C, 30 s at 67.5 °C, 30 s at 72 °C) and a final extension step for 10 min at 72 °C. The PCR product had a size of 840 bp.

PCR 2 (rs4686302)

- 1 mM $MgCl_2$
- 7.5 pmol "hsOXTR rs4686302 ns Exon 3 for"
- 7.5 pmol "hsOXTR rs4686302 ns Exon 3 rev"

Cycling program: 5 min at 94 °C for initial denaturation followed by 35 cycles (30 s at 94 °C, 30 s at 63.2 °C, 30 s at 72 °C) and a final extension step for 10 min at 72 °C. The PCR product had a size of 199 bp.

PCR 3 (rs237897)

- 1 mM $MgCl_2$
- 7.5 pmol primer "hsOXTR rs237897 Intron 3 nfor"
- 7.5 pmol primer „hsOXTR rs237897 Intron 3 nrev"

Cycling program: 5 min at 94 °C for initial denaturation followed by 35 cycles (30 s at 94 °C, 30 s at 59 °C, 30 s at 72 °C) and a final extension step for 10 min at 72 °C. The PCR product had a size of 191 bp.

2.19.2 *Exo-SAP*-procedure

The PCR products were purified for further analysis. Remaining dNTPs and oligonuleotides, which appear as cloud-like structures on agarose gels, would have disturbed the subsequent SNP reaction. This was achieved by treatment of the samples with *Exonuclease I* (*Exo*) and shrimp alkaline phosphatase (*SAP*). *Exo I* degrades single-stranded DNA (oligonucleotides). *SAP* dephosphorylates the 5'- ends of nucleotides (dNTPs). The PCR products were pooled for the *Exo-SAP*-procedure.

Exo-SAP-Mastermix for 10 samples

- 0.5 µl *Exonuclease I* (20 U / µl)
- 5 µl *SAP* (1 U / µl)
- 44.5 µl H_2O

Exo-SAP and PCR products mix

3.25 µl PCR product of PCR 1
4 µl PCR product of PCR 2
4 µl PCR product of PCR 3
5 µl of *Exo-SAP*-Mastermix

Thermocycling conditions: samples were incubated for 60 min at 37 °C followed by a heat inactivation process of 15 min at 80 °C.

The quality of the *Exo-SAP*-procedure was checked by separation of 2 µl of each sample on a 1.5 % agarose gel for 1.5 h.

2.19.3 Single base extension procedure ("SNP reaction")

The *Exo-SAP* and quality-checked samples were taken for single base extension reaction. In a PCR-like reaction, the DNA is heat-denatured and unlabeled interrogation primers hybridize to the template. The interrogation primers hybridize exactly up to one base prior to the SNP position (Figure 2.7).

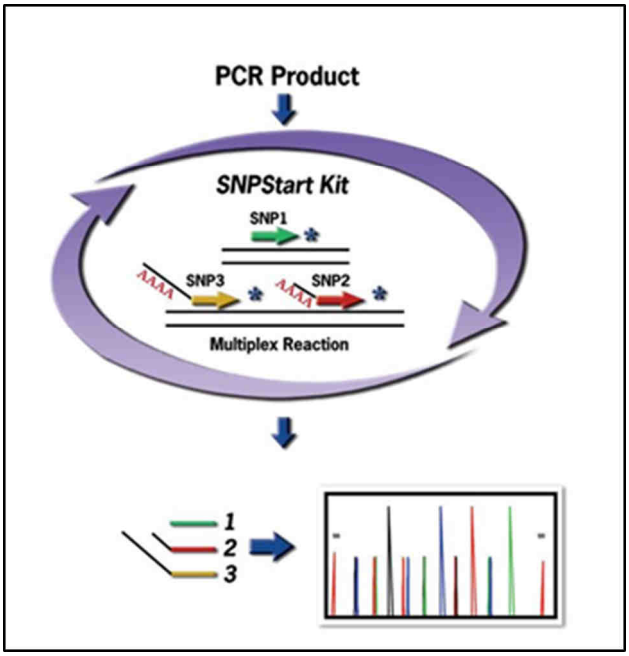

Figure 2.7: Workflow of the single-base extension procedure. The genomic region of interest is amplified via qualitative PCR. The interrogation primers (differing from one another in length) hybridize to their specific target. The SNPStart Kit contains the DNA-Polymerase and the fluorescent dye labeled terminators (asterisks), which are integrated at the 3'– end of the interrogation primer according to the template. In downstream analysis, the single SNPs can be distinguished due to their specific size and dyes (peaks). (BeckmanCoulter, Brea, USA).

The interrogation primers were extended with exactly one base according to the SNP that is encoded on the template by fluorescent dye-labeled terminators (ddNTPs). The different primers were supplied with an adenine stretch at their 3'- end to enable multiplex detection and reaction (2.11.2). The interrogation primers for the different SNPs were pooled prior to use.

Single base reaction

- 1 µl of *Exo-SAP*-treated PCR product mix
- 1 µl interrogation primer pool (1 pmol each)
- 2 µl SNP Start Master Mix
- 6 µl H_2O

Thermocycling conditions: samples were incubated for 10 s at 94 °C and for 20 s at 60 °C. In total, 27 cycles were accomplished.

2.19.4 Purification of the single base reaction products with *SAP*

The reaction products were treated with *SAP* to dephosporylate the 5'- ends of the remaining dye labeled terminators to prevent interference in downstream analysis. Prior to use, a *SAP*-Mastermix was created.

SAP-Mastermix for 10 samples

- 2.5 µl *SAP*
- 13 µl *SAP* buffer
- 14.5 µl H_2O

From this mastermix, 3 µl was added to each single sample.

Thermocycling conditions: samples were incubated for 45 min at 37 °C followed by a heat inactivation process of 15 min at 65 °C.

2.19.5 SNP detection with the CEQ 8000

For SNP detection, the purified samples had to be mixed with a size standard and sample loading solution (SLS) and a drop of mineral oil to prevent evaporation.

Mix for SNP detection

- 1.5 µl of SNP reaction product
- 0.5 µl of size standard 80
- 38 µl of SLS
- 1 drop of mineral oil

The "SNP-1" program of the Beckman CEQ 8000 operating software was used for SNP detection. For 96 samples, the SNP detection process took about 8 h. The raw data was processed with the operating software and SNPs with ambiguous results were manually checked. For further statistical processing, the genotypes were transferred to an Excel file.

2.20 Statistics

2.20.1 Haploview 4.2

Haploview is a software that enables association analyses including visualization (LD plots) of genetic markers such as SNPs in studies designed as either a transmission-disequilibrium-test (TDT) or case-control study (Barrett *et al.*, 2005). This software mandatory needs complete trios consisting of both parents and the affected child for association tests. In statistical terms, Haploview applies the McNemar-Test (McNemar, 1947) for paired samples, where differences of observed and expected frequencies (e.g. alleles) are calculated by χ^2 statistics. The 95 % quantile of the χ^2 distribution with one degree of freedom is 3.84. If the level of significance is set to 5 %, an association is achieved once the value surpasses 3.84. For the association analysis of *C15orf53* (2.18.3), the parameters were set to "case-control data" and "standard TDT". The other parameters were left on their default settings. Haplotypes with an abundance of less than 2 % were excluded. Haploview depicts the haplotype frequencies within the complete investigated sample in percent (haplotype frequencies) as well as the distribution of the haplotype among cases and controls (frequencies cases, controls). The LD plot outputs were set to show the correlation coefficient values between the single genetic markers (r^2) or the D prime (D').

2.20.2 UNPHASED

The software UNPHASED works similar to Haploview. The main difference is its ability to use incomplete trios (Dudbridge, 2008). The missing genotypes are simulated, based on the estimated ones, to have complete trios available for association testing. The statistical procedure of UNPHASED is the so-called Likelihood ratio, which results from the difference of the Log-Likelihoods of null and alternative hypothesis multiplied by minus two. The interpretation of the results is analogous to those of Haploview.

2.20.3 One way analysis of variance (one way ANOVA)

The one way ANOVA was applied as the appropriate statistical procedure to compare the means of the samples derived from cell culture experiments (3.2.4).

3 Results

3.1 *C15orf53* as a candidate gene for the etiology of BD and SCZD10

Previous studies in our department confined a region on chromosome 15q14-15.1 in the multiplex families segregating SCZD10 (Ekawardhani, 2008). A GWAS on BD with 4,387 cases and 6,209 controls identified a strong association in an area containing only four genes (*SPRED1, FAM98B, RASGRP1* and *C15orf53*). On chromosome 15q14, the highest association signal was detected in *C15orf53* (rs2172835, $p = 7.5 \times 10^{-7}$) (Ferreira *et al.*, 2008). Smith and colleagues confirmed this finding in their GWAS on European American and African American individuals (Smith *et al.*, 2009). These findings initiated our interest to fathom this gene within our SCZD10 multiplex families as well as the non-related BD and SCZD10 individual samples, in order to elucidate a potential contribution to the etiology of BD and SCZD10.

3.1.1 Mutational analysis of *C15orf53*

From each of the seven multiplex SCZD10 families, one affected individual was taken for mutational analysis (experimental work accomplished by Ulrike Schuelter). No mutations in exons or splice donor and acceptor sites were found. Only SNPs that were already annotated in the Ensembl database (release 56, May 2009) were found during sequencing, among those the promoter SNP rs7171233 (T/A), the SNP in Exon 1, rs7165988 (T/A) and the SNP in Intron 1, rs2172835 (C/T), which yielded in two different haplotypes; these SNPs were taken for a segregation analysis in our seven SCZD10 families.

3.1.2 Segregation analysis of *C15orf53* haplotypes in multiplex SCZD10 families

The genotyping of the three SNPs, rs7171233 (T/A), rs7165988 (C/G) and rs2172835 (C/T) in our candidate gene *C15orf53* in multiplex family members with SCZD10 revealed two

haplotypes, T-C-C and A-G-T, while no other haplotypes were observed (experimental work accomplished by Michelle Lin and Hans Bauer) (Table 3.1).

Table 3.1: Segregation analysis in SCZD10-affected large families. Within the SCZD10-affected members of all investigated families, the common haplotype (T-C-C) segregated in three (F13, F19, F24), the rare haplotype (A-G-T) in four (F5, F9, F11, F17) of the families.

Family	* non-affected / affected	segregating haplotype in SCZD10 affected individuals
F5	1 / 4	A - G - T
F9	8 / 5	A - G - T
F11	14 / 7	A - G - T
F17	6 / 4	A - G - T
F13	3 / 3	T - C - C
F19	2 / 3	T - C - C
F24	7 / 4	T - C - C

* All mentioned individuals (non-affected / affected) were available at the date of DNA sampling

The common haplotype T-C-C co-segregated in three families (F13, F19, F24) with SCZD10. The rare haplotype A-G-T segregated in the other four families (F5, F9, F11 and F17).

3.1.3 Case-control association analysis and LD of *C15orf53* in BD and SCZD10 samples

The three investigated SNPs, rs7171233 (T/A), rs7165988 (C/G) and rs2172835 (C/T) that were previously identified by segregation analysis in our SCZD10 pedigrees, were in high LD in each investigated cohort (BD & SCZD10 patients) and the combined samples (Figure 3.1).

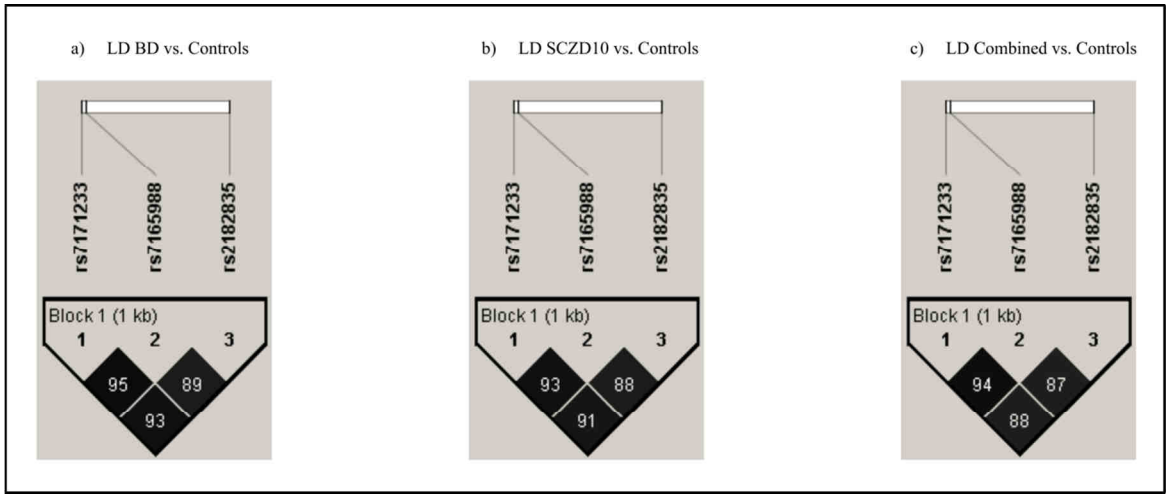

Figure 3.1: Linkage disequilibrium (LD) between investigated loci in the a) BD, b) SCZD10 and c) combined sample vs. control sample. In all three samples, the SNPs were in high LD to each other (r^2 values depicted).

Within all three cohorts, the common haplotype T-C-C was prevalent with more than 61 % and the rare haplotype A-G-T showed a prevalence of about 32 % (Table 3.2). The T variant of rs7171233 and the C variants of rs7165988 and rs2172835 represent the major alleles according to the most recent HapMap-CEU data (HapMap Public Release #28, August 2010).

Table 3.2: Segregating haplotypes of *C15orf53* in case-control samples. Among all investigated samples, the haplotype frequency was very similar. Both haplotypes showed a similar distribution within the BD and SCZD10 samples and the combination of both. None of them was associated with BD or SCZD10. Haplotypes with an abundance of less than 2 % are not depicted.

(a) BD versus controls

Haplotypes	Haplotype frequencies	Frequencies Cases, Controls	Chi Square	p-value
Block 1				
T - C - C	0.640	268.0 : 134.0, 288.0 : 172.0	1.546	0.2137
A - G - T	0.329	124.9 : 277.1, 158.9 : 301.1	1.164	0.2806

(b) SCZD10 versus controls

Haplotypes	Haplotype frequencies	Frequencies Cases, Controls	Chi Square	p-value
Block 1				
T - C - C	0.614	82.0 : 60.0, 287.9 : 172.1	1.077	0.2993
A - G - T	0.350	52.0 : 90.0, 158.9 : 301.1	0.206	0.6502

(c) Combined samples versus controls

Haplotypes	Haplotype frequencies	Frequencies Cases, Controls	Chi Square	p-value
Block 1				
T - C - C	0.633	349.0 : 195.0, 286.9 : 173.1	0.337	0.5616
A - G - T	0.334	176.9 : 367.1, 158.9 : 301.1	0.456	0.4997

We tested *C15orf53* haplotypes for association in 203 patients diagnosed with BD and 71 patients diagnosed with SCZD10 and the pooled SCZD10 and BD samples (n = 274) versus 230 controls without any psychiatric history. None of the haplotypes showed significant association. No deviation from Hardy-Weinberg-Equilibrium was found for any of the three variants in the patients groups or in the control group. None of the single markers showed significant association with BD, SCZD10 or the combination of both phenotypes.

3.1.4 *C15orf53* is expressed in human immune cell lines but not in CNS-derived cell lines and human *post-mortem* brain tissues.

Since hardly any information was available about *C15orf53*, gene expression analyses were accomplished on cDNA derived from human immune and CNS-derived cell lines as well as human *post-mortem* brain tissues (Figure 3.2).

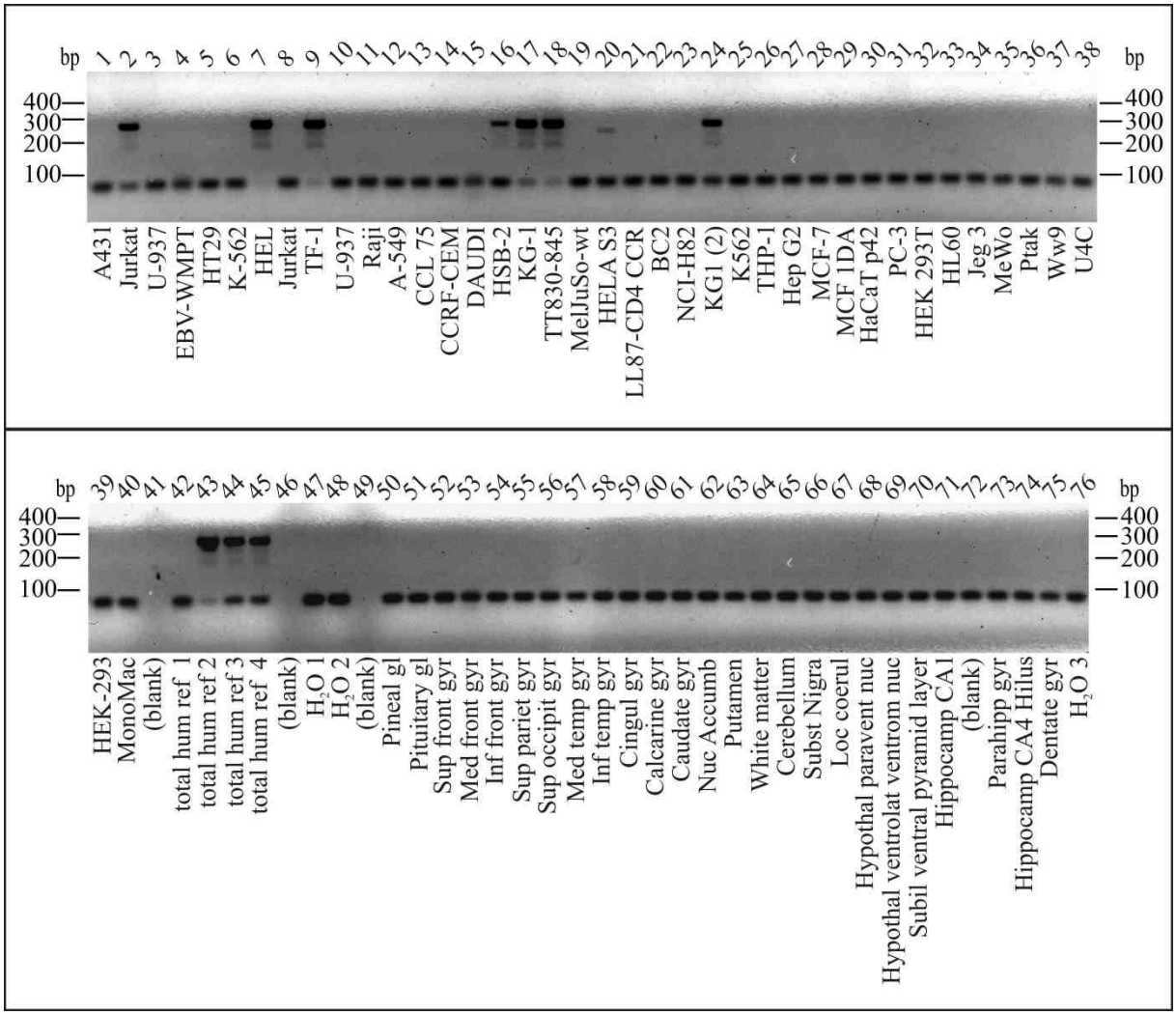

Figure 3.2: *C15orf53* gene expression analysis in 40 human cell lines and 25 human *post-mortem* brain areas. The PCR products were derived from a quantitative PCR reaction; 10 µl of each sample were loaded on a 2 % agarose gel. The following samples showed *C15orf53* gene expression (product size: 293 bp, from left to right): Jurkat, HEL, TF-1, HSB-2, KG-1, TT830-845, KG1 (2) and the positive controls (total human reference cDNA: 43-45). None of the human *post-mortem* brain samples (50-75) showed *C15orf53* gene expression. The negative controls (H_2O: 47, 48 and 76) did not give any signal. Top: running sample numbers. Bottom: sample identification.

C15orf53 expression occurred exclusively in cell lines that are involved in erythropoiesis and derived from the immune system. None of the other cell lines showed any expression of *C15orf53*. Only one of the Jurkat samples (2, 8) revealed *C15orf53* gene expression (2).

Taken into account that all the other immune-cell derived cell lines revealed *C15orf53* gene expression, the most likely explanation for the lack of signal is a technical mistake. From the four positive controls (total human reference cDNA), three were *C15orf53*-positive (43, 44, 45) and one was not (42). As previously described, a technical mistake is the most probable explanation for the lack of signal in sample 42. All negative controls (H_2O) confirmed the accuracy of the PCR reaction (47, 48 and 76). All investigated samples expressing *C15orf53* additionally show by-products at lower sizes on the agarose gel.

A further experiment was conducted to replicate these findings of *C15orf53*-positive cell lines. Furthermore, CNS-derived cell lines (SK-N-SH and U373MG) and human *post-mortem* limbic brain tissues from six Caucasian donors, free of CNS diseases and without any history of long-term psychotropic medication, were tested for *C15orf53* gene expression.

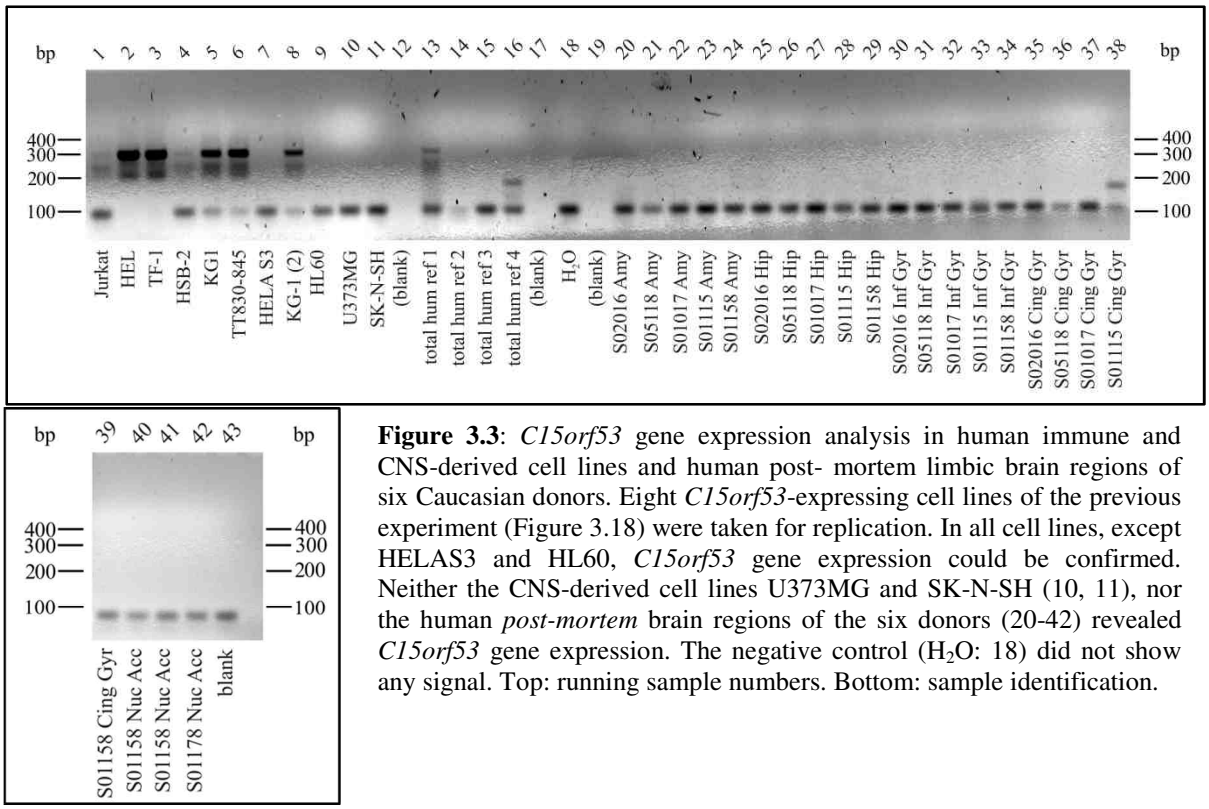

Figure 3.3: *C15orf53* gene expression analysis in human immune and CNS-derived cell lines and human post- mortem limbic brain regions of six Caucasian donors. Eight *C15orf53*-expressing cell lines of the previous experiment (Figure 3.18) were taken for replication. In all cell lines, except HELAS3 and HL60, *C15orf53* gene expression could be confirmed. Neither the CNS-derived cell lines U373MG and SK-N-SH (10, 11), nor the human *post-mortem* brain regions of the six donors (20-42) revealed *C15orf53* gene expression. The negative control (H_2O: 18) did not show any signal. Top: running sample numbers. Bottom: sample identification.

Eight of the ten investigated cell lines showed expression of *C15orf53*. The cell lines HEL, TF-1, KG 1 (two samples) and TT830-845 gave the highest signals on the agarose gel. Jurkat and HSB-2 showed a faint signal and HELA S3, HL60, U373MG and SK-N-SH did not reveal any *C15orf53* gene expression. The results from the immune cell lines in this experiment match with the previous ones. The HELA S3 sample was tested once again

because in the previous experiment, an ambiguous single band of about 200 to 250 bp (Figure 3.2: 20) occurred. In the present experiment, HELA S3 did not show *C15orf53* gene expression (Figure 3.3: 7) once again. The cDNA of the cell lines U373MG and SK-N-SH were tested to check, if *C15orf53* is expressed in CNS-derived tissues. Both cell lines did not express *C15orf53* (10, 11). From the four positive controls (total human reference cDNA: 13-16), only the first (13) yielded a *C15orf53*-positive signal. The fourth positive control (16) resulted in an ambiguous signal due to its lower size than expected. None of the human *post-mortem* limbic brain samples (20-42) showed any expression of *C15orf53*. One cingulate gyrus sample (38) yielded a by-product of 150 bp. The negative control (H_2O: 18) did not give any signal, which confirmed the accuracy of the PCR reactions.

3.1.5 *C15orf53* is not expressed in PBMCs of day profile blood and TSST samples.

Previous experiments have demonstrated that *C15orf53* gene expression is detectable in various human immune cell lines. In a further experiment, we drew 1 ml of whole blood each 15 min from one subject, starting at 07:45 a.m. and ending at 04:00 p.m. (36 samples). In addition, 1 ml of whole blood samples from one subject that had undergone the Trier Social Stress Test (TSST) were collected (14 samples). PBMCs were isolated from all collected samples and tested for *C15orf53* gene expression. The hypothesis should be tested, if *C15orf53* gene expression changes over time in PBCMs.

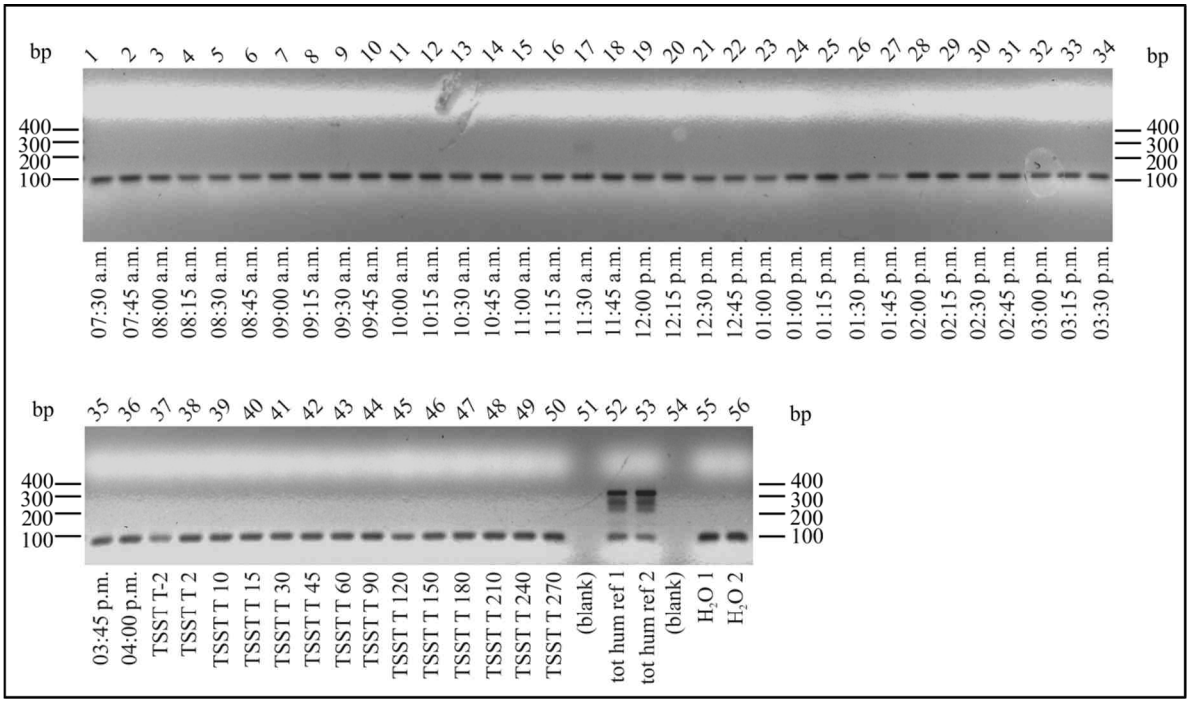

Figure 3.4: No gene expression of *C15orf53* in PBMCs of day profile and TSST blood samples. None of the day profile samples showed any *C15orf53* expression; the blood samples were drawn each 15 min (1-36). Prior to TSST start, one baseline blood sample was drawn (37) followed by further blood samples that had been collected at the indicated times after TSST start (38-50). The positive controls (total human reference cDNA: 52, 53) revealed *C15orf53* gene expression. The negative control (H_2O: 55, 56) samples did not give any signals.

C15orf53 was not expressed in any of the investigated samples with exception of the positive controls (total human reference cDNA: 52, 53). The negative controls (H_2O: 55, 56) confirmed the accuracy of the PCR reaction. Previous successful experiments with the day profile and the TSST samples had confirmed the cDNA integrity (John D. Turner, personal communication). Possibly, the gene expression of *C15orf53* in PBMCs was extremely low and the low-abundant transcripts could not be isolated successfully. The hypothesis for the next experiment was to investigate, whether an increase of the amount of leukocyte subpopulations cDNA leads to the detection of *C15orf53* gene expression.

3.1.6 Human leukocyte subpopulations express *C15orf53*

In the subsequent experiment, 10 ml whole blood of one donor instead of just 1 ml was drawn to increase the total amount of leukocytes and thus the chance of detecting *C15orf53* gene expression. PBMCs, $CD4^+$, $CD8^+$, $CD14^+$ and $CD19^+$ positive cells were isolated. From each of the leukocyte subpopulations, total RNA was isolated and converted into cDNA. The

cDNA of the subpopulations were tested for gene expression of *C15orf53*, together with five human *post-mortem* limbic brain tissues. *GAPDH* gene expression was additionally tested for each of the leukocyte subpopulations and brain tissues (Figure 3.5).

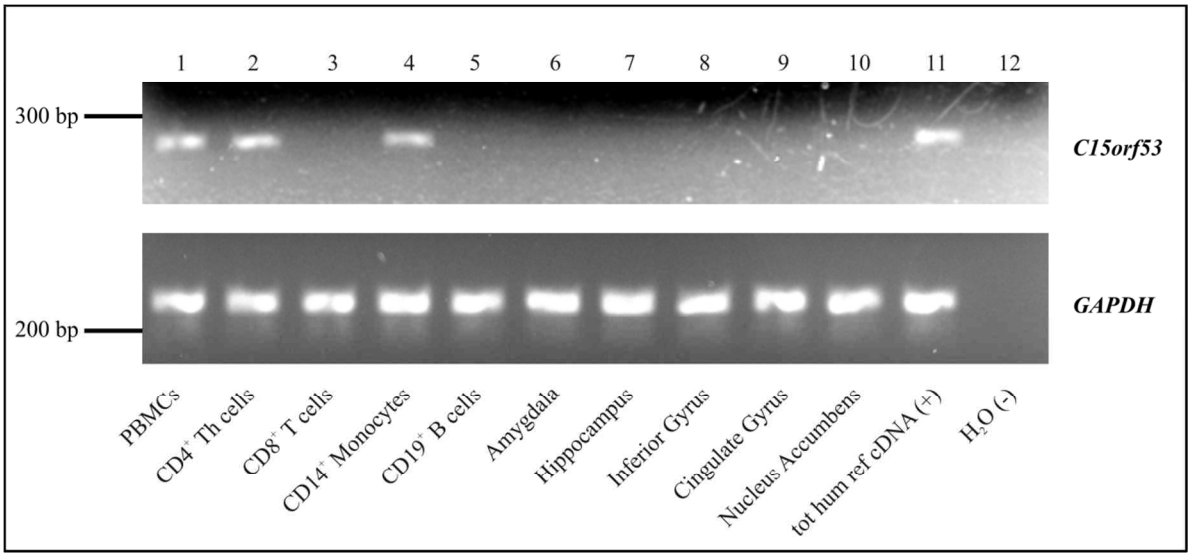

Figure 3.5: *C15orf53* gene expression pattern in cDNAs of leukocyte subpopulations and human post-mortem limbic brain tissues. 10 µl of each PCR sample was separated on a 2 % agarose gel. *C15orf53* (293 bp) was expressed in PBMCs (1), $CD4^+$ (2) and $CD14^+$ (4) cells and the positive control (11). The negative control (H_2O, 12) did neither show expression of *C15orf53* nor *GAPDH* (226 bp). None of the human *post-mortem* limbic brain tissues expressed *C15orf53*. All samples with exception of the negative control expressed *GAPDH*, which confirmed cDNA integrity (1-11).

GAPDH expression could be confirmed for all of the investigated samples with exception of the negative control (1-11). Gene expression of *C15orf53* could be shown for the PBMCs (1), $CD4^+$ (T helper cells, 2) and $CD14^+$ (monocytes, 4) positive cells. Even in this experiment, human *post-mortem* limbic brain tissue did not reveal gene expression *C15orf53* (6-10). The experimental work flow of the gene expression study indicated that *C15orf53* is a gene with a low expression rate and that it is apparently not expressed in the human CNS.

3.2 Association analysis of the *OXTR* gene with ASD

3.2.1 Genotyping of selected *OXTR* SNPs in parent-child trios diagnosed with ASD

The peptide hormone oxytocin is well known for its role in maintaining the uterine contractions during childbirth and for the manifestation of social bonding ("trust hormone") (Gimpl and Fahrenholz, 2001; Kosfeld *et al.*, 2005). Patients diagnosed with ASD are impaired in their social abilities; hence the hormone oxytocin and its receptor (OXTR) have attracted notice for intense investigation (Jacob *et al.*, 2007; Bartz and Hollander, 2008).

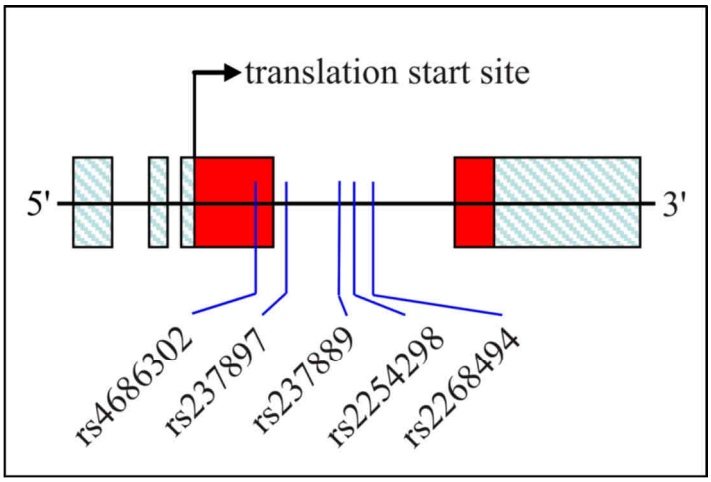

Figure 3.6: Schematic overview of *OXTR* and the location of the five investigated SNPs. Light blue shaded: exons. Red: coding region. Blank: introns

In this study, the four SNPs rs237889 (G/A), rs2254298 (G/A), rs2268494 (T/A), rs237897 (G/A), which are all located in intron 3 and the non-synonymous coding SNP rs4686302 (C/T) of the *OXTR*, leading to an exchange of the amino acid Alanine to Threonine at position 218 (Ala218Thr), were genotyped in our parent offspring trios with ASD-affected children and tested for association (Figure 3.6). A transmission disequilibrium test (TDT) was performed with Haploview 4.2 and UNPHASED.

3.2.2 Association testing with Haploview 4.2, single marker check (all trios)

All available genotyped data was considered for association testing with ASD. At first, the single genotyped markers were quality-checked (Table 3.3).

Table 3.3: Haploview output file on marker check (all trios)

#	Name	Position	ObsHET	PredHET	HWpval	%Geno	FamTrio	MendErr	MAF	Alleles
1	rs2268494	8.802.046	0.132	0.128	1.0	98.1	132	0	0.069	A:T
2	rs2254298	8.802.228	0.198	0.21	0.3969	100	136	0	0.119	C:T
3	rs237889	8.802.483	0.450	0.447	1.0	99.4	135	0	0.337	G:A
4	rs237897	8.808.285	0.443	0.45	0.8234	99.3	135	0	0.342	C:T
5	rs4686302	8.809.222	0.208	0.215	0.6562	91.4	124	0	0.123	G:A

ObsHET: observed heterozygosity, PredHET: predicted heterozygosity, HWpal: Hardy-Weinberg p-value, MendErr: Mendelian errors, MAF: minor allele frequency

The very first column displays the running number, the second the marker name, the following three columns contain the calculation of the allele frequencies of the respective marker alleles with regard to their deviation from the Hardy-Weinberg equilibrium (HWpval). It was tested, if the observed frequency of the heterozygous genotype (ObsHET) significantly deviated from the expected (PredHET). All markers fulfilled the criteria for the Hardy-Weinberg equilibrium ($p < 0.001$). More than 98 % of the patients were successfully genotyped for four of the tested markers (%Geno). The marker rs4686302 was genotyped in 91 % of the samples. The column "FamTrio" displays the amount of families that were included into the calculation. Differences between these numbers within the single markers were correlated to the success of genotyping. The minimum amount of trios considered for calculation was 124, the maximum 136. This difference was due to the incompleteness of some trios meaning missing genotyping data. The level of minimum genotypes for calculation was set to a stringent level of 75 %. The column "MendErr" did not show any genotyping errors. The following column with minor allele frequencies depicted the existence of the minor alleles in the investigated sample as a decimal fraction. The minor allele of rs2268494 (T) was just present in about 7 % of the investigated ASD patients, limiting the explanatory power. Similar conclusions could be drawn for the markers rs2254298 and rs4686302; their minor allele frequencies (MAF) were also low with an abundance of 12 % and 13 %, respectively.

3.2.3 Standard TDT in Haploview 4.2 (all trios)

Subsequent to the marker test, the TDT for single markers was performed (Table 3.4).

Table 3.4: Association of single *OXTR* markers with ASD (all trios)

#	Name	Overtransmitted	T:U	HapMap CEU freq	Chi Square	p-value
1	rs2268494	A	22:12	0.948	2.941	0.0863
2	rs2254298	C	28:22	0.932	0.72	0.3961
3	rs237889	A	66:50	0.372	2.207	0.1374
4	rs237897	T	58:54	0.386	0.143	0.7055
5	rs4686302	A	29:25	0.106	0.296	0.5862

T:U: Transmitted versus Untransmitted, HapMap CEU freq: Allele frequencies from HapMap CEU sample

The column "Overtransmitted" contained the allele that had been transmitted more often from the heterozygous parents to the ASD-affected child. Notably, only the marker rs2254298 revealed an overtransmission of the common allele (C = 0.932). The other four markers showed an overtransmission of their minor alleles from the parents to their children. The Chi square test statistics were calculated with one degree of freedom (df) because there were only two options, either the one or the other allele. A Chi square value of 3.84 corresponded to the 95^{th} quantile of the distribution; the probability was 5 % that the alternative hypothesis (H_1) was accepted although the null hypothesis (H_0) had been valid. The values in Table 3.4 did not fulfill the statistical criteria for significance. Solely rs2268494 with a Chi square value of 2.941 and p = 0.0863 approximated the level of statistical significance.

3.2.4 LD of *OXTR* SNPs and haplotypes in Haploview 4.2 (all trios)

The LD and haplotypes of the five investigated *OXTR* SNPs were calculated (Figure 3.7).

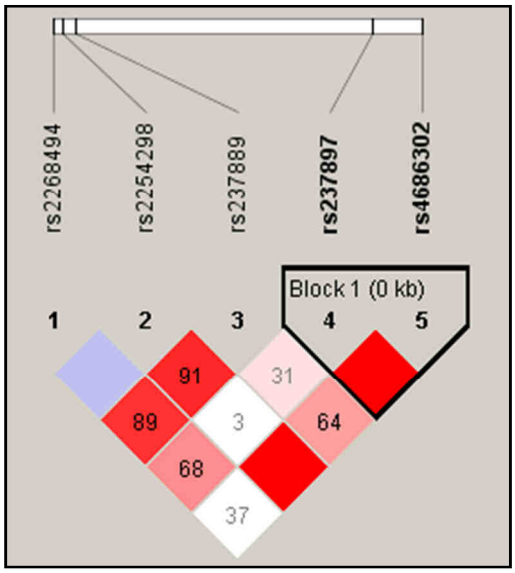

Figure 3.7: LD plot of five *OXTR* SNPs (all trios). The numbers within the squares display the LD (D'). The higher the values, the higher the LD. The colors represent the degree of the LD, red: high LD, white: low LD. Blue: high LD, but low LOD score, no number: D' = 100. The SNPs rs237897 and rs4686302 were considered as one LD block (black frame).

The SNPs rs2268494 and rs2254298 were in high LD but as the LOD score was low (LOD ≤ 2), the validity of this result was low as well. The LD between the markers rs2254298 and rs237889 was high (D' = 91, red), similar to the LD between the markers rs2268494 and rs237889 (D' = 89, red). The highest LD over a distance of seven kilobases could be observed between the SNPs rs2254298 and rs4686302 (D' = 100, red). The SNPs rs237897 and rs4686302 revealed a similar effect: a high LD and a high LOD-score (D' = 100, red). In addition, these two markers are just located in a distance of 1 kb from each other in the genome. In the investigated sample with the occurring genotypes, Haploview 4.2 defined these two markers as one haplotype block. The LD correlated with the genetic distance: the higher the distance, the lower the LD. The only exception was built by the markers rs2254298 and rs4686302. They were in complete LD, whereas the SNPs rs237889 and rs237897 with a smaller genetic distance were in lower LD (D' = 31, rose).

3.2.5 TDT calculation with UNPHASED: allele main effects (all trios)

The genotyped data of the parents-offspring trios were additionally calculated with UNPHASED. The main difference between Haploview and UNPHASED is the ability of UNPHASED to calculate datasets even from incomplete trios and genotypes (missing father or mother). The missing data are simulated on the basis of existing ones. Hence, the results from UNPHASED are more valid and concomitantly, the information density is higher in comparison to datasets calculated by Haploview. UNPHASED calculates the likelihood ratio, which results from the difference of the log-likelihoods of null and alternative hypothesis multiplied by minus two. Equivalently to Haploview, also the data generated by UNPHASED follow a Chi square distribution and can be interpreted analogously.

The results from the calculation by UNPHASED comprising all trios are subsequently displayed (Table 3.5).

Table 3.5: Marginal allele frequency calculation by UNPHASED (all trios)

Marker	Allele	HapMap CEU freq	Trans	Untrans	T-Freq	U-Freq	Null log-likeli	Alt Log-likeli	Likeli-ratio Chi square	p-value
rs2268494	**A**	**0.948**	243	243	**0.9492**	0.9067	-134.217	-132.724	2.9851	0.0840
	T	0.052	13	25	0.0507	0.0932				
rs2254298	**C**	**0.932**	241	246	**0.8993**	0.8786	-190.005	-189.644	0.7217	0.3955
	T	0.068	27	34	0.1007	0.1214				
rs237889	A	0.372	98	89	0.3712	0.3225	-340.742	-339.635	2.2139	0.1367
	G	**0.628**	166	187	**0.6288**	0.6775				
rs237897	**C**	**0.614**	179	193	**0.6533**	0.6748	-349.047	-348.895	0.3052	0.5806
	T	0.386	95	93	0.3467	0.3252				
rs4686302	A	0.106	35	31	0.1389	0.1192	-193.99	-193.847	0.2859	0.5928
	G	**0.894**	217	229	**0.8611**	0.8808				

HapMap CEU freq: allele frequency in HapMap CEU sample, Trans: transmitted allele, Untrans: untransmitted allele, T-Freq: transmission frequency, U-Freq: untransmission frequency, Null log-likeli: null likelihood, Alt log-likeli: alternative likelihood

The transmission rates of the alleles versus the non-transmission rates from the parents to their children differed once compared to the data generated with Haploview. This is explained by the higher number of individuals that UNPHASED used. Instead of 136 trios, 203 were taken for calculation because UNPHASED simulated the data of the missing individuals. Even the calculation with UNPHASED revealed that solely the marker rs2268494 showed a

tendency to statistical significance (χ^2 = 2.9851, p = 0.0840). The other four markers did not reach the level of statistical significance. None of the five markers was associated with ASD. From all markers, the common allele was overtransmitted to the ASD-affected children. The statistical parameters, the Chi square and the p-values, were almost identical to those generated by Haploview for the markers rs2268494, rs2254298, rs237889 and rs4686302. The p-value differences between the UNPHASED and Haploview calculations were lower than five percent. The p-values for marker rs237897 differed more; the p-value generated by UNPHASED was 18 % lower than the one from Haploview (Haploview: 0.7055, UNPHASED: 0.5806). Data generated with both softwares displayed that none of the markers was associated with ASD.

3.2.6 Allele Effects calculated with UNPHASED (all trios)

The Odds ratios were calculated to check the effect sizes of the alleles on the ASD phenotypes among the children (Table 3.6).

Table 3.6: Odds ratios of tested alleles in *OXTR* (all trios)

Marker	Allele	Odds-R	95 % Low	95 % High
rs2268494	A	1	1	1
	T	0.5455	0.2699	1.102
rs2254298	C	1	1	1
	T	0.7857	0.4495	1.373
rs237889	G	1	1	1
	A	1.3199	0.9141	1.9062
rs237897	C	1	1	1
	T	1.107	0.7714	1.589
rs4686302	G	1	1	1
	A	1.1538	0.6826	1.9508

Odds-R: Odds Ratio of Alleles

The major allele was set as the reference allele, by definition its numerical value is one. The alleles of the other markers were compared to their reference alleles, respectively. The markers rs2268494 and rs2254298 had lower odds ratios; the markers rs237889, rs237897 and rs4686302 showed increased ones. All results were not significant as already indicated by the p-values mentioned in Table 3.6, which also explained the high variation of the odds ratio probability range (95 % Low and 95 % High). The odds ratios display whether the minor

allele has a protective or risk-increasing quality with regard to the investigated trait. The extremes of the odds ratios, the T allele of rs2268494 and the A allele of rs237889, can be interpreted as follows: the T allele of rs2268494 had a protective effect; carriers of this allele had a 0.54 fold less risk of ASD diagnosis in comparison to the reference allele. The A allele of rs237889 is a risk allele; carriers had a 1.3 fold increased risk for ASD diagnosis in comparison to the reference allele. Due to the lack of significance (rs2268494: $p = 0.0840$; rs237889: $p = 0.1367$), the results displayed a large spread, which is reflected by the confidence intervals. According to these confidence interval values, the minor alleles of both SNPs could be potentially protective (95 % Low: < 1) or risk-increasing (95 % High > 1). Also the remaining results did not reach the level of statistical significance and could not be evaluated properly.

3.2.7 Haplotype main effects calculated with UNPHASED (all trios)

Besides the single marker effects, the haplotype effects were additionally investigated in this study. Haplotype effects are considered to be more valid than single marker effects because haplotypes combine the effects of two and more single markers. The Haploview LD block analysis revealed a block built by rs237897 and rs4686302 (Figure 3.7). In our complete trio sample, the calculations with UNPHASED resulted in two putative haplotype blocks. The first haplotype block consisted of combinations of the SNPs rs2268494, rs2254298 and rs237889 (markers 1-3). The second block was formed by rs237897 and rs4686302 (markers 4-5).

3.2.8 Haplotype effects of markers rs2268494, rs2254298 and rs237889 (all trios)

The marginal allele frequencies in the all parent-offspring trios were calculated (Table 3.7)

Table 3.7: Marginal allele frequencies for rs2268494, rs2254298 and rs237889 (all trios)

Marker	Allele	HapMap CEU freq	Trans	Untrans	T-Freq	U-Freq	Null log-likeli	Alt log-likeli	Likeli-ratio Chi square	p-value
rs2268494	**A**	**0.948**	251	241	**0.9508**	0.9129	-129.062	-127.569	2.9851	0.0840
	T	0.052	13	23	0.0049	0.0871				
rs2254298	**C**	**0.932**	247	242	**0.8949**	0.8768	-194.123	-193.887	0.4724	0.4919
	T	0.068	29	34	0.1051	0.1232				
rs237889	A	0.372	100	84	0.3676	0.3088	-338.828	-337.740	2.1761	0.1402
	G	**0.628**	172	188	**0.6324**	0.6912				

Trans: transmitted allele, Untrans: untransmitted allele, T-Freq: transmission frequency, U-Freq: untransmission frequency, Null log-likeli: null likelihood, Alt log-likeli: alternative likelihood

The data in this table indicate that there were hardly any differences of the allele frequencies of these three markers in comparison to the complete dataset, which is depicted in Table 3.5. Even in this setting, none of the single markers yielded statistical significance ($p \leq 0.05$). Exclusively the first marker, rs2268494, showed a tendency to statistical significance (Likeli ratio $\chi^2 = 2.9851$, $p = 0.0840$, $df = 1$).

3.2.9 Allele effects of markers rs2268494, rs2254298 and rs237889 (all trios)

The allele effects of the selected three markers were calculated (Table 3.8).

Table 3.8: Allele effects of rs2268494, rs2254298 and rs237889 (all trios)

marker	Allele	Odds-R	95 % Low	95 % High
rs2268494	A	1	1	1
	T	0.5455	0.2699	1.102
rs2254298	C	1	1	1
	T	0.8276	0.4819	1.421
rs237889	G	1	1	1
	A	1.3137	0.9124	1.8910

Odds-R: Odds Ratio of Alleles

The allele effects were not significant; they were comparable to the results shown in Table 3.6. The minor allele of marker rs2254298 revealed a tendency to be protective (Odds-R: 0.8276) compared to the minor alleles of the SNPs rs2268494 (Odds Ratio: 1.8331) and rs237889 (Odds Ratio: 1.3137). The confidence intervals of marker rs22268494 defined a slight protective (0.9074) and risk-increasing effect (3.7051). Here too, the wide spread of the confidence values was explained by the low transmission rate of the minor allele (T-freq: 0.0049). In the next procedure, the different haplotype combinations were tested and calculated.

3.2.10 Haplotype compositions of markers rs2268494, rs2254298 and rs237889 (all trios)

Subsequently, all haplotype compositions including the haplotype frequencies and main effects of the three markers (rs2268494, rs2254298 and rs237889) are depicted (Table 3.9).

Table 3.9: Haplotype frequencies of haplotype block rs2268494, rs2254298 and rs237889 (all trios)

Marker	Haplotype	Trans	Untrans	T-Freq	U-Freq	Null log-likeli	Alt log-likeli	Likeli-ratio Chi Square	p-value
1 & 2	**A-C**	**222**	**208**	**0.8409**	0.7879	-314.169	-312.468	3.3408	0.1882
	A-T	29	33	0.1098	0.1250				
	T-C	13	23	0.0492	0.0871				
1 & 3	A-A	84.03	59.05	0.3207	0.2254	-425.831	-422.361	6.9388	0.0739
	A-G	**165**	**179.9**	**0.6296**	0.6868				
	T-A	11.97	21.95	0.0456	0.0837				
	T-G	1.034	1.055	0.0039	0.0040				
2 & 3	C-A	100	82	0.3676	0.3015	-511.393	-508.71	5.3667	0.1468
	C-G	**143**	**157**	**0.5257**	0.5772				
	T-A	0	2	0	0.0073				
	T-G	29	31	0.1066	0.1140				
1, 2 & 3	A-C-A	84.04	58.06	0.3208	0.2216	-590.557	-586.197	8.7195	0.1208
	A-C-G	**136**	**148.9**	**0.5189**	0.5685				
	A-T-A	0	1	0	0.0038				
	A-T-G	29	31	0.1107	0.1183				
	T-C-A	11.96	21.94	0.0456	0.0837				
	T-C-G	1.04	1.065	0.0039	0.0040				

1: rs2268494 (A/T), 2: rs2254298 (C/T), 3: rs237889 (G/A)

The table values are listed according to alphabetic order of the haplotypes. None of the haplotype calculations fulfilled the criteria for statistical significance. The haplotypes generated by the combination of the markers one and three, rs2268494 and rs237889, approximated the criteria for statistical significance (p = 0.0739). The haplotypes with the highest transmission rates were exclusively composed from major alleles (A-C, A-G, C-G and A-C-G, displayed in bold, Table 3.9).

Table 3.10: Haplotype effects of rs2268494, rs2254298 and rs237889 (all trios)

Marker	Haplotype	Odds-R	95 % Low	95 % High
1 & 2	A-C	1	1	1
	A-T	0.8472	0.4908	1.462
	T-C	0.5427	0.2685	1.097
1 & 3	A-G	1	1	1
	A-A	1.4778	1.0001	2.1834
	T-A	0.6476	0.4541	0.9233
	T-G	0.8083	0.0712	9.1839
2 & 3	C-G	1	1	1
	C-A	1.3728	0.0904	2.0032
	T-A	0	0	0
	T-G	1.0275	0.8143	1.2963
1, 2 & 3	A-C-G	1	1	1
	A-C-A	1.5242	1.0180	2.2821
	A-T-A	0	0	0
	A-T-G	1.0463	0.8414	1.3008
	T-C-A	0.6575	0.4662	0.9271
	T-C-G	0.8166	0.0727	9.1541

1: rs2268494 (A/T), 2: rs2254298 (C/T), 3: rs237889 (G/A)

The haplotype with the highest transmission rate ("major haplotype") was set as the reference value (odds ratios and confidence intervals = 1). None of the haplotype effects fulfilled criteria for statistical significance, according to the p-values depicted in the previous table. The haplotype combinations of the markers 1 & 3 (rs2268494 and rs237889) revealed a tendency to association (p = 0.0739). The haplotype combination, rs2268494 (A) - rs237889 (A), revealed an increased odds ratio (1.4778). Even the lower limit of the confidence interval (95 % Low) showed a minimal tendency of this haplotype for being risk-

contributing (1.0001). The upper limit of the confidence interval (95 % High) also indicated a risk-increasing value (2.1834). Carriers of the haplotype A-A had a 1.47 fold increased risk for ASD in our cohort. The haplotypes T-A and T-G, built from the alleles of rs2268494 and rs237889, both had odds ratios indicating a protective character (Odds-R T-A: 0.6476; Odds-R T-G: 0.8083). Considering the tendency to association, the confidence values of haplotype T-A (95 % Low: 0.4541; 95 % High: 0.9233) underlined the protective character of this haplotype. The odds ratio for haplotype T-G also indicated a protective effect (Odds-R: 0.8083), but the confidence intervals were more spread (95 % Low: 0.0712; 95 % High: 9.1839) due to the extremely low transmission frequency (T-Freq: 0.0039).

3.2.11 Haplotype effects of markers rs237897 and rs4686302 (all trios)

The haplotype effects of the haplotypes built from the alleles of the SNPs rs237897 and rs4686302 are depicted subsequently. The marginal allele frequencies of the markers rs237897 and rs4686302 were calculated (Table 3.11).

Table 3.11: Marginal allele frequencies of rs237897 and rs4686302 (all trios)

Marker	Allele	HapMap CEU freq	Trans	Untrans	T-Freq	U-Freq	Null log-likeli	Alt Log-likeli	Likeli-ratio Chi square	p-value
rs237897	**C**	**0.614**	**182**	189	**0.6500**	0.6750	-348.097	-347.891	0.4120	0.5210
	T	0.386	98	91	0.3500	0.3250				
rs4686302	A	0.106	36	32	0.1395	0.1240	-193.990	-193.847	0.2860	0.5928
	G	**0.894**	**222**	226	**0.8605**	0.8760				

Trans: transmitted allele, Untrans: untransmitted allele, T-Freq: transmission frequency, U-Freq: untransmission frequency, Null log-likeli: null likelihood, Alt log-likeli: alternative likelihood

Similarly to the data of the previous haplotype, the data did not differ from the observation including all markers. None of the two markers reached the level of statistical significance (Likeli ratio $\chi^2 \geq 3.84$, $p \leq 0.05$, df = 1). The major alleles of both markers (rs237897: C; rs4686302: G) were overtransmitted to ASD-affected children.

3.2.12 Allele effects of markers rs237897 and rs4686302 (all trios)

The calculation of the allele effects gave the following results (Table 3.12):

Table 3.12: Allele effects of rs237897 and rs4686302 (all trios)

Marker	Allele	Odds-R	95 % Low	95 % High
rs237897	C	1	1	1
	T	1.125	0.7849	1.612
rs4686302	G	1	1	1
	A	1.1538	0.6826	1.9508

Odds-R: Odds Ratio of Alleles

On closer examination, the odds ratio of marker rs237897 was slightly higher (Odds-R: 1.125) in comparison to its odds ratio, where all five markers were taken for calculation. The confidence interval values were almost similar. The odds ratio and the confidence interval values of marker rs4686302 completely matched with the previous ones. None of the displayed values reached the level of statistical significance (Likeli ratio $\chi^2 \geq 3.84$, $p \leq 0.05$, df = 1).

3.2.13 Haplotype compositions of markers rs237897 and rs4686302 (all trios)

The haplotype compositions are displayed in the subsequent table (Table 3.13).

Table 3.13: Haplotype frequencies of rs237897 and rs4686302 (all trios)

Marker	Haplotype	Trans	Untrans	T-Freq	U-Freq	Null log-likeli	Alt log-likeli	Likeli-ratio Chi Square	p-value
4 & 5	C-A	36	32	0.1417	0.1260	-483.968	-483.755	0.4273	0.8076
	C-G	**130**	136	**0.5118**	0.5354				
	T-G	88	86	0.3465	0.3386				

4: rs237897 (C/T), 5: rs4686302 (G/A)

The haplotype compositions values did not reach the level of statistical significance was not reached at all (likelihood ratio $\chi^2 \geq 5.99$, $p \leq 0.05$, df = 2). Two haplotypes, T-G and C-A, were overtransmitted to ASD-affected children. The haplotype with the second highest transmission frequency (T-G, T-freq: 0.3465) consisted of the minor allele (T) of marker

rs237897 and the major allele (G) of marker rs4686302. The least transmitted one (C-A, T-freq: 0.1417) consisted of the major allele (C) of marker rs237897 and the minor allele of marker rs4686302 (A). The major haplotype C-G revealed the highest transmission rate and was transmitted in over 50 % of the cases (T-freq: 0.5118).

Table 3.14: Haplotype effects rs237897 and rs4686302 (all trios)

Marker	Haplotype	Odds-R	95 % Low	95 % High
4 & 5	C-G	1	1	1
	C-A	1.1922	0.6863	2.0713
	T-G	1.0790	1.0582	1.1009

4: rs237897 (C/T), 5: rs4686302 (G/A)

The major haplotype C-G was set as the reference value. The lack of statistical significance ($p = 0.8076$) did not allow a valid statement on the haplotypes' protective (Odds-R < 1) or risk contributing (Odds-R > 1) qualities. In tendency, the haplotype T-G seemed to have a slightly higher protective quality (Odds-R: 1.0790) than the haplotype C-A (Odds-R: 1.1922). The confidence intervals (95% Low and High), indicated that the effects of both haplotypes could be either protective or risk-increasing. The confidence interval of haplotype T-G was very confined compared that of haplotype C-A. This could be explained by the more than two times higher transmission frequency of T-G compared to that of T-A (T-freq T-G: 0.3465; T-freq C-A: 0.1417), which automatically led to a higher statistical robustness. Thus, the haplotype T-G is exclusively risk-increasing in contrast to haplotype C-A, which is potentially both protective and risk-increasing (95 % Low: 0.6863, 95 % High: 2.0713).

3.2.14 Association testing with Haploview 4.2, single marker check (IQ > 70)

The complete cohort was subdivided into those individuals that had an IQ above 70. The IQ range between 70 and 84 is defined as "borderline intellectual functioning" (Alloway, 2010), IQ values lower than 70 are defined as "mental retardation" (ICD-10 F70 - F74). The results of those children, whose IQ was above 70, are displayed in the subsequent tables. 52 singletons and 90 parents-child trios were taken into consideration for calculation.

Table 3.15: Haploview output of single marker check (IQ > 70)

#	Name	Position	ObsHET	PredHET	HWpval	%Geno	FamTrio	MendErr	MAF	Alleles
1	rs2268494	8.802.046	0.138	0.136	1.0	87.2	86	0	0.074	A:T
2	rs2254298	8.802.228	0.177	0.189	0.4754	100	90	0	0.106	C:T
3	rs237889	8.802.483	0.417	0.442	0.4545	99.2	89	0	0.33	G:A
4	rs237897	8.808.285	0.422	0.443	0.54	99.2	89	0	0.332	C:T
5	rs4686302	8.809.222	0.202	0.211	0.7008	92.0	83	0	0.120	G:A

ObsHET: observerd heterozygosity, PredHET: predicted heterozygosity, HWpal: Hardy-Weinberg p-value, MendErr: Mendelian Errors, MAF: minor allele frequency

As expected, the parameters slightly differed from the results displayed in Table 3.3, where the complete cohort was considered for calculation. In summary, the results displayed in Table 3.15 did not significantly differ from those depicted in Table 3.3. Especially the MAF remained almost exactly the same. The trios and singletons fulfilled the criteria of a minimum completeness of 75 %, the HW p-value cutoff was set to $p < 0.001$.

3.2.15 Standard TDT in Haploview 4.2 (IQ > 70)

Table 3.16: Association test of single markers with ASD (IQ > 70)

#	Name	Overtransmitted	T:U	HapMap CEU freq	Chi Square	p-value
1	rs2268494	A	22:12	0.948	2.941	0.0863
2	rs2254298	C	29:24	0.932	0.472	0.4922
3	rs237889	A	68:52	0.372	2.133	0.1441
4	rs237897	T	60:55	0.386	0.217	0.641
5	rs4686302	A	29:25	0.106	0.296	0.5862

T:U, Transmitted versus Untransmitted

None of the single markers was associated with ASD, the criteria for statistical significance were not fulfilled by any of the markers ($\chi^2 \geq 3.84$, $p \leq 0.05$, $df = 1$). Exclusively marker rs2268494 showed a tendency to association ($\chi^2 = 2.941$, $p = 0.0863$, $df = 1$). Marker rs2254298 had a higher transmission of its major allele (C) in comparison to the results from the investigation of the complete cohort, which led to an increase of its p-value ($p = 0.4922$). The minor allele (A) of rs237889 showed an overtransmission like in the previous analysis with the complete cohort. This observation was also confirmed for rs237897. Once again, the minor allele of this marker (T) was overtransmitted. The transmission rate was higher in this

subpopulation than in the compete cohort, which is reflected in the lowered p-value (p = 0.641). The parameter values for rs4686302 were completely identical to the previous ones.

3.2.16 LD of *OXTR* SNPs and haplotypes in Haploview 4.2 (IQ > 70)

The LD and haplotypes of the five investigated *OXTR* SNPs were calculated (Figure 3.7).

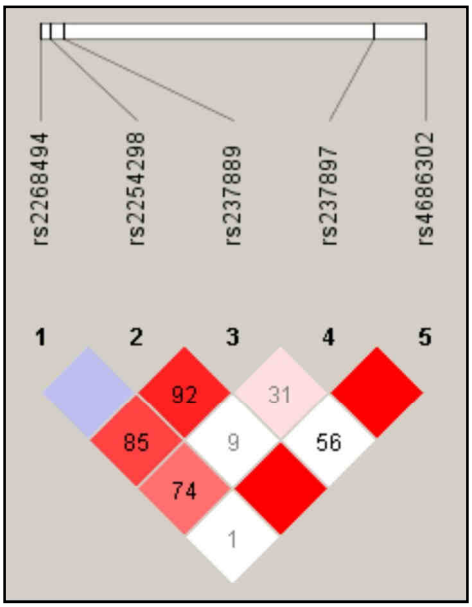

Figure 3.8: LD plot of five *OXTR* SNPs (IQ > 70). The numbers within the squares display the LD (D'). The higher the values, the higher the LD. The colors represent the degree of the LD, red: high LD, white: low LD. Blue: high LD, but low LOD score, no number: D' = 100.

The LD plot values changed in comparison to the previous one. The LD of the markers rs2268494 and rs237889 decreased about 4 % (from 89 to 85), between the markers rs2254298 and rs237889 it increased about 1 % (from 91 to 92). The LD of rs2254298 and rs237897 increased from 3 % to 9 %. A big change of the LD occurred between the markers rs237889 and rs4686302; it decreased about 8 % (from 64 to 56). This also explained color change from light rose to white. The largest change was denoted between the markers with the biggest genetic distance, rs2268494 and rs4686302. The D' values were reduced about 36 % (from 37 % to 1 %), which could be interpreted as non-existing LD.

3.2.17 TDT calculation with UNPHASED: allele main effects (IQ > 70)

The 139 trios and singletons were considered for calculation with UNPHASED. The next table displays the results from the calculation of the allele main effects (Table 3.17).

Table 3.17: Marginal allele frequency calculation by UNPHASED, (IQ > 70)

Marker	Allele	HapMap CEU freq	Trans	Untrans	T-Freq	U-Freq	Null log-likeli	Alt Log-likeli	Likeli-ratio Chi square	p-value
rs2268494	**A**	**0.948**	**163**	159	**0.9368**	0.9138	-90.752	-90.417	0.6698	0.41313
	T	0.052	11	15	0.0632	0.0862				
rs2254298	**C**	**0.932**	**166**	171	**0.8925**	0.9194	-114.240	-113.835	0.8099	0.3681
	T	0.068	20	15	0.1075	0.0807				
rs237889	A	0.372	67	55	0.3712	0.3225	-227.059	-226.055	2.0094	0.1563
	G	**0.628**	**115**	127	**0.6319**	0.6978				
rs237897	**C**	**0.614**	**124**	134	**0.6526**	0.7053	-230.667	-230.008	1.3196	0.2506
	T	0.386	66	56	0.3474	0.2947				
rs4686302	A	0.106	23	25	0.1322	0.1437	-132.557	-132.504	0.1053	0.7455
	G	**0.894**	**151**	149	**0.8678**	0.8563				

Trans: transmitted allele, Untrans: untransmitted allele, T-Freq: transmission frequency, U-Freq: untransmission frequency, Null log-likeli: null likelihood, Alt log-likeli: alternative likelihood

The UNPHASED results differed in many aspects from those that were calculated with Haploview. The most noticeable difference occurred among the overtransmitted alleles. Marker rs4686302 revealed a difference, the G allele ("major allele") was overtransmitted, whereas Haploview reported an overtransmission of the A allele. Once both calculations with UNPHASED were compared to each other (Tables 3.5 and 3.17), the differences became even more obvious. The trend to association of marker rs2268494 disappeared completely (rs2268494 [all trios]: p = 0.0840; rs2268494 [IQ > 70]: p = 0.4131). Also marker rs237897 revealed a big change with respect to its p-value, it decreased about more than 50 % (rs237897 [all trios]: p = 0.5806; rs237897 [IQ > 70]: p = 0.2506). The p-value of marker rs4686302 was further shifted to non-significance (rs4686302 [all trios]: p = 0.5928; rs4686302 [IQ > 70]: p = 0.7455). The p-values of the markers rs2254298 and rs237889 remained almost the same as in the calculation with the complete cohort. The differences of the results of both calculations could be explained different numbers of trios that were used (139 trios in the IQ > 70 subpopulation instead of 203 trios in the complete cohort). Thus, the

amount of alleles that could be considered for calculation was less, which led to a decreased robustness of the statistical parameters.

3.2.18 Allele Effects calculated with UNPHASED (IQ > 70)

Table 3.18: Odds ratios of tested alleles in the *OXTR*, all markers (IQ > 70)

Marker	Allele	Odds-R	95 % Low	95 % High
rs2268494	A	1	1	1
	T	0.7143	0.3173	1.608
rs2254298	C	1	1	1
	T	1.385	0.6784	2.826
rs237889	G	1	1	1
	A	1.3999	0.8764	2.2366
rs237897	C	1	1	1
	T	1.303	0.8279	2.051
rs4686302	G	1	1	1
	A	0.9001	0.4762	1.7013

Odds-R: odds ratios of tested alleles

The minor alleles of two markers revealed a protective effect (rs2268494 and rs4686302, Odds-R < 1); those of the remaining three markers were risk-increasing (rs2254298, rs237889, rs23897, Odds-R > 1). The most striking effects were observed for rs2254298 and rs4686302, their allele effects reversed respectively. In the calculation comprising the complete cohort, the minor allele of marker rs2254298 revealed a protective effect (rs2254298 [all trios]: p = 0.7857) and in the IQ > 70 subpopulation, the allele effect became risk-increasing (rs2254298 [IQ > 70]: p = 1.385). Considering the complete cohort, the minor allele of rs4686302 had a risk-increasing effect (rs4686302 [all trios]: p = 1.1538) and in the IQ > 70 subpopulation, the minor allele effect became protective (rs4686302 [IQ > 70]: p = 0.9001). The confidence intervals of all markers, with exception of rs4686302, in the IQ > 70 subpopulation were more spread than in the calculation comprising the complete cohort. The increase of the p-values and the wider spread of the markers' confidence intervals were due to the lower number of tested alleles (fewer trios). Exclusively for rs4686302, the spread of the confidence intervals remained almost identical, although the absolute values decreased (rs4686302 [all trios]: 0.6826 - 1.9508; rs4686302 [IQ > 70]: 0.4762 - 1.7013).

3.2.19 Haplotype main effects calculated with UNPHASED (IQ > 70)

Similarly to the analysis of the haplotype effects in the complete cohort, the haplotype effects were also calculated for the IQ > 70 subpopulation. The Haploview LD block analysis did not define any block in this sample. Just as in the previous study on the complete cohort, UNPHASED identified two haplotype blocks in our trio subpopulation. The first haplotype block consisted of combinations of the SNPs rs2268494, rs2254298 and rs237889 (markers 1-3). The second block was built by rs237897 and rs4686302 (markers 4-5).

3.2.20 Haplotype effects of markers rs2268494, rs2254298 and rs237889 (IQ > 70)

According to the calculations with the complete cohort, the single markers were grouped into two haplotype blocks. The calculations of the first haplotype block (rs2268494, rs2254298 and rs237889) are displayed (Table 3.19).

Table 3.19: Marginal allele frequencies of rs2268494, rs2254298 and rs237889 (IQ > 70)

Marker	Allele	HapMap CEU freq	Trans	Untrans	T-Freq	U-Freq	Null log-likeli	Alt Log-likeli	Likeli-ratio Chi square	p-value
rs2268494	**A**	**0.948**	**163**	159	**0.9368**	0.9138	-90.751	-90.417	0.6697	0.4131
	T	0.052	11	15	0.0632	0.0862				
rs2254298	**C**	**0.932**	**166**	171	**0.8925**	0.9194	-114.240	-113.835	0.8099	0.3681
	T	0.068	20	15	0.1075	0.0807				
rs237889	A	0.372	67	55	0.3681	0.3022	-227.059	-226.055	2.0093	0.1563
	G	**0.628**	**115**	127	**0.6319**	0.6978				

Trans: transmitted allele, Untrans: untransmitted allele, T-Freq: transmission frequency, U-Freq: untransmission frequency, Null log-likeli: null likelihood, Alt log-likeli: alternative likelihood

These results of the analysis of the first haplotype block were identical to those from the previous analysis, which comprised all markers.

3.2.21 Allele effects of markers rs2268494, rs2254298 and rs237889 (IQ > 70)

The results of the allele effect calculations are depicted in Table 3.20

Table 3.20: Allele effects of markers rs2268494, rs2254298 and rs237889 (IQ > 70)

Marker	Allele	Odds-R	95 % Low	95 % High
rs2268494	A	1	1	1
	T	0.7143	0.3173	1.608
rs2254298	C	1	1	1
	T	1.385	0.6784	2.826
rs237889	G	1	1	1
	A	1.3999	0.8764	2.2366

Odds-R: Odds Ratio of Alleles

According to the values from the calculations of the marginal allele frequencies, the odds ratios were absolutely identical with those of the complete cohort (Table 3.18).

3.2.22 Haplotype compositions of markers rs2268494, rs2254298 and rs237889 (IQ > 70)

The results of the marginal haplotype frequencies are summarized in Table 3.21.

Table 3.21: Haplotype frequencies of rs2268494, rs2254298 and rs237889 (IQ > 70)

Marker	Haplotype	Trans	Untrans	T-Freq	U-Freq	Null log-likeli	Alt log-likeli	Likeli-ratio Chi Square	p-value
1 & 2	**A-C**	**143**	**145**	**0.8218**	0.8333	-197.493	-196.554	1.8779	0.3910
	A-T	20	14	0.1149	0.0805				
	T-C	11	15	0.0632	0.0862				
1 & 3	A-A	53.04	38.05	0.3084	0.2212	-284.809	-283.127	3.3639	0.3389
	A-G	**108**	**118.9**	**0.6277**	0.6916				
	T-A	9.958	13.95	0.0579	0.0811				
	T-C	1.042	1.052	0.0061	0.0061				
2 & 3	C-A	67	54	0.3681	0.2967	-328.053	-324.920	6.2661	0.0993
	C-G	**95**	**114**	**0.5220**	0.6264				
	T-A	0	1	0	0.0055				
	T-G	20	13	0.1099	0.0714				
1 & 2 & 3	A-C-A	53.05	38.06	0.3084	0.2213	-377.738	-374.698	6.0812	0.1932
	A-C-G	**87.95**	**105.9**	**0.5113**	0.6159				
	A-T-G	20	13	0.1163	0.0756				
	T-C-A	9.949	13.94	0.058	0.081				
	T-C-G	1.051	1.059	0.0061	0.0062				

1: rs2268494 (A/T), 2: rs2254298 (C/T), 3: rs237889 (G/A)

The haplotypes compositions 1 & 2 (rs2268494 and rs2254298), 1 & 3 (rs2268494 and rs237889) as well as the combination 2 & 3 (rs2254298 and rs237889) show a similar pattern of transmitted haplotypes in comparison to the complete cohort (Table 3.10). The haplotypes consisting of the major alleles of the single markers were transmitted the most (A-C, A-G, C-G, A-C-G). It is striking that in the IQ > 70 subpopulation, the haplotypes built by the markers 2 & 3 (rs2254298 and rs237889) revealed a tendency to statistical significance ($p = 0.0993$). In contrast to this finding, the haplotype combination of the markers 1 & 3 (rs2268494 and rs237889), which showed a tendency to significance in the calculations comprising the complete cohort ($p = 0.0739$), did not reveal any tendency to significance at all in the IQ > 70 subpopulation ($p = 0.3389$).

Subsequently, the odds ratios and the confidence intervals are displayed (Table 3.22).

Table 3.22: Haplotype effects of rs2268494, rs2254298 and rs237889 (IQ > 70)

Marker	Haplotype	Odds-R	95 % Low	95 % High
1 & 2	A-C	1	1	1
	A-T	1.5	0.7225	3.114
	T-C	0.7143	0.3173	1.608
1 & 3	A-G	1	1	1
	A-A	1.1588	0.9166	2.5176
	T-A	0.8753	0.6108	1.2548
	T-G	0.9467	0.0934	9.6058
2 & 3	C-G	1	1	1
	C-A	1.3729	0.0906	2.003
	T-A	0	0	0
	T-G	1.8562	0.2471	1.3166
1, 2 & 3	A-C-G	1	1	1
	A-C-A	1.6515	0.9833	2.7732
	A-T-G	1.8893	1.3716	2.6018
	T-C-A	0.9123	0.6420	1.2960
	T-C-G	0.9747	0.0973	9.7689

1: rs2268494 (A/T), 2: rs2254298 (C/T), 3: rs237889 (G/A)

The major haplotypes A-C, A-G, C-G and A-C-G were set as the reference values. The haplotype A-T, built from the markers rs2268494 and rs2254298 (1 & 2), revealed a change

from a protective haplotype to a risk haplotype (Odds-R [all trios]: 0.8472; Odds-R [IQ > 70]: 1.5). The spread of the confidence intervals increased as well, especially with respect to the upper limit of the confidence interval for this haplotype (95 % High [all trios]: 1.462; 95 % High [IQ > 70]: 3.114). Another difference was observed for the haplotype A-A, which consisted of the major allele of marker rs2268494 and the minor allele of marker rs237889 (1 & 3). The odds ratio decreased (Odds-R [all trios]: 1.4778; Odds-R [IQ > 70]: 1.1588) and the lower limit of the confidence interval shifted into the protective range of values (95 % Low [all trios]: 1.001; 95 % Low [IQ > 70]: 0.9166). The upper confidence interval limit of haplotype T-A (1 & 3) also shifted towards the risk-increasing range of values. The odds ratio values of the haplotypes T-A and T-G (1 & 3) also lost a small share of their protective character. The upper confidence interval limit of haplotype T-A shifted into the risk-increasing range of values (95 % High: 1.2548). Among the haplotype combinations of the markers 2 & 3 (rs2254298 and rs237889), the combination of the minor allele of rs2254298 (T) and the major allele of rs237889 (G) also revealed an enormous increase of the odds ratio value (Odds-R T-G [all trios]: 1.0275; Odds-R T-G [IQ > 70]: 1.8562). Concomitantly, the lower limit of the confidence interval decreased and the upper limit increased. All of the odds ratios of the haplotype combinations 1, 2 & 3 (rs2268494, rs2254298 and rs237889) showed increased values. The haplotype A-T-A did not occur in this sample. Despite the increase of the odds ratio values, the haplotypes T-C-A and T-C-G remained protective. The most striking change occurred among the values of combination A-T-G. The odds ratio increased about 1.8 fold (Odds-R A-T-G [all trios]: 1.0275; Odds-R A-T-G [IQ > 70]: 1.8893) and the value of the lower confidence interval limit shifted into the risk-increasing range of values (95 % Low [all trios]: 0.8414; 95 % Low [IQ > 70]: 1.3716). The upper limit of the confidence interval has increased by two (95 % High [all trios]: 1.3008; 95 % High [IQ > 70]: 2.6018).

3.2.23 Haplotype effects of markers rs237897 and rs4686302 (IQ > 70)

The results are depicted in Table 3.23

Table 3.23: Marginal allele frequencies of rs237897 and rs4686302 (IQ > 70)

Marker	Allele	HapMap CEU freq	Trans	Untrans	T-Freq	U-Freq	Null log-likeli	Alt Log-likeli	Likeli-ratio Chi square	p-value
rs237897	**C**	**0.614**	**124**	134	**0.6526**	0.6750	-230.667	-230.008	1.13961	0.2507
	T	0.386	66	56	0.3474	0.3250				
rs4686302	A	0.106	23	25	0.1322	0.1437	-132.557	-132.504	0.1053	0.7455
	G	**0.894**	**151**	149	**0.8678**	0.8563				

Trans: transmitted allele, Untrans: untransmitted allele, T-Freq: transmission frequency, U-Freq: untransmission frequency, Null log-likeli: null likelihood, Alt log-likeli: alternative likelihood

The p-value of the marker rs237897 in this cohort was far lower than in the analysis comprising all trios (rs237897 [all trios]: 0.5210; rs237897 [IQ > 70]: 0.2507). The p-value of marker rs4686302 increased (rs4686302 [all trios]: p = 0.5928; rs4686302 [IQ > 70] p = 0.7455). None of the markers fulfilled the criteria of statistical significance ($\chi^2 \geq 3.84$, $p \leq 0.05$, df = 1).

3.2.24 Allele effects of markers rs237897 and rs4686302 (IQ > 70)

The results of the calculation of the allele effects are depicted subsequently (Table 3.24)

Table 3.24: Allele effects of rs237897 and rs4686302 (IQ > 70)

Marker	Allele	Odds-R	95 % Low	95 % High
rs237897	C	1	1	1
	T	1.303	0.8279	2.051
rs4686302	G	1	1	1
	A	0.9001	0.4762	1.7013

Odds-R: Odds Ratio of Alleles

Considering marker rs237897, both the odds ratio (Odds-R [all trios]: 1.125, Odds-R [IQ > 70]: 1.303) and the confidence interval values increased. The minor allele of rs237897 also remained a risk-increasing quality in the IQ > 70 subpopulation. The upper limit of the confidence interval for this allele increased to a value above two (95 % High [all trios]: 1.612; 95 % High [IQ > 70]: 2.051). A bigger change occurred for the minor allele of marker rs4686302. Its odds ratio value turned from risk-increasing to protective (Odds-R [all trios]: 1.1538; Odds-R [IQ > 70]: 0.9001). The confidence interval values decreased (95 % Low [all trios]: 0.6826; 95 % Low [IQ > 70]: 0.4762; 95 % High [all trios]: 1.9508; 95 % High [IQ > 70]: 1.7013).

3.2.25 Haplotype compositions of markers rs237897 and rs4686302 (IQ > 70)

The results of the possible haplotype compositions are displayed subsequently (Table 3.25)

Table 3.25: Haplotype frequencies of rs237897 and rs4386302 (IQ > 70)

Marker	Haplotype	Trans	Untrans	T-Freq	U-Freq	Null log-likeli	Alt log-likeli	Likeli-ratio Chi Square	p-value
4 & 5	C-A	23	25	0.1322	0.1437	-330.123	-329.931	0.3833	0.8257
	C-G	**91**	94	**0.5230**	0.5402				
	T-G	60	55	0.3448	0.3161				

4: rs237897 (C/T), 5: rs4686302 (G/A)

The haplotype C-G, composed of the major alleles of the markers rs237897 and rs4686302, was transmitted the most (91 times). The second most transmitted one was the haplotype T-G, built from the minor allele of marker rs237897 and the major allele of marker rs4686302, with 60 transmissions. The haplotype C-A, consisting of the minor alleles of both markers, was the least transmitted one (23 times). The statistical data from the IQ > 70 subpopulation were almost identical with those from the complete cohort. None of the haplotypes fulfilled the criteria of statistical significance ($\chi^2 \geq 5.99$, $p \leq 0.05$, $df = 2$).

Subsequently, the odds ratios and the confidence intervals are displayed.

Table 3.26: Haplotype effects of rs237897 and rs4686302 (IQ > 70)

Marker	Haplotype	Odds-R	95 % Low	95 % High
4 & 5	C-G	1	1	1
	C-A	0.9524	0.4869	1.8615
	T-G	1.1438	1.1104	1.1747

4: rs237897 (C/T), 5: rs4686302 (G/A)

The major haplotype C-G served as the reference value. The haplotype C-A, composed from the major allele of rs237897 and the minor allele of rs4686302, revealed a slight protective effect (Odds-R: 0.9524). The haplotype T-G, built from the minor allele of rs237897 and the major allele of rs4686302, showed a slight risk increasing effect (Odds-R: 1.1438). The haplotype C-A turned from a risk haplotype into a protective one (Odds-R [all trios]: 1.1922; Odds-R [IQ > 70]: 0.9524). The confidence interval values hardly changed. The odds ratio value for the haplotype T-G slightly increased (Odds-R [all trios]: 1.0790; Odds-R [IQ > 70]: 1.1438). The confidence interval values hardly changed; there was just a minimal increase of both values.

3.2.26 Summary of association analyses of *OXTR* with ASD

In summary, the association analyses did not reveal any association of the five investigated SNPs in the *OXTR* gene with ASD. The consideration of the single markers revealed one SNP, rs2268494 (A/T), which showed a tendency to association in the complete cohort and in the IQ > 70 subpopulation ($\chi^2 > 2.9$, $p < 0.09$, $df = 1$). Among all investigated haplotypes, only the haplotype combinations consisting of the markers rs2268494 and rs237889 (1 & 3) showed a tendency to association ($\chi^2 = 6.93$, $df = 2$, $p = 0.0738$) in the complete cohort. The haplotype consisting of the minor alleles of rs2268494 and rs237889 (T-A) indicated a protective quality with respect to ASD in the complete cohort (Odds-R: 0.64), which was supported by the confidence interval values (95 % Low: 0.45, 95 % High: 0.92). The haplotype A-A, built from the major allele of rs2268494 and the minor allele of rs237889,

revealed a risk-increasing quality in the complete cohort (Odds-R: 1.47), which was also supported by the confidence interval values (95 % Low: 1.0001, 95 % High: 2.1834). In the IQ > 70 subpopulation, exclusively the haplotype combinations consisting of the markers rs2254298 and rs237889 (2 & 3) revealed a tendency to association (χ^2 = 6.26, df = 2, p = 0.09). However, none of the haplotypes was unambiguously protective or risk-increasing. The comparison of the single marker test results of the complete cohort and the IQ > 70 subpopulation confirmed that there were no changes among the overtransmitted alleles, they remained the same in both populations tested (A, C, A, T, A). The p-value of rs2268494 even remained identical (p = 0.0863) in both populations. The comparison of the Haploview results with those from UNPHASED in the complete cohort revealed that there was only a minor change of the p-value for rs237897 (Haploview [all trios]: 0.7055, UNPHASED [all trios]: 0.5806). The remaining p-values were nearly identical. Bigger changes occurred among the Haploview and the UNPHASED results of the IQ > 70 subpopulation. The Haploview result for rs2268494 indicated a tendency to association (p = 0.08), the UNPHASED result did not indicate any tendency to association for this marker (p = 0.41). UNPHASED calculated lower p-values for rs2254298 (p = 0.36) and rs237897 (p = 0.25) in comparison to Haploview (rs2254298: p = 0.49; rs237897: p = 0.64). The p-values of the markers rs237889 and rs4686302 were higher in the UNPHASED calculations (rs237889: p = 0.15; rs4686302: 0.74) in comparison to those done with Haploview (rs237889: p = 0.14; rs4686302: p = 0.58).

3.3 Constitutive *Mlc1* knockout mouse procedure

3.3.1 Validation of pMlc1_KO_mod vector as positive control

Previous genome-wide linkage analyses (Stober *et al.*, 2000, 2001) have revealed a susceptibility locus for SCZD10 on chromosome 22q13 in a single large family. Further refinement of polymorphic markers in this genomic region (Jobst Meyer, unpublished data) confined the genomic area to a 4 cM region to the D22S1160-telomer. The mutational analysis of the putative candidate gene *MLC1* resulted in the identification of the C1121A allele in one family, which leads to an amino acid exchange at position 309 from leucine to methionine (Leu309Met). Further fine-mapping on chromosome 22q13 and the exclusion of

the candidate gene *BRD1* (Ekawardhani, 2008) support *MLC1* as a candidate gene for the etiology of SCZD10. To date, functional data about MLC1 are missing. This pointed to the idea to comprehensively investigate *Mlc1* in a knockout mouse model.

For the creation of a knockout mouse, a positive control was needed during the complete detection procedure. The positive control served the optimization of the screening procedure and enabled to prove PCR specificity. Thus, the pMlc1_KO_mod vector (Ekawardhani, 2008) was taken as a template and later on as the positive control during the whole process (2.15.1). If the PCR reaction worked on the highly diluted positive control, one could expect that the PCR conditions will also be appropriate for ES gDNA. The forward primer bound in the pgk promoter sequence (pgk) of the vector and the reverse primer in the neomycin resistance gene (Neo). Subsequent to the optimization procedure, pMlc1_KO_mod sample revealed the PCR fragment at the expected size of 430 bp, whereas the negative control (H_2O) did not show any PCR fragment, as expected. The PCR fragments were visualized on a 1.5 % agarose gel (Figure 3.9).

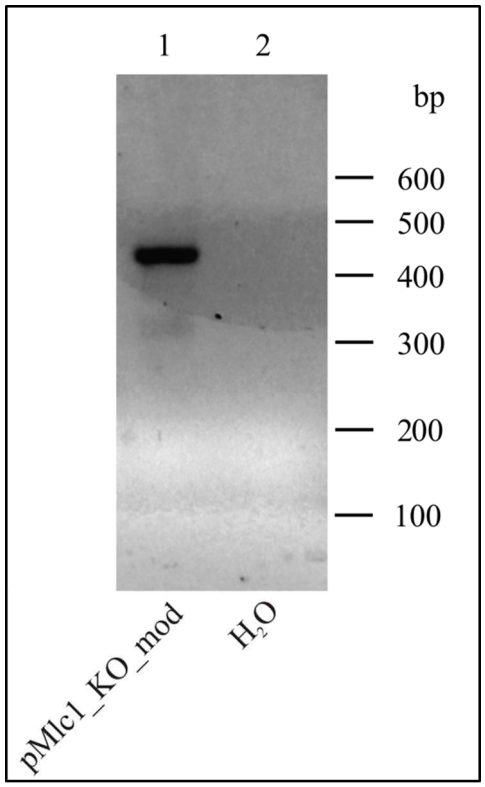

Figure 3.9: PCR optimization on pMlc1_KO_mod. The PCR products were separated on a 1.5 % agarose gel. (1) The PCR reaction on the template pMlc1_KO_mod gave a signal at a size of 430 bp. (2) The negative control did not give any signal as expected.

3.3.2 Screening of ES for sufficient amount of gDNA for further validation process

The ES arrived in 96 well plates with variable amounts of ES in each of the wells. Thus, the putative amount of ES gDNA also varied in a large scale. A PCR reaction requires a minimum amount of DNA to enable gene amplification. Due to the previous selection process only few cells survived, which already set the possible amount of ES gDNA at very low limits. The quantification of ES gDNA by spectrophotometry was technically impossible because the amount of ES gDNA was below the detection limit. Hence, ES gDNA was isolated and the PCR reaction on *Serpina6* (2.16.1) was accomplished to check, if a sufficient amount of ES gDNA was available for subsequent PCR reactions (Figure 3.10).

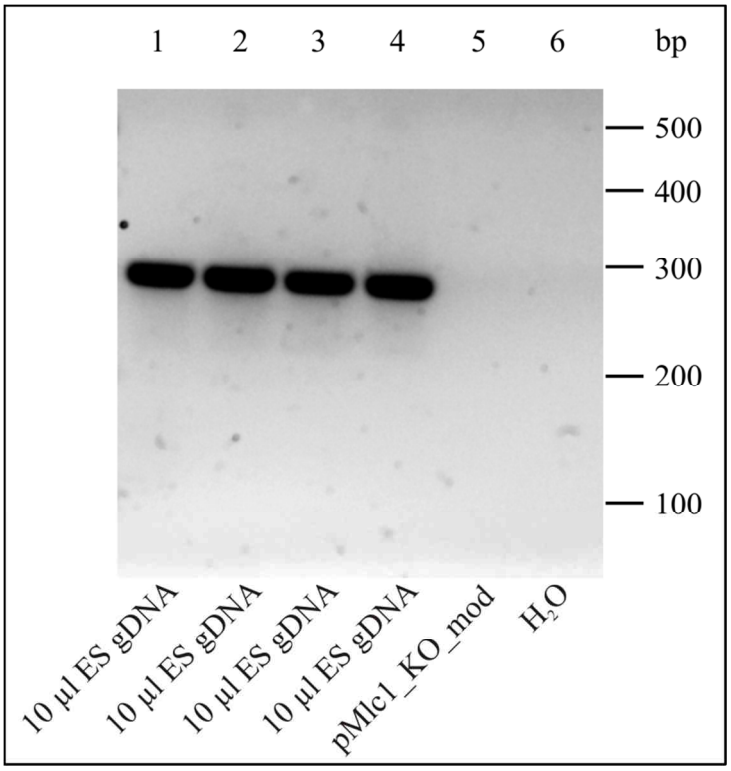

Figure 3.10: Amplification of the *Serpina6* gene. The fragments were detected at the expected size (300 bp) and separated on a 1.5 % agarose gel. (1-4) 10 µl of ES gDNA as a template yielded the expected signal. (5-6) The knockout construct pMlc1_KO_mod and H_2O were used as negative controls (no signals) for verification of the PCR specificity.

The ES gDNA was isolated from each of the single wells. From each sample, 10 µl ES gDNA was taken for the PCR reaction on *Serpina6.* The four tested samples, each derived from a different well, revealed the expected 300 bp fragment of *Serpina6*. This finding confirmed that the PCR conditions were appropriate for ES gDNA detection. If a sample did not yield any signal in the *Serpina6* PCR, it was considered as ES gDNA-free and discarded. The gDNA of C57BL/6 mice was used as a positive control to validate the PCR performance, H_2O as negative control.

3.3.3 Finding aberrant *Mlc1* sequence integration in ES gDNA

Those samples that showed a sufficient amount of ES gDNA (successful *Serpina6* PCR) were considered for further analysis on aberrant *Mlc1* sequence integration into the ES gDNA. The integration of the aberrant *Mlc1* sequence was tested by a PCR reaction. The forward primer bound to the pgk promoter sequence and the reverse primer in the neomycin resistance gene sequence, both not naturally present in mammalian genomes. A positive signal could only occur, once the pMlc1_KO_mod sequence had integrated into the ES gDNA. Some of the tested ES gDNA samples revealed a signal; some others did not (Figure 3.11).

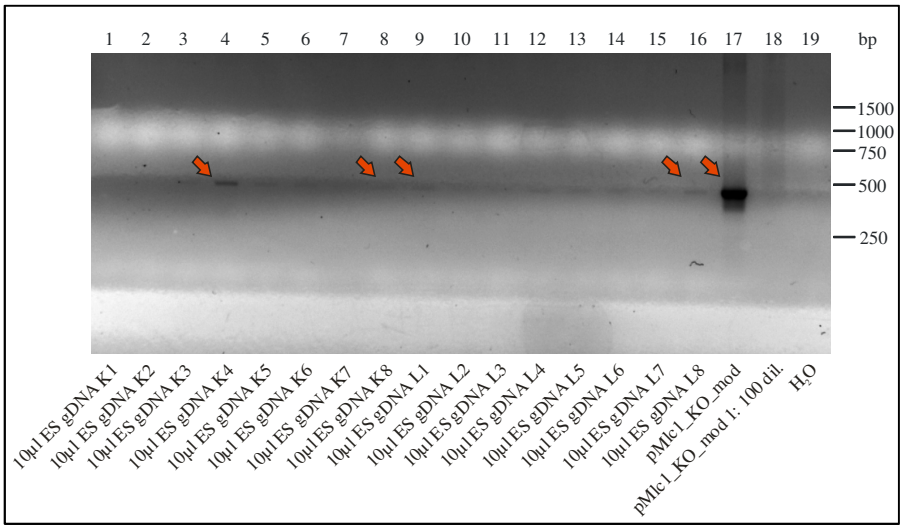

Figure 3.11: Detection of pMlc1_KO_mod sequence in ES gDNA. The recombination of the pMlc1_KO_mod vector and the ES gDNA had occurred in several samples and are indicated with arrows: (1-16) 10 µl ES gDNA from different wells, respectively (17) 10 ng of pMlc1_KO_mod as positive control. (18) 1:100 dilution of pMlc1_KO_mod with H_2O (100 pg / µl). (19) H_2O as negative control.

The positive control and negative controls (17-18) confirmed the accuracy and purity of the PCR. The ES gDNA signals were faint with exception of sample four. To improve the evaluation, 5 µl of the ES PCR products were taken as templates for another PCR with the same primers (reamplification PCR). After reamplification, the signals intensity was high and enabled the distinction of recombinant and non-recombinant samples (Figure 3.12).

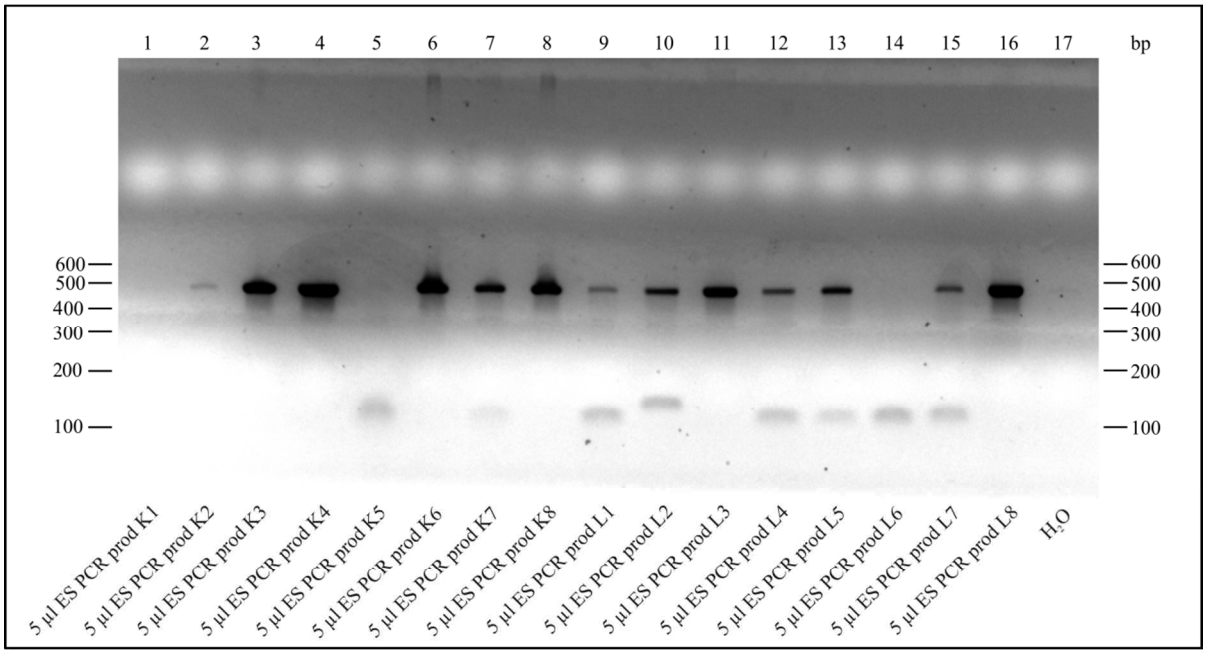

Figure 3.12: Reamplification of PCR products from ES with aberrant *Mlc1* sequence-selective primers. The signals could be intensified for a better distinction of recombined and native ES gDNA. (1-16) 5 µl PCR product of the previous PCR reaction were used for reamplification. (17) H_2O served as negative control (no signal).

The reamplification of the PCR products delivered signals with a higher intensity. Some samples (3, 4, 6, 7, 8, 10, 11, 12, 13, 15 and 16) revealed high signals, others faint ones (2, 9) and a few did not yield any signal after reamplification (1, 5 and 14). No fragment could be detected in the negative control. The samples that presented intense signals confirmed that the knockout vector sequence had undergone recombination with the ES gDNA.

3.3.4 Detection of homologous recombination of aberrant *Mlc1* sequence into ES gDNA

The intention of the knockout vector process was the integration of the aberrant *Mlc1* knockout vector construct at the correct position in the ES gDNA (homologous recombination). Assuming that the homologous recombination had worked, the *Mlc1* would have been disrupted. The identification of homologous recombination was done by a further PCR. In this PCR, the forward primer hybridized to the ES genome sequence of *Mlc1* (native sequence) and the reverse primer to the neomycin resistance gene sequence. The PCR was supposed to deliver a fragment of 1,398 bp, if homologous recombination had occurred (Figure 3.13).

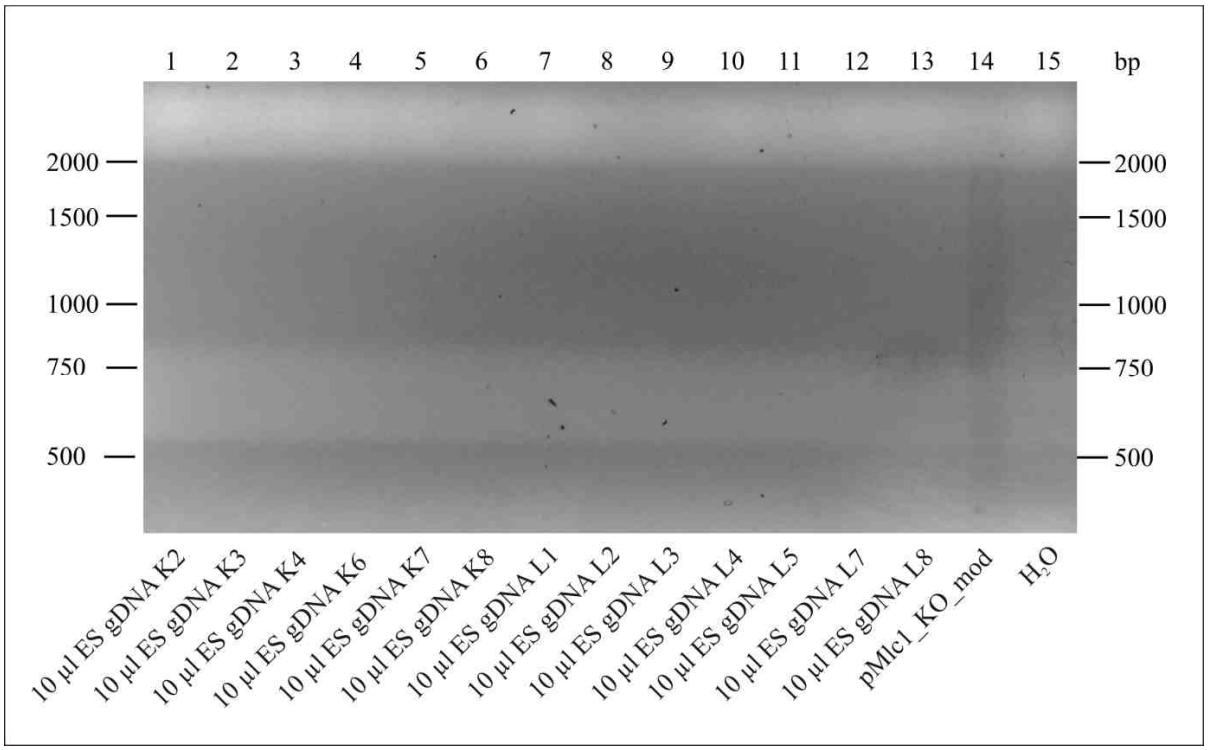

Figure 3.13: No homologous recombination in ES gDNA samples. The expected PCR fragment of 1,398 bp did not occur in any sample. The samples were separated on a 1.5 % agarose gel. (1-13) PCR on ES gDNA did not yield any signal. Homologous recombination could not be confirmed. (14-15) The negative controls pMlc1_mod_KO and H_2O did not show any signal.

None of the samples showed a PCR fragment at the expected size of 1,398 bp. Homologous recombination of the aberrant *Mlc1* sequence into the ES gDNA had obviously not occurred.

The vector pMlc1_KO_mod was used as the first negative control. The forward primer did not have any binding site within the vector sequence thus it was expected that no PCR product should appear on the agarose gel. H_2O as a second negative control confirmed the purity of the PCR reaction. Four PCR plates, each containing 96 different samples, were tested by the complete procedure (3.3.2 – 3.3.4). Most of the ES samples yielded sufficient gDNA. The subsequently accomplished PCR ("detection of aberrant *Mlc1* sequence") also delivered a high number of recombination-positive samples. Yet, none of these samples yielded a signal in the PCR on homologous recombination. Two explanations are possible: 1.) homologous recombination had not occurred in any of the investigated ES samples. 2.) the sensitivity for the detection of homologous recombination in the ES gDNA was too low.

3.4 Effects of miRNAs on *MLC1* and *NR3C1* gene expression in CNS-derived cell lines

3.4.1 Target sites of miRNAs in 3'-UTRs of *MLC1* (NM_015166) and the *NR3C1* genes (NM_000176)

It has been shown for the *MLC1* gene that it is involved in the etiology of periodic catatonia (SCZD10, *605908) in one of our multiplex families (Meyer *et al.*, 2001). Additionally, *MLC1* polymorphisms were found to be associated with SZCD10 (Selch *et al.*, 2007). Psychiatric diseases such as schizophrenia and major depression disorder (MDD) are often triggered by extreme acute or long-termed physical and mental stress episodes, leading to a dysregulation of the hypothalamus–pituitary–adrenal (HPA) axis (de Kloet *et al.*, 2005). The main effect of stress response in mammals is caused by glucocorticoids. Throughout the human brain, there is a high density of receptors for glucocorticoids. The fact that a mutation of the *MLC1* gene had been identified in our multiplex families segregating SCZD10 (Meyer *et al.*, 2001) and that an association of *MLC1* with SCZD10 had been demonstrated (Selch *et al.*, 2007), this study had two goals: 1.) the biological validation of the *in silico*-predicted miR-137 target site in the 3'-UTR of *MLC1* by cell culture experiments. 2.) the identification of a possible implication of *MLC1* in stress response by immunoblot analysis of NR3C1 and MLC1 after miR-137 administration in human and rat CNS-derived cell lines.In this study,

the 3'-UTR of the *MLC1* gene (NCBI accession number: NM_015166) was investigated by the application of the web-based tool TargetScan, Release 5.1 (April 2009).

```
50500191 ACTTCTGAACGCTGGCTGCTCGCTGCCTGTGGCCGAGTGGCGTGTCCACCTTCCCGCCGC 50500132
50500131 ACAGGTGGCCCTGGTGAAGTAACACCTTTCCTGTCTCGGTTGCAGGTGGCCAGGAGCCCC 50500072
50500071 CTGAAGGAGTTCGACAAGGAGAAAGCCTGGAGAGCCGTCGTGGTGCAAATGGCCCAGTGA 50500012
50500011 CCCCCAGACGCGGAAACCGGGTGGCAGCGCCCAGCCTGGCCCCAAGCATGGAAACGCACA 50499952
50499951 ACCCCTAATCGCCCTGAGCTACTGCTTCTAACACCTCTTTTCCCTTGTGTGAGGGCAAAC 50499892
50499891 CAGGCTGCAGGTGGGGTTTTCACTTCCTAGGGTAGTTTAATTTTAAAATAGGCCAATGTT 50499832
50499831 GGCTAGTCTGTGCCTCAGTGAGATCAGTCAGCTCCGAGTGGCTCCCGTGTCGTAACAGCA 50499772
50499771 GGAGCATGGCCGCAACTTCCCAGGCCGAGGAAGGGCCCCCGGCTCGGCCTCTTGAGAGCC 50499712
50499711 CCACCCCTGAACTGGCCCCAGCTCCTCTTCCTGCCTCTCTCATGGCTTGGGCTGGAGTGG 50499652
50499651 GCTCTCTGGACCTGACCAGACTGTGGGTCCCTGCGTCTCCTGCCCACTCTGACCGGGCTT 50499592
50499591 CCTCCCTCCACGCTTAGGGTCTGTCCCGGGTACTCAGTCAGCCCAGTGGGATCTTACCCA 50499532
50499531 CTTCCCTGCAAGGTGCACCTGCCCCAGGCTCAGGCTGCCCAGCGGCTCTTCCTGGACAGT 50499472
50499471 GAGAGCAGGGCTGGGCGCCTCTGTCCTGGCCCGGGAGCCGCAGGGGCCCCTCCTCCAGAG 50499412
50499411 CCTGGGCGCAAGCGACACAGGCTGCCGCTGCTCTCCCAGGTGAAATCCACACCAGTCCAC 50499352
50499351 GCCGGGTCGCCTGCCCTGTCTCCCTACTTAGACCCAGTCATTCTAGAGGGATCCACCGCC 50499292
50499291 ACACTGGCCGGCCCACGTCCTGGGTGCTGTCATGCCCAGCTTGGAGTGCCACGTGGCCGC 50499232
50499231 TGCCCACGTCCCGGGCACTGTCATGCCCAGCTTGGAGTGCCACATGGCCGCTGCCCACGT 50499172
50499171 CCCGGGCACTGTCATGCCCAGCTTGGAGTGCCACGTGGCCGCTGCTGTGACAGGCAGTGT 50499112
50499111 TCTTGGGGGTGGGGCTGCATCCAAGGCTTTGTAAACCGGCTGGACCACGTCTCCCTGGCC 50499052
50499051 CCAGTGACCGGGGGAAGCTGAGCCCCTCCCTCCTGTGTTTGCTCCCATTACTCAAAATGC 50498992
50498991 AGGACAGATCAGGTCAGAGCCCAGGAATTCTCACAGGTTCACCCAGCGCCCTCTACCTCC 50498932
50498931 TAGCAAGTACTTTGTCTTGATCCTCACTGAGAAGGCCCCAGGGCAGCGGTCTTCTCCATC 50498872
50498871 TCCGCTGTTTTGGGGTCTTAGGGTACAGCCCAGGCGGTCACTGCCCACCTGCCAGGCTGC 50498812
50498811 AGGGACAGTTGGGTGTGAGAATAACACTGGCTTTGGGTAGTGCCATGGCCAGGAGTGGGT 50498752
50498751 TTCCCTGCGTCTCCTCGTCCCGAGGGCGCCTGGGTCCTCCCAGCTGACGGCAGTAAATCC 50498692
50498691 ACAGTGAGTTGGGGCGACTGTGAAACTGGAATGCTGTTACTTTGATAATTACTTTCCAGC 50498632
50498631 AGGTGTTTTCCTTCACAATGGTTTTGTTTCTTTCCTTCTGATCTGAGAAGACATGAACGT 50498572
50498571 TTTCTCTTCACCGCCGTGGGGTGTATTGACTGGTCCCCCATGGGCTGCTGGAAAGGCCCG 50498512
50498511 GAGATGCATCTGTGGCCTGGGGCCATCAAGATCAAAGAACCAGGAGGCCTGGGAGATGCA 50498452
50498451 GCTGGATGGGGCGGCCTGCAGACCCTGCCAGGGGGTTTGAGGACCCTCCCAGGTTTCCCA 50498392
50498391 CTGCGGAACAGGAGTGACTCTGGCTGCCAAGATACCTTCATGGTGTTCATGACAAGTGGA 50498332
50498331 ATCATTATTTTCAACCATTGAAGGGGGATGCAGGCAAGACACCTTCCCAGCTGCTCCTAG 50498272
50498271 AGGGGACAAGCCAGGCCCTCTCTGCAGTCCTCGGCAGCTCCGGAAGGACACAGTCAGGGG 50498212
50498211 CCGGGCAAACACTTTGGCCACAGCCCCAAACAAGCGCCACCGTGGGAGAGGAGAGGCTGC 50498152
50498151 TGTCACTGGTACCGGATGCAGACCCCACCCTGTCTGCAGGCCACCCCCACCTCCCTGCAG 50498092
50498091 CTTTGAGGCTGGCGGGGTCTGCTCCTGGGAATGGGGTGGGAGCCACAGGGACGACCCGGG 50498032
50498031 GCGGGCTGATGTCTTCTTGGGGGCAGACCAGAGAGCTCAAGTTTCAGAGTCAGAATTAGG 50497972
50497971 CACTTGGAGCGTTTTTGCTGGCTTGCACTTTCTTATTTTCTTATTTTAGAGCGCTTAAAA 50497912
50497911 AATCCGGAAAAATGGGGTTTAAAAGAACTGTCTCTTTCAGTCTACATTTTTGTTTAATAC 50497852
50497851 GCTTGAGCAATAAACGCTGACTTGCAGACGTGGCTGTGGCTATTTAATATTGTGTCTCAG 50497792
50497791 CAGCGTCAGCTCACTCAGGTCTAAAAACATCGGGACACAGGGAGGAGGGGCGGGTGGAGG 50497732
```

Figure 3.14: The gDNA sequence of the *MLC1* gene surrounding Exon 12 (NM_015166). The coordinate system is depicted on the left and the right side (GRCh37.p5). Purple: non-coding sequence. Light blue: coding sequence. Yellow: 3'-UTR of *MLC1*. Red: predicted target site of miR-137.

Exclusively one highly conserved miRNA target site (miR-137) was predicted by Targetscan (Figure 3.14). A study published by Silber in colleagues in 2008 demonstrated that miR-137 and miR-124 inhibit proliferation of glioblastoma stem cells and induce the expression of *CDK6*, a protein involved in the cell cycle (Silber *et al.*, 2008). For miR-124 it has been shown that it regulates the adult neurogenesis in the subventricular zone (Cheng *et al.*, 2009)

and that it furthermore downregulates the expression of *NR3C1* and of the glucocorticoid-induced leucine zipper (*TSC22D3*) (Vreugdenhil *et al.*, 2009). Most notably, miR-124 is exclusively expressed in the brain (Krichevsky *et al.*, 2006; Vreugdenhil and Berezikov, 2009).

142658637 TAGTAACTTCAGTGAGAGTTGGTTACTCACAACAAATCCTGAAAAGTATTTTTAGTGTTT 142658578
142658577 GTAGGTATTCTGTGGGATACTATACAAGCAGAACTGAGGCACTTAGGACATAACACTTTT 142658518
142658517 GGGGTATATATATCCAAATGCCTAAAACTATGGGAGGAAACCTTGGCCACCCCAAAAGGA 142658458
142658457 AAACTAACATGATTTGTGTCTATGAAGTGCTGGATAATTAGCATGGGATGAGCTCTGGGC 142658398
142658397 ATGCCATGAAGGAAAGCCACGCTCCCTTCAGAATTCAGAGGCAGGGAGCAATTCCAGTTT 142658338
142658337 CACCTAAGTCTCATAATTTTAGTTCCCTTTTAAAAACCCTGAAAACTACATCACCATGGA 142658278
142658277 ATGAAAAATATTGTTATACAATACATTGATCTGTCAAACTTCCAGAACCATGGTAGCCTT 142658218
142658217 CAGTGAGATTTCCATCTTGGCTGGTCACTCCCTGACTGTAGCTGTAGGTGAATGTGTTTT 142658158
142658157 TGTGTGTGTGTGTCTGGTTTTAGTGTCAGAAGGGAAATAAAAGTGTAAGGAGGACACTTT 142658098
142658097 AAACCCTTTGGGTGGAGTTTCGTAATTTCCCAGACTATTTTCAAGCAACCTGGTCCACCC 142658038
142658037 AGGATTAGTGACCAGGTTTTCAGGAAAGGATTTGCTTCTCTCTAGAAAATGTCTGAAAGG 142657978
142657977 ATTTTATTTTCTGATGAAAGGCTGTATGAAAATACCCTCCTCAAATAACTTGCTTAACTA 142657918
142657917 CATATAGATTCAAGTGTGTCAATATTCTATTTTGTATATTAAATGCTATATAATGGGGAC 142657858
142657857 AAATCTATATTATACTGTGTATGGCATTATTAAGAAGCTTTTTCATTATTTTTTATCACA 142657798
142657797 GTAATTTTAAAATGTGTAAAAATTAAAACCAGTGACTCCTGTTTAAAAATAAAAGTTGTA 142657738
142657737 GTTTTTTATTCATGCTGAATAATAATCTGTAGTTAAAAAAAAAGTGTCTTTTTACCTACG 142657678
142657677 CAGTGAAATGTCAGACTGTAAAACCTTGTGTGGAAATGTTTAACTTTTATTTTTTCATTT 142657618
142657617 AAATTTGCTGTTCTGGTATTACCAAACCACACATTTGTACCGAATTGGCAGTAAATGTTA 142657558
142657557 GCCATTTACAGCAATGCCAAATATGGAGAAACATCATAATAAAAAAATCTGCTTTTTCAT 142657498
142657497 TATGTGACTCCAACATGCTTTTGTAGAACTTGTACAGTTCCGATTGTCCAATCTGATTTT 142657438

Figure 3.15: The gDNA sequence of the *NR3C1* gene surrounding Exon 9 (NM_000176). The coordinate system is depicted on the left and on the right side of the sequence. Purple: non-coding sequence. Light blue: coding sequence. Yellow: 3'-UTR of *NR3C1*. Red: predicted target sites of miRNAs.

TargetScan Version 5.1 predicted 15 potential target sites of miRNAs (Figure 3.15) in the 3'-UTR of the *NRC31* gene. Three target sites were predicted for miRNA-124. According to the results of the *in silico* investigation, the aim of this study was to test whether the application of the precursor molecule of miR-137 had any detectable effect on the expression of *MLC1* and *NR3C1*. Furthermore, a part of the *NR3C1* 3'-UTR gDNA sequence, encompassing the target sites from miR-183 until miR-410, was cloned into the pMIR-REPORT vector for subsequent investigation of the predicted miRNA target sites.

3.4.2 MLC1 protein expression in human CNS-derived cell lines

Before starting the investigation of a certain protein in cell lines, it is generally required to clarify whether these cell lines reveal endogenous expression of the protein of interest. The NR3C1 protein is practically ubiquitously expressed and its expression pattern within CNS-derived cell lines of human and animal origin is well characterized. Concerning the MLC1 protein, the expression pattern is not yet well characterized among the variety of cell lines. The glioblastoma cell line U373MG served as a positive control for MLC1; one study had previously confirmed endogenous expression of MLC1 in this cell line (Ambrosini *et al.*, 2007). The protein expression pattern of MLC1 was tested in four cell lines (SH-SY5Y, TR14, SK-N-MC, U-373MG).

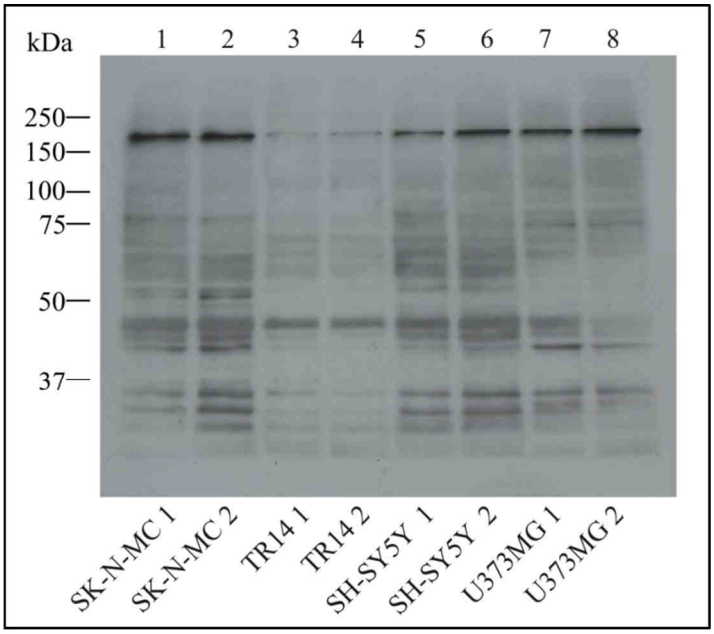

Figure 3.16: MLC1 protein expression in human CNS-derived cell lines. SK-N-MC (1-2), TR14 (3-4), SH-SY5Y (5-6) and U373MG (7-8). In each lane, 20 ng of total protein were separated on a 10 % SDS-PAGE. The rabbit anti-human MLC1 antibody targets the N-terminal region of the MLC1 protein. The applied primary antibody (Abcam, Cambridge, UK) was obviously unspecific (multiple bands on immunoblot). The band with the highest signal intensity revealed a molecular weight of 160 kDa. The signal intensity of the 160 kDa band in the cell lines SK-N-MC and U373MG appeared to be similar (lanes 1-2 and 7-8). The signal intensity of the SH-SY5Y) samples (5-6) was weaker than in those derived from SK-N-MC and U373MG. The TR14 samples (3-4) showed the faintest signals.

Two antibodies (Table 2.9) were used for the identification of MLC1 expression in the four CNS-derived cell lines. Figure 3.16 displays the immunoblot created with the antibody, which was raised against the immunogenic sequence encompassing the amino acids 180-229 of the MLC1 protein sequence (Abcam, Cambridge, UK). Multiple changes of the protocol (blocking of nitrocellulose membrane with BSA instead of low-fat milk powder, decrease of antibody concentration from 1:200 in steps to 1:1000, more stringent washing episodes, elongation of washing episodes) did not yield any improvement. Tejido and colleagues (2004) described that MLC1 has a lower molecular weight than expected (about 10 kDa less) and that it obviously forms multimers (Teijido *et al.*, 2004). Apart from our observation that the immunoblots always resulted in a "bar-code"- like pattern, one could recognize a very intense signal at a molecular weight of about 160 kDa. Following the explanation given by Teijido and colleagues (2004), this band could potentially represent a tetramer of MLC1 (Teijido *et al.*, 2004). However, the immunoblot signals should have been clear without ambiguity to draw appropriate conclusions. The cell lines U373MG and SK-N-MC and PC12 were used for further experiments because MLC1 expression both on the mRNA and protein level had been proven for these cell lines (Ambrosini *et al.*, 2007; Lukk *et al.*, 2010; Henseler, 2010). In conclusion, the MLC1 protein could not be displayed on immunoblots without ambiguity. Consequently, the focus of this study was shifted to the investigation of miR-137 effects on *NR3C1* expression for two reasons: 1.) immunoblot analysis of the NR3C1 protein was

possible due to the availability of appropriate antibodies. 2.) detectable effects of miR-137 on NR3C1 protein expression have not ever been described in any publication before.

3.4.3 NR3C1 protein expression is reduced by miR-137 in cell lines U373MG, SK-N-MC and PC12

In silico analysis by TargetScan Human release 5.1 predicted one poorly-conserved target site for miR-137 in the 3'-UTR of *NR3C1*. One study had shown morphological changes in mouse embryonic stem cells and modified gene expression subsequent to miR-137 and miR-124 transfections (Silber *et al.*, 2008). The study by Silber and colleagues provided the first indication for a potential influence of miR-137 on *NR3C1* expression. As positive control, miR-124 was applied because it had been demonstrated to knockdown *NR3C1* expression in human neuronal tissues (Vreugdenhil *et al.*, 2009). One poorly-conserved miR-137 target site had been predicted for miR-137, thus indicating a possible link of *MLC1* and *NR3C1* in the modulation of mental disorders. The results are illustrated in Figure 3.17.

U373MG and SK-N-MC

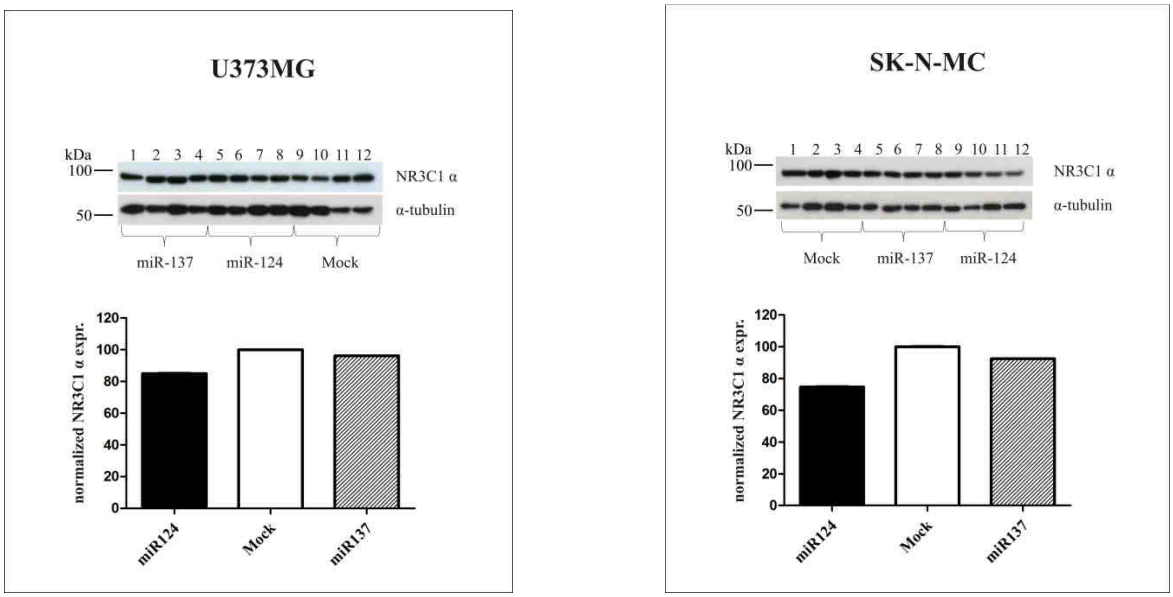

Figure 3.17: NR3C1 α protein expression is reduced by miR-137 and miR-124 in U373MG and SK-N-MC cells. Immunoblot analysis was performed to measure steady-state NR3C1 α protein expression levels. The data were normalized against α-tubulin. The experiments were performed with two biological samples and repeated twice (n = 4). The addition of 100 nM miR-124 and miR137 led to a decrease of NR3C1 α levels in both cell lines, albeit not statistically significant.

These experiments have shown that the application of 100 nM miR-137 lead to a decrease of NR3C1 α expression in U373MG and SK-M-MC cells. Due to a low number of samples tested (n = 4) per cell line, the data were did not fulfill the criteria for statistical significance ($p \leq 0.05$). Interestingly, the effect of miR-124 was obviously higher in U373MG cells than in SK-N-MC, leading to a lower NR3C1 α protein expression in U373MG cells. A higher number of samples and repeated measurements will be needed to validate our findings and to draw conclusions about the biological effect of miR-137 in U373MG and SK-N-MC cells respectively.

PC12

The cell line PC12 was used to investigate miR-137 effects in a neuronal phenotype. PC12 cells were differentiated into the neuronal phenotype by NGF prior to experimental use. The results are displayed in Figure 3.18.

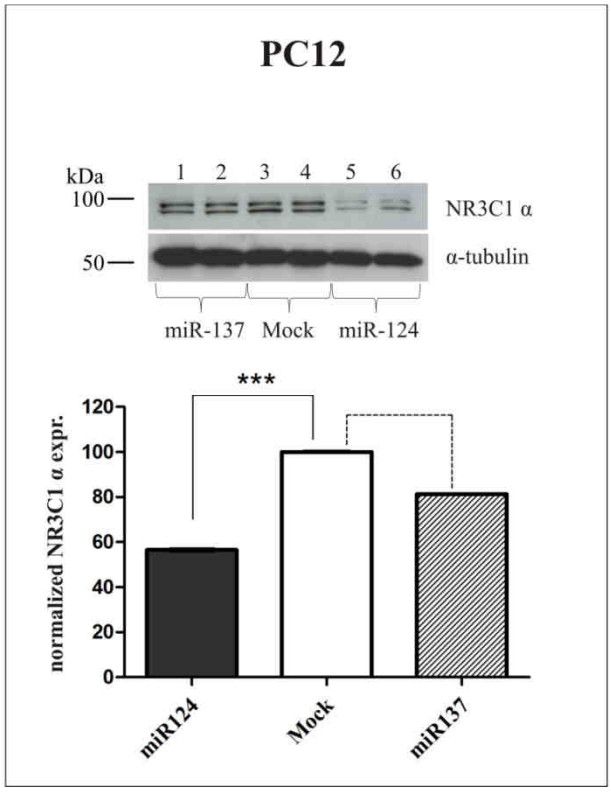

Figure 3.18: NR3C1 α protein expression is reduced by miR-137 and miR-124 in PC12 cells. Immunoblot analysis was applied to measure steady-state NR3C1 α protein expression levels. The data were normalized against alpha-tubulin. The experiments were performed with two biological samples and repeated four times (n = 8). Bar graph represents means ± SEM, post-hoc. Mock vs. miR124, solid line, $p < 0.0001$ (***); Mock vs. miR137, dashed line, trend effect ($p = 0.064$).

As depicted in Figure 3.18, the overall analysis of the different treatments (Mock, miR-124, miR-137) performing a one way ANOVA led to a highly statistical significant effect ($F_{(2,23)} = 11.57$; $p \leq 0.001$, $n = 8$). Post-hoc analysis showed that the addition of 100 nM miR-124 resulted in a significant decrease of NR3C1 α protein expression level (≈ 40 %) in comparison to the Mock condition. There was also the tendency of miR-137 treatment to downregulate NR3C1 α protein expression at about 20 %, albeit the observed effect did not reach statistical significance ($p = 0.064$, $n = 4$). These results indicate that miR-137 has an observable influence on the NR3C1 α protein expression in CNS-derived cell lines from humans and rats. However, a higher number of biological samples and repeated measurements will be necessary for validation of our results with respect to statistical significance.

3.4.4 *NR3C1* pMIR-REPORT construct

The investigation of *in silico*-predicted miRNA target sites was planned to be performed in a reporter gene construct called pMIR-REPORT. The complete 3'-UTR of *NR3C1* is too large for being cloned at once. Hence, a distinct region of the *NR3C1* 3'-UTR (red box) was cloned into the pMIR-REPORT vector for downstream analysis of the predicted miRNA target sites (Figure 3.19).

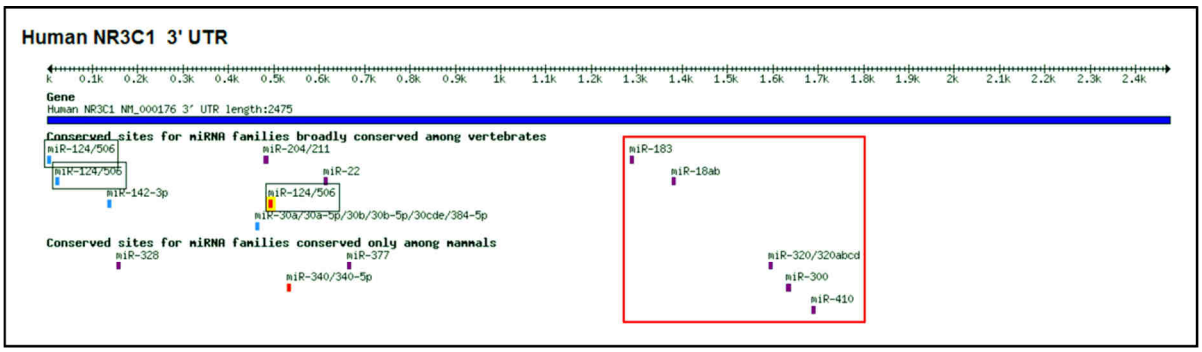

Figure 3.19: TargetScanHuman output of *NR3C1* 3'-UTR (NM_000176). The red box indicates the fragment that was cloned into the pMIR-REPORT vector.

Vreugdenhil *et al.* (2009) have demonstrated that miR-18 (red box) leads to a reduced expression of the murine *Nr3c1* in NS-1 cells (Vreugdenhil *et al.*, 2009). This kind of experiment was planned to be replicated with a human *NR3C1* pMIR-REPORT construct to confirm the previous findings in human tissue. In addition, the other *in silico*-predicted miRNA target sites (miR-183, miR-320/320abcd, miR-300 and miR-410) should also be biologically validated as no study characterizing their potential effects on *NR3C1* gene expression had been published yet.

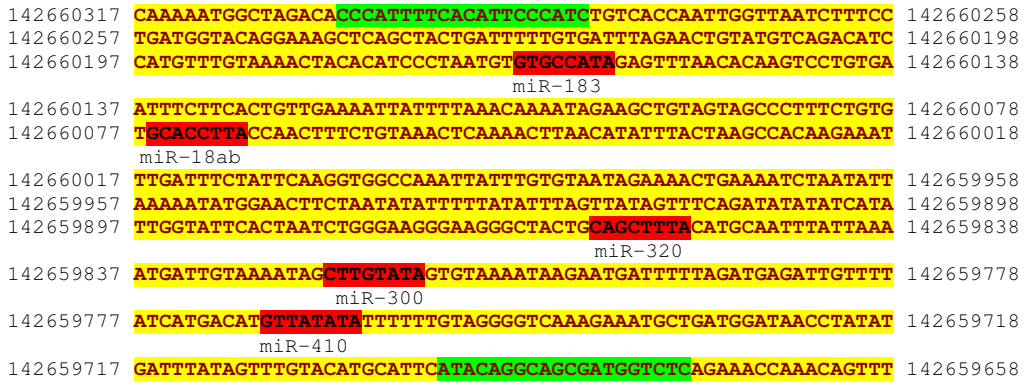

Figure 3.20: 3'-UTR fragment of *NR3C1* gene (NM_000176). The fragment size is 628 bp. The coordinate system is depicted on the left and on the right side of the sequence. The primer binding sites are highlighted in green. The *in silico*-predicted miRNA target sites are highlighted in red.

The fragment of interest was amplified by PCR with human gDNA as a template and the previously mentioned primers (highlighted in green in Figure 3.20). The fragment size was 628 bp. The PCR result was unambiguous; the samples containing gDNA yielded high signals of the expected size on the agarose gel. The negative control (H_2O) did not reveal any signal as expected (Figure 3.21).

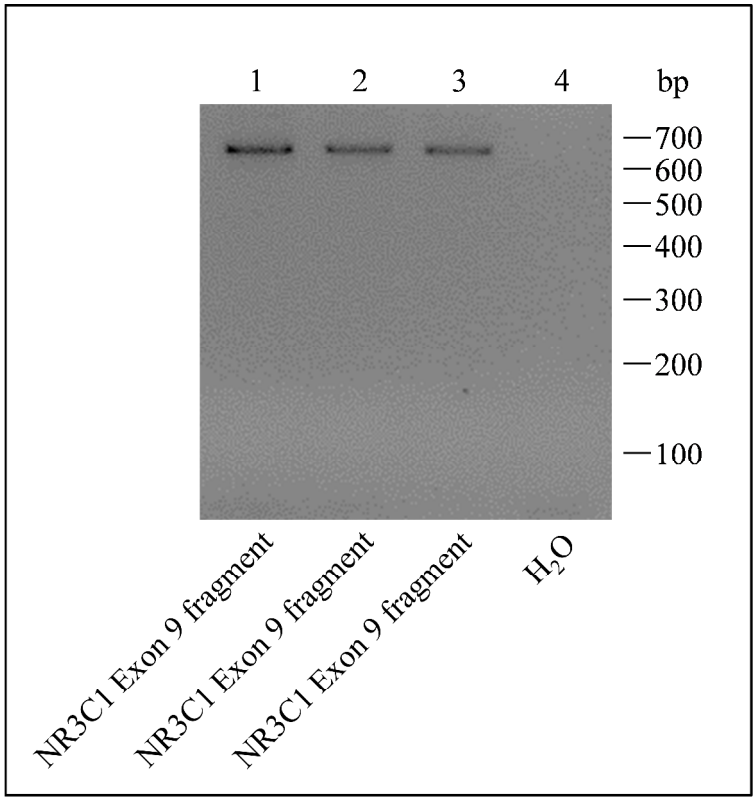

Figure 3.21: *NR3C1* 3'-UTR fragment encompassing *in silico*-predicted miR-410 and miR-183 target sites. 100 ng human gDNA were used for fragment amplification. The samples were separated on a 1.5 % agarose gel. (1-3) *NR3C1* 3'-UTR fragments showing expected size of 628 bp. (4) Negative control (H2O) template did not yield any signal.

The PCR fragment was extracted from the agarose gel and validated by restriction digest. The validated PCR fragment was cloned into the pMIR-REPORT vector. The clones were investigated by colony PCR; pMIR-REPORT-positive clones were considered for inoculation of LB medium with subsequent isolation of pMIR-REPORT plasmids. The plasmids were checked, if they contained the fragment of interest (Figure 3.22).

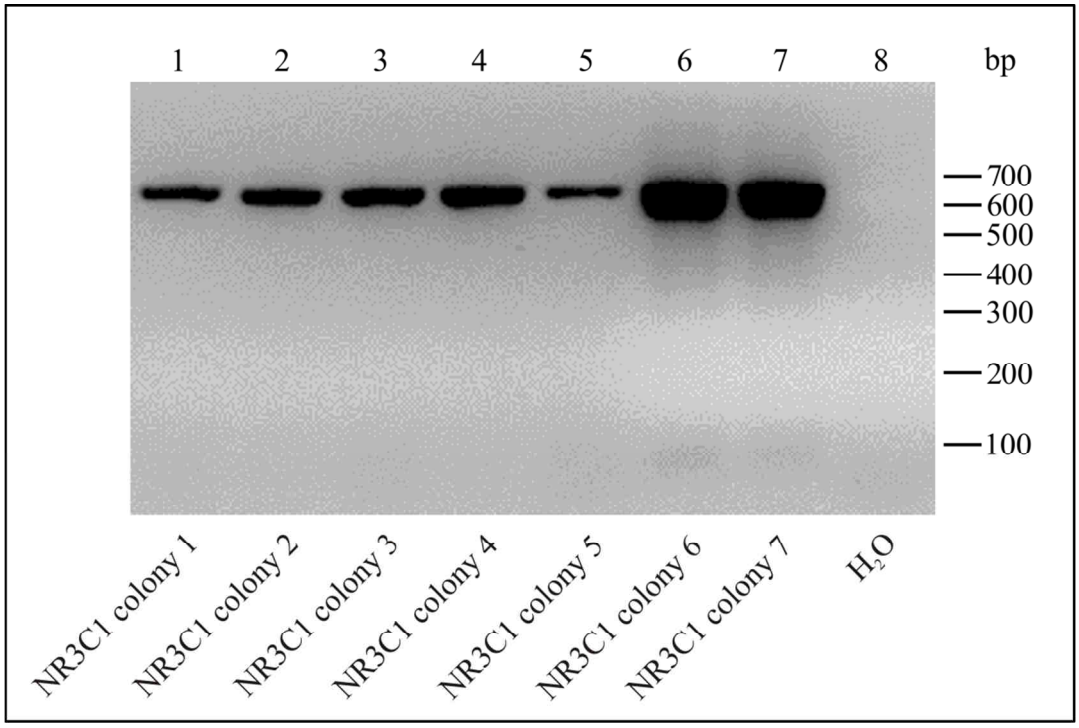

Figure 3.22: Colony PCR on selected pMIR-REPORT *NR3C1* 3'-UTR clones. The samples were separated on a 1.5 % agarose gel. (1-7) The clones showed the expected fragment at a size of 628 bp. (8) The negative control (H_2O) did not show any signal.

All investigated pMIR-REPORT constructs obviously contained the fragment of interest. For final validation, the pMIR-REPORT construct was checked by DNA sequencing. The DNA sequencing confirmed that the cloned *NR3C1* 3'-UTR fragment did not reveal any mutation and that it had been inserted both in sense orientation and correct reading frame. Cell culture experiments with this construct are planned and accomplished by Erno Vreugdenhil and colleagues at the Department of Medical Pharmacology, University of Leiden (NL).

4 Discussion

4.1 The chromosome 15q14 locus for bipolar disorder and schizophrenia: Is *C15orf53* a major candidate gene?

Previous linkage studies conducted in our multiplex families segregating periodic catatonia (SCZD10) revealed linkage to chromosome 15q14-15 (Stober *et al.*, 2001; 2002). Several putative candidate genes located in this segregating genomic region have already been excluded (Meyer *et al.*, 2002; 2003; Ekici, 2004; McKeane *et al.*, 2005). A fine-mapping on chromosome 15q14-15 led to a refinement of the segregating region to a size of 4.38 Mb (Ekawardhani, 2008). The gene *SPRED1*, which is located in this genomic region and expressed in the CNS, could be further excluded as a candidate gene for the pathogenesis of SCZD10 by mutational analysis of SCZD10-affected individuals in our multiplex families (Ekawardhani, 2008). Ferreira and colleagues (2008) performed a GWAS on bipolar disorder (BD) patients of European ancestry and identified three susceptibility loci: *ANK3* on chromosome 10q21 and *CACNA1C* on chromosome 12p13 with the strongest associations and a region in proximity of *C15orf53* on chromosome 15q14 (Ferreira *et al.*, 2008). A further GWAS conducted by Smith and colleagues (2009) on BD patients confirmed two of the previous susceptibility loci in patients of European ancestry: *ANK3* and *C15orf53* (Smith *et al.*, 2009). The latter gene is located exactly in the region defined by our SCZD10 families on chromosome 15q14-15.1. The length of its genomic DNA sequence is 3.44 kb, the gene consists of two exons and the only characterized transcript has a length of 2,043 bp (Ensembl genome browser, rel. 66, February 2012). *In silico* analysis of this gene predicts a putative protein consisting of 179 amino acids (AA), whose existence has not been biologically validated yet. Based on findings from our previous studies and the two GWAS both supporting this locus, the putative candidate gene *C15orf53* was investigated in this study with various approaches: 1.) mutation and segregation analysis in multiplex families segregating SCZD10. 2.) case-control association analyses with individuals diagnosed with BD or SCZD10 versus controls and the combination of both cohorts versus controls. 3.) extended gene expression analysis in human cell lines, leukocyte subpopulations and *post-mortem* limbic brain tissue.

The DNA sequencing of *C15orf53* did not reveal any mutations within the seven tested SCZD10-affected family members (one person from each family), neither in the proximal promoter region, nor 5'-UTR, coding regions and intron-exon boundaries. Thus, *C15orf53* did not seem to be causative for the etiology of SCZD10. Nevertheless, a subsequent segregation analysis was performed in the multiplex families with all available DNA samples. The gene is rather small with a genomic sequence of 3.44 kb. Three SNPs were chosen for the segregation analysis: the promoter SNP rs7171233 (T/A), furthermore a SNP located in the first exon, rs7165988 (C/G) and rs2172835 (C/T), which is located in the only intron and had been genotyped by Ferreira and colleagues (2008). We identified two haplotypes segregating in our SCZD10 families: the first haplotype T-C-C, composed of the major alleles of the SNPs, was segregating in three families (F13, F19 and F24) and the second haplotype A-G-T, consisting of the minor alleles of all SNPs, was segregating in the other four multiplex families (F5, F9, F11 and F17; experimental work accomplished by Michelle Lin, Hans Bauer and Ulrike Schuelter). This result confirmed that the three investigated SNPs in *C15orf53* are in high linkage disequilibrium (LD) in our families, since no other haplotype occurred among our family members.

The genotyping of the three SNPs in 203 BD and 71 SCZD10 individuals revealed that the common haplotype T-C-C had a prevalence of 61 % and the rare haplotype A-G-T one of 32 %. The other calculated haplotypes had a prevalence of less than 2 % respectively and were not considered for analysis. The LD plots by Haploview revealed a high LD in the BD, the SCZD10 and the combined sample. The case-control association analysis yielded negative results. None of the haplotypes was associated with BD, SCZD10 or the combined samples. Additionally, the single markers were not associated with BD, SCZD10 or the combined samples. The unambiguous interpretation of our findings is impossible due to the lack of statistical power. The number of individuals in the tested samples was too low; hence it cannot be excluded that the results of the case-control association study were false-negative. There exist further explanations for this phenomenon that are equally probable. A general problem that occurs with association studies of biologically unrelated subjects is the unpredictability of the exact effect sizes that single markers or haplotypes deliver. Effect sizes of alleles detected in GWAS are considered to be predominantly small (Thapar *et al.*, 2009). However, the individual samples diagnosed with BD and SCZD10 have been exclusively recruited in the area of Würzburg. Thus, the probability of population stratification is rather low. Hypothesis-based association studies with patient samples of comparable sizes, which

originated from the same geographic region, had been successfully conducted in the past (Meyer *et al.*, 2005; de Bakker *et al.*, 2005; Selch *et al.*, 2007). Hence, the case-control sample might have been of sufficient size to detect reasonably strong gene effects, which reveals itself in the SCZD10 multiplex families. The fact that we were unable to detect any association albeit investigating a genetically highly homogenous group of individuals allowed the conclusion that the effect sizes of all three investigated SNPs has to be rather low.

Extensive screening in databases providing information about gene expression such as NCBI and EMBL only delivered very few information concerning *C15orf53*. The function and regulation of *C15orf53* is largely unknown. The cDNA of this gene has been first isolated in 2002 by the Mammalian Gene Collection (MGC), GenBank: BC119810.1 (Strausberg *et al.*, 2002) and in parallel, by the "full-length long Japan" (FLJ) collection (Ota *et al.*, 2003). Its existence has been confirmed in further studies for human spleen tissue (Kimura *et al.*, 2006), the immune system and at extremely low abundance in whole human brain samples, while human limbic brain samples have not been explicitly analyzed (Dezso *et al.*, 2008). In our study, we confirm that *C15orf53* is expressed in the human immune system but not in the human limbic brain (amygdala, hippocampus, inferior gyrus, cingulate gyrus and nucleus accumbens). The very low abundant gene expression of *C15orf53* reported by Dezso and colleagues (Dezso *et al.*, 2008) and the undetectable gene expression in human limbic brain tissues do not support a major impact of this gene in the human brain functions and the etiology of psychoses. The question remains, why Deszo and colleagues (2008) detected a very low abundant gene expression in their *post-mortem* brain tissue samples and in our study, we did not. We had not extracted and processed the human *post-mortem* brain tissues ourselves; thus we were dependent on the accuracy and speed of the pathologists that had performed the brain extraction and cutting into cubes. The most critical phase is the time delay from the time of death until the time of extraction and immediate ultra-deep freezing. The amount of mRNA molecules decreases once the patient is dead and gene transcription stops. Furthermore, mRNA molecules are not thermostable and sensitive towards RNases, which are highly present on human skin. Genes revealing a low transcription rate could not be identified because their transcripts would have degraded at the time of investigation due to time delay, temperature of the tissue and slight contaminations with RNases at the time of extraction. Hence, it is possible that *C15orf53* is in fact expressed in human limbic brain tissues and due to degradation of *C15orf53* transcripts in our brain samples we were unable to detect those. The extent of mRNA degradation prior to conversion into cDNA is difficult to

evaluate; our quantitative PCR on *GAPDH,* a high abundant housekeeping gene, had proven that the mRNA had not been completely degraded prior to conversion into cDNA. However, it is possible that the *C15orf53* gene had been active in our investigated brain samples and due to the multiple processing steps, the transcripts had degraded and thus the gene expression analysis delivered a false-negative result. Another scenario is possible to explain, why Deszo and colleagues identified *C15orf53* expression in their brain samples. Maybe *C15orf53* is in fact not expressed in the CNS. Hence, the detection of *C15orf53* gene expression in human brain tissues could be explained by slight contaminations of their samples with blood and rapid subsequent processing of their tissues for gene expression analysis. Hence, a false-positive result could be possible. The human brain is a highly perfused organ with a blood flow of 1000 ml / min and a constant blood volume of about 100 ml (Walters, 1998). Once the human brain is extracted and cut into appropriate samples, a contamination with blood is practically inevitable. Since we have proven in this study that *C15orf53* is expressed in leukocyte subpopulations, the detection of *C15orf53* gene expression in human brain samples by Deszo and colleagues could be due to blood contamination. Furthermore, due to the high sensitivity and fidelity of microarrays used by Deszo and colleagues, the risk of receiving false-positive gene expression signals is relatively high (Vartanian *et al.*, 2009). Most of the studies on gene expression profiling in psychiatric disorders only focus on gene expression in peripheral sources in a case-control design (Gladkevich *et al.*, 2004; Segman *et al.*, 2005; Tsuang *et al.*, 2005; Bowden *et al.*, 2006; Hu *et al.*, 2006; Numata *et al.*, 2007; Hu *et al.*, 2009a; Hu *et al.*, 2009b). The contamination problem remains, especially when PBMCs are compared with different target tissues. One example is the study by Rollins and colleagues (2010). Seeking valid and robust biomarkers for psychiatric disorders, they compared the gene expression pattern of PBMCs and distinct brain tissues. Contamination of brain tissue with whole blood seems to be an ubiquitary problem that leads to biased findings in gene expression analyses. As a control experiment, they perfused rats with saline prior to brain tissue dissection. Subsequent to this procedure, the gene expression pattern of genes expressed both in brain and PBMCs did not differ significantly, but it revealed that contamination by PBMCs indeed is a given fact that should not be ignored (Rollins *et al.*, 2010).

In our study, none of the analyzed brain regions revealed expression of *C15orf53*. If contamination with PBMCs had played a significant role, one could assume that *C15orf53* expression should have been detected. This would be a limited point of view. In fact, a

contamination with PBMCs in the investigated brain tissues is highly probable. *C15orf53* is obviously expressed at such a low level even in PBMCs that the total amount of transcripts available in the target tissues is limited. Based on the fact that *C15orf53* expression could be neither detected in *post-mortem* human limbic brain tissues nor in human CNS-derived cell lines, it is highly improbable that *C15orf53* is expressed in a large scale in the human CNS. The ability to amplify the housekeeping gene *GAPDH* emphasizes that the cDNA quality was acceptable, albeit *GAPDH* is expressed at such high levels due to its key function in glycolysis that its "marker" quality for cDNA integrity has to be considered carefully.

The most recent version of TargetScan Human (release 6, November 2011) predicted target sites for miR-34a and miR-449 in the 3'-UTR of *C15orf53*. To date, these miRNA target sites have not been experimentally validated yet. Therefore, the dimensions of their potential functionality remain unclear. However, miR-34a seems to be targeted by p53 (Chang *et al.*, 2007; Aranha *et al.*, 2011; Choi *et al.*, 2011) and miR-34a is involved in the differentiation of mouse embryonic stem cells (Aranha *et al.*, 2011). Furthermore, its expression is decreased in mutant-p53 gliomas (Guessous *et al.*, 2010; Luan *et al.*, 2010). These studies underline the implication of miR-34a in necessary regulatory functions in the CNS.

It is known about miR-449 that it is a key regulator of vertebrate multiciliogenesis (Marcet *et al.*, 2011). Furthermore, this miRNA is downregulated in gastric cancer (Bou Kheir *et al.*, 2011). Interestingly, there is also a link of miR-34a and miR-449 to schizophrenia and BD. Transcriptome analysis in the prefrontal cortex of patients diagnosed with schizophrenia and BD showed a dysregulation of miR-34a and miR-449 compared to controls (Kim *et al.*, 2010). Wistar rats administered with the mood stabilizers valproate and lithium demonstrated a reversible change in gene expression of miR-34a. Hence, miR-34a is a potential effector of psychotherapeutic medication (Zhou *et al.*, 2009). In another study by Lai and colleagues (2011), miR-34a was correlated with the negative symptoms of schizophrenia (SCZ) and it was even suggested as a potential biomarker (Lai *et al.*, 2011). These studies support the assumption that *C15orf53* is involved in a not yet characterized network of genes, which influence the occurrence of schizophrenia and/or BD.

4.2 Transmission disequilibrium test (TDT) of *OXTR* with parents–child trios with ASD–affected child

Children diagnosed with ASD show mannerisms in social interaction, deficits in communication and stereotypical behaviors (Levy *et al.*, 2009). The peptide hormone oxytocin (OXT), which is synthesized in the nucleus paraventricularis (PVN) in the hypothalamus and stored in the posterior pituitary gland, is responsible for a variety of physiological processes in humans, among those parturition, lactation and the formation of the mother–child bonding (Heinrichs and Domes, 2008; Lee *et al.*, 2009). OXT acts by binding to the oxytocin receptor (OXTR), which belongs to the G-coupled receptor protein family (Gimpl and Fahrenholz, 2001). It is expressed in the endo and myometrium of the uterus, the mammary gland and in the CNS. Due to the obvious social deficits that patients with ASD exhibit, OXTR as the facilitator of oxytocin effects became a candidate gene in ASD research. A number of association studies on *OXTR* with ASD (Wu *et al.*, 2005; Jacob *et al.*, 2007; Lerer *et al.*, 2008; Liu *et al.*, 2010) as well as functional studies on oxytocin knockout mice (Winslow and Insel, 2002; Modi and Young, 2012; Pobbe *et al.*, 2012) corroborate the implication of the OXT–OXTR system in the pathogenesis of ASD. In one study, the OXTR protein expression in different brain regions in rats was analyzed, among those the olfactory bulb, prefrontal cortex, hippocampus and the striatum. The OXTR protein expression level was associated with the licking behavior of low licking (LL) and high licking (HL) rats. LL mothers revealed a significantly higher expression of OXTR in the olfactory bulb and in the hippocampus. In the maternal aggressive behavior test, the HL mothers showed a higher biting frequency in comparison to LL mothers, supporting the importance of the *OXTR* gene for the modulation and its influence on behavior (Ruthschilling *et al.*, 2012).

In this study, a TDT of five SNPs of *OXTR* was conducted in parents-child trios with ASD-affected children. The SNPs rs2268494, rs2254298, rs237889 and rs237897 were chosen because they had already been tested in previous association studies on ASD (Wu *et al.*, 2005; Lerer *et al.*, 2008). The non-synonymous coding SNP rs4686302 (pAla218Thr) was chosen on our own from the Ensembl database. The single marker allele and putative haplotype effects were estimated with two different bioinformatics tools for family-based association studies, Haploview 4.2 and UNPHASED. The intelligence quotient (IQ) was examined in all

ASD-affected children and calculations were performed in two groups: the complete cohort and trios with children revealing an IQ above 70.

In contrast to previous association studies of *OXTR* with ASD (Wu *et al.*, 2005; Jacob *et al.*, 2007; Lerer *et al.*, 2008; Liu *et al.*, 2010), none of our tested SNPs revealed association with ASD in our cohort. Exclusively for SNP rs2268494, a tendency for association ($p = 0.08$) with a protective effect (OR = 0.54 for T allele) was calculated by both Haploview 4.2 and UNPHASED in the complete cohort and solely with Haploview 4.2 in the IQ > 70 subpopulation. The other four investigated SNPs did not even show a tendency to association, neither in the complete cohort, nor in the IQ > 70 subpopulation. The finding that rs2268494 revealed a tendency for association with ASD matched with the results of Lerer and colleagues (2008), who also described an association of this SNP with ASD ($p = 0.011$) in 152 ASD subjects from 133 families after TDT (Lerer *et al.*, 2008). This SNP had additionally been associated with the trait "empathy" in a cohort of non-related Chinese subjects (Houenou *et al.*, 2012). These subjects, like ours, had also been diagnosed according to ADI-R and ADO-S. In our study, more subjects (n = 203) were investigated than in the study of Lerer and colleagues. The IQ > 70 subpopulation (n = 139) did not reveal any different result for rs2268494 in comparison to the complete cohort, if the calculations were performed with Haploview 4.2. The calculations done with UNPHASED in this subpopulation did not reveal any tendency to association for rs2268494 ($p = 0.4131$). The different data is explained by the different sample sizes and algorithms. The data of the IQ > 70 subpopulation are derived from trios of 139 families. Among these 139 families, there had been only 90 complete trios, the rest consisted of singletons. Haploview 4.2 accomplished its calculations solely based on the 90 complete trios because it cannot calculate with singletons or incomplete trios. The 52 singletons were not taken for TDT calculation, whereas UNPHASED simulated the accordant missing genotypes of the incomplete trios and singletons to make them complete. Hence, although both tools are used for TDT calculations, the calculations performed with UNPHASED are supposed to be more informative (Christine M. Freitag, personal communication) due to the larger amount of data that are used.

The bottom line is that both tools, Haploview and UNPHASED, did not identify any association of rs2268494 with ASD. The reason why rs2268494 is associated with ASD in the cohort of Lerer and colleagues (2008) and in our cohorts we did not find an association can be explained as follows: 1.) we did not know the precise diagnostic criteria that Lerer and

colleagues (2008) applied during the recruitment of their patients. The endophenotyping of the cohorts were completely unknown to us. There could be slight differences of the diagnostic stringency that could explain the different results, although similar cohort sizes were considered for association analysis. The reliability of these diagnostic procedures is generally problematic as ADO-S and ADI-R are interview-based and dependent on the observation of the patient. Clinicians evaluate similar behaviors with different cut-off scores, thus there is a chance of a bias. 2.) Nothing is known about potential population stratification. Lerer and colleagues (2008) recruited their cohort in Israel. According to our knowledge, the share of genetic identity in Israel is very high due to cultural and religious reasons (Atzmon *et al.*, 2010). However, unknown and minor population stratification in our cohort could explain the different association results.

The calculation of haplotype main effects by UNPHASED in the complete cohort resulted in one haplotype, rs2268494 (A) – rs237889 (G), which showed a tendency to association ($\chi^2 = 6.92$, df = 3, p = 0.07). Lerer and colleagues did not report the occurrence of this haplotype in their study. The haplotype rs2268494 (A) – rs2254298 (C) revealed the highest transmission frequency in the complete cohort (T-freq: 0.84), but did not reach the level of statistical significance (p = 0.18). In the cohort of Lerer and colleagues, the same haplotype also revealed the highest frequency (T-freq: 0.63) and was significantly associated with ASD (p = 0.023). Another haplotype, rs2268494 (T) – rs2254298 (C), occurred both in our complete cohort as well as in the study by Lerer and colleagues. In the study by Lerer and colleagues, it was significantly associated with ASD (p = 0.012) and showed a minor transmission frequency (T-freq: 0.17). In our complete cohort, this haplotype had the lowest transmission frequency (T-freq: 0.04) and was not associated with ASD (p = 0.18). However, one haplotype occurred in the complete cohort, rs2268494 (A) – rs2254298 (T), which had not been reported by Lerer and colleagues. In the complete cohort, this haplotype revealed the second highest transmission frequency (T-freq: 0.10). The previously mentioned haplotypes also occurred in the IQ > 70 subpopulation, the transmission frequencies were almost exactly the same and there was also no association of any haplotype with ASD (p = 0.39). Another haplotype composition that occurred in the study by Lerer *et al.* and ours consisted of the SNPs rs2268494, rs2254298 and rs237889. Neither in our complete cohort nor in the IQ > 70 subpopulation, these haplotype compositions reached the level of statistical significance (complete cohort: p = 0.14; IQ > 70 subpopulation: p = 0.19). The cohort of Lerer *et al.* revealed association with ASD for two haplotypes (rs2268494-rs2254298-rs237889): T-C-A

(T-freq: 0.16, p = 0.004) and A-C-A (T-freq: 0.27, p = 0.011). In both of our samples, the haplotype A-C-A showed the second highest transmission frequency (T-Freq [complete cohort]: 0.32; T-freq [IQ > 70 subpopulation]: 0.30). These results are very close to those of Lerer and colleagues. The haplotype T-C-A also appeared in both of our tested populations at a very low abundance (T-freq [complete cohort]: 0.04; T-freq [IQ > 70 subpopulation]: 0.05). In the cohort of Lerer *et al.*, this haplotype was much more frequent (T-freq: 0.16) and in contrast to our calculations, it was associated with ASD (p = 0.004). While Lerer and colleagues only reported two haplotypes built from these SNPs, we detected five (IQ > 70 subpopulation) and six (complete cohort) haplotypes with UNPHASED. In our cohorts, the haplotype A-C-G revealed the highest occurrence (T-Freq in both samples: 0.51). In the study by Lerer and colleagues, this haplotype only existed as a part of extended haplotypes with at least five markers with very low abundances (T-freq ≤ 0.06). Furthermore, in our study we detected both variants of rs2254298 (C/T) in haplotypes. Lerer and colleagues exclusively reported the occurrence of the major allele (C) in haplotypes.

In our study, none of the single markers was associated with ASD. Exclusively rs2268494 (T/A) revealed tendency to association (p = 0.08) in our complete cohort. This SNP was associated with ASD in the study by Lerer and colleagues (p = 0.0117). None of the other existing association studies (Wu *et al.*, 2005; Jacob *et al.*, 2007; Liu *et al.*, 2010; Wermter *et al.*, 2010) of *OXTR* with ASD had tested this SNP in their cohort. The A allele of SNP rs2254298 had been associated with ASD in a Chinese and a Japanese cohort (Wu *et al.*, 2005; Liu *et al.*, 2010). In an association study on a Caucasian sample, the G allele of this SNP was associated with ASD (Jacob *et al.*, 2007). In our study, this SNP did not reveal any tendency to association with ASD (complete cohort: p = 0.39; IQ > 70 subpopulation: p = 0.36). This SNP had additionally been associated further traits: unipolar depression (Costa *et al.*, 2009), amygdala volume (Furman *et al.*, 2011), loneliness in adults (Lucht *et al.*, 2009) and physical as well as social anxiety (Thompson *et al.*, 2011). Brune (2012) discusses in his review that there is a high evidence for an evolutionary advantage of the non-ancestral A allele of rs2254298. Due to its association with increased amygdala size and the link of the amygdala with social complexity, it appears to be plausible that there is a positive selection mechanism (Brune, 2012). The other three SNPs that we tested in our cohort (rs237889, rs237897 and rs4686302) were neither associated with ASD in our samples nor did they reveal any association in the studies on ASD patients of Japanese, Chinese, Caucasian and Israeli origin.

Interestingly, in our study it became obvious that the item "IQ" shifted the tendencies of association within the haplotype compositions. In our complete cohort, the haplotype compositions rs2268494 – rs237889 showed a tendency to association ($p = 0.07$) and in the IQ > 70 subpopulation, this tendency disappeared completely ($p = 0.33$). In the IQ > 70 subpopulation, the haplotype composition rs2254298 – rs237889 revealed a tendency to association ($p = 0.09$), which did not occur in the complete cohort ($p = 0.14$). Both of these haplotypes were not explicitly tested in the study by Lerer and colleagues. Obviously, the factor "IQ > 70" has an effect on both single marker as well as haplotype associations with ASD. Furthermore, the association studies in different populations (Japanese, Chinese, Caucasian, Israeli) demonstrated for rs2254298 (C/T) that either the major allele (Lerer *et al.*, 2008) or the minor allele (Wu *et al.*, 2005; Liu *et al.*, 2010) was overtransmitted to ASD-affected patients. The findings about the variable allele frequencies in these studies underline the importance of a very homogenous population sample with respect to ethnical origin to enable comparability of association studies.

The definition of clear endophenotypes is mandatory for meaningful research on ASD. The LD outputs by Haploview indicate that these SNPs are in high linkage disequilibrium in our cohorts. In fact, there are two linkage blocks, one consisting of the SNPs rs2268494 – rs2254298 – 237889 (Intron 3) and the other one consisting of the SNPs rs4686302 – rs237897 (located in Exon 3 and in proximity to exon 3 – intron 3 boundary). This is supported by data on the CEU sample available in the HapMap project (version 3, release 27). Thus, the identification of the same or similar haplotypes matches with the results by Lerer and colleagues.

However, we could not find any association of a single SNP or a haplotype with ASD in our cohort. We could not reproduce any finding of other association studies in different populations. Three explanations are probable for the missing association of *OXTR* in our cohort with ASD: 1.) we lack the information about the exact diagnostic procedures from the other studies. 2.) different endophenotyping in the other studies and a putative population stratification in our sample. 3.) the sample size of our cohort was too low to identify possible associations although tendencies were already detectable for one SNP and two haplotype blocks.

4.3 Identification of homologous recombinant *Mlc1* embryonic stem cells

Previous studies on *MLC1* in humans and its orthologue in mice indicate that this gene remains a candidate gene for the etiology of SCZD10. To date, no constitutive *Mlc1* knockout mouse is available. The knockout vector for the creation of a constitutive *Mlc1* knockout mouse model had already been set up in our facilities (Ekawardhani, 2008). We submitted this vector to the Department of Clinical Neurobiology, University of Würzburg, which is already experienced in the creation of knockout mice. The transfected and selected ES were delivered to our department to identify homologous recombinant clones.

Transgenic organism models are highly valuable tools for research. Especially the discovery and development of transgenic mice (Capecchi, 1989) has opened huge possibilities for researchers around the word to investigate genes of interest. The genetic similarity of mice and humans in combination with easy handling and fast reproduction makes them the ideal candidate organisms to work on. The verification of the applied knockout vector construct, pMLC1_KO_mod (Figure 2.4), revealed that there were no problems with respect to its assembly and sequence validity. Two striking points that limited the success of this study were the generally low gDNA abundance and the unequal distribution of ES among the single wells. The gDNA content was below the measurement range of the spectrophotometer.

The detection of recombinant ES gDNA by southern blot requires a minimum gDNA amount of 5 µg (Brown, 2001). The low amount of gDNA in all of the tested wells did not allow detection by southern blot (≤ 100 ng in total). Hence, the appropriate technique was PCR to amplify the low abundant gDNA. Personal communication with experienced scientists from the Department of Clinical Biology in Würzburg (Michael Glinka, personal communication) and from the Department of Psychiatry, Psychosomatics and Psychotherapy in Würzburg (Lisa Gutknecht, personal communication) confirmed the adequacy of this technique. The first step was to find a method to validate an appropriate gDNA amount in the single wells. A PCR amplifying the gene *Serpina6* was considered for validation of sufficient gDNA amount. As expected, many samples did not show enough gDNA material and were not considered for further analysis. Those samples that revealed a sufficient amount of ES gDNA were investigated for the presence of aberrant *Mlc1* sequences in the ES genome. This procedure was divided in two parts: 1.) detection of the aberrant *Mlc1* sequence (pMlc1_KO_mod) in

the ES genome (recombination). 2.) identification of homologous recombination in the ES genome.

The knockout vector sequence could be identified in about seventy percent of all investigated samples. The other thirty percent of the samples did either not contain sufficient gDNA or even none. First of all, the detection of the pMlc1_KO_mod sequence in the ES genome indicated that the electroporation had been successful and recombination had occurred. The next step was the identification of homologous recombination. Smithies and colleagues who had inserted DNA sequences into the human beta-globulin locus reported that the homologous recombination frequency is about 1:1000 (Smithies *et al.*, 1985). The homologous recombination frequency is defined as the amount of homologous recombination events per number of ES. Hence, in statistical terms there occurs exactly one homologous recombination in 1,000 ES. This value appears to be a very optimistic estimation as further studies on gene targeting report recombination frequencies that are far less. Estimations on homologous recombination frequencies vary between 1:1,000,000 and 1:10,000 (Deng and Capecchi, 1992; Fujitani *et al.*, 1995). The authors of these studies explain this huge variance by the length of the homology sequences that were used during knockout vector assembly. There is a linear relationship between homology length and recombination frequency, if the homology arms have a length between 2 and about 14 kb. Beyond that size it obviously reaches the level of saturation (Deng and Capecchi, 1992). The highest efficiency of gene targeting was achieved once the short homology arm had a length in between 1 and 2 kb and the long homology arm a length of 5 to 6 kb (Hasty *et al.*, 1991). The short arm of our knockout vector had a size of 1.2 kb and thus it perfectly fulfilled the recommendations from literature. The long arm with a size of 4.8 kb was slightly shorter than recommended. Anyhow, this only allows the assumption that the efficiency of homologous recombination could be lowered but not completely abolished. Another important fact that influences recombination success is the avoidance of repetitive DNA elements within the homology arms (Wu *et al.*, 2008). Repetitive DNA sequences, such as CpG islands or microsatellites negatively affect the homologous recombination success as they lower the degree of homology of the homology arms to their target sites. The higher the degree of repetitive DNA within the knockout construct vector, the higher the probability of unspecific recombination occasions in the target genome. We could even exclude this option in our applied knockout vector construct; neither CpG islands nor extended microsatellite elements could be detected within the homology arms. There remain three reasonable explanations for the failure to identify a homologous

recombined clone: 1.) the DNA isolation procedure never yields all available molecules. Maybe, those ES containing the homologous recombined genome got lost. This assumption is supported by the fact that the rate of homologous recombination can be considered to be very low in average; a recombination rate of 1:1,000,000 is obviously very realistic (Hasty *et al.*, 1991; Deng and Capecchi, 1992; Fujitani *et al.*, 1995). 2.) homologous recombination did not occur in any of the investigated cells. This is rather speculation than empirical knowledge; it can neither be proven nor denied for sure. Nevertheless, from a statistical point of view it is possible that in the investigated cells, homologous recombination did not occur (Fujitani *et al.*, 1995). Random recombination is favored up to 10,000x over specific, which supports our assumption (Hasty *et al.*, 1991; te Riele *et al.*, 1992; Lodish, 2000). 3.) specific recombination occurred but remained undetected. This assumption could also be explained by the low abundance of specific recombination events in ES. The detection of specific recombination requires a PCR reaction that is highly sensitive to detect even the least abundance of recombined target DNA. Considering that the abundance of recombined DNA is extremely low and that the total number of samples tested was less than 1,000 colonies, this scenario could also explain why a positive clone could not be identified. In the end, it is proverbially impossible to accomplish a detailed troubleshooting, especially because the ES electroporation and selection process had not been performed in our facilities. The low ES gDNA in each of the investigated wells indicates that the propagation of ES had not been performed sufficiently before they were distributed into the 96 well plates.

We have not been able to identify homologous recombined ES clones in our samples. However, in the meantime the availability of *Mlc1*-knockout positive stem cells has been reported. The International Knockout Mouse Consortium (IKMC, http://www.knockoutmouse.org) announced the availability of homologous recombinant and quality-controlled ES (KOMP-CSD project ID: 32104 and KOMP-Regeneron project ID: VG12047). The IKMC performs mutations of all characterized protein-coding genes by high-throughput BAC recombineering techniques; about 9,000 conditional targeted alleles have been produced up to now (Skarnes *et al.*, 2011). The genetic background of these ES differs from ours. We used the ES from the common mouse strain for genetic manipulation, 129/Ola, whereas the IKMC used ES derived from mouse strain C57BL/6N. The strain C57BL/6N is supposed to be the best characterized inbred mouse strain and at the same time, it is the reference strain for the mouse genome sequence (Waterston *et al.*, 2002). Both projects of the IKMC offer the microinjection of the targeted ES into blastocysts; the

customer is guaranteed to receive a litter of weaned pups including at least one male 50 % plus chimera for further cross-breeding in your own facilities for null allele production. Thus, the way to the *Mlc1* knockout mouse has been abbreviated and within the near future, *Mlc1* knockout mice could be available for behavioral, morphological and histological investigations.

4.4 The expression of the NR3C1 protein is decreased by miR-137 in CNS-derived cell lines

Gene expression is a complex process, which is regulated by a variety of factors. Modifications of mRNAs and proteins are important processes in gene expression: post-transcriptional modifications such as RNA processing and post-translational modifications such as glycosylation. These modifications define both mRNA targeting and protein solubility. The characterization of another process modifying gene expression has emerged since the beginning of this century: RNA interference (Zamore *et al.*, 2000; Bagasra and Prilliman, 2004; Siomi and Siomi, 2009). The mRNA amount can be exactly regulated by RNA interference and thus, the availability and amount of proteins in an organism.

One mechanism of RNA interference is the targeting of mRNAs by miRNAs. Specific miRNAs hybridize to their target mRNAs and initiate mRNA degradation. This enables the regulation of the target mRNA availability and consequently, the amount of target protein. To date, no study has been reported that investigated the effect of miRNAs on *MLC1* gene expression and its orthologues. *MLC1* is supposed to be contributing or even causative for the etiology of SCZD10 in our families. Due to the lack of the *Mlc1* knockout mouse model, *MLC1* and its rat orthologue were supposed to be knocked down by miR-137 in CNS-derived cell lines. In addition, the concomitant effects of miR-124 and miR-137 on gene expression of *NR3C1* and *MLC1* including their orthologues were tested. Psychiatric disorders are notably triggered by environmental factors. Long-term psychological and physical stress is accepted as one major influential factor for their pathogenesis (Akil, 2005; de Kloet *et al.*, 2005; Billing *et al.*, 2012). *NR3C1* is the main receptor molecule for cortisol in mammals and thus the ideal candidate gene to measure stress effects in heterologous systems such as mammalian cell cultures and in animal studies.

The Figures 3.14 and 3.15 illustrate the 3'-UTR of human *NR3C1* and *MLC1*. Conspicuously, exclusively one miRNA target site (miR-137) was predicted for *MLC1*, whereas for *NR3C1*, fifteen miRNA target sites were predicted. The first task was the characterization of the protein expression of MLC1 and its orthologues in CNS-derived cell lines. As Figure 3.16 depicts, the applied commercially available polyclonal antibodies directed against human MLC1 constantly gave a high noise. Various changes in the protocol and the application of different antibodies did not lead to an improvement of the MLC1 immunoblot results. Hence, we exclusively investigated the effects of miR-137 on the gene expression of NR3C1 and its orthologue. In the human neuroblastoma cell lines U373MG and the neuronal cell line SK-N-MC, miR-137 led to a non-significant decrease of the NR3C1 protein level (Figure 3.17). The addition of miR-124, which had been previously described to decrease the NR3C1 protein expression effectively (Vreugdenhil *et al.*, 2009), confirmed the realiability of the transfection process. The decreasing effect of miR-137 on NR3C1 protein expression in both cell lines was just about 15 %. The effect of miR-124 was obviously higher; about 17 % reduction of NR3C1 protein expression in U373MG cells and 22 % in SK-N-MC cells. Due to the low sample number (n = 4), a proper statistical analysis was not accomplishable and therefore, these results only provide an indication of miR-137 effects. For the neuronal rat cell line PC12, the effect of miR-137 on NR3C1 protein level almost reached the level of statistical significance ($p = 0.064$) with a knockdown effect on NR3C1 expression of 18 %. The knockdown effect of miR-124 on NR3C1 protein expression was highly significant ($p = 0.001$) and considerably high with 42 %.

The evidence derived from our cell culture experiments is supported by a study of Silber and colleagues (2008), who investigated diverse glioblastomal multiforme cell lines (U87 and U251) with respect to their endogenous miRNA expression. In these cell lines, miR-124 and miR-137 are downregulated in comparison to the steadily expressed miRNA let-7a. Treatment of these cell lines with the DNA demethylating agent 5-aza-2'-deoxycytidine (5-aza-dC) led to an increase of miR-137 expression, which indicates the epigenetic modification of transcriptional regulatory sequences. A further finding of Silber and colleagues was the influence of miR-137 on cell cycle arrest and the regulation of neuronal differentiation due to its knockdown effect on *CDK6* expression (Silber *et al.*, 2008). In adult hippocampal neuroprogenitor cells derived from E18 mice, *in situ* hybridization targeting miR-137 revealed a high expression in the dentate gyrus and in the molecular layer. Overexpression of miR-137 in neurons leads to high expression levels of doublecortin (*DCX*, a marker for

immature neurons). Furthermore, the ubiquitin ligase *Mib1*, which is known to be involved in neurogenesis and -development, was confirmed to be targeted by miR-137 (Smrt *et al.*, 2010). Hence, miR-137 obviously modifies gene expression of those genes involved in neuronal formation and synaptic plasticity. Further evidence is provided by the loss of function of the maternal allele of the gene *UBE3A,* which leads to the Angelman syndrome. This syndrome is mainly characterized by motor dysfunction and mental impairment. The lack of UBE3A protein results in affected spine morphology, length and number in pyramidal neurons of the hippocampus (Dindot *et al.*, 2008). Sun and colleagues (2011) conducted *in utero* electroporation of miR-137 into embryonic mice and identified a decrease of neural stem cell development and differentiation because miR-137 acts on the histone deacetylase complex gene *KDM1A* (Mittal *et al.*, 2007). Further experiments will be required to elucidate the further target genes and effects of miR-137. Previous studies describing that miR-137 affects gene expression of various genes and our own findings about miR-137 affecting NR3C1 protein expression in CNS-derived cell lines indicate that this miRNA is important for the regulation of neurogenesis and neuronal development.

In summary, the data collection from the three different experiments in CNS-derived cell lines of human and rat origin confirm that miR-137 affects protein expression of NR3C1 and its orthologue. Especially the results from experiment with PC12 cells, which are able to mimic a neuronal phenotype after differentiation with nerve growth factor (NGF), appear very promising and convincing (Figure 3.18). Future experiments with higher sample numbers will provide confirmation for statistical robustness. At the time the study was accomplished, TargetScan Human predicted one target site of miR-137 in *MLC1*, but none for *NR3C1*. In contrast, the most recent version of TargetScan Human, version 6.0 (November 2011), predicted a target of miR-137 in *NR3C1*. The target site of this miRNA perfectly matched with the target sequence (7mer). Thus, the tendency to a significant knockdown effect of miR-137 on NR3C1 protein expression provides a good indication for the validity of the *in silico* predicted target site. However, the same miRNAs target the 3'-UTRs of several genes; our experiments only allow a correlation and not a causal relationship of the miR-137 effects on NR3C1 protein expression (Lim *et al.*, 2005; Lee *et al.*, 2007; Zhang and Su, 2009). At this time it is impossible to determine, whether the miR-137 effects on *NR3C1* and its rat orthologue are direct or indirect. Possibly it is a network of genes interacting with each other and thus finally downregulating *NR3C1* expression. Reporter gene assays containing the miR-137 target sites of both genes will be required to validate our previous results and to

answer the question, whether there is an immediate effect of miR-137 on *NR3C1* and *MLC1* gene expression (Vreugdenhil *et al.*, 2009; Smrt *et al.*, 2010).

4.5 Summary

The gene *C15orf53* was comprehensively investigated. The association study with bipolar disorder (BD) and SCZD10 individual samples did not show any association of single nucleotide polymorphisms (SNPs) in *C15orf53* neither with BD or SCZD10, nor the combination of both samples. The mutational analysis of *C15orf53* in seven SCZD10-affected individuals from multiplex families did not reveal any mutations in the 5' untranslated region, the coding region and the intron-exon boundaries. The gene expression data revealed that *C15orf53* is expressed in a subpopulation of leukocytes, but expression was not detectable in human *post-mortem* limbic brain tissue. According to the results of these studies, *C15orf53* is unlikely to be a strong candidate gene for the etiology of BD or SCZD10.

Five SNPs in the *OXTR* gene were taken for transmission-disequilibrium test (TDT) in parents-child trios with autism spectrum disorder (ASD)-affected children. Association was neither found in the complete sample nor in the subgroup with children that had an intelligence quotient (IQ) above 70, independent from the application of Haploview or UNPHASED for analysis.

Mutations in the *MLC1* gene lead to megalencephalic leukoencephalopathy with subcortical cysts (MLC) and one variant coding for the amino acid methionine (Met) instead of leucine (Leu) at position 309 was identified to segregate in a family affected with periodic catatonia (SCZD10). Mouse embryonic stem cells (ES) for creation of a constitutive *Mlc1* knockout mouse were analyzed for homologous recombination of the knockout construct with the genomic DNA (gDNA) of the ES. Polymerase chain reaction (PCR) on the available stem cell clones did not reveal any homologous recombined ES. However, the International Knockout Mouse Consortium (IKMC) recently published the information that validated *Mlc1* knockout stem cells from the mouse strain C57BL/6 are available. Thus, the creation of the *Mlc1* knockout mouse is significantly abbreviated.

The bioinformatics tool TargetScan predicted a binding site for miR-137 in the *MLC1* and the human glucocorticoid receptor (*NR3C1*) genes. Due to the unavailability of appropriate antibodies for MLC1, the immunoblot analysis was exclusively performed on the glucocorticoid receptor. In the human glioblastomal cell line U373MG, the neuroblastoma cell line SK-N-MC and the rat cell line PC12, miR-137 led to a decrease of glucocorticoid receptor protein expression. In PC12 cells, the decrease showed a tendency to statistical

significance. Thus, it is proven that miR-137 has a regulatory effect on glucocorticoid receptor expression.

5 Concluding remarks

5.1 ASD, bipolar disorder and SCZD10 reveal overlapping symptomatology and share susceptibility loci

This study focused on three different genetic loci (*OXTR*: 3p25, *C15orf53*: 15q14 and *MLC1*: 22q13.33) in multiplex families segregating SCZD10, parents-child trios and BD- and SCZD10-affected individuals cohorts. Although three different genes located in three completely different loci were investigated, there is a connection between all of them. Psychiatric disorders are heterogeneous in their occurrence. Several approaches exist to explain the etiologies of psychiatric disorders. Most researchers share the opinion that psychiatric diseases are complex traits and their etiology is based on an extended interacting and complex genetic network (Kato, 2007b; Gaiteri and Sibille, 2011). However, several studies exist, which support the idea that psychiatric disorders exceptionally accumulate in families and thus show a Mendelian inheritance pattern (St. Clair *et al.*, 1990; Meyer *et al.*, 2001; Verma *et al.*, 2004; Knight HM *et al.*, 2009). A Swedish group published a study in 2008, where the parents of individuals diagnosed with ASD are frequently affected by a psychiatric disorder themselves (Daniels *et al.*, 2008). Further strong evidence for familial aggregation of complex disorders is given by a study of Greenwood *et al.* (2004), where 183 relative pairs affected by intellectual disability (ID) reveal a high chance to have relatives diagnosed with SCZ (Greenwood *et al.*, 2004). The results of Greenwood *et al.* (2004) are further supported by a population-based study on individuals with ID by Morgan and colleagues (2008). In their study, the comorbidity of ID and SCZ individuals is 32 % (Morgan *et al.*, 2008).

Among the scientific community, psychiatric disorders are considered to be both, genetically and environmentally evoked and modified. Especially the heritability of psychiatric disorders is strikingly high. A study on twins diagnosed with BD in Finland revealed a concordance rate of 0.43 among monozygotic and of 0.06 among dizygotic twins (Kieseppa *et al.*, 2004). Edvardsen *et al.* (2008) accomplished a twin study on the complete bipolar spectrum (BD I, BD II and cyclothymia) and analyzed the cross-concordances between the single diagnoses. The concordance rates in their cohort for BD I was 0.73, for BD I and BD II combined 0.77

and for BD I, BD II and cyclothymia combined 0.71 (Edvardsen *et al.*, 2008). A twin study of McGuffin and colleagues (2003) even came to a concordance rate of 85 % for BD (McGuffin P *et al.*, 2003). Despite the fact that heritability and concordance rates vary between the studies, a high heritability of psychiatric disorders, as demonstrated for BD above, is proven.

Autism, BD and SCZD10 appear to be differently characterized disorders, once their symptomatology is exclusively considered. Interestingly, many psychiatric disorders do not occur as just "one precisely delimited disorder on their own" but they share a high proportion of comorbidities with further psychiatric disorders. ASD reveals a high comorbidity with attention-deficit hyperactivity syndrome (ADHD) (Reiersen and Todd, 2008; Freitag, 2006; Freitag *et al.*, 2012) and BD (McElroy, 2004; Freitag, 2006; Freitag *et al.*, 2012). Although pervasive developmental disorders (PDD) such as ASD co-occur with ADHD at rates between 50 – 75 % (Goldstein and Schwebach, 2004; Reiersen *et al.*, 2007; Reiersen and Todd, 2008; Grzadzinski *et al.*, 2011), a transcriptomics study on monoaminergic candidate genes on PBMCs in ASD and ADHD patients identified that dopamine receptor D5 (*DRD5*) expression level of ASD patients is significantly decreased in comparison to ADHD patients (Taurines *et al.*, 2011). A functional magnetic resonance imaging (fMRI) study on 20 boys each diagnosed with either ASD or ADHD identified a significant underactivation of the dorso-lateral prefrontal cortex (DLPFC) in ADHD boys compared to ASD boys (Christakou *et al.*, 2012). A meta-analysis on 30 twin studies investigating the etiology and heritability of ASDs and the comorbidity with other psychiatric disorders concluded that there is a high merge of symptoms and that the latest findings in genetics argue against a strict separation of these syndromes (Ronald and Hoekstra, 2011). These reports evoke the question, if there is a link between ASD, BD and SCZD10 as well. Incontrovertibly, there is a symptomatological overlap of ASDs, BD and schizophrenia (SCZ), especially once considering self-perception, motoric impairment and sensorimotor gating. In fact, all of these disorders form overlapping spectra (Stahlberg *et al.*, 2004; Rapoport *et al.*, 2009; King and Lord, 2011), which means that an entire separation and allocation of patients into ASD, BD an SCZ is exclusively possible without ambiguity at their symptomatological extremes. Moreover, diagnostic overlaps of ASD and SCZ have been described explicitly. In one study, fourteen males were differentially diagnosed with either ASD or SCZ. Seven ASD patients revealed comorbidity with SCZ and in addition, five patients revealed positive and six patients negative symptoms of SCZ according to the scales for the assessment of positive (SAPS) and negative (SANS) symptoms (Konstantareas and Hewitt, 2001). These studies support the observation that in the center of

all three previously mentioned spectra, common or at least overlapping symptomatology is rather the rule than the exception. Furthermore, the findings about common symptomatology allow tracing back to common susceptibility loci in the human genome.

Genes are known to have pleiotropic effects, so certain allele variants in genes can have advantageous or disadvantageous properties on the organism in various characteristics. Pleiotropic effects mainly show their impact in the immune system; e.g. genetic variability in the interleukin-1 system has been identified to favor the etiology of SCZ (Katila *et al.*, 1999; Xu and He, 2010). Crespi *et al.* (2011) report variants in the major histocompatibility complex gene *HLA-DRB1*, which reveal both protective and risk-increasing effects against rheumatoid arthritis and autism but increase the risk of getting affected by SCZ and vice versa (Crespi and Thiselton, 2011). Meyer *et al.* (2011) consider SCZ as a neuroinflammatory process, which is caused by abnormal expression of inflammatory genes. Psychological and physical stress leads to an overactivation of microglia and further cells via a complex signaling cascade, which causes low-grade inflammations in the brain. Abnormal HPA axis activity further facilitates this effect and leads to progredient deterioration of the patients' health state (Meyer *et al.*, 2011). A further example for pleiotropic gene effects mediated by the immune system is the study by Nelson and colleagues (2006). They investigated the blood of newborn children diagnosed with autism or Down syndrome and identified variations among cytokine levels, depending from age and disorder (Nelson *et al.*, 2006). These studies provide insight into the implications of genetic variations. Genetic variability, especially among immune system relevant genes, leads to maladaptations or obviously even to the etiology of psychiatric disorders.

The success of a treatment of a psychiatric disorder is highly dependent on validity and accuracy of the diagnostic procedure. Nevertheless, the diagnostic differentiation between psychiatric disorders can become complicated due to overlapping symptomatology as already mentioned before: the differentiation between ASD and SCZ seems to be extraordinary complicated, especially when SCZ appears in its early-onset form. Dossetor *et al.* (2007) write in their publication that "not all that glitters is gold". They underline the obvious problems that occur once clinicians are supposed to accomplish differential diagnosis on ASD and early-onset SCZ because many of their symptoms resemble each other (Dossetor, 2007). The review by Carroll *et al.* (2009) elucidates the genetic overlap of ASD, BD and SCZ. A large amount of copy-number variants (CNVs) in ASD, SCZ and BD have been identified

during the last years. Some of those are located in genes that have been previously associated with all three psychiatric disorders. Two known genes are neurexin-1 (*NRXN1)* and the contactin associated protein-like 2 (*CNTNAP2*). Both genes are responsible for formation of synapses and the maintenance of their architecture, especially the formation of the synaptic cleft (Reichelt *et al.*, 2012). Recent technologies enable further insight into the genetic architecture of psychiatric diseases. Next-generation sequencing techniques open new possibilities of 1.) genome sequencing and 2.) gene expression profiling. The latter aspect was investigated in a study by Lin *et al.* (2011). Inducible human pluripotent stem cells (iPSCs) were differentiated into neurons. During this transition, several significant changes on the gene expression level of developmentally crucial genes were identified, including candidate genes for ASD, BD and SCZ (Lin *et al.*, 2011). The authors of this study did not use pluripotent stem cells derived from psychiatric patients, hence an extrapolation of the results to the real situation in psychiatric disorder-affected individuals has to be regarded with caution. However, the identification of upregulated genes that are also considered to be candidate genes for psychiatric disorders is striking. These findings additionally support the "neurodevelopmental hypothesis" of SCZ published in 1986 by Nasrallah and colleagues (Nasrallah and Weinberger, 1986) as well as Murray and colleagues (Murray and Lewis, 1988; Murray *et al.*, 1992; Murray, 1994). Recently, this hypothesis was reappraised by Owen and colleagues (Owen *et al.*, 2011). The neurodevelopmental hypothesis of SCZ bases upon the assumption that molecular and morphological aberrations of the brain during ontogenesis are considered to be responsible for the etiology of SCZ. Owen *et al.* (2011) refocused on this hypothesis on the background of recent studies, which were predominantly conducting functional genomics and fMRI. They wonder if it is reasonable to confine this hypothesis to SCZ and if it should not be expanded to PDDs and BD. The arguments for an extension of this hypothesis sound reasonable, as findings from recent studies on functional genomics in different psychiatric disorders with overlapping symptomatology support this idea. One item that is shared by ASD, BD and SCZ is the cognitive impairment. It appears to be a common trait, even a core symptom shared by all psychiatric disorders; hence this trait is a good indicator for a common etiology of them (Millan *et al.*, 2012). Craddock *et al.* (2010) defined a concept describing a gradient of decreasing severity of neurodevelopmental impairment among psychiatric disorders: intellectual disability, autism, ADHD, SCZ, BD (Craddock and Owen, 2010).

Most of the risk susceptibility loci, which were associated with ASD, BD and SCZ, refer to genes that are involved in synaptic plasticity and development, mostly around neurexins and neuroligins (Littleton and Sheng, 2003; Doherty *et al.*, 2012). Further support of the implication of neurexins and neuroligins in the etiology of psychiatric disorders is provided by a mutation analysis in Old Order Amish people, which are affected by the Cortical Dysplasia–Focal Epilepsy Syndrome (CDFE). CDFE is characterized by seizures, impulsive and aggressive behavior, language regression and progressive mental retardation. A mutation in *CNTNAP2* (3709delG), leading to a truncated protein, was identified among the patients. Additionally to this finding, 67 % of the children affected by CDFE were co-diagnosed with ASD (Strauss *et al.*, 2006). A linkage analysis comprising 72 multiplex families from the NIMH repository and a subsequent TDT in 145 trios revealed a genetic marker within the *CNTNAP2* gene that increases the familial risk for autism (Arking *et al.*, 2008). In three non-related Caucasian patients, haploinsufficiency of *CNTNAP2* was associated with SCZ, epilepsy and cognitive impairment (Friedman *et al.*, 2008a). A report of Burbach and colleagues (2008) supports the idea of a shared etiology between ASD and SCZ with a special focus on *CNTNAP2* (Burbach and van, 2009). Wang and colleagues (2010) performed a genome-wide meta-analysis of GWAS data on BD and SCZ, which supports common genetic variants influencing BD and SCZ including *CNTNAP2* (Wang *et al.*, 2010).

Two susceptibility loci of this study, chromosome 15q14 and 22q13, have already been investigated in a number of linkage and association studies. In a linkage study by Hong and colleagues (2004), they found an association of the *CHRNA7* gene on chromosome 15q14 with BD in a Chinese cohort (Hong *et al.*, 2004). A meta-analysis on CNVs discovered in ASD and SCZ described an enrichment of CNVs on chromosome 15q13-14 and 22q11-13 for both disorders, thus encouraging the authors to define these genomic areas as rearrangement hotspots (Itsara *et al.*, 2009). *OXTR* on chromosome 3p25 is not exclusively a candidate gene for the etiology of ASDs. The SNP rs2740204 located in *OXTR* was significantly associated with treatment response and negative symptoms in schizophrenic individuals that had received clozapine (Souza *et al.*, 2010). In addition, the *OXTR* SNPs rs53576 and rs2254298 were associated with unipolar depression (Costa *et al.*, 2009a).

Genetic and translational studies corroborate that psychiatric disorders should be rather considered as continua than entities (Craddock, 2005; Craddock and Owen, 2010). The complexity of research on psychiatric disorders is demonstrated by a variety of factors:

comorbidities of several psychiatric disorders at the same time, heritability and the development-dependent changes of symptomatology during ontogenesis. Based on the obvious complexity of psychiatric disorders, a holistic perspective instead of a reductionist seems to be the more reasonable approach. Present data of our study as well as data from further studies support the perspective that psychiatric disorders form continua with overlapping core symptoms, e.g. cognitive dysfunction (Millan *et al.*, 2012). In fact, two strategies appear reasonable to unravel the complexity of psychiatric disorders: 1.) reductionist concepts will be still required to understand not yet characterized molecular mechanisms within cells, especially neurons. The interaction of proteins at the pre- and postsynaptic membranes such as neuroligins and neurexins are not yet completely characterized. The elucidation of these basic protein functions and interactions will still require some years. 2.) holistic approaches will gain further importance. The intense application of bioinformatic tools will provide further information and insight into interacting genetic networks. The growth and expansion of the internet, interacting machine systems and their increasing performance in data management will enable a completely new insight into interacting systems in biology. Only a cybernetic approach will be appropriate to clarify, whether psychiatric disorders really form continua or in other words, smooth transitions from one symptomatologic pool to the next.

The Macy conferences during the 1940s and 1950s proclaimed to fathom the human mind and cognition. These conferences are considered to be the initiator of a transdisciplinary approach called cybernetics. It connects research in human behaviors, reciprocal transmission and exchange of messages and human decisions, which are specified in game theory (Wiener, 1961). Heinz von Förster (1911 – 2002) and Humberto Maturana (born 1928), both researchers in the topic of second-order cybernetics and autopoiesis, held two opinions: 1.) humans are observers and consequently, they may merely act as “observers of observers” or “participant observers”. 2.) organisms are organized in a principle that they always maintain and reproduce themselves. An organism produces those components, which are required to reproduce itself (“recursive organization”). The homeostasis is the most extended complex system assumable in organisms. Homeostasis is the regulation of the internal environment to reach stable conditions and works via positive and negative regulatory feedback systems (Albrecht, 2012). These days, we have not yet completely elucidated all regulatory systems, including those in the CNS of humans. From day to day, our datasets grow and likewise their complexity. However, it will hardly be possible to receive datasets,

which can be combined to a system theory about the CNS without accepting gaps. Although humans are able to perform self-referentiality ("thinking about thinking"), Paul Watzlawick (1921 – 2007), Heinz von Förster and Humberto Maturana deny that the human mind will ever be able to completely comprehend the complexity and the principles of human cognition (Abramovitz and von Foerster, 1974; Maturana, 1975; Maturana, 1980; Maturana and Varela, 1992; von Foerster *et al.*, 1997; Watzlawick, 2008).

In spite of the previous discussed allegedly limitations of the human mind, it is personal curiosity and the desire to identify the truth behind not yet characterized behaviors and mechanisms, which drives researchers to continue their investigations. To date, three among the multiple hypotheses about the etiology of psychiatric disorders are most frequently discussed and investigated among the scientific community: 1.) neurodevelopmental alterations, which lead to subtle brain lesions and thus cause the occurrence of psychiatric disorders e.g. schizophrenia (Murray and Lewis, 1988; Murray, 1994; McGrath *et al.*, 2003; Owen *et al.*, 2011). 2.) aberrations of immune system function leading to chronic inflammations in the CNS and thus to degradation of brain tissue (Saetre *et al.*, 2007; Rook and Lowry, 2008; Hope *et al.*, 2009; Monji *et al.*, 2009; Watanabe *et al.*, 2010; Dean, 2011). 3.) general models of psychiatric psychosis like the biopsychosocial model and unitary models, which try to merge different hypotheses in one (Andreasen, 1999; Keshavan and Hogarty, 1999; Keshavan, 2005; Ghaemi, 2006; Andreasen, 2010). Remarkably, the number of studies concerning general models, which try to integrate several coexisting hypothesis, is increasing. Concomitantly, some researchers intensify the discussions from a pluralistic view on psychiatric disorders back to a unitaristic.

The core feature merging all of the different coexisting hypotheses about the etiology of psychiatric disorders is the gene-environment interaction. Each of the previously mentioned studies discusses the necessity of a certain genetic predisposition and a disorder-triggering environment to evoke the onset of a psychiatric disorder. The genetic predisposition may affect genes that encode for proteins necessary for brain morphology or the immune system. The functionality of the immune system in turn is influenced by the environment e.g. nutrition, physical and psychological stress, socioeconomic status. An impaired immune system may have two major effects: 1.) reactivation of endogenous retroviruses (ERV). Neither the complete number nor the function of endogenous retroviruses is known to date.

They have been conserved for at least 30 million years in primates and represent about 8 % of the human genome (Belshaw *et al.*, 2004). Since humans and chimpanzees have diverged approximately 6 million years ago, one family of viruses, HERV-K(HML2), has been active in humans and some humans were identified to carry more copies of viruses than others (Belshaw *et al.*, 2005). It is neither known what kind of diseases this virus family is able to evoke nor the exact circumstances that lead to its reactivation in humans. Due to the striking abundance of ERV DNA in the human genome, an implication to evoke or influence the development of psychiatric disorders seems possible and should be investigated in further detail. 2.) the etiology of autoimmune diseases such as Hashimoto's thyroiditis or rheumatic disorders. In several studies it has been reported that either inflammatory processes have been observed in patients diagnosed with SCZ and BD and that inflammation-related genes were upregulated (Saetre *et al.*, 2007; Hope *et al.*, 2009; Dimitrov *et al.*, 2011; Meyer *et al.*, 2011). Hashimotos's thyroiditis is a chronic inflammation of the thyroid gland leading to its complete deterioration. Patients affected by Hashimoto's thyroiditis suffer from symptoms with enormous severity, including depressive mood, listlessness and hallucinations. If pharmacological intervention occurs too late, patients may develop Hashimoto's encephalopathy. This disease is characterized by a variety of neurological and psychiatric symptoms (e.g. seizures, psychosis, ataxia) and in rare cases even dementia and SCZ phenotypes (Lin and Liao, 2009; Chong *et al.*, 2011; Santoro *et al.*, 2011). Brain atrophy and neurodegeneration in SCZ are supposed to be caused by inflammatory processes. Only few studies are existent to date, which focus on a link rheumatic and psychiatric disorders. Systemic lupus erythematosus (SLE) may affect the CNS and cause psychiatric symptoms (Fietta *et al.*, 2011). However, there exist only few data about SLE and psychiatric disorders.

The existence of various hypotheses confirms that psychiatric disorders remain an enigma to date. Yet, transcriptomic studies with psychiatric patients could reveal possible reactivation of ERVs or indicate autoimmune processes. Thus, potential misdiagnoses could be prevented and patients treated properly according to the real cause of their symptoms. Eventually, pharmacological intervention with antipsychotics could be significantly reduced in many cases by application of virostatics, anti-inflammatory compounds and hormone supplementation. Hence, the patients' life quality could be essentially and sustainably improved.

However, further research is required to integrate all of these findings. World-wide interaction through computers and further automation of experiments by machines will enable researchers to unravel the mystery of psychiatric disorders.

The results of this thesis provide further insight into the mechanisms of psychiatric disorder-associated genes. Three different loci each linked to different psychiatric disorders were investigated. The studies on *C15orf53* on chromosome 15q14 have resulted in extensive understanding of its gene expression pattern. To date, only few gene expression data about *C15orf53* is published. To our knowledge, this study shows for the first time that *C15orf53* is expressed in PBMCs, $CD4^+$ and $CD14^+$ cells and in specific human immune cell lines. Furthermore, it is shown in this study that *C15orf53* is not expressed in human *post-mortem* limbic brain tissue. Mutational analysis of SCDZ10-affected family members and a case-control association study on BD and SCZD10 individuals were both negative. Hence, there is high evidence that *C15orf53* is most probably not a major candidate gene for the etiology of BD and SCZD10, neither in our families nor in unrelated individuals. In summary, this gene is most probably not suitable for translational research with regards to identify new targets for patient treatment. In a separate study in this thesis, a TDT on trios with ASD-affected children was performed on five polymorphisms in the *OXTR* gene. The complete cohort and a subgroup with children having an IQ above 70 were separately taken for calculation with both Haploview and UNPHASED. No association was found with ASD, neither in the complete cohort nor in the subgroup. Thus, our study does not support previous findings claiming that the *OXTR* gene is associated with ASD. However, other studies also do not report association of *OXTR* with ASD. Our study will be included in a meta-analysis on *OXTR* polymorphisms. The meta-analysis will provide insight into the robustness and validity of previous studies and thus assist to indicate potential target sites in *OXTR* that could be used for the development of personalized pharmacological intervention. The study to create an *Mlc1* knockout mouse model ended with the identification process of homologous recombined ES. In our ES sample, no homologous recombination-positive clone could be detected. This reveals the difficulties of such a project and the need to perform ES screening at large numbers (Smithies *et al.*, 1985; Deng and Capecchi, 1992; Fujitani *et al.*, 1995). Meanwhile, the IKMC has reported the availability of positive *Mlc1* knockout clones. Hence, the way to create the *Mlc1* knockout mouse has been remarkably abbreviated. In a further study of this thesis, the bioinformatics

tool TargetScan was used to find potential miRNA target sites in the 3'-UTRs of *MLC1* and *NR3C1*. Only one miRNA target site was predicted for *MLC1*: miR-137. This target site was additionally predicted in *NR3C1*. Protein expression analysis could not be performed for *MLC1* in default of appropriate antibodies but for *NR3C1* it was demonstrated that the transfection of miR-137 leads to a downregulation of the *NR3C1* protein in three different cell lines derived from two species. As soon as appropriate antibodies for *MLC1* are available, the experiments should be repeated with regard to this protein. Potentially, *MLC1* protein expression is also affected by miR-137. The putative interference of *MLC1* and *NR3C1* by miR-137 could indicate potential targets for pharmacological treatment of SCZD10, but further studies will be required to evaluate this.

Although these studies have contributed to a better understanding of molecular mechanisms of certain candidate genes in ASD, BD and SCZD10, further functional studies (pharmacogenomics and transcriptomics) will be necessary in patients with different psychiatric disorders to confirm the results of this thesis.

6 Outlook

QVO VADIS, PSYCHIATRIC RESEARCH ?

6.1 Translational methods to fathom psychiatric disorders

Research has always undergone changes in paradigms. Technological advance enables new ways to enlighten problems that have been in the dark. It was not before the drafts of the complete human genome (Lander *et al.*, 2001b; Venter *et al.*, 2001) had been published and the announcement in 2003 that the Human Genome Project had been declared as finalized (Collins, 2003) that translational epidemiology could be performed in a large-scale manner. The International HapMap project has gained increasing knowledge about variabilities within the human genome such as SNPs and CNVs and the identification of tag SNPs, which serve as representative SNPs for genomic regions with high LD (International HapMap Consortium, 2003, 2005; Frazer *et al.*, 2007). Evolving from this knowledge, the era of GWAS was born. In 2002, the very first GWAS was published; it investigated 93,000 SNPs in about 1,000 cases and controls with respect to myocardial infarction (Ozaki *et al.*, 2002). From 2005 onwards, array-based SNP assays have become available, first covering about 100,000 SNPs with up to 1.5 million SNPs and CNVs in the most recent generation (Psychiatric GWAS Consortium, 2009). The 1,000 Genomes project, launched in 2008, initially aimed to sequence at least 1,000 genomes from various ethnic origins in order to receive more profound understanding of genetic variation among humans. In 2010, the results of the pilot study were published. Three projects were accomplished in parallel, each reporting different gene coverages of the investigated individuals. The first study contained 180 samples from four different populations, where the whole genome was sequenced at low-coverage, the second study focused on deep sequencing of six individuals in two trios and the third one analyzed more than 8,000 exons in about 700 individuals from seven populations (Durbin *et al.*, 2010). At the end of 2010, they reported 2,700 complete human genomes and the estimation for the end of 2011 was a total number of 30,000 human genomes (Patterson *et al.*, 2011). The increase of data at such a fast pace leads to a high validity and comprehension on the human genome data and opens the insight into the genetic variation within one and among different

ethnic groups. The 1,000 Genomes project would not have become feasible without the invention and application of so-called "high throughput" DNA sequencing technologies. With respect to price and speed, the currently existing next generation sequencing platforms outclass the conventional and well-established Sanger sequencing technology. The Sanger sequencing technology is based on dye-terminating sequencing (Sanger *et al.*, 1977) and therefore it is limited to 700-900 bp per read and 384 samples in one run and 24 runs a day in the most recent machines. In the best case, 8.3 Mb can be sequenced with this technique a day. The next generation sequencing technologies enable reads of 100 to 600 Mb per day, depending on the platform used, due to the possibility of large genome enrichment based on high-fidelity PCR reactions (ten Bosch and Grody, 2008). The most widespread platforms for high throughput DNA sequencing are currently provided by 454 Life sciences/Roche with the 454 FLX system, Illumina/Solexa with the Illumina/Solexa Genome Analyzer and the Applied Biosystems SOLiD™ system (Mardis, 2008). For medical genetics, the latest development is of high impact as the data density and validity, especially with respect to SNPs and CNVs, is increasing. The low-coverage sequencing of 60 CEU samples revealed almost 8 million novel SNPs that had not been annotated before as well as 259 duplications representing an increase of 33 % for the SNPs and even 90 % for the duplications (Durbin *et al.*, 2010).

Based on the detailed insight into human genetic variations, translational research can be conducted. Translational research ("from bench to bedside") attempts to unify knowledge of basic researchers and clinicians for the amelioration of patient health care and therapy (Woolf, 2008). It is supposed to be a symbiotic work: the basic researchers provide the clinicians with new potential therapeutic tools for the treatment of disorders and the clinicians on the opposite report their observations from clinical trials back to the basic researchers, so that these are able to improve their tools for clinical practice. Sung and colleagues (2003) present in their publication that translational research has to be divided into two blocks. They name them T1 and T2. In the first block (T1) researchers attempt to identify new disease mechanisms and subsequently the development of new methods for diagnosis and therapy as well as prevention, performed in clinical studies. The second block (T2) takes the findings from the clinical studies into daily practice and leads to prophylactic health care politics. According to Sung and colleagues, the biggest challenge is the recruitment and accomplishment of clinical trials, as both the total number of volunteers as well as the financial support has to be increased tremendously (Sung *et al.*, 2003). In the United States,

the National Institute of health (NIH) has launched the Clinical and Translational Science Award (CTSA) program in 2006. The NIH declared in a report from July 2009 that seven institutions have been funded over five years with $171 million (http://www.nih.gov/news/health/jul2009/ncrr-14.htm). Until the end of 2012, the NIH predicts a network of 60 institutions working together on translational science (http://commonfund.nih.gov/clinicalresearch/overview-translational.aspx), being funded with $500 million per year. According to an article by Woolf (2008), the European commission has allocated €6 billion to health-related research (Woolf, 2008). These numbers underline that translational research has moved into the focus of applied research.

The map of the human genome is getting more accurate by the day and thus, new potential target sites in the human genome are identified. These target sites will serve as starting points to unravel the etiology of psychiatric disorders and complex disorders in general. The novel variants, common or rare, represent new potential targets for the development of appropriate therapeutic intervention.

6.2 Personalized medicine due to genome-based endophenotyping

Since next generation sequencing technologies have been established, "personalized medicine" has become a realistic scenario, although there is still some way to go and questions to clarify (Ng *et al.*, 2009). For many years, researchers were not convinced by its feasibility due to the lack of profound information about the human genome. Since 2003, the human genome has been declared as "deciphered" (Collins, 2003) and by application of next generation sequencing (NGS), each individual's genome turns out to become an "open resource". One example for that is the genetic endophenotyping of ASD patients that show aberrations on chromosome 16p11.2, better known as the "16p11.2 deletion and duplication syndrome", spanning an area of about 500 kb with 30 estimated genes located inside. This syndrome has been identified in patients diagnosed with SCZ and BD (Kirov, 2010; van Winkel *et al.*, 2010) and in ASDs (Abrahams and Geschwind, 2008b; Tabet *et al.*, 2012). Personalized medicine together with genome-based endophenotyping has two major aims: 1.) grouping patients with similar genomic aberrations 2.) developing compounds that suppress or mimic the effects of those genes that are either deleted or multiplied. The long-term vision is to find therapy improvements not only for an entity but for the complete

continuum of psychiatric disorders for patients, which share common genomic rearrangements and aberrations. The term "personalized medicine" should not be misinterpreted as "individualized medicine". Personalized medicine aims to elucidate the risk of certain population subgroups to suffer from distinct complex disorders. As the nature of complex disorders is not yet completely understood at all, in most of the cases medical genetics may not deliver more than risk predictions for certain disorders. Complex disorders may accumulate within families. Thus, one famous example is the hereditary breast-ovary cancer syndrome. A meta-analysis on 74 studies on breast cancer calculated a relative risk for individuals developing breast cancer of 2.1, if a first-degree relative had been diagnosed with breast cancer and 1.9 for any relative diagnosed with that disease (Pharoah *et al.*, 1997). Major candidate genes for the etiology of familial breast cancer are the genes *BRCA1* on chromosome 17q21.31 and *BRCA2* on chromosome 13q12.3. A meta-analysis on 8,139 index cases comprising 500 individuals with a mutation in either *BRCA1* or *BRCA2* calculated a risk to develop breast cancer at the age of 70 of 65 % and for 39 % for ovarian cancer for *BRCA1* mutation carriers. If the carriers had mutations in the *BRCA2* gene, the risk for breast cancer at the age of 70 was 45 % and for ovarian cancer 11 %. From all these individuals, 289 carried a *BRCA1* and 221 a *BRCA2* mutation (Antoniou *et al.*, 2003). A meta-analysis by Chen *et al.* (2007) incorporated the study by Anoniou *et al.* (2003) and nine others with 1023 *BRCA1* and 661 *BRCA2* mutation carriers in total. The risk for *BRCA1* mutation carriers to develop breast cancer at the age of 70 was 55 %, the risk for ovarian cancer remained the same with 39 %. *BRCA2* mutation carriers showed a slightly increased risk to develop breast cancer with 47 % and ovarian cancer with 17 % (Chen and Parmigiani, 2007). In 2010, Kurian and colleagues published a survival analysis for *BRCA1/2* mutation carriers. If the mutation carriers do not receive medical intervention, the survival probability by the age of 70 is 53 % for *BRCA1* and 71 % for *BRCA2* mutation carriers (Kurian *et al.*, 2010).

These studies demonstrate that valid risk prediction is possible for specific complex disorders such as breast and ovary cancer. Once the individual risk is calculated for a mutation carrier, genetic counselors are able to recommend measurements, in the extreme case indication of prophylactic mastectomy and/or oophorectomy. Based on the achievements in the treatment of specified cancers, the improvement of treatment of psychiatric disorders seems probable. First researchers need a detailed insight into the genomics of psychiatric disorders. The genetics of psychiatric disorders are not yet as well characterized as for complex disorders

like breast and ovary cancer. Nowadays, appropriate techniques are at hand to identify susceptibility variants and genes. Subsequent to their validation in studies comprising large cohorts derived from various ethnicities, the chance to develop personalized medical intervention will become feasible.

6.3 Functional neurogenetics and genomic neuroimaging will expand our comprehension for psychiatric disorder etiology and lead to new opportunities for biomarker identification

To date, no reliable biomarker or reliable physiological test has been identified for none of the psychiatric disorders; one example for that is the prepulse inhibition (PPI) that obviously works reliably in an animal model but the transition to the human situation, especially its applicability in SCZ patients, remains unreliable (Swerdlow and Geyer, 1998; Swerdlow *et al.*, 2008). Reasons are most likely to find in the diagnostic procedure itself and the heterogeneity of the symptomatology. Further subgrouping of cohorts according to more specific endophenotypes and genotypes will help to facilitate a more stringent and directed research. Whole transcriptome analysis by RNAseq, which is based on the principle of next generation sequencing, will enable the acquisition of individualized patient transcriptomes (Mehta *et al.*, 2010; Lin *et al.*, 2011; Voineagu *et al.*, 2011). Especially for research on psychiatric disorders, RNAseq is the ideal technical approach. It is possible to collect the total cDNA from a patient at variable time points and to compare these to each other. This will become of special interest for research on bipolar disorder, where manic and depressive episodes are alternating. Mostly depending on the patient's compliance, the transcriptomes of a patient in a certain mood phase will allow further insight into gene activity. Another important advantage of RNAseq is the possibility to receive unbiased data about novel transcripts and a global understanding in alternative splicing in genes. Furthermore, RNAseq does not require intermediate steps such as hybridization in comparison to microarrays and it also captures low expressed transcripts (Mehta *et al.*, 2010). RNAseq may be even combined with compound treatment and the observation of rapid gene expression changes within a certain time period, before and after compound treatment. New biological pathways will be elucidated and the effector of genes can be observed in a time-course like manner (Abrahams and Geschwind, 2008b).

Imaging studies have revealed alterations in brain size and connectivity, especially decreased grey matter volume and increased ventricle volume, in patients diagnosed with BD (Brambilla *et al.*, 2008; Baldacara *et al.*, 2011), SCZ (Brandt and Bonelli, 2008; Greenstein *et al.*, 2011; Radonic *et al.*, 2011;) and ASD (Saitoh and Courchesne, 1998; Murphy *et al.*, 2012). The knowledge derived from microarray or RNAseq-derived gene expression profiling ("functional neuroanatomy") in combination with risk genotypes in psychiatric patients and fMRI based approaches will enable further insight and understanding of functional connectivity phenotypes (Scott-Van Zeeland *et al.*, 2010). To date, the results from various studies on psychiatric disorders still remain partially contradictory. Merging transcriptomics and imaging studies will allow researchers to receive a better understanding on psychiatric disorders.

7 References

Abrahams BS, Geschwind D (2008a) Advances in autism genetics: on the threshold of a new neurobiology. Nat Rev Genet 9:341–355.

Abrahams BS, Geschwind DH (2008b) Advances in autism genetics: on the threshold of a new neurobiology. Nat Rev 9:341–355.

Abrahams BS, Geschwind D (2010) Connecting genes to brain in the autism spectrum disorders. Arch Neurol 67:395–399.

Abramovitz R, von Foerster H (1974) Cybernetics of cybernetics or the control of control and the communication of communication: [result of a course, fall semester 1973, continued through spring semester 1974]. Urbana III: Lab.

Abuhatzira L, Makedonski K, Kaufman Y, Razin A, Shemer R (2007) MeCP2 deficiency in the brain decreases BDNF levels by REST/CoREST-mediated repression and increases TRKB production. Epigenetics 2:214–222.

Adelman J, Bond C, Pessia M, Maylie J (1995) Episodic ataxia results from voltage-dependent potassium channels with altered functions. Neuron 15:1449–1454.

Akil H (2005) Stressed and depressed. Nat Med. 11:116–118.

Albrecht U (2012) Timing to perfection: the biology of central and peripheral circadian clocks. Neuron 74:246–260.

Alloway T (2010) Working memory and executive function profiles of individuals with borderline intellectual functioning. J Intellect Disabil Res 54:448–456.

Al-Sabi A, Shamotienko O, Dhochartaigh S, Muniyappa N, Le Berre M, Shaban H, Wang J, Sack J, Dolly J (2010) Arrangement of Kv1 alpha subunits dictates sensitivity to tetraethylammonium. J Gen Physiol 136:273–282.

Alt SR, Turner JD, Klok MD, Meijer OC, Lakke EAJF, DeRijk RH, Muller CP (2010) Differential expression of glucocorticoid receptor transcripts in major depressive disorder is not epigenetically programmed. Psychoneuroendocrinology 35:544–556.

Ambros V (2011) MicroRNAs and developmental timing. Curr Opin Genet Dev 21:511–517.

Ambrosini E, Serafini B, Lanciotti A, Tosini F, Scialpi F, Psaila R, Raggi C, Di Girolamo F, Petrucci T, Aloisi F (2007) Biochemical characterization of MLC1 protein in astrocytes and its association with the dystrophin-glycoprotein complex. Mol Cell Neurosci 37:480-493

Andreasen NC (1999) A Unitary Model of Schizophrenia: Bleuler's "Fragmented Phrene" as Schizencephaly. Archives of General Psychiatry 56:781–787.

Andreasen NC (2010) The lifetime trajectory of schizophrenia and the concept of neurodevelopment. Dialogues Clin Neurosci 12:409–415.

Antoniou A *et al.* (2003) Average risks of breast and ovarian cancer associated with BRCA1 or BRCA2 mutations detected in case Series unselected for family history: a combined analysis of 22 studies. Am J Hum Genet 72:1117–1130.

Aranha M, Santos D, Sola S, Steer C, Rodrigues C (2011) miR-34a regulates mouse neural stem cell differentiation. PLoS One 6:e21396.

Arking D, Cutler D, Brune C, Teslovich T, West K, Ikeda M, Rea A, Guy M, Lin S, Cook E, Chakravarti A (2008) A common genetic variant in the neurexin superfamily member CNTNAP2 increases familial risk of autism. Am J Hum Genet 82:160–164.

Atzmon G, Hao L, Pe'er I, Velez C, Pearlman A, Palamara P, Morrow B, Friedman E, Oddoux C, Burns E, Ostrer H (2010) Abraham's children in the genome era: major Jewish

diaspora populations comprise distinct genetic clusters with shared Middle Eastern Ancestry. Am J Hum Genet 86:850–859.

Bagasra O, Prilliman KR (2004) RNA interference: the molecular immune system. J Mol Histol 35:545–553.

Bakker PIW de, Yelensky R, Pe'er I, Gabriel SB, Daly MJ, Altshuler D (2005) Efficiency and power in genetic association studies. Nat Genet 37:1217–1223.

Baldacara L, Nery-Fernandes F, Rocha M, Quarantini LC, Rocha GG, Guimaraes JL, Araujo C, Oliveira I, Miranda-Scippa A, Jackowski A (2011) Is cerebellar volume related to bipolar disorder? J Affect Disord 135:305–309.

Bale T, Davis A, Auger A, Dorsa D, McCarthy M (2001) CNS region-specific oxytocin receptor expression: importance in regulation of anxiety and sex behavior. J Neurosci 21:2546–2552.

Barrett JC, Fry B, Maller J, Daly MJ (2005) Haploview: analysis and visualization of LD and haplotype maps. Bioinformatics 21:263–265.

Bartel D (2004) MicroRNAs: genomics, biogenesis, mechanism, and function. Cell 116:281–297.

Bartel D (2009) MicroRNAs: target recognition and regulatory functions. Cell 136:215–233.

Bartz J, Hollander E (2008) Oxytocin and experimental therapeutics in autism spectrum disorders. Prog Brain Res 170:451-462.

Belshaw R, Dawson ALA, Woolven-Allen J, Redding J, Burt A, Tristem M (2005) Genomewide screening reveals high levels of insertional polymorphism in the human endogenous retrovirus family HERV-K(HML2): implications for present-day activity. J Virol 79:12507–12514.

Belshaw R, Pereira V, Katzourakis A, Talbot G, Paces J, Burt A, Tristem M (2004) Long-term reinfection of the human genome by endogenous retroviruses. Proc Natl Acad Sci U S A 101:4894–4899.

Ben-Zeev B, Levy-Nissenbaum E, Lahat H, Anikster Y, Shinar Y, Brand N, Gross-Tzur V, MacGregor D, Sidi R, Kleta R, Frydman M, Pras E (2002) Megalencephalic leukoencephalopathy with subcortical cysts; a founder effect in Israeli patients and a higher than expected carrier rate among Libyan Jews. Hum Genet 111:214–218.

Berney TP (2000) Autism--an evolving concept. Br J Psychiatry 176:20–25.

Bernstein E, Caudy A, Hammond S, Hannon G (2001) Role for a bidentate ribonuclease in the initiation step of RNA interference. Nature 409:363–366.

Beurs E, Comijs H, Twisk JR, Sonnenberg C, Beekman A, Deeg D (2005) Stability and change of emotional functioning in late life: modelling of vulnerability profiles. J Affect Disord 84:53–62.

Beveridge N, Gardiner E, Carroll A, Tooney P, Cairns M (2010) Schizophrenia is associated with an increase in cortical microRNA biogenesis. Mol Psychiatry 15:1176–1189.

Bhugra D (2005) The Global Prevalence of Schizophrenia. PLoS Med 2:e151.

Billing AM, Revets D, Hoffmann C, Turner JD, Vernocchi S, Muller CP (2012) Proteomic profiling of rapid non-genomic and concomitant genomic effects of acute restraint stress on rat thymocytes. J Proteomics 75:2064–2079.

Binder E (2009) The role of FKBP5, a co-chaperone of the glucocorticoid receptor in the pathogenesis and therapy of affective and anxiety disorders. Psychoneuroendocrinology 34 Suppl 1:186-195.

Binder E, Bradley R, Liu W, Epstein M, Deveau T, Mercer K, Tang Y, Gillespie C, Heim C, Nemeroff C, Schwartz A, Cubells J, Ressler K (2008) Association of FKBP5 polymorphisms and childhood abuse with risk of posttraumatic stress disorder symptoms in adults. JAMA 299:1291–1305.

Bjarkam C, Corydon T, Olsen I, Pallesen J, Nyegaard M, Fryland T, Mors O, Borglum A (2009) Further immunohistochemical characterization of BRD1 a new susceptibility gene for schizophrenia and bipolar affective disorder. Brain Struct Funct 214:37–47.

Blattner R, Moers A von, Leegwater PAJ, Hanefeld FA, van der Knaap MS, Köhler W (2003) Clinical and genetic heterogeneity in megalencephalic leukoencephalopathy with subcortical cysts (MLC). Neuropediatrics 34:215–218.

Boor I, Nagtegaal M, Kamphorst W, van der Valk P, Pronk J, van Horssen J, Dinopoulos A, Bove K, Pascual-Castroviejo I, Muntoni F, Estévez R, Scheper GC, van der Knaap M (2007) MLC1 is associated with the dystrophin-glycoprotein complex at astrocytic endfeet. Acta Neuropathol. 114:403–410.

Boor IPK, de Groot K, Mejaski-Bosnjak V, Brenner C, van der Knaap M, Scheper G, Pronk J (2006) Megalencephalic leukoencephalopathy with subcortical cysts: an update and extended mutation analysis of MLC1. Hum.Mutat. 27:505–512.

Boor P, de Groot K, Waisfisz Q, Kamphorst W, Oudejans C, Powers J, Pronk J, Scheper G, van der Knaap M (2005) MLC1: a novel protein in distal astroglial processes. J Neuropathol Exp Neurol. 64:412–419.

Bou Kheir T, Futoma-Kazmierczak E, Jacobsen A, Krogh A, Bardram L, Hother C, Grønbæk K, Federspiel B, Lund A, Friis-Hansen L (2011) miR-449 inhibits cell proliferation and is down-regulated in gastric cancer. Mol Cancer 10:29.

Bowden N, Weidenhofer J, Scott R, Schall U, Todd J, Michie PT, Tooney P (2006) Preliminary investigation of gene expression profiles in peripheral blood lymphocytes in schizophrenia. Schizophr Res 82:175–183.

Brambilla P, Hatch J, Soares J (2008) Limbic changes identified by imaging in bipolar patients. Curr Psychiatry Rep 10:505–509.

Brandt G, Bonelli R (2008) Structural neuroimaging of the basal ganglia in schizophrenic patients: a review. Wien Med Wochenschr 158:84–90.

Brignone M, Lanciotti A, Macioce P, Macchia G, Gaetani M, Aloisi F, Petrucci T, Ambrosini E (2011) The beta1 subunit of the Na,K-ATPase pump interacts with megalencephalic leucoencephalopathy with subcortical cysts protein 1 (MLC1) in brain astrocytes: new insights into MLC pathogenesis. Hum Mol Genet 20:90–103.

Brown T (2001) Southern blotting. Curr Protoc Protein Sci 4:Appendix 4G.

Brownawell A, Macara I (2002) Exportin-5, a novel karyopherin, mediates nuclear export of double-stranded RNA binding proteins. J Cell Biol 156:53–64.

Browne D, Brunt E, Griggs R, Nutt J, Gancher S, Smith E, Litt M (1995) Identification of two new KCNA1 mutations in episodic ataxia/myokymia families. Hum Mol Genet 4:1671–1672.

Browne D, Gancher S, Nutt J, Brunt E, Smith E, Kramer P, Litt M (1994) Episodic ataxia/myokymia syndrome is associated with point mutations in the human potassium channel gene, KCNA1. Nat Genet 8:136–140.

Brune M (2012) Does the oxytocin receptor polymorphism (rs2254298) confer 'vulnerability' for psychopathology or 'differential susceptibility'? Insights from evolution. BMC Med 10:38.

Brunner HG, Nelen M, Breakefield XO, Ropers HH, van Oost BA (1993) Abnormal behavior associated with a point mutation in the structural gene for monoamine oxidase A. Science 262:578–580.

Burbach J, van d (2009) Contact in the genetics of autism and schizophrenia. Trends Neurosci 32:69–72.

Bushati N, Cohen S (2007) microRNA functions. Annu Rev Cell Dev Biol 23:175–205.

Bymaster F, Hemrick-Luecke S, Perry K, Fuller R (1996) Neurochemical evidence for antagonism by olanzapine of dopamine, serotonin, alpha 1-adrenergic and muscarinic receptors in vivo in rats. Psychopharmacology 124:87–94.

Bymaster F, Rasmussen K, Calligaro D, Nelson D, DeLapp N, Wong D, Moore N (1997) In vitro and in vivo biochemistry of olanzapine: a novel, atypical antipsychotic drug. J Clin Psychiatry 58 Suppl 10:28–36.

Calhoun V, Sui J, Kiehl K, Turner J, Allen E, Pearlson G (2011) Exploring the psychosis functional connectome: aberrant intrinsic networks in schizophrenia and bipolar disorder. Front Psychiatry 2:75.

Cannon TD, Kaprio J, Lonnqvist J, Huttunen M, Koskenvuo M (1998) The genetic epidemiology of schizophrenia in a Finnish twin cohort. A population-based modeling study. Arch Gen Psychiatry 55:67–74.

Capecchi MR (1989) The new mouse genetics: altering the genome by gene targeting. Trends Genet 5:70–76.

Caricasole A, Bettini E, Sala C, Roncarati R, Kobayashi N, Caldara F, Goto K, Terstappen G (2002) Molecular cloning and characterization of the human diacylglycerol kinase beta (DGKbeta) gene: alternative splicing generates DGKbeta isotypes with different properties. J Biol Chem 277:4790–4796.

Carroll B, Yoho S, Bottoms J (2011) Periodic catatonia. Ann Clin Psychiatry 23:150–151.

Carroll L, Owen M (2009) Genetic overlap between autism, schizophrenia and bipolar disorder. Genome Med 1:102.

Cases O, Seif I, Grimsby J, Gaspar P, Chen K, Pournin S, Muller U, Aguet M, Babinet C, Shih JC (1995) Aggressive behavior and altered amounts of brain serotonin and norepinephrine in mice lacking MAOA. Science 268:1763–1766.

Caspi A, McClay J, Moffitt TE, Mill J, Martin J, Craig IW, Taylor A, Poulton R (2002) Role of genotype in the cycle of violence in maltreated children. Science 297:851–854.

Caspi A, Moffitt T (2006) Gene-environment interactions in psychiatry: joining forces with neuroscience. Nat Rev Neurosci 7:583–590.

Caspi A, Moffitt T, Cannon M, McClay J, Murray R, Harrington H, Taylor A, Arseneault L, Williams B, Braithwaite A, Poulton R, Craig I (2005) Moderation of the effect of adolescent-onset cannabis use on adult psychosis by a functional polymorphism in the catechol-O-methyltransferase gene: longitudinal evidence of a gene X environment interaction. Biol Psychiatry 57:1117–1127.

Caspi A, Sugden K, Moffitt T, Taylor A, Craig IW, Harrington H, McClay J, Mill J, Martin J, Braithwaite A, Poulton R (2003) Influence of life stress on depression: moderation by a polymorphism in the 5-HTT gene. Science 301:386–389.

Catholic Church (2005) Catechism of the Catholic Church. New York: Doubleday.

Cawley S, Bekiranov S, Ng H, Kapranov P, Sekinger E, Kampa D, Piccolboni A, Sementchenko V, Cheng J, Williams A, Wheeler R, Wong B, Drenkow J, Yamanaka M, Patel S, Brubaker S, Tammana H, Helt G, Struhl K, Gingeras T (2004) Unbiased mapping of transcription factor binding sites along human chromosomes 21 and 22 points to widespread regulation of noncoding RNAs. Cell 116:499–509.

Cerullo M, Fleck D, Eliassen J, Smith M, Delbello M, Adler C, Strakowski S (2012) A longitudinal functional connectivity analysis of the amygdala in bipolar I disorder across mood states. Bipolar Disord 14:175–184.

Chang T, Wentzel E, Kent O, Ramachandran K, Mullendore M, Lee K, Feldmann G, Yamakuchi M, Ferlito M, Lowenstein CJ, Arking DE, Beer MA, Maitra A, Mendell J (2007) Transactivation of miR-34a by p53 broadly influences gene expression and promotes apoptosis. Mol Cell 26:745–752.

Chen S, Parmigiani G (2007) Meta-analysis of BRCA1 and BRCA2 penetrance. J Clin Oncol 25:1329–1333.

Cheng H, Obrietan K (2007) Revealing a role of microRNAs in the regulation of the biological clock. Cell Cycle 6:3034–3035.

Cheng L, Pastrana E, Tavazoie M, Doetsch F (2009) miR-124 regulates adult neurogenesis in the subventricular zone stem cell niche. Nat Neurosci 12:399–408.

Choi Y, Lin C, Ho J, He X, Okada N, Bu P, Zhong Y, Kim S, Bennett M, Chen C, Ozturk A, Hicks GG, Hannon GJ, He L (2011) miR-34 miRNAs provide a barrier for somatic cell reprogramming. Nat Cell Biol 13:1353–1360.

Chong CSY, Leung JLM, Wong IHH, Ng PW, Miao MYK (2011) Presenile dementia: a case of Hashimoto's encephalopathy. East Asian Arch Psychiatry 21:32–36.

Christakou A, Murphy CM, Chantiluke K, Cubillo AI, Smith AB, Giampietro V, Daly E, Ecker C, Robertson D, Murphy DG, Rubia K (2012) Disorder-specific functional abnormalities during sustained attention in youth with Attention Deficit Hyperactivity Disorder (ADHD) and with Autism. Mol Psychiatry:1-9

Chrousos GP (1998) Stressors, stress, and neuroendocrine integration of the adaptive response. The 1997 Hans Selye Memorial Lecture. Ann. N. Y. Acad. Sci. 851:311–335.

Coleman S, Newcombe J, Pryke J, Dolly J (1999) Subunit composition of Kv1 channels in human CNS. J Neurochem 73:849–858.

Collins FS (2003) The Human Genome Project: Lessons from Large-Scale Biology. Science 300:286–290.

Comu S, Giuliani M, Narayanan V (1996) Episodic ataxia and myokymia syndrome: a new mutation of potassium channel gene Kv1.1. Ann Neurol 40:684–687.

Costa B, Pini S, Gabelloni P, Abelli M, Lari L, Cardini A, Muti M, Gesi C, Landi S, Galderisi S, Mucci A, Lucacchini A, Cassano GB, Martini C (2009) Oxytocin receptor polymorphisms and adult attachment style in patients with depression. Psychoneuroendocrinology 34:1506–1514.

Courchesne E, Pierce K, Schumann C, Redcay E, Buckwalter J, Kennedy D, Morgan J (2007) Mapping early brain development in autism. Neuron 56:399–413.

Craddock N (2005) The beginning of the end for the Kraepelinian dichotomy. Br J Psychiatry 186:364–366.

Craddock N, Owen MJ (2010) The Kraepelinian dichotomy - going, going… but still not gone. Br J Psychiatry 196:92–95.

Craddock N, Owen MJ, O'Donovan M (2006) The catechol-O-methyl transferase (COMT) gene as a candidate for psychiatric phenotypes: evidence and lessons. Mol Psychiatry 11:446–458.

Crespi BJ, Thiselton DL (2011) Comparative immunogenetics of autism and schizophrenia. Genes Brain Behav 10:689–701.

Cullen B (2005) RNAi the natural way. Nat Genet 37:1163–1165.

Daniels JL, Forssen U, Hultman CM, Cnattingius S, Savitz DA, Feychting M, Sparen P (2008) Parental psychiatric disorders associated with autism spectrum disorders in the offspring. Pediatrics 121:e1357-62.

de Kloet C, Vermetten E, Geuze E, Lentjes E, Heijnen CJ, Stalla GK, Westenberg HG (2008) Elevated plasma corticotrophin-releasing hormone levels in veterans with posttraumatic stress disorder. Prog Brain Res 167:287–291.

de Kloet ER, Joëls M, Holsboer F (2005) Stress and the brain: from adaptation to disease. Nat Rev Neurosci 6:463–475.

De Peri L, Crescini A, Deste G, Fusar-Poli P, Sacchetti E, Vita A (2012) Brain structural abnormalities at the onset of schizophrenia and bipolar disorder: a meta-analysis of controlled magnetic resonance imaging studies. Curr Pharm Des 18:486–494.

Dean B (2011) Understanding the role of inflammatory-related pathways in the pathophysiology and treatment of psychiatric disorders: evidence from human peripheral studies and CNS studies. Int J Neuropsychopharmacol 14:997–1012.

Del Rio-Albrechtsen T, Kiontke K, Chiou S, Fitch D (2006) Novel gain-of-function alleles demonstrate a role for the heterochronic gene lin-41 in C. elegans male tail tip morphogenesis. Dev Biol 297:74–86.

Deng C, Capecchi MR (1992) Reexamination of gene targeting frequency as a function of the extent of homology between the targeting vector and the target locus. Mol Cell Biol 12:3365–3371.

Devaney J, Donarum E, Brown K, Meyer J, Stöber G, Lesch K, Nestadt G, Stephan D, Pulver A (2002) No missense mutation of WKL1 in a subgroup of probands with schizophrenia. Mol Psychiatry 7:419–423.

Devuyst O, Guggino W (2002) Chloride channels in the kidney: lessons learned from knockout animals. Am J Physiol Renal Physiol 283:F1176-91.

Dezso Z, Nikolsky Y, Sviridov E, Shi W, Serebriyskaya T, Dosymbekov D, Bugrim A, Rakhmatulin E, Brennan RJ, Guryanov A, Li K, Blake J, Samaha RR, Nikolskaya T (2008) A comprehensive functional analysis of tissue specificity of human gene expression. BMC Biol 6:49.

D'Hulst C, Kooy R (2009) Fragile X syndrome: from molecular genetics to therapy. J Med Genet 46:577–584.

Dimitrov HD, Braida N, Walss-Bass C (2011) The Link Between Immune System Dysregulation and Schizophrenia. A Look at the Genetic Evidence. Psychiatric Times 28.

Dindot SV, Antalffy BA, Bhattacharjee MB, Beaudet AL (2008) The Angelman syndrome ubiquitin ligase localizes to the synapse and nucleus, and maternal deficiency results in abnormal dendritic spine morphology. Hum Mol Genet 17:111–118.

Doherty JL, O'Donovan MC, Owen MJ (2012) Recent genomic advances in schizophrenia. Clin Genet 81:103–109.

Dossetor D (2007) 'All that glitters is not gold': misdiagnosis of psychosis in pervasive developmental disorders--a case series. Clin Child Psychol Psychiatry 12:537–548.

Duarri A, Lopez Heredia M de, Capdevila-Nortes X, Ridder M, Montolio M, Lopez-Hernandez T, Boor I, Lien C, Hagemann T, Messing A, Gorecki DC, Scheper GC, Martinez A, Nunes V, van der Knaap MS, Estevez R (2011) Knockdown of MLC1 in primary astrocytes causes cell vacuolation: a MLC disease cell model. Neurobiol Dis 43:228–238.

Duarri A, Teijido O, Lopez-Hernandez T, Scheper G, Barriere H, Boor I, Aguado F, Zorzano A, Palacin M, Martinez A, Lukacs G, van der Knaap MS, Nunes V, Estevez R (2008) Molecular pathogenesis of megalencephalic leukoencephalopathy with subcortical cysts: mutations in MLC1 cause folding defects. Hum Mol Genet 17:3728–3739

Dudbridge F (2008) Likelihood-based association analysis for nuclear families and unrelated subjects with missing genotype data. Hum Hered 66:87–98.

Duggal H, Gandotra G (2005) Risperidone treatment of periodic catatonia. Can J Psychiatry 50:241–242.

Durbin RM, Abecasis GR, Altshuler DL, Auton A, Brooks LD, Gibbs RA, Hurles ME, McVean GA (2010) A map of human genome variation from population-scale sequencing. Nature 467:1061–1073.

Dwivedi Y (2009) Brain-derived neurotrophic factor: role in depression and suicide. Neuropsychiatr Dis Treat 5:433–449.

Ebstein RP, Israel S, Lerer E, Uzefovsky F, Shalev I, Gritsenko I, Riebold M, Salomon S, Yirmiya N (2009) Arginine vasopressin and oxytocin modulate human social behavior. Ann NY Acad Sci 1167:87–102.

Ecker C, Suckling J, Deoni S, Lombardo M, Bullmore E, Baron-Cohen S, Catani M, Jezzard P, Barnes A, Bailey A, Williams S, Murphy D (2012) Brain anatomy and its relationship to behavior in adults with autism spectrum disorder: a multicenter magnetic resonance imaging study. Arch Gen Psychiatry 69:195–209.

Edvardsen J, Torgersen S, Roysamb E, Lygren S, Skre I, Onstad S, Oien PA (2008) Heritability of bipolar spectrum disorders. Unity or heterogeneity? J Affect Disord 106:229–240.

Egashira N, Tanoue A, Matsuda T, Koushi E, Harada S, Takano Y, Tsujimoto G, Mishima K, Iwasaki K, Fujiwara M (2007) Impaired social interaction and reduced anxiety-related behavior in vasopressin V1a receptor knockout mice. Behav Brain Res 178:123–127.

Ekawardhani S (2008) Dissection of schizophrenia susceptibility loci at chromosomes 15q14-15.1 and 22q13.33. University of Trier, Germany.

Ekici A (2004) Periodic Catatonia: systematic analysis of candidate genes in a schizophrenia locus on chromosome 15q15. Eur J Hum Genet 282:12.

Elgar G, Vavouri T (2008) Tuning in to the signals: noncoding sequence conservation in vertebrate genomes. Trends Genet 24:344–352.

Engel G (1977) The need for a new medical model: a challenge for biomedicine. Science 196:129–136.

Engelmann M, Ebner K, Wotjak CT, Landgraf R (1998) Endogenous oxytocin is involved in short-term olfactory memory in female rats. Behav Brain Res. 90:89–94.

Esquirol E (1838) Des maladies mentales. Bruxelles: Tircher.

Ettinger U, Williams SC, Meisenzahl EM, Moller HJ, Kumari V, Koutsouleris N (2011) Association between brain structure and psychometric schizotypy in healthy individuals. World J Biol Psychiatry:1–6

Ewald H, Lundorf M (2002) The missense mutation in the WKL1 gene not found in patients with bipolar affective disorder. Mol Psychiatry 7:340–341.

Fallin MD, Lasseter VK, Avramopoulos D, Nicodemus K, Wolyniec P, McGrath J, Steel G, Nestadt G, Liang K, Huganir R, Valle D, Pulver A (2005) Bipolar I disorder and schizophrenia: a 440-single-nucleotide polymorphism screen of 64 candidate genes among Ashkenazi Jewish case-parent trios. Am J Hum Genet 77:918–936.

Ferguson J, Young L, Hearn E, Matzuk M, Insel T, Winslow J (2000) Social amnesia in mice lacking the oxytocin gene. Nat Genet 25:284–288.

Ferreira M *et al.* (2008) Collaborative genome-wide association analysis supports a role for ANK3 and CACNA1C in bipolar disorder. Nat Genet 40:1056–1058.

Fietta P, Fietta P, Delsante G (2011) Psychiatric and neuropsychological manifestations of systemic lupus erythematosus. Acta Biomed 82:97–114.

Fink M, Shorter E, Taylor M (2010) Catatonia is not schizophrenia: Kraepelin's error and the need to recognize catatonia as an independent syndrome in medical nomenclature. Schizophr Bull 36:314–320.

Fink M, Taylor M (2009) The catatonia syndrome: forgotten but not gone. Arch Gen Psychiatry 66:1173–1177.

Fischer M (1973) Genetic and environmental factors in schizophrenia. A study of schizophrenic twins and their families. Acta Psychiatr Scand Suppl 238:9–142.

Fombonne E (2003) Epidemiological surveys of autism and other pervasive developmental disorders: an update. J Autism Develop Disord 33:365–382.

Fombonne E (2009) Epidemiology of pervasive developmental disorders. Pediatr. Res. 65:591–598.

Frazer KA *et al.* (2007) A second generation human haplotype map of over 3.1 million SNPs. Nature 449:851–861.

Freitag CM (2006) The genetics of autistic disorders and its clinical relevance: a review of the literature. Mol Psychiatry 12:2–22.

Freitag CM, Asherson P, Hebebrand J (2012) Behavioural Genetics of Childhood Disorders. Curr Top Behav Neurosci 12:395–428

Friedman JI, Vrijenhoek T, Markx S, Janssen IM, van d, Faas BH, Knoers NV, Cahn W, Kahn RS, Edelmann L, Davis KL, Silverman JM, Brunner HG, van K, Wijmenga C, Ophoff RA, Veltman JA (2008) CNTNAP2 gene dosage variation is associated with schizophrenia and epilepsy. Mol Psychiatry 13:261–266.

Friedman R, Farh K, Burge CB, Bartel D (2008) Most mammalian mRNAs are conserved targets of microRNAs. Genome Res 19:92–105.

Fries E, Dettenborn L, Kirschbaum C (2009) The cortisol awakening response (CAR): facts and future directions. Int J Psychophysiol 72:67–73.

Fujitani Y, Yamamoto K, Kobayashi I (1995) Dependence of frequency of homologous recombination on the homology length. Genetics 140:797–809.

Furman DJ, Chen MC, Gotlib IH (2011) Variant in oxytocin receptor gene is associated with amygdala volume. Psychoneuroendocrinology 36:891–897.

Gaiteri C, Sibille E (2011) Differentially expressed genes in major depression reside on the periphery of resilient gene coexpression networks. Front Neurosci 5:95.

Gardier AM (2009) Mutant mouse models and antidepressant drug research: focus on serotonin and brain-derived neurotrophic factor. Behav Pharmacol 20:18–32.

Gee S, Madhavan R, Levinson S, Caldwell J, Sealock R, Froehner S (1998) Interaction of muscle and brain sodium channels with multiple members of the syntrophin family of dystrophin-associated proteins. J Neurosci 18:128–137.

Ghaemi SN (2006) Paradigms of psychiatry: eclecticism and its discontents. Curr Opin Psychiatry 19:619–624.

Gimpl G, Fahrenholz F (2001) The oxytocin receptor system: structure, function, and regulation. Physiol Rev 81:629–683.

Given JB (2001) Inquisition and medieval society. Power, discipline, and resistance in Languedoc. London: Cornell University Press.

Gladkevich A, Kauffman H, Korf J (2004) Lymphocytes as a neural probe: potential for studying psychiatric disorders. Prog Neuropsychopharmacol Biol Psychiatry 28:559–576.

Gogos J, Santha M, Takacs Z, Beck K, Luine V, Lucas L, Nadler J, Karayiorgou M (1999) The gene encoding proline dehydrogenase modulates sensorimotor gating in mice. Nat Genet 21:434–439.

Goldstein S, Schwebach A (2004) The comorbidity of Pervasive Developmental Disorder and Attention Deficit Hyperactivity Disorder: results of a retrospective chart review. J Autism Dev Disord 34:329–339.

Greenstein D, Lenroot R, Clausen L, Chavez A, Vaituzis AC, Tran L, Gogtay N, Rapoport J (2011) Cerebellar development in childhood onset schizophrenia and non-psychotic siblings. Psychiatry Res 193:131–137.

Greenwood CMT, Husted J, Bomba MD, Hodgkinson KA, Bassett AS (2004) Elevated rates of schizophrenia in a familial sample with mental illness and intellectual disability. J Intellect Disabil Res 48:531–539.

Gregory R, Chendrimada T, Cooch N, Shiekhattar R (2005) Human RISC couples microRNA biogenesis and posttranscriptional gene silencing. Cell 123:631–640.

Groenink L, van Bogaert M, van der Gugten J, Oosting R, Olivier B (2003) 5-HT1A receptor and 5-HT1B receptor knockout mice in stress and anxiety paradigms. Behav Pharmacol 14:369–383.

Gross J, Grimm O, Ortega G, Teuber I, Lesch KP, Meyer J (2001) Mutational analysis of the neuronal cadherin gene CELSR1 and exclusion as a candidate for catatonic schizophrenia in a large family. Psychiatr Genet. 11:197–200.

Grosse G, Draguhn A, Höhne L, Tapp R, Veh R, Ahnert-Hilger G (2000) Expression of Kv1 potassium channels in mouse hippocampal primary cultures: development and activity-dependent regulation. J Neurosci 20:1869–1882.

Grubb B, Gabriel S (1997) Intestinal physiology and pathology in gene-targeted mouse models of cystic fibrosis. Am J Physiol 273:G258-266.

Grunnet M, Rasmussen H, Hay-Schmidt A, Rosenstierne M, Klaerke D, Olesen S, Jespersen T (2003) KCNE4 is an inhibitory subunit to Kv1.1 and Kv1.3 potassium channels. Biophys J 85:1525–1537.

Grzadzinski R, Di Martino A, Brady E, Mairena MA, O'Neale M, Petkova E, Lord C, Castellanos FX (2011) Examining autistic traits in children with ADHD: does the autism spectrum extend to ADHD? J Autism Dev Disord 41:1178–1191.

Guastella A, Einfeld S, Gray K, Rinehart N, Tonge B, Lambert T, Hickie I Intranasal Oxytocin Improves Emotion Recognition for Youth with Autism Spectrum Disorders. Biol Psychiatry 67:692–694.

Guessous F, Zhang Y, Kofman A, Catania A, Li Y, Schiff D, Purow B, Abounader R (2010) microRNA-34a is tumor suppressive in brain tumors and glioma stem cells. Cell Cycle 9:1031–1036.

Gura T (1999) Gene defect linked to Rett syndrome. Science 286:27.

Guy J, Hendrich B, Holmes M, Martin J, Bird A (2001) A mouse Mecp2-null mutation causes neurological symptoms that mimic Rett syndrome. Nat Genet 27:322–326.

Guzman C, Myung V, Wang Y (2008) Treatment of periodic catatonia with atypical antipsychotic olanzapine. Psychiatry Clin Neurosci 62:482.

Hadjantonakis AK, Sheward WJ, Harmar AJ, Galan L de, Hoovers JM, Little PF (1997) Celsr1, a neural-specific gene encoding an unusual seven-pass transmembrane receptor, maps to mouse chromosome 15 and human chromosome 22qter. Genomics 45:97–104.

Harteneck C, Reiter B (2007) TRP channels activated by extracellular hypo-osmoticity in epithelia. Biochem Soc Trans 35:91–95.

Hartmann A, Blaesse P, Kranz T, Wenz M, Schindler J, Kaila K, Friauf E, Nothwang H (2009) Opposite effect of membrane raft perturbation on transport activity of KCC2 and NKCC1. J Neurochem 111:321–331.

Hasler G, Northoff G (2011) Discovering imaging endophenotypes for major depression. Mol Psychiatry 16:604–619.

Hasty P, Rivera-Pérez J, Bradley A (1991) The length of homology required for gene targeting in embryonic stem cells. Mol Cell Biol 11:5586–5591.

Hecker E (1871) Die Hebephrenie. Ein Beitrag zur klinischen Psychiatrie. Arch Pathol Anat Physiol Klin Med 52:394–429

Hecker E (2003) Cyclothymia, a Circular Mood Disorder. History of Psychiatry 14:377–390.

Heinrichs M, Baumgartner T, Kirschbaum C, Ehlert U (2003) Social support and oxytocin interact to suppress cortisol and subjective responses to psychosocial stress. Biol Psychiatry 54:1389–1398.

Heinrichs M, Domes G (2008) Neuropeptides and social behaviour: effects of oxytocin and vasopressin in humans. Prog Brain Res 170:337–350.

Henseler D (2010) Untersuchung potentieller Kandidatengene für Periodische Katatonie und Schizophrenie: Strukturelle und funktionelle Promotoranalyse von Mlc1, Mutationsanalyse von BUB1B und Assoziationsstudien zu CHRNA7, DAOA und BRD1. Trier.

Henseler D, Turner J, Eckhardt M, van der Mark M, Revsin Y, Lin M, Kranz T, Muller C, Meyer J (2011) Unusual 5'-regulatory structure and regulation of the murine Mlc1 gene: Lack of promoter-specific functional elements. J Nucleic Acids Invest 2:70–76.

Higashida H, Yokoyama S, Munesue T, Kikuchi M, Minabe Y, Lopatina O (2011) CD38 gene knockout juvenile mice: a model of oxytocin signal defects in autism. Biol Pharm Bull 34:1369–1372.

Hillegers MHJ (2004) Impact of stressful life events, familial loading and their interaction on the onset of mood disorders: Study in a high-risk cohort of adolescent offspring of parents with bipolar disorder. Br J Psychiatry 185:97–101.

Hollander E, Bartz J, Chaplin W, Phillips A, Sumner J, Soorya L, Anagnostou E, Wasserman S (2007) Oxytocin Increases Retention of Social Cognition in Autism. Biol Psychiatry 61:498–503.

Hollander E, Novotny S, Hanratty M, Yaffe R, DeCaria C, Aronowitz B, Mosovich S (2003) Oxytocin infusion reduces repetitive behaviors in adults with autistic and Asperger's disorders. Neuropsychopharmacology 28:193–198.

Hong C, Lai I, Liou L, Tsai S (2004) Association study of the human partially duplicated alpha7 nicotinic acetylcholine receptor genetic variant with bipolar disorder. Neurosci Lett 355:69–72.

Hope S, Melle I, Aukrust P, Steen NE, Birkenaes AB, Lorentzen S, Agartz I, Ueland T, Andreassen OA (2009) Similar immune profile in bipolar disorder and schizophrenia: selective increase in soluble tumor necrosis factor receptor I and von Willebrand factor. Bipolar Disord 11:726–734.

Houenou J, d'Albis M, Vederine F, Henry C, Leboyer M, Wessa M (2012) Neuroimaging biomarkers in bipolar disorder. Front Biosci (Elite Ed) 4:593–606.

Hu V, Frank B, Heine S, Lee NH, Quackenbush J (2006) Gene expression profiling of lymphoblastoid cell lines from monozygotic twins discordant in severity of autism reveals differential regulation of neurologically relevant genes. BMC Genomics 7:118.

Hu V, Nguyen A, Kim K, Steinberg M, Sarachana T, Scully M, Soldin SJ, Luu T, Lee N (2009a) Gene expression profiling of lymphoblasts from autistic and nonaffected sib pairs: altered pathways in neuronal development and steroid biosynthesis. PLoS One 4:e5775.

Hu V, Sarachana T, Kim K, Nguyen A, Kulkarni S, Steinberg M, Luu T, Lai Y, Lee N (2009b) Gene expression profiling differentiates autism case-controls and phenotypic variants of autism spectrum disorders: evidence for circadian rhythm dysfunction in severe autism. Autism Res 2:78–97.

Hudson J, Mangweth B, Pope H, Col C de, Hausmann A, Gutweniger S, Laird N, Biebl W, Tsuang M (2003) Family study of affective spectrum disorder. Arch Gen Psychiatry 60:170–177.

Inoue T, Kimura T, Azuma C, Inazawa J, Takemura M, Kikuchi T, Kubota Y, Ogita K, Saji F (1994) Structural organization of the human oxytocin receptor gene. J Biol Chem 269:32451–32456.

International HapMap Consortium (2003) The International HapMap Project. Nature 426:789–796.

International HapMap Consortium (2005) A haplotype map of the human genome. Nature 437:1299–1320.

Itsara A, Cooper GM, Baker C, Girirajan S, Li J, Absher D, Krauss RM, Myers RM, Ridker PM, Chasman DI, Mefford H, Ying P, Nickerson DA, Eichler EE (2009) Population analysis of large copy number variants and hotspots of human genetic disease. Am J Hum Genet 84:148–161.

Jacob S, Brune C, Carter C, Leventhal B, Lord C, Cook E (2007) Association of the oxytocin receptor gene (OXTR) in Caucasian children and adolescents with autism. Neurosci Lett 417:6–9.

Jansen L, de Gispen W, Wiegant V, Westenberg H, Lahuis B, van Engeland H (2006) Autonomic and neuroendocrine responses to a psychosocial stressor in adults with autistic spectrum disorder. J Autism Dev Disord 36:891–899.

Jaspers K (1973) Allgemeine Psychopathologie. Heidelberg: Springer.

Jin D *et al.* (2007) CD38 is critical for social behaviour by regulating oxytocin secretion. Nature 446:41–45.

Jin P, Zarnescu D, Ceman S, Nakamoto M, Mowrey J, Jongens T, Nelson D, Moses K, Warren S (2004) Biochemical and genetic interaction between the fragile X mental retardation protein and the microRNA pathway. Nat Neurosci 7:113–117.

Jirikowski GF, Sanna PP, Bloom FE (1990) mRNA coding for oxytocin is present in axons of the hypothalamo-neurohypophysial tract. Proc Natl Acad Sci U S A 87:7400–7404.

Jorgensen T, Børglum A, Mors O, Wang A, Pinaud M, Flint T, Dahl H, Vang M, Kruse T, Ewald H (2002) Search for common haplotypes on chromosome 22q in patients with schizophrenia or bipolar disorder from the Faroe Islands. Am J Med Genet 114:245–252.

Kaganovich M, Peretz A, Ritsner M, Bening Abu-Shach U, Attali B, Navon R (2004) Is the WKL1 gene associated with schizophrenia? Am J Med Genet B Neuropsychiatr Genet 125:31–37.

Kahlbaum K (1874) Die Katatonie oder das Spannungsirresein. Eine klinische Form psychischer Krankheit. Berlin: Hirschwald.

Kakefuda K, Oyagi A, Ishisaka M, Tsuruma K, Shimazawa M, Yokota K, Shirai Y, Horie K, Saito N, Takeda J, Hara H (2010) Diacylglycerol kinase beta knockout mice exhibit lithium-sensitive behavioral abnormalities. PLoS One 5:e13447.

Kapferer R, Sticker G (1934) Die Werke des Hippocrates. Die hippokratische Schriftensammlung in neuer deutscher Übersetzung. Stuttgart: Hippokrates-Verlag

Karayiorgou M, Morris M, Morrow B, Shprintzen R, Goldberg R, Borrow J, Gos A, Nestadt G, Wolyniec P, Lasseter V (1995) Schizophrenia susceptibility associated with interstitial deletions of chromosome 22q11. Proc Natl Acad Sci U S A 92:7612–7616.

Katila H, Hanninen K, Hurme M (1999) Polymorphisms of the interleukin-1 gene complex in schizophrenia. Mol Psychiatry 4:179–181.

Kato T (2007) Molecular genetics of bipolar disorder and depression. Psychiatry Clin Neurosci 61:3–19.

Keshavan MS (2005) Neurobiology of early psychosis. Br J Psychiatry187:s8.

Keshavan MS, Hogarty GE (1999) Brain maturational processes and delayed onset in schizophrenia. Dev Psychopathol 11:525–543.

Kieseppa T, Partonen T, Haukka J, Kaprio J, Lonnqvist J (2004) High concordance of bipolar I disorder in a nationwide sample of twins. Am J Psychiatry 161:1814–1821.

Kim A, Reimers M, Maher B, Williamson V, McMichael O, McClay J, van den Oord E, Riley B, Kendler KS, Vladimirov V (2010) MicroRNA expression profiling in the prefrontal cortex of individuals affected with schizophrenia and bipolar disorders. Schizophr Res 124:183–191.

Kimura K *et al.* (2006) Diversification of transcriptional modulation: large-scale identification and characterization of putative alternative promoters of human genes. Genome Res 16:55–65.

King BH, Lord C (2011) Is schizophrenia on the autism spectrum? Brain Res 1380:34–41.

Kirov G (2010) The role of copy number variation in schizophrenia. Expert Rev Neurother 10:25–32.

Kirsch P, Esslinger C, Chen Q, Mier D, Lis S, Siddhanti S, Gruppe H, Mattay V, Gallhofer B, Meyer-Lindenberg A (2005) Oxytocin modulates neural circuitry for social cognition and fear in humans. J Neurosci 25:11489–11493.

Kirschbaum C, Pirke KM, Hellhammer DH (1993) The 'Trier Social Stress Test' - a tool for investigating psychobiological stress responses in a laboratory setting. Neuropsychobiology 28:76–81.

Klein ME, Lioy DT, Ma L, Impey S, Mandel G, Goodman RH (2007) Homeostatic regulation of MeCP2 expression by a CREB-induced microRNA. Nat Neurosci 10:1513–1514.

Kleist K (1928) Über zykloide, paranoide und epileptoide Psychosen und über die Frage der Degenerationspsychosen. Schweiz Arch Neurol Neurochir 23:3–37.

Knight HM, Pickard BS, Maclean A, Malloy MP, Soares DC, McRae AF, Condie A, White A, Hawkins W, McGhee K, van Beck M, MacIntyre DJ, Starr JM, Deary IJ, Visscher PM, Porteous DJ, Cannon RE, St Clair D, Muir WJ, Blackwood DH (2009) A cytogenetic abnormality and rare coding variants identify ABCA13 as a candidate gene in schizophrenia, bipolar disorder, and depression. Am J Hum Genet 85:833–846.

Knight LA, Yong MH, Tan M, Ng IS (1995) Del(3) (p25.3) without phenotypic effect. J Med Genet 32:994–995.

Koike H (2006) Disc1 is mutated in the 129S6/SvEv strain and modulates working memory in mice. Proc Natl Acad Sci U S A 103:3693–3697.

Konstantareas M, Hewitt T (2001) Autistic disorder and schizophrenia: diagnostic overlaps. J Autism Dev Disord 31:19–28.

Kosfeld M, Heinrichs M, Zak P, Fischbacher U, Fehr E (2005) Oxytocin increases trust in humans. Nature 435:673–676.

Krichevsky A, Sonntag K, Isacson O, Kosik K (2006) Specific microRNAs modulate embryonic stem cell-derived neurogenesis. Stem Cells 24:857–864.

Kurian AW, Sigal BM, Plevritis SK (2010) Survival analysis of cancer risk reduction strategies for BRCA1/2 mutation carriers. J Clin Oncol 28:222–231.

Kushima I, Aleksic B, Ikeda M, Yamanouchi Y, Kinoshita Y, Ito Y, Nakamura Y, Inada T, Iwata N, Ozaki N (2010) Association study of bromodomain-containing 1 gene with schizophrenia in Japanese population. Am J Med Genet B Neuropsychiatr Genet 153:786–791.

Kwon E, Wang W, Tsai L (2011) Validation of schizophrenia-associated genes CSMD1, C10orf26, CACNA1C and TCF4 as miR-137 targets. Mol Psychiatry: 1–2

Lagos-Quintana M, Rauhut R, Lendeckel W, Tuschl T (2001) Identification of novel genes coding for small expressed RNAs. Science 294:853–858.

Lai C, Yu S, Hsieh M, Chen C, Chen H, Wen C, Huang Y, Hsiao P, Hsiao CK, Liu C, Yang P, Hwu H, Chen W (2011) MicroRNA expression aberration as potential peripheral blood biomarkers for schizophrenia. PLoS One 6:e21635.

Lanciotti A, Brignone M, Camerini S, Serafini B, Macchia G, Raggi C, Molinari P, Crescenzi M, Musumeci M, Sargiacomo M, Aloisi F, Petrucci TC, Ambrosini E (2008) MLC1 trafficking and membrane expression in astrocytes: Role of caveolin-1 and phosphorylation. Neurobiol Dis 37:581–595

Lanciotti A, Brignone M, Molinari P, Visentin S, Nuccio C, Macchia G, Aiello C, Bertini E, Aloisi F, Petrucci TC, Ambrosini E (2012) Megalencephalic leukoencephalopathy with subcortical cysts protein 1 functionally cooperates with the TRPV4 cation channel to activate the response of astrocytes to osmotic stress: dysregulation by pathological mutations. Hum Mol Genet 21:2166–2180.

Lander ES *et al.* (2001) Initial sequencing and analysis of the human genome. Nature 409:860–921.

Lasseter VK, Pulver AE, Wolyniec PS, Nestadt G, Meyers D, Karayiorgou M, Housman D, Antonarakis S, Kazazian H, Kasch L (1995) Follow-up report of potential linkage for schizophrenia on chromosome 22q: Part 3. Am J Med Genet 60:172–173.

Lee C, Risom T, Strauss WM (2007) Evolutionary conservation of microRNA regulatory circuits: an examination of microRNA gene complexity and conserved microRNA-target interactions through metazoan phylogeny. DNA Cell Biol 26:209–218.

Lee H, Macbeth A, Pagani J, Scott Young W (2009) Oxytocin: The great facilitator of life. Prog Neurobiol 88:127–151.

Lee RC, Ambros V (2001) An extensive class of small RNAs in Caenorhabditis elegans. Science 294:862–864.

Lee Y, Ahn C, Han J, Choi H, Kim J, Yim J, Lee J, Provost P, Rådmark O, Kim S, Kim V (2003) The nuclear RNase III Drosha initiates microRNA processing. Nature 425:415–419.

Lee Y, Jeon K, Lee J, Kim S, Kim V (2002) MicroRNA maturation: stepwise processing and subcellular localization. EMBO J. 21:4663–4670.

Leegwater P, Boor P, Yuan B, van der Steen J, Visser A, Konst A, Oudejans CB, Schutgens R, Pronk J, van der Knaap M (2002) Identification of novel mutations in MLC1 responsible for megalencephalic leukoencephalopathy with subcortical cysts. Hum Genet 110:279–283.

Leegwater P, Yuan B, van der Steen J, Mulders J, Könst A, Boor P, Mejaski-Bosnjak V, van der Maarel S, Frants R, Oudejans C, Schutgens R, Pronk J, van der Knaap M (2001) Mutations of MLC1 (KIAA0027), encoding a putative membrane protein, cause megalencephalic leukoencephalopathy with subcortical cysts. Am J Hum Genet 68:831–838.

Leonhard K, Beckmann H (1999) Classification of endogenous psychoses and their differential etiology. Wien: Springer.

Lerer E, Levi S, Salomon S, Darvasi A, Yirmiya N, Ebstein R (2008) Association between the oxytocin receptor (OXTR) gene and autism: relationship to Vineland Adaptive Behavior Scales and cognition. Mol Psychiatry 13:980–988.

Levy S, Mandell D, Schultz R (2009) Autism. Lancet 374:1627–1638.

Lewis CM *et al.* (2003) Genome scan meta-analysis of schizophrenia and bipolar disorder, part II: Schizophrenia. Am J Hum Genet 73:34–48.

Lightman SL, Wiles CC, Atkinson HC, Henley DE, Russell GM, Leendertz JA, McKenna MA, Spiga F, Wood SA, Conway-Campbell BL (2008) The significance of glucocorticoid pulsatility. Eur J Pharmacol 583:255–262.

Lim L, Lau N, Garrett-Engele P, Grimson A, Schelter J, Castle J, Bartel DP, Linsley PS, Johnson J (2005) Microarray analysis shows that some microRNAs downregulate large numbers of target mRNAs. Nature 433:769–773.

Lin M, Pedrosa E, Shah A, Hrabovsky A, Maqbool S, Zheng D, Lachman H (2011) RNA-Seq of human neurons derived from iPS cells reveals candidate long non-coding RNAs involved in neurogenesis and neuropsychiatric disorders. PLoS One 6:e23356.

Lin Y, Liao S (2009) Hashimoto encephalopathy presenting as schizophrenia-like disorder. Cogn Behav Neurol 22:197–201.

Linacre T, Payne JF (1881) Galeni Pergamensis De temperamentis. Et De inaeqvali intemperie libri tres, Thomas Linacro Anglo interprete. Opus non medicis modo, sed et philosophis oppido q[uem] necessariu[m] nunc primum prodit in lucem cvm gratia & priuilegio. Cambridge: Macmillan.

Littleton JT, Sheng M (2003) Neurobiology: Synapses unplugged. Nature 423:931–932.

Liu H, Heath S, Sobin C, Roos J, Galke B, Blundell M, Lenane M, Robertson B, Wijsman E, Rapoport J, Gogos J, Karayiorgou M (2002) Genetic variation at the 22q11

PRODH2/DGCR6 locus presents an unusual pattern and increases susceptibility to schizophrenia. Proc Natl Acad Sci U S A 99:3717–3722.

Liu J, Carmell M, Rivas F, Marsden C, Thomson J, Song J, Hammond S, Joshua-Tor L, Hannon G (2004) Argonaute2 is the catalytic engine of mammalian RNAi. Science 305:1437–1441.

Liu X, Kawamura Y, Shimada T, Otowa T, Koishi S, Sugiyama T, Nishida H, Hashimoto O, Nakagami R, Tochigi M, Umekage T, Kano Y, Miyagawa T, Kato N, Tokunaga K, Sasaki T (2010) Association of the oxytocin receptor (OXTR) gene polymorphisms with autism spectrum disorder (ASD) in the Japanese population. J Hum Genet 55:137–141.

Liu Z, Huang T, Smith C (2012) Lithium reverses increased rates of cerebral protein synthesis in a mouse model of fragile X syndrome. Neurobiol Dis 45:1145–1152.

Lodish HF (2000) Molecular cell biology. New York: W.H. Freeman.

López-Hernández T, Ridder M, Montolio M, Capdevila-Nortes X, Polder E, Sirisi S, Duarri A, Schulte U, Fakler B, Nunes V, Scheper GC, Martínez A, Estévez R, van der Knaap M (2011) Mutant GlialCAM causes megalencephalic leukoencephalopathy with subcortical cysts, benign familial macrocephaly, and macrocephaly with retardation and autism. Am J Hum Genet 88:422–432.

Lord C, Risi S, Lambrecht L, Cook EH, JR, Leventhal BL, DiLavore PC, Pickles A, Rutter M (2000) The autism diagnostic observation schedule-generic: a standard measure of social and communication deficits associated with the spectrum of autism. J Autism Dev Disord 30:205–223.

Lord C, Rutter M, Le Couteur A (1994) Autism Diagnostic Interview-Revised: a revised version of a diagnostic interview for caregivers of individuals with possible pervasive developmental disorders. J Autism Dev Disord 24:659–685.

Luan S, Sun L, Huang F (2010) MicroRNA-34a: a novel tumor suppressor in p53-mutant glioma cell line U251. Arch Med Res 41:67–74.

Lucht MJ, Barnow S, Sonnenfeld C, Rosenberger A, Grabe HJ, Schroeder W, Völzke H, Freyberger HJ, Herrmann FH, Kroemer H, Rosskopf D (2009) Associations between the oxytocin receptor gene (OXTR) and affect, loneliness and intelligence in normal subjects. Prog Neuropsychopharmacol Biol Psychiatry 33:860–866.

Lucki I (1997) The forced swimming test as a model for core and component behavioral effects of antidepressant drugs. Behav Pharmacol 8:523–532.

Lucki I, Dalvi A, Mayorga A (2001) Sensitivity to the effects of pharmacologically selective antidepressants in different strains of mice. Psychopharmacology (Berl) 155:315–322.

Lukk M, Kapushesky M, Nikkilä J, Parkinson H, Goncalves A, Huber W, Ukkonen E, Brazma A (2010) A global map of human gene expression. Nat Biotechnol 28:322–324.

Mackay C, Institoris H, Sprenger J (2006) Malleus maleficarum. Cambridge: Cambridge University Press.

Malavasi F, Deaglio S, Funaro A, Ferrero E, Horenstein A, Ortolan E, Vaisitti T, Aydin S (2008) Evolution and function of the ADP ribosyl cyclase/CD38 gene family in physiology and pathology. Physiol Rev 88:841–886.

Marcet B, Chevalier B, Luxardi G, Coraux C, Zaragosi L, Cibois M, Robbe-Sermesant K, Jolly T, Cardinaud B, Moreilhon C, Giovannini-Chami L, Nawrocki-Raby B, Birembaut P, Waldmann R, Kodjabachian L, Barbry P (2011) Control of vertebrate multiciliogenesis by miR-449 through direct repression of the Delta/Notch pathway. Nat Cell Biol 13:693–699.

Mardis ER (2008) Next-generation DNA sequencing methods. Annu Rev Genomics Hum Genet 9:387–402.

Marneros A (2008) Psychiatry's 200th birthday. Br J Psychiatry193:1–3.

Marneros A, Pillmann F (2005) Das Wort Psychiatrie wurde in Halle geboren. Von den Anfängen der deutschen Psychiatrie. Stuttgart: Schattauer.

Martin T, Grishanin R (2003) PC12 cells as a model for studies of regulated secretion in neuronal and endocrine cells. Methods Cell Biol 71:267–286.

Maturana HR (1975) The organization of the living: A theory of the living organization. Int J Man-Machine Studies 7:313–332

Maturana HR (1980) Autopoiesis and cognition: the realization of the living. Dordrecht: Reidel Pub Co.

Maturana HR, Varela FJ (1992) The tree of knowledge. The biological roots of human understanding. New York: Shambhala Pub.

McCullagh P, Chaplin T, Meerabux J, Grenzelias D, Lillington D, Poulsom R, Gregorini A, Saha V, Young B (1999) The cloning, mapping and expression of a novel gene, BRL, related to the AF10 leukaemia gene. Oncogene 18:7442–7452.

McElroy SL (2004) Diagnosing and treating comorbid (complicated) bipolar disorder. J Clin Psychiatry 65 Suppl 15:35–44.

McGlashan T (2011) Eugen Bleuler: Centennial Anniversary of His 1911 Publication of Dementia Praecox or the Group of Schizophrenias. Schizophr Bull 37:1101–1103.

McGrath JJ, Féron FP, Burne THJ, Mackay-Sim A, Eyles DW (2003) The neurodevelopmental hypothesis of schizophrenia: a review of recent developments. Ann Med 35:86–93.

McGuffin P, Rijsdijk F, Andrew M, Sham P, Katz R, Cardno A (2003) The heritability of bipolar affective disorder and the genetic relationship to unipolar depression. Arch Gen Psychiatry 60:497–502.

McKeane DP, Meyer J, Dobrin SE, Melmed KM, Ekawardhani S, Tracy NA, Lesch KP, Stephan DA (2005) No causative DLL4 mutations in periodic catatonia patients from 15q15 linked families. Schizophr Res 75:1–3.

McNemar Q (1947) Note on the sampling error of the difference between correlated proportions or percentages. Psychometrika 12:153–157.

McQuillin A, Kalsi G, Moorey H, Lamb G, Mayet S, Quested D, Baker P, Curtis D, Gurling H (2002) A novel polymorphism in exon 11 of the WKL1 gene shows no association with schizophrenia. Eur J Hum Genet 10:491–494.

Mehta D, Menke A, Binder EB (2010) Gene Expression Studies in Major Depression. Curr Psychiatry Rep 12:135–144.

Mellios N, Huang H, Grigorenko A, Rogaev E, Akbarian S (2008) A set of differentially expressed miRNAs, including miR-30a-5p, act as post-transcriptional inhibitors of BDNF in prefrontal cortex. Hum Mol Genet 17:3030–3042.

Meltzer H, Huang M (2008) In vivo actions of atypical antipsychotic drug on serotonergic and dopaminergic systems. Prog Brain Res 172:177–197.

Meyer J, Huberth A, Ortega G, Syagailo Y, Jatzke S, Mossner R, Strom T, Ulzheimer-Teuber I, Stober G, Schmitt A, Lesch K (2001) A missense mutation in a novel gene encoding a putative cation channel is associated with catatonic schizophrenia in a large pedigree. Mol Psychiatry 6:302–306.

Meyer J, Johannssen K, Freitag CM, Schraut K, Teuber I, Hahner A, Mainhardt C, Mossner R, Volz HP, Wienker TF, McKeane D, Stephan DA, Rouleau G, Reif A, Lesch KP (2005) Rare variants of the gene encoding the potassium chloride co-transporter 3 are associated with bipolar disorder. Int J Neuropsychopharmacol 8:495–504.

Meyer J, Ortega G, Schraut K, Nurnberg G, Ruschendorf F, Saar K, Mossner R, Wienker T, Reis A, Stober G, Lesch K (2002) Exclusion of the neuronal nicotinic acetylcholine receptor alpha7 subunit gene as a candidate for catatonic schizophrenia in a large family supporting the chromosome 15q13-22 locus. Mol Psychiatry 7:220–223.

Meyer J, Ruschendorf F, Lesch K (2003) A second large family with catatonic schizophrenia supports the region distally of CHRNA7 on chromosome 15q14-15. Mol Psychiatry 8:259–260.

Meyer U, Schwarz MJ, Muller N (2011) Inflammatory processes in schizophrenia: a promising neuroimmunological target for the treatment of negative/cognitive symptoms and beyond. Pharmacol Ther 132:96–110.

Millan M *et al.* (2012) Cognitive dysfunction in psychiatric disorders: characteristics, causes and the quest for improved therapy. Nat Rev Drug Discov 11:141–168.

Miller S, Dykes D, Polesky H (1988) A simple salting out procedure for extracting DNA from human nucleated cells. Nucleic Acids Res 16:1215.

Minshew N, Keller T (2010) The nature of brain dysfunction in autism: functional brain imaging studies. Curr Opin Neurol 23:124–130.

Mittal V, Dhruv S, Tessner K, Walder D, Walker E (2007) The relations among putative biorisk markers in schizotypal adolescents: minor physical anomalies, movement abnormalities, and salivary cortisol. Biol Psychiatry 61:1179–1186.

Modahl C, Green L, Fein D, Morris M, Waterhouse L, Feinstein C, Levin H (1998) Plasma oxytocin levels in autistic children. Biol Psychiatry 43:270–277.

Modi M, Young L (2012) The oxytocin system in drug discovery for autism: animal models and novel therapeutic strategies. Horm Behav 61:340–350.

Monji A, Kato T, Kanba S (2009) Cytokines and schizophrenia: Microglia hypothesis of schizophrenia. Psychiatry Clin Neurosci 63:257–265.

Monroe SM, Simons AD (1991) Diathesis-stress theories in the context of life stress research: implications for the depressive disorders. Psychol Bull 110:406–425.

Morel B (1860) Traité des maladies mentales. Paris: Victor Masson.

Morgan V, Leonard H, Bourke J, Jablensky A (2008) Intellectual disability co-occurring with schizophrenia and other psychiatric illness: population-based study. Br J Psychiatry 193:364–372.

Mowry BJ *et al.* (2004) Multicenter linkage study of schizophrenia loci on chromosome 22q. Mol Psychiatry 9:784–795.

Muhle R, Trentacoste S, Rapin I (2004) The Genetics of Autism. Pediatrics 113:e472-486.

Murphy C, Deeley Q, Daly EM, Ecker C, O'Brien FM, Hallahan B, Loth E, Toal F, Reed S, Hales S, Robertson DM, Craig MC, Mullins D, Barker GJ, Lavender T, Johnston P, Murphy KC, Murphy DG (2012) Anatomy and aging of the amygdala and hippocampus in autism spectrum disorder: an in vivo magnetic resonance imaging study of Asperger syndrome. Autism Res 5:3–12.

Murray RM (1994) Neurodevelopmental schizophrenia: the rediscovery of dementia praecox. Br J Psychiatry Suppl:6–12.

Murray RM, Lewis SW (1988) Is schizophrenia a neurodevelopmental disorder? Br Med J (Clin Res Ed) 296:63.

Murray RM, O'Callaghan E, Castle DJ, Lewis SW (1992) A neurodevelopmental approach to the classification of schizophrenia. Schizophr Bull 18:319–332.

Nasrallah H, Weinberger D (1986) The Neurology of schizophrenia. New York: Elsevier

Nelson PG, Kuddo T, Song EY, Dambrosia JM, Kohler S, Satyanarayana G, Vandunk C, Grether JK, Nelson KB (2006) Selected neurotrophins, neuropeptides, and cytokines: developmental trajectory and concentrations in neonatal blood of children with autism or Down syndrome. Int J Dev Neurosci 24:73–80.

Ng PC, Murray SS, Levy S, Venter JC (2009) An agenda for personalized medicine. Nature 461:724–726.

Nguyen T, Mehta N, Conant K, Kim K, Jones M, Calabresi P, Melli G, Hoke A, Schnaar R, Ming G, Song H, Keswani S, Griffin J (2009) Axonal Protective Effects of the Myelin-Associated Glycoprotein. J Neurosci 29:630–637.

Nickl-Jockschat T, Schneider F, Pagel A, Laird A, Fox P, Eickhoff S (2011) Progressive pathology is functionally linked to the domains of language and emotion: meta-analysis of brain structure changes in schizophrenia patients. Eur Arch Psychiatry Clin Neurosci 261 Suppl 2:S166-71.

Nishimori K, Young L, Guo Q, Wang Z, Insel T, Matzuk M (1996) Oxytocin is required for nursing but is not essential for parturition or reproductive behavior. Proc Natl Acad Sci U S A . 93:11699–11704.

Noll R (2007) Encyclopedia of Schizophrenia. New York: Facts on File.

Nothen MM, Nieratschker V, Cichon S, Rietschel M (2010) New findings in the genetics of major psychoses. Dialogues Clin Neurosci 12:85–93.

Numata S, Ueno S, Iga J, Yamauchi K, Hongwei S, Hashimoto R, Takeda M, Kunugi H, Itakura M, Ohmori T (2007) Gene expression in the peripheral leukocytes and association analysis of PDLIM5 gene in schizophrenia. Neurosci Lett 415:28–33.

Nyegaard M *et al.* (2010) Support of association between BRD1 and both schizophrenia and bipolar affective disorder. Am J Med Genet B Neuropsychiatr Genet 153:582–591.

Ota T *et al.* (2003) Complete sequencing and characterization of 21,243 full-length human cDNAs. Nat Genet 36:40–45.

Owen M, O'Donovan M, Thapar A, Craddock N (2011) Neurodevelopmental hypothesis of schizophrenia. Br J Psychiatry 198:173–175.

Oyagi A, Oida Y, Kakefuda K, Shimazawa M, Shioda N, Moriguchi S, Kitaichi K, Nanba D, Yamaguchi K, Furuta Y, Fukunaga K, Higashiyama S, Hara H, Linden R (2009) Generation and Characterization of Conditional Heparin-Binding EGF-Like Growth Factor Knockout Mice. PLoS One 4:e7461.

Ozaki K, Ohnishi Y, Iida A, Sekine A, Yamada R, Tsunoda T, Sato H, Sato H, Hori M, Nakamura Y, Tanaka T (2002) Functional SNPs in the lymphotoxin-alpha gene that are associated with susceptibility to myocardial infarction. Nat Genet 32:650–654.

Patrono C, Di Giacinto G, Eymard-Pierre E, Santorelli FM, Rodriguez D, de Stefano N, Federico A, Gatti R, Benigno V, Megarbane A, Tabarki B, Boespflug-Tanguy O, Bertini E (2003) Genetic heterogeneity of megalencephalic leukoencephalopathy and subcortical cysts. Neurology 61:534–537.

Patterson K (2011) 1000 GENOMES: A World of Variation. Circ Res 108:534–536.

Perälä J, Suvisaari J, Saarni S, Kuoppasalmi K, Isometsä E, Pirkola S, Partonen T, Tuulio-Henriksson A, Hintikka J, Kieseppä T, Härkänen T, Koskinen S, Lönnqvist J (2007) Lifetime prevalence of psychotic and bipolar I disorders in a general population. Arch Gen Psychiatry 64:19–28.

Pereira A, Tiemensma J, Romijn J (2010) Neuropsychiatric disorders in Cushing's syndrome. Neuroendocrinology 92 Suppl 1:65–70.

Perkins D, Jeffries C, Jarskog L, Thomson J, Woods K, Newman M, Parker J, Jin J, Hammond S (2007) microRNA expression in the prefrontal cortex of individuals with schizophrenia and schizoaffective disorder. Genome Biol 8:R27.

Pharoah PD, Day NE, Duffy S, Easton DF, Ponder BA (1997) Family history and the risk of breast cancer: a systematic review and meta-analysis. Int J Cancer 71:800–809.

Pillai R, Bhattacharyya S, Artus C, Zoller T, Cougot N, Basyuk E, Bertrand E, Filipowicz W (2005) Inhibition of translational initiation by Let-7 MicroRNA in human cells. Science 309:1573–1576.

Pilowsky L, Bressan R, Stone J, Erlandsson K, Mulligan R, Krystal J, Ell P (2006) First in vivo evidence of an NMDA receptor deficit in medication-free schizophrenic patients. Mol Psychiatry 11:118–119.

Pobbe R, Pearson B, Defensor E, Bolivar V, Young W, Lee H, Blanchard DC, Blanchard R (2012) Oxytocin receptor knockout mice display deficits in the expression of autism-related behaviors. Horm Behav 61:436–444.

Popik P, Vetulani J, van Ree J (1992) Low doses of oxytocin facilitate social recognition in rats. Psychopharmacology 106:71–74.

Porsolt R, Le P, Jalfre M (1977) Depression: a new animal model sensitive to antidepressant treatments. Nature 266:730–732.

Posner J, Nagel B, Maia T, Mechling A, Oh M, Wang Z, Peterson B (2011) Abnormal amygdalar activation and connectivity in adolescents with attention-deficit/hyperactivity disorder. J Am Acad Child Adolesc Psychiatry 50:828-37.e3.

Psychiatric GWAS Consortium (2009) Genomewide Association Studies: History, Rationale, and Prospects for Psychiatric Disorders. Am J Psychiatry 166:540–556.

Radonic E, Rados M, Kalember P, Bajs-Janovic M, Folnegovic-Smalc V, Henigsberg N (2011) Comparison of hippocampal volumes in schizophrenia, schizoaffective and bipolar disorder. Coll Antropol 35 Suppl 1:249–252.

Ramsey A (2009) NR1 knockdown mice as a representative model of the glutamate hypothesis of schizophrenia. Prog Brain Res 179:51–58.

Rapoport J, Chavez A, Greenstein D, Addington A, Gogtay N (2009) Autism spectrum disorders and childhood-onset schizophrenia: clinical and biological contributions to a relation revisited. J Am Acad Child Adolesc Psychiatry 48:10–18.

Realmuto GM, August GJ (1991) Catatonia in autistic disorder: a sign of comorbidity or variable expression? J Autism Dev Disord 21:517–528.

Reed U (2009) Congenital muscular dystrophy. Part I: a review of phenotypical and diagnostic aspects. Arq Neuropsiquiatr 67:144–168.

Reichelt AC, Rodgers RJ, Clapcote SJ (2012) The role of neurexins in schizophrenia and autistic spectrum disorder. Neuropharmacology 62:1519–1526.

Reiersen A, Constantino J, Volk H, Todd R (2007) Autistic traits in a population-based ADHD twin sample. J Child Psychol Psychiatry 48:464–472.

Reiersen AM, Todd RD (2008) Co-occurrence of ADHD and autism spectrum disorders: phenomenology and treatment. Expert Rev Neurother 8:657–669.

Reinhart B, Slack F, Basson M, Pasquinelli A, Bettinger J, Rougvie A, Horvitz H, Ruvkun G (2000) The 21-nucleotide let-7 RNA regulates developmental timing in Caenorhabditis elegans. Nature 403:901–906.

Ridder M, Boor I, Lodder J, Postma N, Capdevila-Nortes X, Duarri A, Brussaard A, Estevez R, Scheper G, Mansvelder H, van der Knaap M (2011) Megalencephalic leucoencephalopathy with cysts: defect in chloride currents and cell volume regulation. Brain 134:3342–3354.

Ripke S *et al.* (2011) Genome-wide association study identifies five new schizophrenia loci. Nat Genet 43:969–976.

Riquelme R, Miralles C, de Blas AL (2002) Bergmann glia GABA(A) receptors concentrate on the glial processes that wrap inhibitory synapses. J Neurosci 22:10720–10730.

Rollins B, Martin M, Morgan L, Vawter M (2010) Analysis of whole genome biomarker expression in blood and brain. Am J Med Genet B Neuropsychiatr Genet 153:919–936.

Ronald A, Hoekstra RA (2011) Autism spectrum disorders and autistic traits: A decade of new twin studies. Am J Med Genet B Neuropsychiatr Genet 156B:255-274

Rook GAW, Lowry CA (2008) The hygiene hypothesis and psychiatric disorders. Trends Immunol 29:150–158.

Rubie C, Lichtner P, Gartner J, Siekiera M, Uziel G, Kohlmann B, Kohlschutter A, Meitinger T, Stober G, Bettecken T (2003) Sequence diversity of KIAA0027/MLC1: are megalencephalic leukoencephalopathy and schizophrenia allelic disorders? Hum Mutat 21:45–52.

Rupniak HT, Rein G, Powell JF, Ryder TA, Carson S, Povey S, Hill BT (1984) Characteristics of a new human neuroblastoma cell line which differentiates in response to cyclic adenosine 3':5'-monophosphate. Cancer Res 44:2600–2607.

Ruthschilling C, Albiero G, Lazzari V, Becker R, Moura A, Lucion A, Almeida S, Veiga AB, Giovenardi M (2012) Analysis of transcriptional levels of the oxytocin receptor in different areas of the central nervous system and behaviors in high and low licking rats. Behav Brain Res 228:176–184.

Sabol SZ, Hu S, Hamer D (1998) A functional polymorphism in the monoamine oxidase A gene promoter. Hum Genet 103:273–279.

Saetre P, Emilsson L, Axelsson E, Kreuger J, Lindholm E, Jazin E (2007) Inflammation-related genes up-regulated in schizophrenia brains. BMC Psychiatry 7:46.

Saitoh O, Courchesne E (1998) Magnetic resonance imaging study of the brain in autism. Psychiatry Clin Neurosci 52:S219-22.

Sanger F, Nicklen S, Coulson AR (1977) DNA sequencing with chain-terminating inhibitors. Proc Natl Acad Sci U S A 74:5463–5467.

Santoro D, Colombo I, Ghione I, Peverelli L, Bresolin N, Sciacco M, Prelle A (2011) Steroid-responsive Hashimoto encephalopathy mimicking Creutzfeldt-Jakob disease. Neurol Sci 32:719–722.

Sarapas C, Cai G, Bierer LM, Golier JA, Galea S, Ising M, Rein T, Schmeidler J, Müller-Myhsok B, Uhr M, Holsboer F, Buxbaum JD, Yehuda R (2011) Genetic markers for PTSD risk and resilience among survivors of the World Trade Center attacks. Dis Markers 30:101–110.

Scantamburlo G, Hansenne M, Fuchs S, Pitchot W, Marechal P, Pequeux C, Ansseau M, Legros JJ (2007) Plasma oxytocin levels and anxiety in patients with major depression. Psychoneuroendocrinology 32:407–410.

Schatzberg A, Nemeroff C (2009) The American Psychiatric Publishing textbook of psychopharmacology. Washington, D.C: American Psychiatric Pub.

Scheer FA, Buijs RM (1999) Light affects morning salivary cortisol in humans. J Clin Endocrinol Metab 84:3395–3398.

Schmitt A, Gofferje V, Weber M, Meyer J, Mossner R, Lesch K (2003) The brain-specific protein MLC1 implicated in megalencephalic leukoencephalopathy with subcortical cysts is expressed in glial cells in the murine brain. Glia 44:283–295.

Schneider K (1992) Klinische Psychopathologie. New York: Thieme.

Schratt G, Tuebing F, Nigh E, Kane C, Sabatini M, Kiebler M, Greenberg M (2006) A brain-specific microRNA regulates dendritic spine development. Nature 439:283–289.

Schultz J, Hoffmüller U, Krause G, Ashurst J, Macias M, Schmieder P, Schneider-Mergener J, Oschkinat H (1998) Specific interactions between the syntrophin PDZ domain and voltage-gated sodium channels. Nat Struct Biol 5:19–24.

Segal D, Koschnick J, Slegers L, Hof P (2007) Oligodendrocyte pathophysiology: a new view of schizophrenia. Int J Neuropsychopharmacol 10:503–511.

Segman R, Shefi N, Goltser-Dubner T, Friedman N, Kaminski N, Shalev A (2005) Peripheral blood mononuclear cell gene expression profiles identify emergent post-traumatic stress disorder among trauma survivors. Mol Psychiatry 10:500–513.

Selch S, Strobel A, Haderlein J, Meyer J, Jacob CP, Schmitt A, Lesch K, Reif A (2007) MLC1 polymorphisms are specifically associated with periodic catatonia, a subgroup of chronic schizophrenia. Biol Psychiatry 61:1211–1214.

Selye H (1946) The general adaptation syndrome and the diseases of adaptation. J Clin Endocrin & Metab 6:117–230.

Selye H (1974) Stress without distress. Philadelphia: Lippincott.

Seong E, Seasholtz A, Burmeister M (2002) Mouse models for psychiatric disorders. Trends Genet 18:643–650.

Severinsen JE, Bjarkam CR, Kiaer-Larsen S, Olsen IM, Nielsen MM, Blechingberg J, Nielsen AL, Holm IE, Foldager L, Young BD, Muir WJ, Blackwood DHR, Corydon TJ, Mors O, Børglum AD (2006) Evidence implicating BRD1 with brain development and susceptibility to both schizophrenia and bipolar affective disorder. Mol Psychiatry 11:1126–1138.

Silber J, Lim DA, Petritsch C, Persson AI, Maunakea AK, Yu M, Vandenberg SR, Ginzinger DG, James CD, Costello JF, Bergers G, Weiss WA, Alvarez-Buylla A, Hodgson JG (2008) miR-124 and miR-137 inhibit proliferation of glioblastoma multiforme cells and induce differentiation of brain tumor stem cells. BMC Med 6:14.

Simpson D (2005) Phrenology and the neurosciences: contributions of F. J. Gall and J. G. Spurzheim. ANZ J Surg 75:475–482.

Siomi H, Siomi M (2009) On the road to reading the RNA-interference code. Nature 457:396–404.

Skarnes WC, Rosen B, West AP, Koutsourakis M, Bushell W, Iyer V, Mujica AO, Thomas M, Harrow J, Cox T, Jackson D, Severin J, Biggs P, Fu J, Nefedov M, de Jong PJ, Stewart AF, Bradley A (2011) A conditional knockout resource for the genome-wide study of mouse gene function. Nature 474:337–342.

Smith E *et al.* (2009) Genome-wide association study of bipolar disorder in European American and African American individuals. Mol Psychiatry 14:755–763.

Smithies O, Gregg RG, Boggs SS, Koralewski MA, Kucherlapati RS (1985) Insertion of DNA sequences into the human chromosomal beta-globin locus by homologous recombination. Nature 317:230–234.

Smrt R, Szulwach K, Pfeiffer R, Li X, Guo W, Pathania M, Teng Z, Luo Y, Peng J, Bordey A, Jin P, Zhao X (2010) MicroRNA miR-137 regulates neuronal maturation by targeting ubiquitin ligase mind bomb-1. Stem Cells 28:1060–1070.

Song K, Li S, Okamoto T, Quilliam L, Sargiacomo M, Lisanti M (1996) Co-purification and Direct Interaction of Ras with Caveolin, an Integral Membrane Protein of Caveolae Microdomains. J Biol Chem 271:9690–9697.

Sonino N, Fallo F, Fava G (2010) Psychosomatic aspects of Cushing's syndrome. Rev Endocr Metab Disord 11:95–104.

Souza RP, de Luca V, Meltzer HY, Lieberman JA, Kennedy JL (2010) Schizophrenia severity and clozapine treatment outcome association with oxytocinergic genes. Int J Neuropsychopharmacol 13:793–798.

St Clair D, Blackwood D, Muir W, Carothers A, Walker M, Spowart G, Gosden C, Evans HJ (1990) Association within a family of a balanced autosomal translocation with major mental illness. Lancet 336:13–16.

Stahlberg O, Soderstrom H, Rastam M, Gillberg C (2004) Bipolar disorder, schizophrenia, and other psychotic disorders in adults with childhood onset AD/HD and/or autism spectrum disorders. J Neural Transm 111:891–902.

Stark K, Xu B, Bagchi A, Lai W, Liu H, Hsu R, Wan X, Pavlidis P, Mills AA, Karayiorgou M, Gogos J (2008) Altered brain microRNA biogenesis contributes to phenotypic deficits in a 22q11-deletion mouse model. Nat Genet 40:751–760.

Stober G, Pfuhlmann B, Nurnberg G, Schmidtke A, Reis A, Franzek E, Wienker TF (2001) Towards the genetic basis of periodic catatonia: pedigree sample for genome scan I and II. Eur Arch Psychiatry Clin Neurosci 251 Suppl 1:I25-I30.

Stober G, Saar K, Ruschendorf F, Meyer J, Nurnberg G, Jatzke S, Franzek E, Reis A, Lesch KP, Wienker TF, Beckmann H (2000) Splitting schizophrenia: periodic catatonia-susceptibility locus on chromosome 15q15. Am J Hum Genet 67:1201–1207.

Stober G, Seelow D, Ruschendorf F, Ekici A, Beckmann H, Reis A (2002) Periodic catatonia: confirmation of linkage to chromosome 15 and further evidence for genetic heterogeneity. Hum Genet 111:323–330.

Strausberg RL *et al.* (2002) Generation and initial analysis of more than 15,000 full-length human and mouse cDNA sequences. Proc Natl Acad Sci U S A 99:16899–16903.

Strauss K, Puffenberger E, Huentelman M, Gottlieb S, Dobrin S, Parod J, Stephan D, Morton D (2006) Recessive symptomatic focal epilepsy and mutant contactin-associated protein-like 2. N Engl J Med 354:1370–1377.

Sullivan PF, Kendler KS, Neale MC (2003) Schizophrenia as a complex trait: evidence from a meta-analysis of twin studies. Arch Gen Psychiatry 60:1187–1192.

Sultan M, Schulz M, Richard H, Magen A, Klingenhoff A, Scherf M, Seifert M, Borodina T, Soldatov A, Parkhomchuk D, Schmidt D, O'Keeffe S, Haas S, Vingron M, Lehrach H, Yaspo M (2008) A global view of gene activity and alternative splicing by deep sequencing of the human transcriptome. Science 321:956–960.

Sung NS, Crowley WF, JR, Genel M, Salber P, Sandy L, Sherwood LM, Johnson SB, Catanese V, Tilson H, Getz K, Larson EL, Scheinberg D, Reece EA, Slavkin H, Dobs A, Grebb J, Martinez RA, Korn A, Rimoin D (2003) Central challenges facing the national clinical research enterprise. JAMA 289:1278–1287.

Swerdlow N, Weber M, Qu Y, Light G, Braff D (2008) Realistic expectations of prepulse inhibition in translational models for schizophrenia research. Psychopharmacology (Berl) 199:331–388.

Swerdlow NR, Geyer MA (1998) Using an animal model of deficient sensorimotor gating to study the pathophysiology and new treatments of schizophrenia. Schizophr Bull 24:285–301.

Tabares-Seisdedos R, Rubenstein J (2009) Chromosome 8p as a potential hub for developmental neuropsychiatric disorders: implications for schizophrenia, autism and cancer. Mol Psychiatry 14:563–589.

Tabet AC, Pilorge M, Delorme R, Amsellem F, Pinard JM, Leboyer M, Verloes A, Benzacken B, Betancur C (2012) Autism multiplex family with 16p11.2p12.2 microduplication syndrome in monozygotic twins and distal 16p11.2 deletion in their brother. Eur J Hum Genet 20:540–546

Takao K, Yamasaki N, Miyakawa T (2007) Impact of brain-behavior phenotypying of genetically-engineered mice on research of neuropsychiatric disorders. Neurosci Res 58:124–132.

Takayanagi Y, Yoshida M, Bielsky I, Ross H, Kawamata M, Onaka T, Yanagisawa T, Kimura T, Matzuk M, Young L, Nishimori K (2005) Pervasive social deficits, but normal parturition, in oxytocin receptor-deficient mice. Proc Natl Acad Sci U S A 102:16096–16101.

Tang G (2005) siRNA and miRNA: an insight into RISCs. Trends Biochem Sci 30:106–114.

Tansey K, Brookes K, Hill M, Cochrane L, Gill M, Skuse D, Correia C, Vicente A, Kent L, Gallagher L, Anney R (2010) Oxytocin receptor (OXTR) does not play a major role in the aetiology of autism: Genetic and molecular studies. Neurosci Lett 474:163–167.

Tarantino C, Paolella G, Cozzuto L, Minopoli G, Pastore L, Parisi S, Russo T (2010) miRNA 34a, 100, and 137 modulate differentiation of mouse embryonic stem cells. FASEB J 24:3255–3263.

Taurines R, Grünblatt E, Schecklmann M, Schwenck C, Albantakis L, Reefschläger L, Walitza S, Renner T, Gerlach M, Thome J, Romanos M (2011) Altered mRNA expression

of monoaminergic candidate genes in the blood of children with attention deficit hyperactivity disorder and autism spectrum disorder. World J Biol Psychiatry 12 Suppl 1:104–108.

Taylor MA, Fink M (2003) Catatonia in psychiatric classification: a home of its own. Am J Psychiatry 160:1233–1241.

te Riele H, Maandag ER, Berns A (1992) Highly efficient gene targeting in embryonic stem cells through homologous recombination with isogenic DNA constructs. Proc Natl Acad Sci U S A 89:5128–5132.

Teijido O, Casaroli-Marano R, Kharkovets T, Aguado F, Zorzano A, Palacin M, Soriano E, Martinez A, Estevez R (2007) Expression patterns of MLC1 protein in the central and peripheral nervous systems. Neurobiol Dis 26:532–545.

Teijido O, Martinez A, Pusch M, Zorzano A, Soriano E, del Rio J, Palacin M, Estevez R (2004) Localization and functional analyses of the MLC1 protein involved in megalencephalic leukoencephalopathy with subcortical cysts. Hum Mol Genet 13:2581–2594.

ten Bosch JR, Grody WW (2008) Keeping up with the Next Generation. J Mol Diagn 10:484–492.

Thapar A, Rice F, Hay D, Boivin J, Langley K, van d, Rutter M, Harold G (2009) Prenatal smoking might not cause attention-deficit/hyperactivity disorder: evidence from a novel design. Biol Psychiatry 66:722–727.

Thompson RJ, Parker KJ, Hallmayer JF, Waugh CE, Gotlib IH (2011) Oxytocin receptor gene polymorphism (rs2254298) interacts with familial risk for psychopathology to predict symptoms of depression and anxiety in adolescent girls. Psychoneuroendocrinology 36:144–147.

Tomasi D, Volkow N (2012) Abnormal functional connectivity in children with attention-deficit/hyperactivity disorder. Biol Psychiatry 71:443–450.

Topçu M, Gartioux C, Ribierre F, Yalçinkaya C, Tokus E, Oztekin N, Beckmann JS, Ozguc M, Seboun E (2000) Vacuoliting megalencephalic leukoencephalopathy with subcortical cysts, mapped to chromosome 22qtel. Am J Hum Genet 66:733–739.

True WR, Rice J, Eisen SA, Heath AC, Goldberg J, Lyons MJ, Nowak J (1993) A twin study of genetic and environmental contributions to liability for posttraumatic stress symptoms. Arch Gen Psychiatry 50:257–264.

Tsai Y, Tsai P, Jiang M, Chang C (2007) Designer mice for human disease - A close view of Nobel Laureate: Oliver Smithies. Research Express@NCKU 2:2

Tsuang M, Nossova N, Yager T, Tsuang M, Guo S, Shyu K, Glatt S, Liew C (2005) Assessing the validity of blood-based gene expression profiles for the classification of schizophrenia and bipolar disorder: a preliminary report. Am J Med Genet B Neuropsychiatr Genet 133B:1–5.

Vainzof M, Ayub-Guerrieri D, Onofre P, Martins P, Lopes V, Zilberztajn D, Maia L, Sell K, Yamamoto L (2008) Animal models for genetic neuromuscular diseases. J Mol Neurosci 34:241–248.

van der Knaap M, Valk J, Barth P, Smit L, van Engelen B, Tortori D (1995) Leukoencephalopathy with swelling in children and adolescents: MRI patterns and differential diagnosis. Neuroradiology 37:679–686.

van Os J, Kapur S (2009) Schizophrenia. Lancet 374:635–645.

van Winkel R, Esquivel G, Kenis G, Wichers M, Collip D, Peerbooms O, Rutten B, Myin-Germeys I, van Os J (2010) REVIEW: Genome-wide findings in schizophrenia and the role of gene-environment interplay. CNS Neurosci Ther 16:e185-92.

Van Zeeland S, Abrahams B, Alvarez-Retuerto A, Sonnenblick L, Rudie J, Ghahremani D, Mumford J, Poldrack R, Dapretto M, Geschwind D, Bookheimer S (2010) Altered

functional connectivity in frontal lobe circuits is associated with variation in the autism risk gene CNTNAP2. Sci Transl Med 2:56ra80.

Vandebrouck A, Sabourin J, Rivet J, Balghi H, Sebille S, Kitzis A, Raymond G, Cognard C, Bourmeyster N, Constantin B (2007) Regulation of capacitative calcium entries by alpha1-syntrophin: association of TRPC1 with dystrophin complex and the PDZ domain of alpha1-syntrophin. FASEB J 21:608–617.

Vartanian K, Slottke R, Johnstone T, Casale A, Planck SR, Choi D, Smith JR, Rosenbaum JT, Harrington CA (2009) Gene expression profiling of whole blood: comparison of target preparation methods for accurate and reproducible microarray analysis. BMC Genomics 10:2.

Vawter M, Usen N, Thatcher L, Ladenheim B, Zhang P, VanderPutten D, Conant K, Herman M, van Kammen D, Sedvall G, Garver D, Freed W (2001) Characterization of human cleaved N-CAM and association with schizophrenia. Exp Neurol 172:29–46.

Venter JC *et al.* (2001) The sequence of the human genome. Science 291:1304–1351.

Verma R, Chauhan C, Saleem Q, Gandhi C, Jain S, Brahmachari SK (2004) A nonsense mutation in the synaptogyrin 1 gene in a family with schizophrenia. Biol Psychiatry 55:196–199.

Verma R, Mukerji M, Grover D, B-Rao C, Das S, Kubendran S, Jain S, Brahmachari S (2005) MLC1 gene is associated with schizophrenia and bipolar disorder in Southern India. Biol Psychiatry 58:16–22.

Vermeulen A, Behlen L, Reynolds A, Wolfson A, Marshall W, Karpilow J, Khvorova A (2005) The contributions of dsRNA structure to Dicer specificity and efficiency. RNA 11:674–682.

Voineagu I, Wang X, Johnston P, Lowe JK, Tian Y, Horvath S, Mill J, Cantor RM, Blencowe BJ, Geschwind DH (2011) Transcriptomic analysis of autistic brain reveals convergent molecular pathology. Nature 474:380–384.

von Foerster H, von Glasersfeld E, Hejl PM, Schmidt SJ, Watzlawick P (1997) Einführung in den Konstruktivismus. München: Piper.

Vreugdenhil E, Berezikov E (2009) Fine-tuning the brain: MicroRNAs. Front Neuroendocrinol 31:128–133

Vreugdenhil E, Kolk S, Boekhoorn K, Fitzsimons C, Schaaf M, Schouten T, Sarabdjitsingh A, Sibug R, Lucassen P (2007) Doublecortin-like, a microtubule-associated protein expressed in radial glia, is crucial for neuronal precursor division and radial process stability. Eur J Neurosci 25:635–648.

Vreugdenhil E, Verissimo CS, Mariman R, Kamphorst JT, Barbosa JS, Zweers T, Champagne DL, Schouten T, Meijer OC, de Kloet ER, Fitzsimons CP (2009) MicroRNA 18 and 124a down-regulate the glucocorticoid receptor: implications for glucocorticoid responsiveness in the brain. Endocrinology 150:2220–2228.

Walters F (1998) Intracranial Pressure and Cerebral Blood Flow. Physiology 8:1–4.

Wang J, Shang J, Wu Y, Gu Q, Xiong H, Ding C, Wang L, Gao Z, Wu X, Jiang Y (2011) Identification of novel MLC1 mutations in Chinese patients with megalencephalic leukoencephalopathy with subcortical cysts (MLC). J Hum Genet 56:138–142.

Wang K, Liu X, Aragam N (2010) A genome-wide meta-analysis identifies novel loci associated with schizophrenia and bipolar disorder. Schizophr Res 124:192–199.

Wang Y, Medvid R, Melton C, Jaenisch R, Blelloch R (2007) DGCR8 is essential for microRNA biogenesis and silencing of embryonic stem cell self-renewal. Nat Genet 39:380–385.

Watanabe Y, Someya T, Nawa H (2010) Cytokine hypothesis of schizophrenia pathogenesis: evidence from human studies and animal models. Psychiatry Clin Neurosci 64:217–230.

Waterston R *et al.* (2002) Initial sequencing and comparative analysis of the mouse genome. Nature 420:520–562.

Watzlawick P (2008) Die erfundene Wirklichkeit. Wie wissen wir, was wir zu wissen glauben? Beiträge zum Konstruktivismus. München: Piper.

Wermter A, Kamp-Becker I, Hesse P, Schulte-Körne G, Strauch K, Remschmidt H (2010) Evidence for the involvement of genetic variation in the oxytocin receptor gene (OXTR) in the etiology of autistic disorders on high-functioning level. Am. J. Med. Genet. B Neuropsychiatr Genet 153:629–639.

Wernicke C (2007) Grundriss der Psychiatrie in klinischen Vorlesungen. Saarbrücken: VDM Verlag Dr. Müller.

Wiener N (1961) Cybernetics. Or control and communication in the animals and the machine. Cambridge (Massachusetts): MIT press.

Willemsen M, Vallès A, Kirkels L, Mastebroek M, Olde Loohuis N, Kos A, Wissink-Lindhout WM, de Brouwer APM, Nillesen WM, Pfundt R, Holder-Espinasse M, Vallée L, Andrieux J, Coppens-Hofman MC, Rensen H, Hamel BCJ, van Bokhoven H, Aschrafi A, Kleefstra T (2011) Chromosome 1p21.3 microdeletions comprising DPYD and MIR137 are associated with intellectual disability. J Med Genet 48:810-818

Williams H, Glaser B, Williams N, Norton N, Zammit S, MacGregor S, Kirov G, Owen M, O'Donovan M (2005) No association between schizophrenia and polymorphisms in COMT in two large samples. Am J Psychiatry 162:1736–1738.

Willmann R, Possekel S, Dubach-Powell J, Meier T, Ruegg M (2009) Mammalian animal models for Duchenne muscular dystrophy. Neuromuscul Disord 19:241–249.

Winslow J, Insel T (2002) The social deficits of the oxytocin knockout mouse. Neuropeptides 36:221–229.

Wismer F, Ziegler T, Kurian J, Jacoris S, Pollak S (2005) Early experience in humans is associated with changes in neuropeptides critical for regulating social behavior. Proc Natl Acad Sci U S A 102:17237–17240.

Wolkowitz O, Burke H, Epel E, Reus V (2009) Glucocorticoids. Mood, memory, and mechanisms. Ann N Y Acad Sci 1179:19–40.

Wood G, Tomasiewicz H, Rutishauser U, Magnuson T, Quirion R, Rochford J, Srivastava L (1998) NCAM-180 knockout mice display increased lateral ventricle size and reduced prepulse inhibition of startle. Neuroreport 9:461–466.

Woolf SH (2008) The meaning of translational research and why it matters. JAMA 299:211–213.

Wu S, Jia M, Ruan Y, Liu J, Guo Y, Shuang M, Gong X, Zhang Y, Yang X, Zhang D (2005) Positive Association of the Oxytocin Receptor Gene (OXTR) with Autism in the Chinese Han Population. Biol Psychiatry 58:74–77.

Wu S, Ying G, Wu Q, Capecchi MR (2008) A protocol for constructing gene targeting vectors: generating knockout mice for the cadherin family and beyond. Nat Protoc 3:1056–1076.

Wust S, Wolf J, Hellhammer DH, Federenko I, Schommer N, Kirschbaum C (2000) The cortisol awakening response - normal values and confounds. Noise Health 2:79–88.

Xiu M, Hui L, Dang Y, Hou T, Zhang C, Zheng Y, Chen D, Kosten T, Zhang X (2009) Decreased serum BDNF levels in chronic institutionalized schizophrenia on long-term treatment with typical and atypical antipsychotics. Prog Neuropsychopharmacol Biol Psychiatry 33:1508–1512.

Xu M, He L (2010) Convergent evidence shows a positive association of interleukin-1 gene complex locus with susceptibility to schizophrenia in the Caucasian population. Schizophr Res 120:131–142.

Yagi T, Takeichi M (2000) Cadherin superfamily genes: functions, genomic organization, and neurologic diversity. Genes Dev 14:1169–1180.

Yamada K, Watanabe M (2002) Cytodifferentiation of Bergmann glia and its relationship with Purkinje cells. Anat Sci Int 77:94–108.

Yamashita M, Fukushima S, Shen H, Hall F, Uhl G, Numachi Y, Kobayashi H, Sora I (2006) Norepinephrine transporter blockade can normalize the prepulse inhibition deficits found in dopamine transporter knockout mice. Neuropsychopharmacology 31:2132–2139.

Yehuda R (2001) Biology of posttraumatic stress disorder. J Clin Psychiatry 62 Suppl 17:41–46.

Yehuda R, Halligan S, Golier J, Grossman R, Bierer L (2004) Effects of trauma exposure on the cortisol response to dexamethasone administration in PTSD and major depressive disorder. Psychoneuroendocrinology 29:389–404.

Yehuda R, Halligan S, Grossman R, Golier J, Wong C (2002) The cortisol and glucocorticoid receptor response to low dose dexamethasone administration in aging combat veterans and holocaust survivors with and without posttraumatic stress disorder. Biol Psychiatry 52:393–403.

Yehuda R, Koenen K, Galea S, Flory J (2011) The role of genes in defining a molecular biology of PTSD. Dis Markers 30:67–76.

Yeom K, Lee Y, Han J, Suh M, Kim V (2006) Characterization of DGCR8/Pasha, the essential cofactor for Drosha in primary miRNA processing. Nucleic Acids Res 34:4622–4629.

Yi R (2003) Exportin-5 mediates the nuclear export of pre-microRNAs and short hairpin RNAs. Genes & Development 17:3011–3016.

Yolken R (2002) Subtraction libraries for the molecular characterization of gene-environmental interactions in bipolar disorder. Bipolar Disorders 4:77–80.

Yüzbaşioğlu A, Topçu M, Cetin K, Ozgüç M (2011) Novel mutations of the MLC1 gene in Turkish patients. Eur J Med Genet 54:281–283.

Zamore P, Tuschl T, Sharp P, Bartel D (2000) RNAi: double-stranded RNA directs the ATP-dependent cleavage of mRNA at 21 to 23 nucleotide intervals. Cell 101:25–33.

Zhang R, Su B (2009) Small but influential: the role of microRNAs on gene regulatory network and 3'UTR evolution. J Genet Genomics 36:1–6.

Zhou R, Yuan P, Wang Y, Hunsberger J, Elkahloun A, Wei Y, Damschroder-Williams P, Du J, Chen G, Manji H (2009) Evidence for selective microRNAs and their effectors as common long-term targets for the actions of mood stabilizers. Neuropsychopharmacology 34:1395–1405.

Zingg H, Laporte S (2003) The oxytocin receptor. Trends Endocrinol Metab 14:222–227.

Acknowledgement

At first, I like to thank Professor Jobst Meyer for his offer work on this project and to accomplish my work in his facilities with his support. I also thank Professor Claude Muller for his willingness to be my second reviewer of this thesis and the opportunity to perform a big share of my work in his facilities at the Laboratoire National de Santé in Luxembourg-City.

I want to thank Ulrike Schülter, Dr. Andrea Schote-Frese, Rita Reinke and all the other colleagues of the Department of Neurobehavioural Genetics that arrived and left for their continuous support within the lab and the creation and correction of manuscripts for publication. Furthermore, I thank all of them for their enjoyable time we shared together including a lot of informal chats.

I thank all the diploma students for the time we shared together and their enormous help concerning my scientific work: Katharina Berens, Susanne Weyand, Frauke Steiger and Fabian Streit. I am very grateful for interdisciplinary discussions in order to bridge the different ways psychologists and biologists focus on the same matter. Special thanks to all of you for your support in statistical questions and the pleasant atmosphere in and outside the lab.

Thanks to Dr. Andreas Chiocchetti, Dr. Regina Waltes and Marnie Kopp from the clinic of psychiatry, psychosomatics and psychotherapy of children and adolescents for the good collaboration and the nice time we spent together during the WCPG 2010 in Athens.

I am indebted to my colleagues at the Institute of Immunology in Luxembourg-City, especially Professor Claude Muller for giving me the opportunity to work in his facilities. I thank Dr. Jonathan Turner and Dr. Simone Alt for their extraordinary support and the excellent collaboration with respect to planning and accomplishment of the studies that I conducted in their lab.

I thank all the people from the Department of Medical Pharmacology. Thanks to Professor Ron de Kloet, Professor Melly Oitzl and most notably, Professor Erno Vreugdenhil for his

offer to conduct my experiments in his facilities. I explicitly want to thank Dirk-Jan Saaltink and Robert Eendebak for their care and assistance during my experimental work and the nice spare time we shared together “op de uitkijkpunt” and biking around.

I thank the German Research foundation and the International Research Training Group “From Molecules and Genes to Affect and Cognition”, GRK 1389/1, for their financial support that enabled the realization of this thesis.

I feel indebted to all my friends that have been accompanying me most of my life for their belief in my ideas and their help. I am grateful that they always supported me once I needed them.

My biggest thanks go to my girlfriend Natascha who always encouraged me to hang on with my work and who gave me all the love I needed to “keep swimming”.
Thank you very much ☺ !!!

Zum Schluss möchte ich meinen Eltern dafür danken, dass sie mein ganzes Leben lang für mich da waren und sind und mich in jeglicher Hinsicht zur Durchführung der vorliegenden Arbeit ermutigt und unterstützt haben. Sie haben an mich geglaubt. Vielen Dank an Euch!

Versicherung an Eides statt

Hiermit erkläre ich an Eides statt, dass ich die vorliegende Arbeit selbständig und nur mit den darin angegebenen Hilfsmitteln verfasst habe und die wörtlich oder dem Inhalt nach aus fremden Arbeiten entnommenen Stellen als solche genau kenntlich gemacht sind.

Insbesondere habe ich hierfür nicht die entgeltliche Hilfe von Vermittlungs- bzw. Beratungsdiensten (Promotionsberater oder andere Personen) in Anspruch genommen. Niemand hat von mir unmittelbar oder mittelbar geldwerte Leistungen für Arbeit erhalten, die im Zusammenhang mit dem Inhalt der vorliegenden Dissertation stehen. Die Arbeit wurde bisher weder im In- noch im Ausland in gleicher oder ähnlicher Form einer anderen Prüfungsbehörde vorgelegt.

_____ _____

Ort, Datum Unterschrift